R-11-06

SFR site investigation

Bedrock Hydrogeochemistry

Ann-Chatrin Nilsson, Geosigma AB

Eva-Lena Tullborg, Terralogica AB

John Smellie, Conterra AB

María J Gimeno, Javier B Gómez, Luis F Auqué
University of Zaragoza

Björn Sandström, WSP Sverige AB

Karsten Pedersen, Micans AB

November 2011

SKB

SFR site investigation

Bedrock Hydrogeochemistry

Ann-Chatrin Nilsson, Geosigma AB

Eva-Lena Tullborg, Terralogica AB

John Smellie, Conterra AB

María J Gimeno, Javier B Gómez, Luis F Auqué
University of Zaragoza

Björn Sandström, WSP Sverige AB

Karsten Pedersen, Micans AB

November 2011

Update notice

The original report, dated November 2011, was found to contain factual errors which have been corrected in this updated version. The corrected factual errors are presented below.

Updated 2013-08

Location	Original text	Corrected text
Page 125, Figure 5-46c	Wrong data used in figure	Figure updated with correct data

Abstract

There are plans that the final repository for low and intermediate level radioactive waste, SFR, located about 150 km north of Stockholm, will be extended. Geoscientific studies to define and characterise a suitable bedrock volume for the extended repository have been carried out from 2007 to 2011, and have included the drilling and evaluation of seven new core drilled and four percussion boreholes. These new data, together with existing data extending back to 1985, have been interpreted and modelled in order to provide the necessary information for safety assessment and repository design. This report presents the final hydrogeochemical site description for the SFR site, and will constitute a background report for the integrated site description (the SFR Site Descriptive Model version 1.0) together with corresponding reports from the geological and hydrogeological disciplines.

Most of the hydrogeochemical data from the field investigations consist of major ions and isotopes together with sporadic gas, microbe and measured redox data. Despite the close proximity of the Forsmark site, few data from this source are of relevance because of the shallow nature of the SFR site, the fact that SFR is located beneath the Baltic Sea and also the drawdown/upconing impacts of its construction on the hydrogeochemistry. This artificially imposed dynamic flow system is naturally more prevalent along major deformation fracture zones of higher transmissivity, whilst lower transmissive fractures together with the less transmissive bedrock masses between major deformation zones, still retain some evidence of the natural groundwater mixing patterns established prior to the SFR construction.

The groundwaters in the SFR dataset cover a depth down to –250 m.a.s.l. with single sampling locations at –300 and –400 m.a.s.l. and represent a relatively limited salinity range (1,500 to 5,500 mg/L chloride). However, the $\delta^{18}O$ values show a wide variation (–15.5 to –7.5‰ V-SMOW) similar to that reported from the Forsmark site investigations (Laaksoharju et al. 2008). At the SFR, marine indicators such as Mg/Cl, K/Cl and Br/Cl also show relatively large variations considering the limited salinity range. This information together with palaeoclimatic considerations were used to differentiate the groundwaters into four major types; 1) local Baltic Seawater type, 2) Littorina type water with a glacial component, 3) brackish-glacial water type, and 4) mixed brackish water (transition type). Based on these types, explorative analyses using traditional geochemical approaches have been performed initially to describe groundwater conditions (origin and evolution) followed by further detailed evaluation using different modelling approaches such as mixing modelling, geochemical equilibrium modelling and redox modelling.

From measured Eh values, and in accordance with the chemistry of Fe, Mn, S and U, it is concluded that mildly reduced conditions (–140 to –190 mV) generally prevail in the investigated groundwaters and, importantly, also for the youngest Baltic Sea type groundwaters. In terms of redox buffer capacity, the most important fracture minerals available are the Fe(II)-bearing minerals coating the water conductive fractures, which at SFR comprise mainly chlorite, clay minerals and pyrite. Calcite coatings are also frequent, which results in a rapid response to changes in pH by dissolution or precipitation and thereby provides an important buffering capacity against acidification.

The division into different groundwater types has facilitated interaction and integration with the geological and hydrogeological models making it possible to construct a hydrogeochemical site descriptive model for the SFR site. The distribution of the different groundwater types shows that the major deformation zones have served as important groundwater flow pathways over long periods of geological time while single discrete fractures in rock volumes between zones generally contain older and more isolated groundwater. Presently, the steeply dipping structures in particular have facilitated the drawdown of modern Baltic Seawater which has been observed since excavation and construction of the SFR commenced some twenty years ago. Although this intrusion is not reversible, the system maintains stable hydrochemical conditions in terms of pH and Eh and the resulting changes in chemical composition have been relatively small.

Understanding the evolution of the groundwater system over time, i.e. since the last glaciation and more recently since excavation and construction of the SFR repository, shows that; 1) present day hydraulic conditions have preserved groundwater patterns which replicate to a large extent what will occur during the next deglaciation (long term perspective), and 2) the future impact of extended excavations and underground construction on groundwater chemistry can be predicted from past to present day observations at the SFR site (short term perspective).

Uncertainties have been treated indicating high confidence in defining the different groundwater types and their mixing flow paths in the bedrock, the major processes (major reactions, Eh and pH) influencing the groundwaters, and the successful integration of the hydrogeological and hydrogeo-chemical conceptual models.

Sammanfattning

Vid slutförvaret för låg- och medelaktivt radioaktivt driftavfall, SFR, lokaliserat cirka 150 km norr om Stockholm, planeras för en utbyggnad. Syftet med platsundersökningsprojektet, som omfattar tiden 2007–2011, är att definiera och karakterisera en lämplig bergvolym för denna utbyggnad. Detta inbegriper borrning och geovetenskapliga undersökningar i sju kärnborrhål och fyra hammarborrhål samt efterföljande tolknings- och modelleringsarbete baserat på erhållna resultat för att leverera nödvändig information för säkerhetsanalys och projektering. Denna rapport presenterar en slutlig hydrogeokemisk platsbeskrivning för SFR och aktuellt område för utbyggnaden. Rapporten kommer att utgöra en bakgrundsrapport till den integrerade platsbeskrivningen (SFR Site Descriptive Model version 1.0) tillsammans med motsvarande rapporter för disciplinerna hydrogeologi och geologi.

De avslutade hydrogeokemiska fältundersökningarna har bidragit med kemiska data huvudsakligen bestående av vanliga grundvattenanalyser inkluderande huvudkomponenter och isotoper samt ett fåtal gas-, mikrob- och mätta redoxdata. Trots närheten till kandidatområdet för slutförvaret för utbränt kärnbränsle i Forsmark är det bara en mindre datamängd därifrån som är relevant i samman-hanget på grund av att SFR förvaret är beläget relativt ytligt, att det är beläget under Östersjön och dessutom påverkar hydrokemin i form av avsänknings och uppkoningseffekter. Detta artificiellt skapade dynamiska flödessystem är företrädesvis verkande längs deformationszoner med högre hydraulisk transmissivitet medan spricksystem med lägre transmissivitet och mindre transmissiva bergmassor mellan större deformationszoner har bibehållit spår av det naturliga blandningsmönstret som rådde innan SFR konstruerades.

Datasetet från SFR täcker ett maximalt djup ner till –250 m.ö.h. med enstaka provpunkter vid –300 och –400 m.ö.h. och representerar ett relativt begränsat salinitetsintervall (1 500 till 5 500 mg/Lklorid). Värdena för $\delta^{18}O$ däremot visar en större variation (–15,5 till –7,5 ‰ V-SMOW) vilket är samma intervall som har rapporterats från platsundersökningarna i Forsmark (Laaksoharju et al. 2008). Marina indikatorer som Mg/Cl, K/Cl och Br/CL visar också relativt stora variationer med tanke på det begrän-sade salinitetsintervallet. Denna information tillsammans med palaeoklimathistorik har använts för att dela upp grundvatten i fyra huvudsakliga grundvattentyper; 1) lokal Östersjövattentyp, 2) Littorina-typ med en glacial komponent, 3) bräckt glacial vattentyp och 4) ett blandvatten av övergångstyp. Baserat på dessa vattentyper, har en första utvärdering gjorts med hjälp av traditionella geokemiska tolkningsmetoder för att beskriva grundvattenförhållandena (ursprung och utveckling), därefter har mer detaljerade utvärderingar utförts med hjälp av modelleringsverktyg för blandningsberäkningar, jämviktsberäkningar och redoxmodellering.

Från mätta redoxvärden och i överenstämmelse med kemin för Fe, Mn, S och U, är slutsatsen att det generellt råder måttligt reducerade förhållanden (–140 till –190 mV) i de undersökta grundvatten. Av vikt är att detta gäller också för de yngsta grundvatten av Östersjötyp. Den redoxbuffertkapacitet som tillhandahålls av sprickmineral utgörs till största delen av Fe(II) mineral (klorit, lermineral och pyrit) som finns på sprickväggarna längs de vattenförande strukturerna i berget. Kalcitbeläggningen som också är vanligt förekommande i de vattenförande sprickorna reagerar snabbt med upplösning/ utfällning om de grundvattenkemiska förhållandena förändras och kommer därigenom att fungera som en pH buffert.

Uppdelningen i vattentyper har underlättat samverkan och integration med de hydrogeologiska modellerna och möjliggjort konstruktionen av den hydrogeokemiska platsbeskrivningen för SFR. Distributionen av de olika vattentyperna i bergvolymen visar att de större deformationszonerna har tjänat som viktiga flödesvägar för grundvattnet under långa geologiska tidsperioder medan enstaka sprickor i bergvolymer mellan zoner generellt innehåller ett äldre och mer isolerat grund-vatten. I nutid underlättar i synnerhet de brantstående zonerna för den inträngning av modernt Östersjövatten som har observerats sedan utsprängningen och konstruktionen av SFR, för cirka tjugu år sedan. Denna inträngning är inte reversibel, men systemet bibehåller stabila hydrokemiska förhållanden när det gäller pH och Eh och de orsakade förändringarna i kemisk sammansättning har varit relativt begränsade.

Förståelsen för utvecklingen av grundvattensystemet över tid, sedan den sista deglaciationen och fram till modern tid inkluderande utsprängningen och konstruktionen av SFR förvaret, visar att; 1) dagens hydrauliska förhållanden har bevarat grundvattenmönster som replikerar till stor del vad som förväntas bli resultatet av nästa deglaciation (långtidsperspektiv), och 2) framtida påverkan på grundvattenkemin från utgrävning och underjordskonstruktioner kan förutsägas från observationer gjorda under nuvarande SFRs existenstid (korttidsperspektiv).

Osäkerheterna i den hydrokemiska beskrivningen har utvärderats och indikerar hög trovärdighet i beskrivningen av de olika vattentyperna och deras blandning och flödesvägar i berggrunden, vilka huvudsakliga processer (huvudsakliga reaktioner, Eh och pH) som påverkar grundvattensamman-sättningen samt överensstämmelsen i integrationen mellan de hydrogeologiska och hydrogeokemiska konceptuella modellerna.

Contents

1 Introduction

1.1 Background

During 2008, the Swedish Nuclear Fuel and Waste Management Company (SKB) initiated an investigation programme for a future extension of the final repository for low and medium level radioactive operational waste, SFR, located about 150 km north of Stockholm. The repository was inaugurated in April 1988 and, at present, the stored waste volume is about 30,000 m^3 (total capacity is 63,000 m^3) consisting of operational waste from the Swedish nuclear power plants and radioactive waste from hospitals. The purpose of the investigations was to define and characterise a bedrock volume large enough to allow further storage of operational waste from existing Swedish nuclear power plants and future waste from the decommissioning and dismantling of nuclear power plant reactors (SKB 2008). Of several alternatives, a selected location was investigated southwest of the present SFR tunnel system (Figure 1-1).

The geoscientific investigation programme for the SFR extension project is clearly less extensive than the previous investigation programme at Forsmark (henceforth referred to as the 'Forsmark site investigations' or 'PLU'(SKB 2001)) and the number of drilled boreholes is comparatively few. The stated reasons are: 1) The candidate area is relatively small. 2) The investigation and construction phase as well as the operational phase have already provided a rather detailed understanding of the repository area and its vicinity. 3) The issues to consider in the safety assessment are somewhat different from the site investigations in Forsmark. The implication for the hydrogeochemical part of the investigation programme is, besides the more limited analytical protocol, that the number of new sampling locations (borehole sections) amounts to less than fifteen. However, when already available hydrogeochemical data from early SFR boreholes are included, and considering the small area, the data density for the SFR extension site turns out to be quite high (one borehole per 90,000 m^2 for the SFR regional area compared to one per 450,000 m^2 for the Forsmark local area).
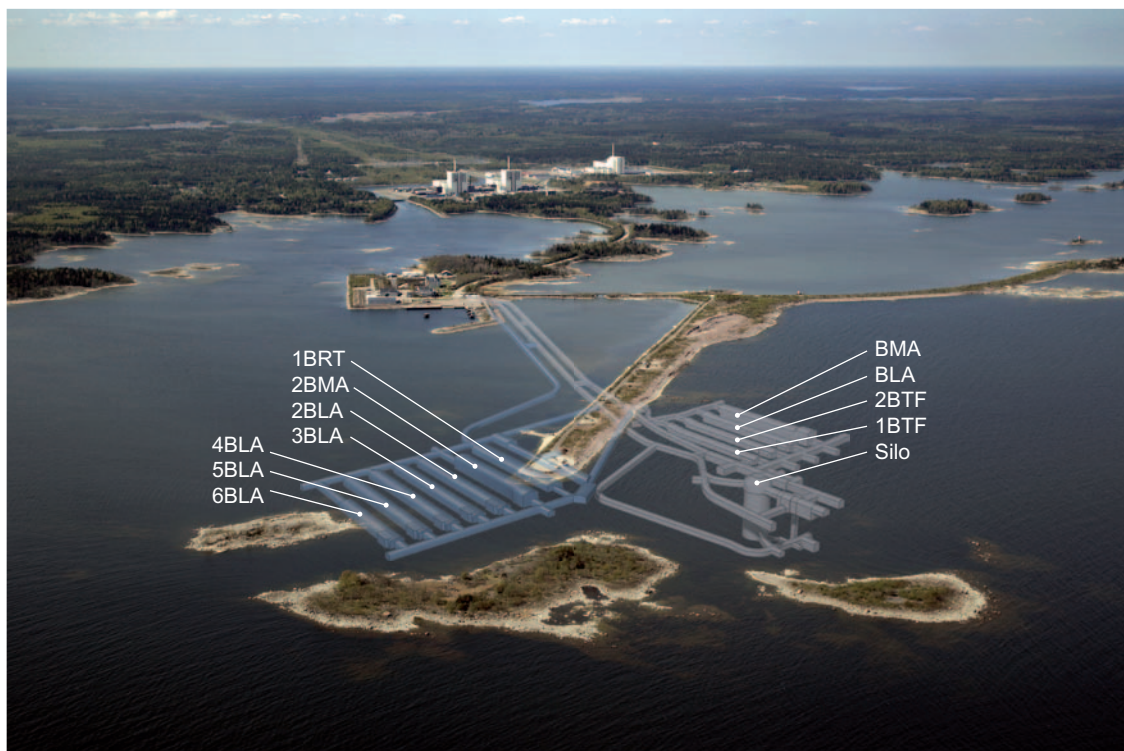
Figure 1-1. One of several lay out proposals for the extension of the SFR repository. The present SFR repository is located to the right (light grey colour) while the planned new tunnel system is shown to the left (light blue colour). Both existing and planned facilities are situated about 60 m below the seabed of the Baltic Sea. The abbreviations are explained in Table 1-2.

The SFR site investigation, including also the interpretation and modelling work to follow, is based to a large extent on methodologies that were established during the preceding Forsmark site investigations (2002 to 2007) for a deep repository for spent fuel. However, it is intended that the new storage capacity will connect with the existing SFR facility and thus the target area for the location of the extension is already defined.

The regional and local SFR model areas as well as the Forsmark site investigation local model area are shown in Figure 1-2. The SFR local model volume extends from elevation +100 m.a.s.l. (metres above sea level) to –300 m.a.s.l., while the regional model volume extends from +100 m.a.s.l. to –1,100 m.a.s.l. The coordinates defining the model areas are provided in Table 1-1. The distinct rectangular volumes primarily concern the geological model.

Table 1-1. Coordinates defining the model areas for SFR in metres (SKB 2008). RT90 (RAK) coordinate system.

Regional model volume		Local model volume	
Easting	**Northing**	**Easting**	**Northing**
1631920.0000	6701550.0000	1632550.0000	6701880.0000
1633111.7827	6702741.1671	1633059.2484	6702388.9854
1634207.5150	6701644.8685	1633667.2031	6701780.7165
1633015.7324	6700453.7014	1633157.9547	6701271.7311
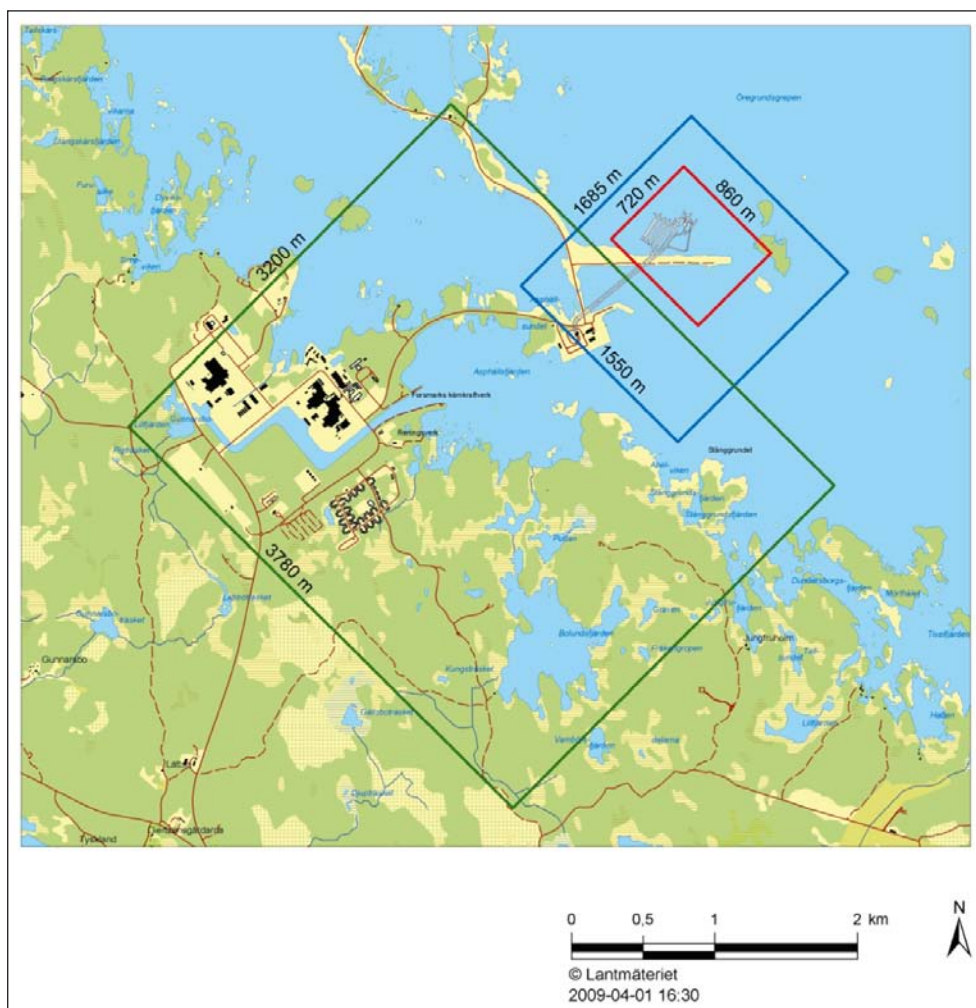
Figure 1-2. *Regional (blue) and local (red) model domains for SFR model v. 0.1, in relation to the local model area of the Forsmark site investigation, model v. 2.2 (green) (SKB 2008).*

1.2   Objectives and scope

The overall objectives of the hydrochemical interpretation and modelling work for the SFR site are to establish a detailed understanding of the hydrogeochemical conditions at the site, and to develop models to describe and visualise the site. The focus is to describe the chemistry, origin and the distribution of groundwaters in the bedrock and the hydrogeochemical processes involved in the evolution of the groundwaters as well as the short term impacts since 1984 from the construction and operation of the present SFR repository. Hydrogeochemical information, for example salinity distribution, groundwater residence time and palaeohydrogeochemical input, are of concern also for the hydrogeology in order to constrain the hydrogeological descriptive model. The hydrogeochemical modelling work has been performed in three steps, resulting in three model versions (0.1, 0.2 and 1.0).

Version 0.1, presented in SFR P-09-45 (Nilsson A-C 2009), comprised a systematic data evaluation and retrospective QA of data from the early SFR boreholes (cf. Table 4-2), including the period 1984 to 2007, rather than the construction of a hydrogeochemical model. The hydrogeochemical data were extracted from the database Sicada (Sicada-08-200 0:1 "data delivery reference"). A simple initial check of both borehole information and data was performed by comparison with corresponding SKB documentation in earlier reports from the SFR. Further evaluation was performed by using trend plots, different x-y scatter plots, charge balance calculations, and 3D visualisations of a few selected parameters/components (e.g. Cl, Mg and $\delta^{18}O$) etc. The main purpose was to become acquainted with the dataset and groundwater variability, as well as to discover inconsistencies and outliers among the data. The revealed errors were subsequently corrected in Sicada and questionable data were highlighted in the report.

The specific aim with the version 0.2 interpretation and modelling work (Nilsson et al. 2010a) was to produce a preliminary hydrogeochemical site description model based on both the early SFR data and most of the new data from the SFR extension project (i.e. data deliveries Sicada-09-182 (0:1), Sicada-09-189 (0:1) and a few complementary data made available in April 2010 (Nilsson K 2011)). Explorative analyses using traditional geochemical approaches were performed to describe the data and to provide an early insight and understanding of the site, i.e. to construct a preliminary conceptual model. The report was rather an early progress report, documenting the initial achievements in the interpretation and modelling work, than a complete hydrogeochemical site description for the SFR site. However, the groundwaters were interpreted in relation to their origin, evolution and composition, and the preliminary conceptual model was used to describe and visualise the site.

The present final hydrogeochemical site description version 1.0 includes also subsequent complementary data from the SFR extension project (Sicada-11-056 0:1), (Nilsson K 2011) and the data are further evaluated using additional modelling approaches and techniques. The Hydrochemistry Site Description version 1.0, together with the corresponding site descriptions from the Geology and Hydrogeology disciplines, will serve as background reports prior to being finally integrated into the SFR Site Descriptive Model version (SDM) 1.0. The purpose of the final SFR SDM will be to fulfil the needs of the repository design and safety assessment groups.

1.3   Report structure

This report presents the final hydrochemical site description version 1.0 for the SFR site. The introduction also addresses the performed investigations and the impact on sampling and sampling conditions from different sources such as grouting, drilling/drilling water, sampling techniques, hydrogeology and other forms of contamination. The geological and hydrogeological input is outlined in Chapter 2 and also included in this chapter are the fracture mineralogical data. The evolutionary effects which have influenced the SFR site area from the Holocene and beyond are presented in Chapter 3. This includes a preliminary palaeohydrogeochemical conceptual model adapted for the SFR site, based on the recent conceptual model for the Forsmark site. The model

forms the basis for the explorative analyses and especially for the identification/definition of the four different groundwater types, i.e. Local Baltic type, Littorina type, Mixed transition type and Brackish-glacial type. Chapter 4 focuses on the hydrogeochemical data, i.e. data availability, the databases and the quality assured and categorised data. Chapter 5 addresses the explorative analysis and modelling of the data, mainly centred on the four main groundwater types described in Chapter 3, by means of; a) scatter plots illustrating depth trends and the evolutionary relationships between major ion-ion/isotopes using cross plots, b) groundwater composition of different bedrock features, c) changes in groundwater composition since construction of the SFR, d) mixing calculations, e) description of groundwater mineral systems, f) measured and modelled Eh values as well as redox sensitive elements, g) uranium, radium and radon contents, g) microorganisms and gases, and h) groundwater residence times. A separate section discussing very recent data from borehole KFR104 in the Central Block has been added to Chapter 5 at a late stage. The constructed conceptual hydrogeochemical SDM model is visualised and described in Chapter 6, and the uncertainties in the model are listed in Chapter 7. Finally, the main conclusions to the SFR investigation and future issues to be addressed are outlined in Chapter 8.

1.4   Nomenclature and abbreviations

Special nomenclature and abbreviations used in this report are explained in this section and relate to distinguishing the different groundwater types and the bedrock division into structural domains.

Groundwater nomenclature:

1) Water types (Local Baltic type, Littorina type, Brackish-glacial type etc, (cf. Section 3.3) that are used to distinguish between different current groundwaters as measured today. The nomenclature of these present waters is related to the perceived main origin of the waters (Baltic Seawater, Littorina Seawater, glacial meltwater etc) but their compositions have subsequently been altered by mixing and reactions.

2) Original waters (or end members, cf. Section 3.2) contributing to the groundwater mixture present in the bedrock. This essentially means the main origin of the currently defined major groundwater types, i.e. the actual Baltic Seawater, Littorina Seawater and glacial meltwater, and to a minor extent precipitation.

The site is divided into three structural domains (cf. Figure 2-3) to facilitate localisation for the reader **(**Curtis et al. 2011).

1) The Southern boundary belt is dominated by deformation zone ZFMWNW0001 (Singö zone).

2) The SFR Central Block, or just the Central Block, indicates the domain between the Southern and Northern boundary belts.

3) The Northern boundary belt is dominated by deformation zones ZFMNW0805A and B (formerly Zone 8).

Table 1-2 explains terms, symbols, subscripts and abbreviations that are frequently used in this report, and Table 1-3 presents the former names of the deformation zones as well as the presently preferred names.

Table 1-2. Explanation of terms, symbols, subscripts and abbreviations used in this report.

Symbol/abbreviation	Description
BIPS	Borehole Image Processing System.
BLA	*(Bergssal för Lågativt Avfall)* Rock gallery for low level radioactive waste.
BMA	*(Bergsal för Medelaktivt Avfall)* Rock gallery for intermediate level radioactive waste.
BRT	*(Bergssal för ReaktorTankar)* Rock gallery for reactor tanks.
BTF	*(BetongTankFörråd)* Concrete tank storage space.
CCC	Complete Chemical Characterisation.
CDT	Cañon Diablo Troilite (standard used for $\delta^{34}S$).
Central Block	Target area inbetween the Southern and Northern boundary belts.
EC	Electrical Conductivity.
Early SFR boreholes	Boreholes drilled between 1984 and 1987 from the present SFR tunnel system (cf. Figure 4-2).
Formation groundwater	Groundwater originating directly from fracture systems in the bedrock.
Forsmark site investigation	Site investigation in Forsmark (2002–2007).
HTHB	Hydraulic test equipment for percussion boreholes.
ICV	Input 'Compositional Variables' in M3 mixing calculations.
Idcode	Name of sampling locations or other investigated objects in the Sicada database.
M3	Computer software for mixing calculations.
M.a.s.l.	Metres above sea level. Coordinate system RT 90- RHB 70.
Mbl	Metre borehole length (length measured from top of casing, the zero point, along the borehole).
Northern boundary belt	Boundary composed by zones ZFMNW0805A and ZFMNW0805B (zones 8a and 8b).
PFL logging	Flow logging using Posiva Flow Log equipment.
PFL-f	Descrete inflow detected by the Posiva flow logging method .
PLU	Site investigation projects carried out in Forsmark and Oskarshamn (2002–2007) to select locations for the planned repository for radioactive waste. The PLU data notation in x/y scatter plots is restricted to data from the Forsmark site.
RHB 70	An improvement of the elevation reference system RH 70.
SBA1, SBA2 etc	Shallow Bedrock Aquifers (cf. Section 2.2.3).
Secup, Secmid, Seclow	Upper, midpoint and lower borehole section limit (mbl).
Silo	Silo shaped storage facility.
Southern boundary belt	Boundary mainly consisting of ZFMWNW0001 (the Singö zone).

Table 1-3. Clarification between zone nomenclature used in the SFR investigations and the one based on the Forsmark site investigation.

SFR terminology	Forsmark site investigation terminology
Singö zone	ZFMWNW0001
Zone H2	ZFM871
Zone 3	ZFMNNE0869
Zone 6	ZFMNNW1209
Zone 8	ZFMNW0805A
Zone 9a	ZFMNE0870A
Zone 9b	ZFMNE0870B

1.5 Investigations and investigation prerequisites

1.5.1 Drilling and borehole investigations

The investigation programme within the SFR extension project was performed between 2007 and 2009 with some complementary studies conducted during Oct. 2010 and as late as June 2011. Although the approach shows close similarities to the Forsmark site investigations, the area is much smaller, the rock volume studied is mostly shallow (generally down to ~ 250 m.a.s.l., single locations at –300 and –400 m.a.s.l.) and almost completely covered by the Baltic Sea, and the location is close to an existing repository facility, the construction of which has had a marked impact on the groundwater chemistry, and to some extent continues to do so. Together, these conditions present a special set of circumstances which have not been addressed before within the SKB site investigation programmes.

Besides the present investigations carried out in the target area southeast of the SFR facility, earlier boreholes remaining in the present tunnel system from the construction phase of the repository were also available for additional investigations. The latter are equipped with packer installations (to seal off borehole sections) of varying age and condition. Erroneous or imprecise section lengths, leakages between sections, as well as contamination from different metals in the equipment, are therefore complications that cannot be completely excluded, cf. Nilsson A-C (2009). New equipment was installed in twelve of the boreholes (KFR01, KFR02, KFR03, KFR04, KFR05, KFR7A, KFR7B, KFR08, KFR13, KFR19, KFR55 and KFR56) during 2008 and at the same time borehole lengths and section lengths were checked.

The geoscientific investigations entailed the drilling of four percussion boreholes and seven cored boreholes. All the cored boreholes are of the conventional type apart from one telescopic type borehole similar to those frequently used during the Forsmark site investigations (Laaksoharju et al. 2008). Furthermore, all percussion boreholes and six of the cored boreholes are drilled from the surface (from the pier and from the little islet close to the pier) and one cored borehole is drilled from the construction tunnel in the present SFR facility (cf. Figure 1-3). Time saving considerations and the exposed location for rough climate conditions on the pier were the conclusive arguments for the choice of conventional boreholes. For the same time saving reasons, groundwater sampling in preinstalled fixed borehole sections was preferred over the more advanced downhole equipment previously used during the site investigations at Forsmark (Laaksoharju et al. 2008) and capable of sampling and measuring variable section depths and section lengths.

However, the use of these simpler conventional type cored boreholes implies some limitations and consequences for the overall geoscientific investigation programme and in particular for the hydrogeochemical investigations. First, air lift pumping using nitrogen gas cannot be conducted during drilling and therefore the amounts of drilling water, as well as drilling debris remaining in the boreholes after drilling, will be greater than in telescopic type boreholes. Consequently, the telescopic borehole and one conventional borehole drilled from the tunnel were selected for the most important and extensive hydrogeochemical investigations. In the tunnel borehole there is little risk of contamination from drilling, drilling water or other borehole activities since the groundwater flow is directed towards the tunnel, effectively flushing out unwanted contaminants. Secondly, the maximum number of borehole sections for pressure measurements possible to install in conventional surface boreholes is restricted to three because there is limited space for stand pipes in the narrow upper borehole diameter. For the same reason circulation sections, which are the most suitable ones for groundwater sampling, cannot be installed and therefore air lift pumping using nitrogen gas is the only possible technique to pump the groundwater to the ground surface. Possible impacts on the quality of the groundwater samples are described in Section 1.5.2. The boreholes, drilling techniques, locations, and the number of sampled borehole sections are summarised in Table 1-4.

The basic investigation programme following completion of a new borehole included:

1. BIPS logging (Borehole Image Processing System).

2. Geophysical logging.

3. Differential flow logging using the Posiva flow log.

4. Packer installation to isolate borehole sections based on information from BIPS and flow logging; start of regular pressure monitoring.

5. Groundwater sampling was performed in selected borehole sections in some of the boreholes. Generally, groundwater sampling was performed within two to three months after completion of the borehole.

Table 1-4. Summary of borehole information.

Borehole idcode	Drilling technique	From tunnel (T) or surface (S)	Groundwater sampling and no. of sampled borehole sections[1]
HFR101	Percussion	S	Yes[2], entire borehole
HFR102	Percussion	S	Insufficient water yield
HFR103	Not drilled	–	–
HFR104	Not drilled	–	–
HFR105	Percussion	S	Yes[2], entire borehole
HFR106	Percussion	S	Yes[2], 2 sections
KFR101	Cored conven*	S	Yes[3], 1 section (bottom)
KFR102A	Cored telescopic	S	Yes[4], 2 sections
KFR102B	Cored conven*	S	No
KFR103	Cored conven*	S	No
KFR104	Cored conven*	S	Yes[3], 1 section (bottom), late sampling in June 2011
KFR105	Cored conven*	T	Yes[5], 5 sections (along the entire borehole)
KFR106	Cored conven*	S	Yes[3], 2 long sections

* Conventionally drilled core boreholes, in contrast to telescopic boreholes.

[1] The section lengths and elevations are displayed in Table 4-1.

[2] Sampling using HTHB equipment (Hydraulic test equipment for percussion boreholes).

[3] Sampling by air-lift pumping (nitrogen gas) in the installed fixed section for pressure monitoring.

[4] Sampling by pumping in wide standpipe connected to circulation section.

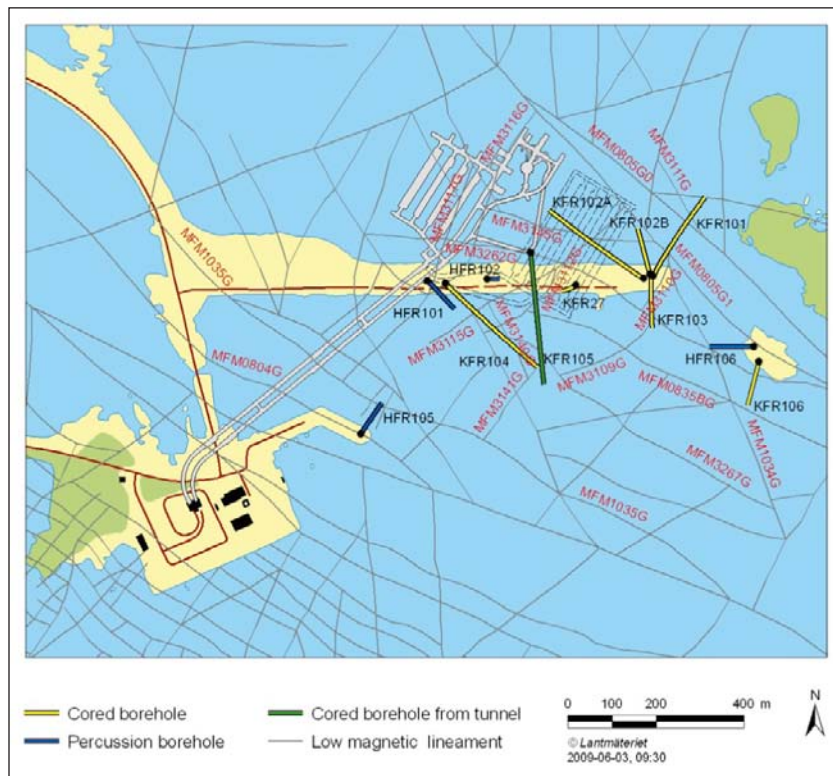[5] No pumping is necessary; over pressure.

Figure 1-3. Locations of recent boreholes drilled within the SFR extension project.

1.5.2 Impacts on sampling and sampling conditions

Groundwater sampling in boreholes drilled from the SFR repository, or in the vicinity of the repository, is by necessity impacted by changed hydraulic conditions due to the presence of the repository as well as by anthropogenic activities carried out within or close to the tunnel system. In contrast to the site investigations at Forsmark, the SFR extension modelling (SDM SFR) should describe an artificially imposed dynamic flow system and most of the hydraulic impacts from the SFR are included in this description. In order to interpret the hydrogeochemical data correctly it is necessary to understand the hydraulic conditions and consider possible causes of sample contamination, for example from grouting or, however unlikely, ultimately from the stored low and intermediate radioactive waste.

The possible impacts on groundwater sampling that may result in reduced sample representativity or quality are identified and described below. However, it should be remembered that impacts on the quality of the groundwater data (and also the quality of the chemical analyses) may to some extent be excluded or verified by other samples from the same borehole sections. Most of the early SFR borehole section samples represent a sample series, i.e. single samples have been collected at several occasions over a time period of more than twenty years, and generally show either a quite stable water composition or a clear trend due to changes in hydraulic conditions from the impact of the SFR repository. Besides long sample series, time series data also exist, i.e. regular and frequent samples collected during a period of days or weeks during continuous discharge from the borehole section being sampled. Time series were collected as normal routine practice from the recent SFR extension project boreholes and a limited number have also been collected from the early SFR boreholes on several occasions. Consistent results from sample series and sample time series increases confidence in the data, and even if samples with a questionable groundwater composition, or if outliers in the datasets do occur, they are generally possible to identify and disregard.

Impacts from grouting

When analysing and interpreting the hydrogeochemical data from the early boreholes in the SFR facility, possible impacts on the water composition from grouting were considered also. Generally, contamination due to injection of cement increases the pH, the calcium concentration and probably also different trace metal concentrations. Furthermore, the ^{14}C signature may be diluted/lowered due to addition of inorganic carbon. The largest grouting efforts were made in the excavated passage through the Singö zone and zone ZFMNNE0869 (formerly Zone 3) and in the deepest tunnel sections penetrating the gently dipping deformation zone ZFM871 (formerly Zone H2) (cf. Öhman et al. 2011). The only borehole from the access tunnel in the vicinity of the grouted passage through Singö is KFR01; no sampled boreholes are located close to the passage through zone ZFMNNE0869 or associated with the grouted part in the lower, deep tunnel section penetrating zone ZFM871. Boreholes KFR7A, B and C which provide important data in this deep region are located at some distance from the grouted areas and the risk of any impact is small. However, since large volumes of groundwaters from different excavated locations may have been pumped and discharged on several occasions during the last twenty years or so, it is difficult to completely rule out that different types of contamination and mixing situations may have occurred also at some distance away. For example, four samples from borehole KFR83 collected in 1987 showed high pH values and an unusual groundwater composition and were classified as unsuitable for modelling (Dataset II) due to possible contamination from cement, despite that this borehole is far from any known grouting location. The effects on the ^{14}C signature are, however, more difficult to verify; samples collected in autumn 2010 from five sections in borehole KFR02, located in zone ZFM NE0870 (formerly Zone 9) and penetrating zone ZFM871, all show quite low pmC values and all are within the same order of magnitude. This is in contrast to what is expected since the groundwater type is changing towards younger water in the intercept with zone ZFM871. It is possible that this is an effect of grouting/injection of cement.

Impacts from drilling and drilling water

Drilling of percussion boreholes, conventional boreholes and telescopic boreholes imply first of all mixing of different groundwaters due to the high pressures used, and in the case of core drilling the introduction of large quantities of drilling water to cool the drill bit. Secondly, impacts related

to open borehole conditions following drilling when flow gradients can become established in the borehole resulting, for example, in possible short circuiting and mixing of natural groundwater flow conditions as described below. Furthermore, contamination from drilling debris and from metals due to wear and tear of the drilling equipment may occur.

If the pumped volume from the borehole section prior to groundwater sampling is insufficient, the drilling water content in the samples may remain unacceptably high. During drilling of the recent boreholes, uranine dye was added to the drilling water as a tracer (0.2 mg/L) to allow calculation of the drilling water content. Tap water was used as drilling water for boreholes KFR101 and KFR102A in order to avoid any change in the groundwater marine signature that might impact on the evaluation of groundwater origin. Borehole KFR106 was not initially planned for hydrogeochemical investigations and was unfortunately drilled using seawater. Borehole KFR105 was drilled from the construction tunnel in the SFR repository where the water flow is directed towards the tunnel and therefore there was little risk of contamination from drilling, drilling water or other borehole activities. Remaining drilling water was not expected to be a problem and the lower drainage basin in the SFR repository was accepted as a source of drilling water. The drilling water budget calculations for KFR105 verified that all the drilling water was recovered (Nilsson G 2009, Lindquist and Nilsson 2010). The same pressure conditions are of course valid also for the early SFR boreholes drilled from the tunnel system. Furthermore, it is more than 20 years since they were drilled and possible traces of drilling water should have disappeared a long time ago.

Hydrogeological impacts

The presence of the tunnel system has an impact on the hydrogeological conditions in terms of changed flow paths and groundwater drawdown effects. These effects are observed from long term hydrochemical trends as very slow but systematic changes in the groundwater composition, i.e. dilution with modern marine water from the Baltic Sea or increased mixing of groundwaters of different origin. However, this has not disqualified any samples since at the present time they are representative for the groundwater development close to the repository. The slow dilution is mainly observed in boreholes intersecting major vertical to subvertical deformation zones.

Pressure gradients (most probably an impact from the adjacent SFR tunnel system) between borehole sections may cause an initial downward transport of large volumes of shallow water into the borehole before installation of fixed packers to isolate the borehole sections. This will affect subsequent sampling and sample quality. Two examples of boreholes recording pressure gradients are borehole HFR106 and especially KFM11A where samples are generally excluded from the approved dataset for modelling due to interpretation problems.

During sampling, fracture networks intersecting the boreholes may lead to short circuiting of the groundwater flow in the surrounding bedrock and also to bypassing the packer system used to isolate the borehole section being sampled. This means that the section sampled may have been supplied by mixed groundwaters from higher or lower levels in the bedrock, and/or mixed borehole waters above or below the packers. In both cases the sampled groundwaters when interpreted in isolation may be evaluated erroneously as being of suitable quality.

Different sampling conditions/techniques

The groundwater data used for the SDM SFR originate from groundwaters sampled under different conditions, for example different discharged volumes prior to sampling and different section lengths and pumping techniques.

Insufficient exchange of water from the borehole section prior to sampling may result in samples consisting partly of section water and partly of formation groundwater. In addition, the water initially present in the borehole section may differ considerably in composition from that of the desired formation groundwater in the bedrock. It may represent a water mixture from the entire borehole or a different part(s) of the borehole. Furthermore, processes, for example microbial production of sulphide, may be more pronounced in the borehole section compared to the surrounding water conducting fracture system in the bedrock. Plug flow calculations have been used to estimate the percentage of section water in samples from the SFR extension project, cf. Nilsson et al. (2010b).

The percussion boreholes (HFR101, HFR105, HFM34 and HFM35) were sampled along the entire borehole during hydraulic tests using the HTHB equipment. The exception is borehole HFM106 where two packed off borehole sections (36–41 mbl and 175–190.4 mbl) were sampled using the HTHB equipment (HydroTestutrustning för HammarBorrhål) (Jönsson et al. 2008, Thur et al. 2009). Samples collected from a certain length of a borehole will comprise an average groundwater composition representing contributions from all the water yielding flow anomalies in the isolated borehole section and their different hydraulic transmissivities. Sampling from entire boreholes or long borehole sections will therefore reduce the possibility to resolve the differences in water composition along the borehole. Furthermore, if the volume pumped out of the borehole section before sampling is insufficient to include all the anomalies in the pumped water (and this risk increases with increasing length of the sampled section, see above), the samples will also contain significant contributions of waters that have remained in the borehole for some time.

Air lift pumping was used for sampling in boreholes KFR101 and KFR106 (later also in KFR104, cf. Appendix 2) as these boreholes do not have installed circulation sections with wide stand pipes that otherwise allows the lowering of a pump for groundwater sampling (Thur and Nilsson 2009a, Sandström et al. 2011). In borehole sections routinely used for pressure measurements, the only possible sampling method is by air lift pumping using nitrogen gas to lift the water volume in the borehole section to the ground surface. It is possible that this pumping method affects the sample quality differently compared to conventional pumping, and therefore the following effects might be expected: 1) Depending on the borehole section geometry and volume it may be difficult to obtain sufficient exchange of initial section water due to both low pumping efficiency and gas consumption. 2) The groundwater in the section will probably experience a vigorous turbulence effect compared with the slow mechanical groundwater extraction normally encountered when pumping in the stand pipe. This may affect parameters such as sulphide (i.e. through changed microbe activity, addition of precipitation to the waters etc), trace metals and TOC/DOC. 3) Because the groundwater reaches the surface as a series of pulses, this may affect parameters related to gas phases, for example causing loss of radon and other dissolved gases, and moreover it is more difficult to avoid air intrusion when collecting samples for sulphide analyses since the water volume from one pulse may be insufficient to fill a Winkler sample bottle.

2   Geology and hydrogeology

2.1   Geological setting

The following description of the geological setting is based mainly on the final geological site descriptive model version 1.0 (Curtis et al. 2011) and provides a short summary of the bedrock geology (Section 2.1.1) and introduces the rock domain (Section 2.1.2) and deformation zone (Section 2.1.3) submodels. The fracture mineralogy is described in Section 2.1.4. The deformation zone submodel as well as the fracture mineralogy interpretation have a direct importance for the hydrogeochemical interpretations, in contrast to the rock domain submodel, and have therefore been presented in more detail.

No GeoDFN, Fracture domain, or Regolith modelling was conducted as part of the SFR extension project. With respect to fracture domains, there were not enough data for their classification and subdivision and therefore this concept has not been used in the geological and hydrogeological characterisations, and therefore not in the hydrogeochemical interpretations. However, with reference to the regolith, the conceptual model of the distribution of Quaternary deposits that was developed within the Forsmark site investigation programme is relevant as it covers also the marine sediments above the SFR (Hedenström et al. 2008). The importance of the sediment thickness for hydraulic contact between the SFR and the Baltic Sea is discussed in the hydrogeology description (Section 2.2.1).

2.1.1   Bedrock geology

The SFR extension project has increased the detailed knowledge concerning the geology in the SFR regional model area but no new data or interpretations have been forthcoming that affect the established interpretation of the regional geological setting as described by (Söderbäck 2008) from the earlier site investigations in Forsmark (PLU).

The SFR bedrock is dominated by different types of metamorphosed granitoids with subordinate felsic to intermediate metavolcanic rocks, metamorphosed diorite or gabbro, and pegmatite or pegmatitic granite (Figure 2-1). These rocks formed between 1.89 and 1.85 billion years ago (1.89–1.85 Ga). A penetrative, ductile tectonic fabric developed between 1.87–1.85 Ga during the Svecokarelian orogeny, when temperatures exceeded 600°C and the rocks were situated at mid-crustal depths. After 1.85 Ga, the rocks started to cool below 500°C. Areas where the bedrock is banded and/or affected by a strong, ductile tectonic foliation can be separated from areas where the bedrock is folded and more lineated in character (Figure 2-2). The former are inferred to have been affected by higher ductile strain and anastomose around the more folded and lineated bedrock with lower ductile strain that is restricted to several tectonic lenses. Following these early developments, ductile-brittle and brittle deformation occurred several times during the Proterozoic, related to major tectonic activity probably during the later part of the Svecokarelian (1.80–1.70 Ga), Gothian (1.70–1.60 Ga) and Sveconorwegian (1.10–0.90 Ga) orogenies. This has resulted in the activation and subsequent reactivation of the different fracture systems.

Secondary geological processes have also affected the bedrock at several times during the Proterozoic and Phanerozoic. These have involved loading by sedimentary rocks or by ice during cold glacial periods, followed subsequently by unloading related to denudation of this younger sedimentary material and/or melting of an accumulated ice mass. These processes have occurred at several times during the long geological history of the bedrock and each loading/unloading phase has resulted in exposure of the Proterozoic crystalline bedrock accompanied by stress release effects.

The major structures comprising the SFR area are shown in the magnetic total field image in Figure 2-3. The SFR site is situated within a high strain belt that forms the northeasterly margin to the so-called Forsmark tectonic lens, and is separated from the Forsmark area by the regionally significant Singö deformation zone (ZFMWNW0001; Southern boundary belt) which dips steeply and strikes WNW-ENE. Further to the northeast the SFR site locality is bounded by the steeply dipping zone ZFMNW0805A (formerly Zone 8; Northern boundary belt). These two major deformation zones therefore dominate the Southern and Northern boundary belts respectively to the SFR site area, with the central part referred to as the Central Block.
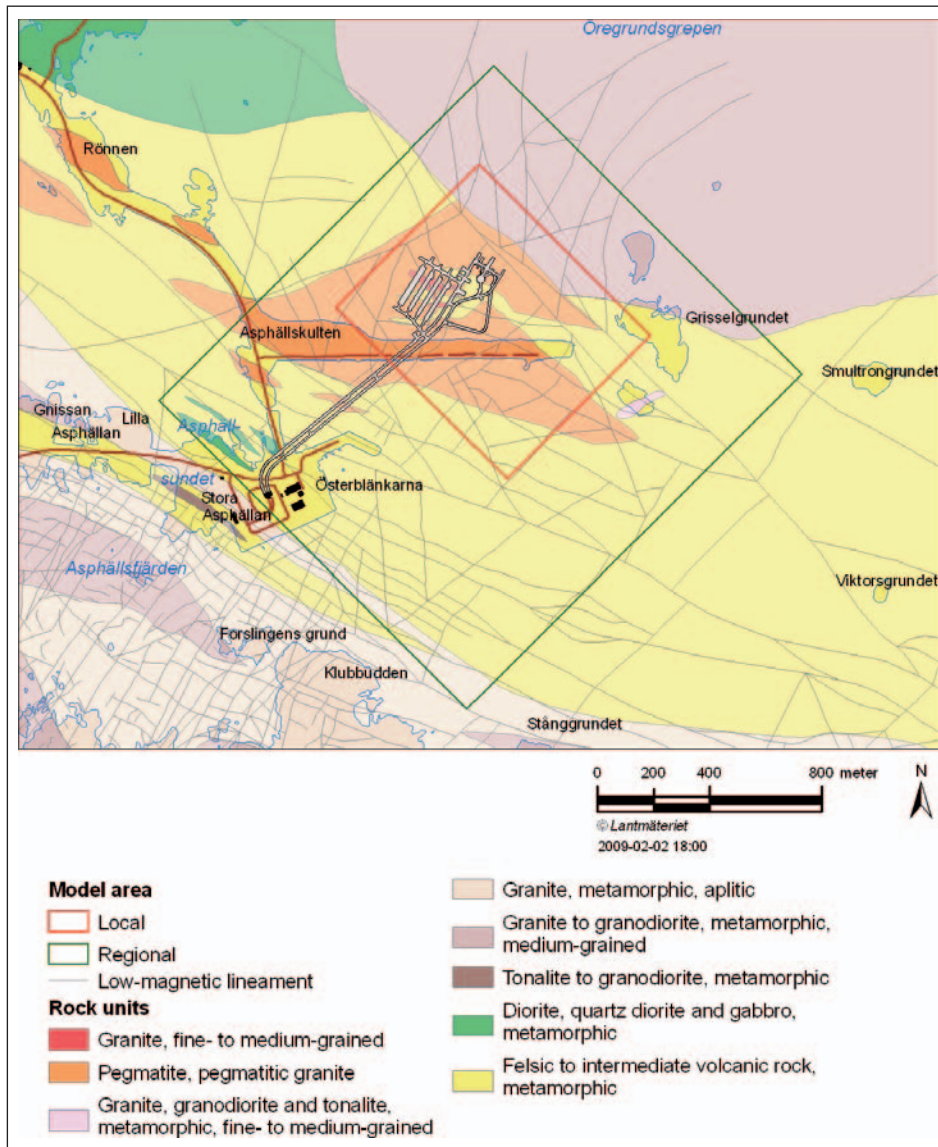
Figure 2-1. Bedrock geological map of the area around SFR produced during the Forsmark site investigation. The inferred low magnetic lineaments in the area, based on model stage 2.3 in the Forsmark site investigation, and the local and regional SFR model areas, are also shown. The paler shades for each colour on the map indicate that the corresponding rock unit is under water (Curtis et al. 2011).
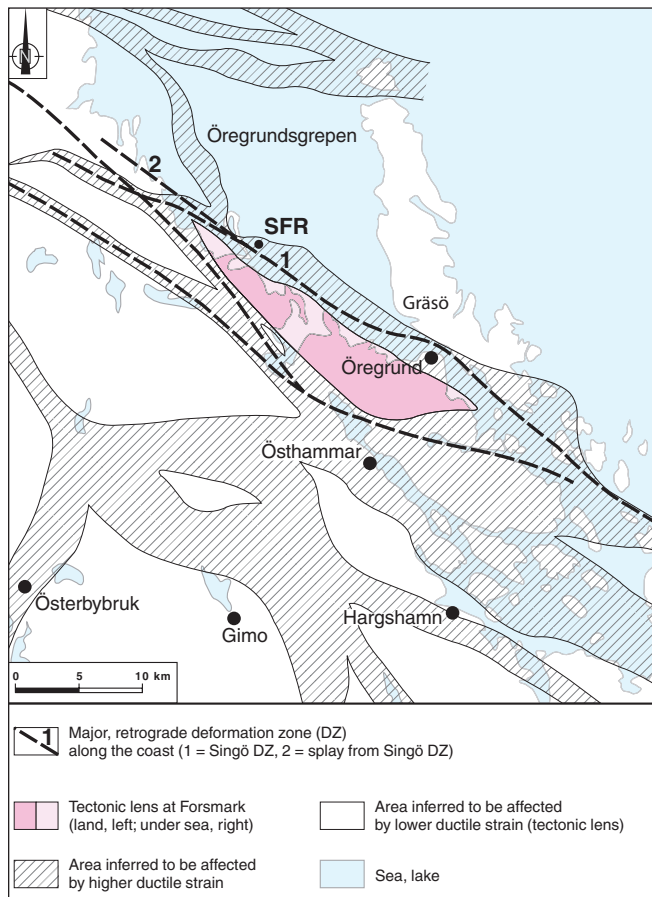
Figure 2-2. Map showing the structural framework in the Forsmark area with ductile high strain belts that anastomose around tectonic lenses of lower ductile strain. The major retrograde deformation zones surrounding the Forsmark tectonic lens are also shown (modified after Stephens et al. 2007).
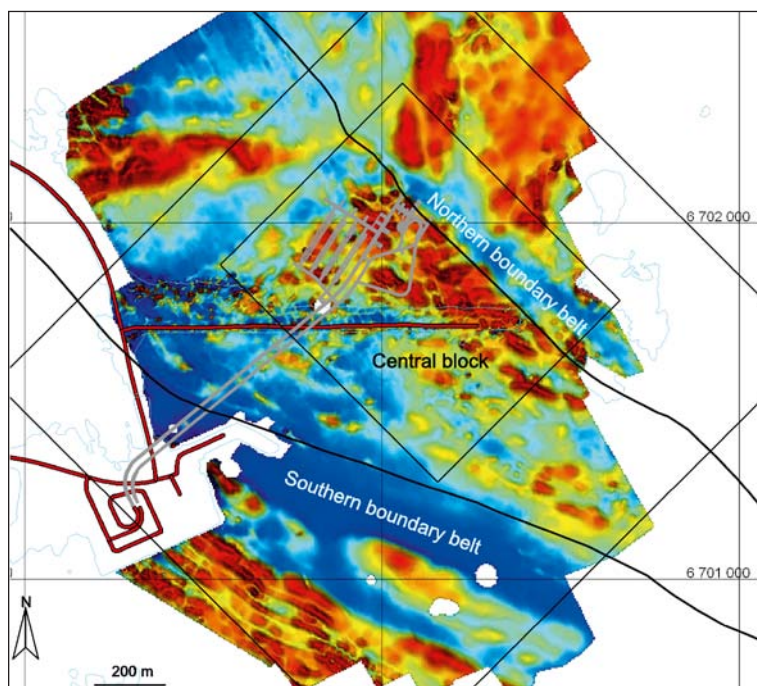
Figure 2-3. Magnetic total field demarcating the SFR Central Block containing the existing SFR storage facility, the Northern boundary belt (dominated by deformation zone ZFMNW0805A) and the Southern boundary belt (dominated by deformation zone ZFMWNW0001) (Curtis et al. 2011).

2.1.2 Local rock domains

Individual rock domains have been defined on the basis of an integration of the composition, grain size, heterogeneity and character of ductile deformation in various rock units, as employed in the Forsmark site investigation (Stephens et al. 2007). A single model consisting of four rock domains has been established for the local SFR model volume; no regional model was developed. It should be noted that the degree of fracturing has not been considered during the division into rock domains. The four rock domains are arranged in a fashion with a central domain (RFR02) surrounded by three marginal domains (RFR01, RFR03 and RFR04). The conceptual thinking that involves major folding in the SFR area is the basis for the modelling of domains RFR01 and RFR03, and these two folded marginal domains are recognised by their low intensity in the magnetic total field. Information from boreholes and the SFR tunnel system is restricted to rock domains RFR01 and RFR02; no data are available for rock domains RFR03 and RFR04 (Curtis et al. 2011). The three dimensional distribution of the rock domains is presented in Figure 2-4 and their major properties are given in Table 2-1.

2.1.3 Deformation zones

The conceptual geological understanding and the definition of deformation zones from the Site Investigations in Forsmark (Stephens et al. 2007) were adopted also in the SFR extension project. This current SKB definition of a deformation zone differs from that applied in the previous structural models of the SFR locality. The prime criterion to define a zone core is a highly increased fracture frequency (including sealed as well as open fractures) relative to the damage zone. This implies that a defined zone or large parts of a zone may have insignificant hydraulic transmissivity in contrast to previous SFR structural models which focussed on water conducting structures. In the final geological model version 1.0 separate local and regional deformation zone models were produced; both the modelled regional and local deformation zones are displayed in Figure 2-5 (Curtis et al. 2011).

Table 2-1. Rock domain description.

Rock domain	Structural description	Dominating rock types	Subordinate rock types	Homogeneous or heterogeneous
RFR01	Major fold structure; the boundary is defined by the inferred folded axes based on stretching lineation data.	Mainly pegmatitic granite and pegmatite; also fine to finely medium-grained metagrandiorite.	Subordinate rock types (~10%).	Relatively high degree of homogeneity compared to RFR02.
RFR02	–	Fine to finely medium-grained metagrandiorite, or felsic to intermediate metavolcanic rock.	Pegmatitic granite and pegmatitic younger granite, amphibolite and aplitic metagranite.	Far more heterogeneous compared to RFR01.
RFR03	Low magnetic belt forms the surface expression of RFR03; the unclear boundary between RFR02 and RFR03 was modelled to define a major fold structure.	Pegmatitic granite and pegmatite.	–	–
RFR04	The boundary between RFR02 and RFR04 is based on the magnetic total field and follows the contact between RFM021 and RFM033 in the regional rock domain model for Forsmark.	Lack data.	Lack data.	Lack data.
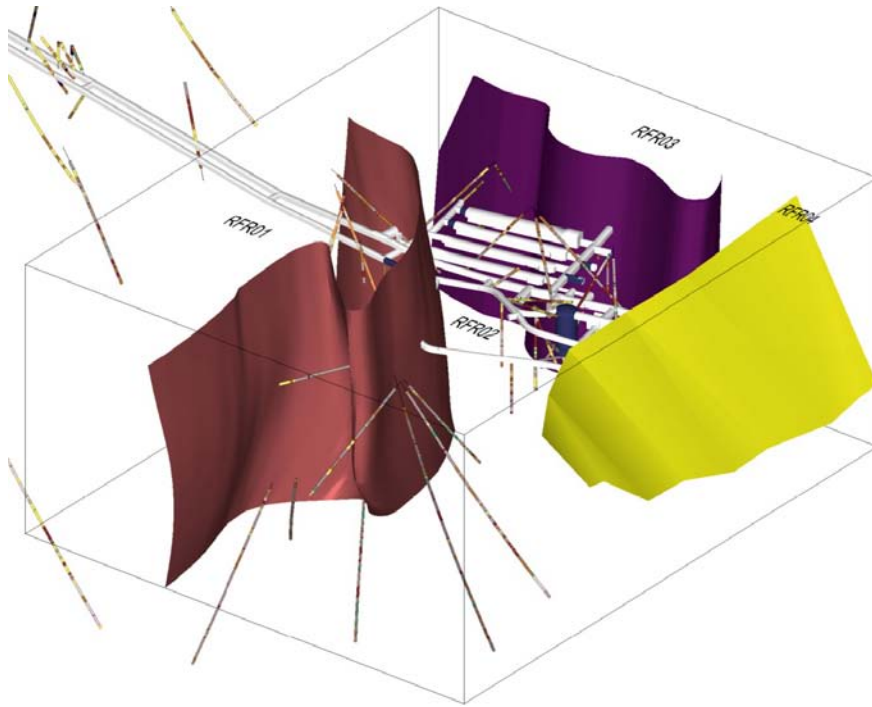
Figure 2-4. *Three dimensional model view from the east showing the four rock domains within the local SFR model volume relative to the boreholes and the SFR facility. The boundary between rock domains RFR01–RFR02 is pinkish brown, RFR02–RFR03 violet and RFR03–RFR04 yellow (Curtis et al. 2011).*
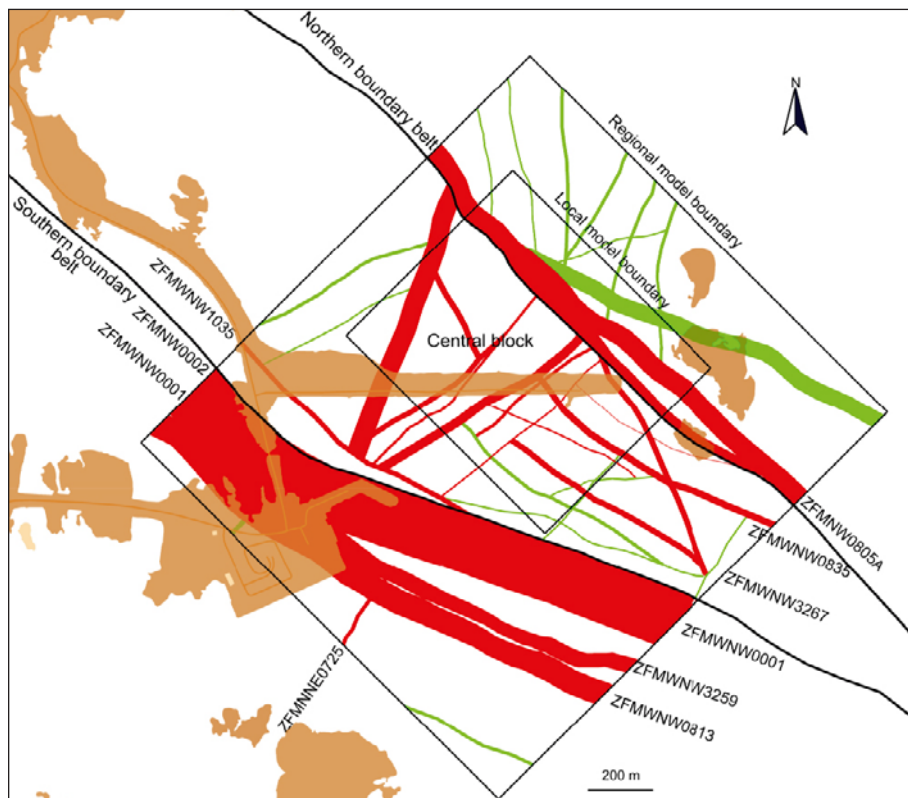
Figure 2-5. *Intersection at the current ground surface of deformation zone traces of all sizes inside the regional model area, i.e. a combined model version. The regional deformation zones ZFMWNW0001 and ZFMNW0805A, along with their major splays, demarcate the Southern and Northern boundaries of the central SFR tectonic block. Confidence in existence; high = red, medium = green (Curtis et al. 2011).*

The modelled zones in the regional and the local model include zones that are inferred to have a traceable length of at least 300 m and 1,000 m at the ground surface, respectively. The subdivision into four orientation sets of deformation zones (Stephens et al. 2007) has been maintained also in the present SFR study. The sets of modelled deformation zones at the SFR (cf. Figures 2-6 to 2-9) are; 1) the vertical to steeply dipping NNE to ENE set, 2) the vertical to steeply dipping WNW to NW set, 3) the vertical to steeply dipping NNE to ENE set, and 4) the gently dipping zones.

Of the Central Block deformation zones, the vertical to steeply dipping NNE to ENE set are generally shorter than the WNW to NW set (cf. Figure 2-7) and they are generally narrow (around 5–15 m) except for ZFMNNE869 (formerly Zone 3, 60 m) and ZFMENE3115 (28 m). These zones formed in the brittle regime and are dominated by sealed fractures. Quartz dissolution (vuggy granite) is present in zones ZFMENE3115, ZFMNE3118 and ZFMNNE0725.
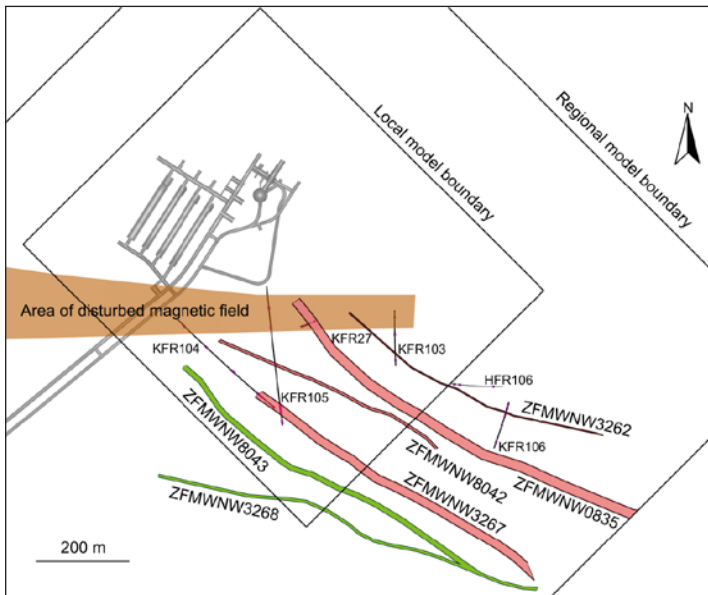
Figure 2-6. *Modelled deformation zones of the WNW to NW group lying within the Central Block (all zone dips are greater than 85°). The different colours refer to confidence in existence; high = red, medium = green (Curtis et al. 2011).*
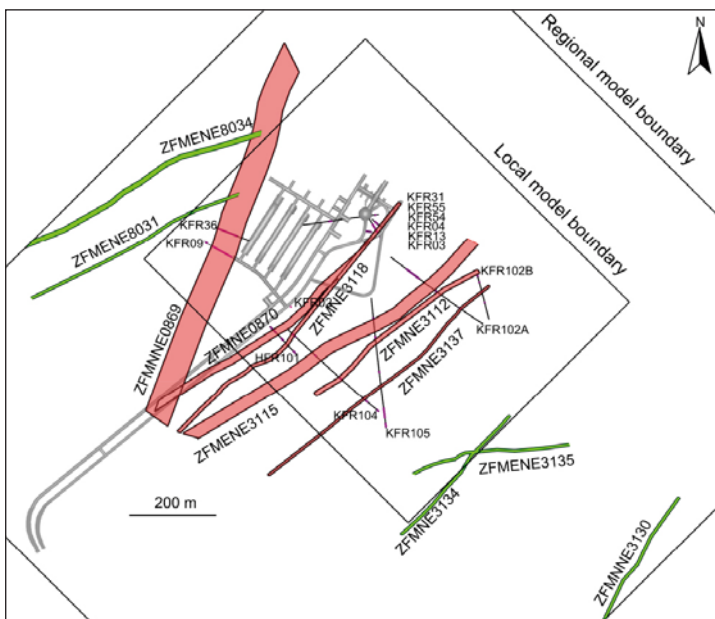
Figure 2-7. *NNE to ENE deformation zones penetrating the Central Block between ZFMWNW0001 and ZFMNW0805A. The different colours refer to confidence in existence; high = red, medium = green (Curtis et al. 2011).*

Of the five zones in the N-S to NNW group, ZFMNNW0999, ZFMNNW1034, ZFMNNW1209 (formerly Zone 6), ZFMNNW3113 and ZFMNS3154, only ZFMNNW1209 and ZFMNNW1034 lie within the Central Block and have been identified with high confidence based on tunnel and borehole data (cf. Figure 2-8); they have similar modelled thicknesses of 17 m and 18 m. The other three zones are located to the north of zone ZFMNW0805A (formerly Zone 8a). In general, these zones are dominated by sealed fractures and, based on their low frequency of occurrence, are judged to be less significant relative to other orientations.

Three gently dipping zones are included in the model (cf. Figure 2-9); ZFMA1 of medium confidence on the southern side of ZFMWNW0001 (the Singö zone), ZFMB10 of low confidence at depth beneath the local model volume, and ZFM871 (formerly Zone H2) of high confidence within the local model volume. None of the zones are interpreted to intercept the ground surface. Zone ZFM871 is interpreted to be of importance as a horizontal transport pathway for groundwater; however, the geological evidence of its extension west of zone ZFMNNW1209 is very weak. Only one borehole (KFR02) penetrates the modelled zone to the west side while several boreholes exist on the east side.
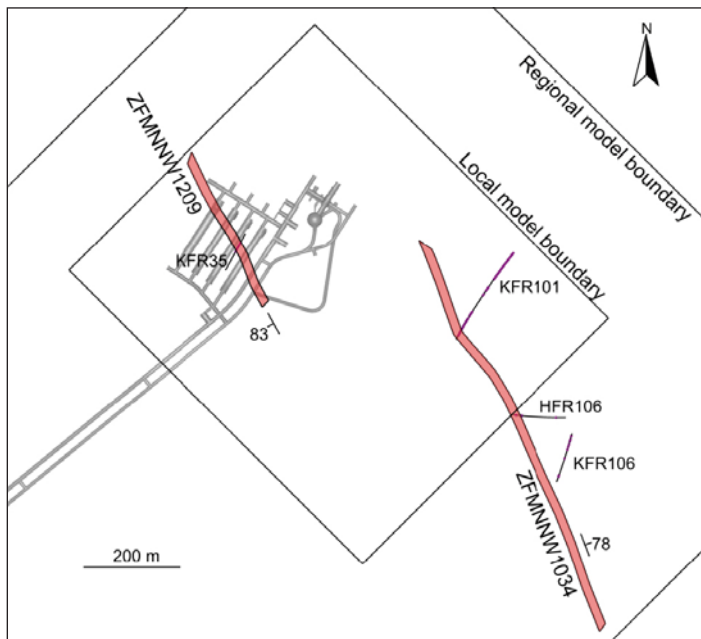
Figure 2-8. N-S to NNW deformation zones penetrating the Central Block between ZFMWNW0001 and ZFMNW0805A (Curtis et al. 2011).
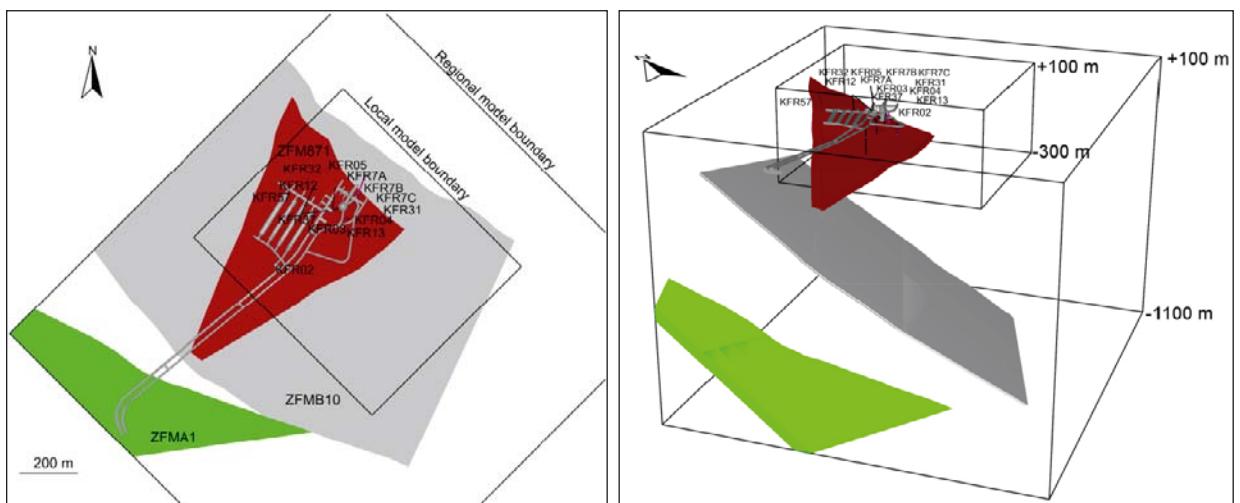
Figure 2-9. Gently dipping zones penetrating the SFR regional model volume. Deformation zone ZFM871 (red, high confidence), zone ZFMA1 (green, medium confidence) and zone ZFMB10 (grey, low confidence) (Curtis et al. 2011).

2.1.4 Fracture mineralogy

Detailed studies of fracture mineralogy and wall rock alteration were carried out during the site investigations for a deep repository of spent nuclear fuel in Forsmark (PLU) between 2002 and 2007 (Sandström and Tullborg 2009, Sandström et al. 2006, 2008, 2009, 2010). However, within the SFR extension investigation programme detailed fracture mineralogical has only been carried out on a limited set of samples which corresponds to the borehole sections sampled for groundwater chemistry and Eh (Sandström and Tullborg 2011).

Table 2-2. SFR borehole sections included in the detailed fracture mineralogy study.

Borehole (Idcode)	Secup (m)	Secup (m)	Elevation Secmid (m.a.s.l.)
KFR01	44.5	62.3	−94.23
KFR08	63.0	104.0	−80.94
KFR10	87.0	107.3	−146.99
KFR19	95.0	110.0	−56.35
KFR7A	48.0	74.7	−134.43
KFR105	120.0	134.0	−128.38
KFR105	265.0	306.8	−153.59

Generally, data from the drillcore mapping (Curtis et al. 2011) indicate that there are no major differences between the fracture mineralogy in the SFR area and in the Forsmark area (Stephens et al. 2007, Sandström et al. 2008). It is also evident that the sequence of four major events of fracture mineralisation distinguished based on, for example, cross-cutting relations, stable isotopes and $^{40}Ar/^{39}Ar$ dating during the Forsmark site investigation, is valid also for the SFR area. The sequence is summarised below:

Generation 1: Precipitation of epidote, chlorite and quartz occurred under hydrothermal conditions at temperatures between about 200° and 300°C in preferably subhorizontal to gently dipping fractures and fracture zones, but some also in steep WNW-ENE to NW-SE fractures. The wall rock was hydrothermally altered and red stained by hematite dissemination during this event. The minerals precipitated during the Proterozoic between 1.8 and 1.1 Ga and it is suggested that precipitation occurred close to 1.8–1.7 Ga as a result of fracturing and fluid circulation during the waning stages of the Svecokarelian orogeny, at conditions close to the ductile-brittle transition.

Generation 2: Hydrothermal precipitation of a sequence of fracture minerals occurred at temperatures between about 150° and 250°C. The fracture mineral generation is dominated by hematite stained adularia and laumontite, together with albite, prehnite, calcite and chlorite, and all preferentially precipitated along steep ENE-WSW to NNE-SSW and NNW-SSE fractures. $^{40}Ar/^{39}Ar$ ages of adularia and K-feldspar in breccias indicate, at the very least, the last event of precipitation of what is considered generation 2 minerals that occurred as a response to far-field effects from the Sveconorwegian orogeny around $1,107 \pm 7$ to $1,034 \pm 3$ Ma. Both reactivation of older structures and formation of new fractures and breccias are inferred during this period. The wall rock was hydrothermally altered, causing red staining by hematite dissemination. After precipitation of the generation 2 minerals a period with some dissolution of fracture minerals occurred, of which the age and cause is uncertain.

Generation 3: Fracture minerals were precipitated at temperatures between 60° and 190°C (mainly < 100°C) during several episodes in the Palaeozoic. $^{40}Ar/^{39}Ar$ ages of adularia indicate that the main stage of precipitation occurred after 460 Ma and before 277 ± 1 Ma. Generation 3 is dominated by quartz, calcite and pyrite with minor occurrences of, for example, asphaltite, analcime, corrensite, galena, adularia and fluorite. Downward penetration of fluids emanating from an organic-rich sedimentary sequence overlying the basement during this period, and mixing with a deep basinal brine, is suggested to have promoted the precipitation of generation 3 minerals. The orientation of fractures lined with these minerals indicates significant reactivation of older fractures during the Palaeozoic, preferably steep ENE-WSW to NNE-SSW and subhorizontal to gently-dipping fractures. However, formation of new fractures during this period is also inferred. Far-field effects from the Caledonian orogeny and/or elevated hydrostatic pressure due to the overburden of the Caledonian foreland basin is suggested to have caused reactivation and formation of fractures and associated migration of fluids.
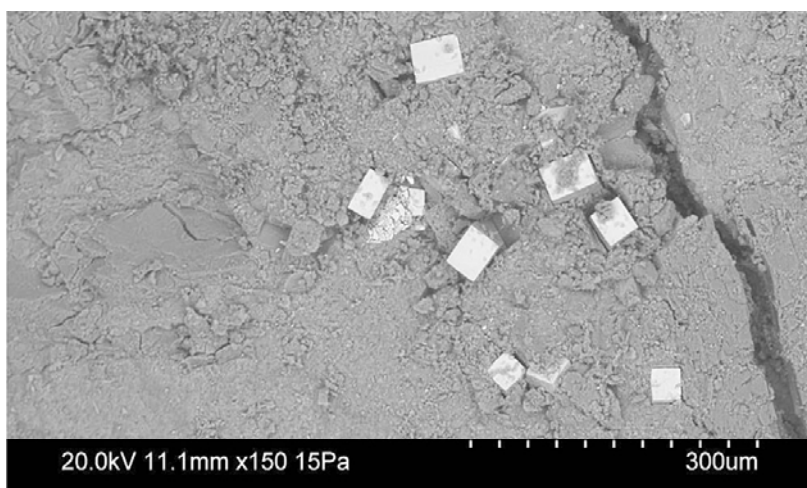
Figure 2-10. Electron image of euhedral pyrite crystals (bright) on a fracture surface coated with illite and quartz (Generation 3) KFR105:283.38 m (Sandström and Tullborg 2011).

Generation 4: Predominantly clay minerals and thin precipitates of calcite in hydraulically conductive fractures, and zones and in open fractures in the upper part of the bedrock, were formed at this stage; minor occurrences of pyrite and goethite are also found. Precipitation has probably occurred at low temperatures (< 50°C) during a prolonged period, possibly since the late Palaeozoic until present by groundwater circulation. Generation 4 minerals are mostly found in subhorizontal to gently dipping fractures, but also in steep NNE, ENE and NW trending fractures indicating that most of these fracture minerals have precipitated in older Proterozoic to Palaeozoic fractures. Some formation of subhorizontal to gently dipping fractures is also likely in the upper part of the bedrock due to stress release during loading and unloading cycles related to sedimentation episodes during the late Palaeozoic to Mesozoic, and to glaciations during the Quaternary.

No major differences are evident between the fracture mineralogy of the sampled SFR drillcores and samples investigated during the Forsmark site investigation (Sandström and Tullborg 2011). However, minor differences, some of which may be of significant importance for the understanding of past and present groundwater-mineral interaction, have been identified:

- The relative abundance of different clay minerals; in the SFR a mixed layer clay consisting of smectite-illite dominates together with illite in the water conductive fractures. Within the Forsmark site investigation area, corrensite, a mixed layer clay consisting of smectite-chlorite, was totally dominating. However, only a few occurrences of corrensite were recorded above −100 m.a.s.l. during the Forsmark site investigations (Sandström et al. 2008), in agreement with the results from the SFR. There are also indications that the amounts of clay minerals are greater in the SFR drillcores compared with Forsmark.

- REE-carbonate has been identified in many of the SFR drillcore samples; no REE-carbonates were identified within the Forsmark site investigations.

- Barite is more common in the SFR drillcores; a few occurrences of a Sr-rich barite have also been identified (solid solution barite-celestine series).

- Uranium minerals have been detected in 20% of the analysed samples (total number of studied samples 29) from the SFR drillcores. At the Forsmark site investigation, only one uranium mineral was identified in more than 200 sampled fractures.

These observations indicate that fluids rich in REEs, barium and uranium have circulated in the area at some period. Based on the association with generation 3 minerals, it is inferred that the main phase of precipitation of minerals from these fluids occurred during the Palaeozoic. The precipitation of uranium minerals is believed to represent remobilisation of uranium already present in the fracture system. The absence of these minerals within the Forsmark area suggests a more open system outside the tectonic lens with fluid migration along major deformation zones. This is in agreement with the conceptual geological understanding of the area where the tectonic lens is considered to represent a hydraulically tighter and isolated part of the bedrock compared to its surroundings

(Stephens et al. 2007, Laaksoharju et al. 2008, Sandström et al. 2009, Curtis et al. 2011). Barite, as the latest precipitated mineral on fracture surfaces, generally occurs as small crystals and may be of recent origin. This is supported by the observation that most of the SFR groundwaters are in equilibrium with respect to barite (Gimeno et al. 2011).

Fracture mineralogical studies can never provide a satisfactory statistical overview due to time and cost constraints. For a statistical analysis of fracture minerals, quantitative data obtained from the drillcore mapping needs to be extracted from SKB's database Sicada and processed. Furthermore, when using these data (Boremap data) it is necessary to keep in mind that it is gathered via macroscopical inspections and therefore minor phases may have been overlooked, whereas others may be overrepresented (e.g. due to pigmentation etc). Moreover, some minerals are difficult to separate from each other without XRD analysis. Examples of possible bias are:

a) The Fe-oxides and Fe-oxyhydroxides. The separation between hematite, goethite and less crystalline Fe(OOH) can be problematic without detailed analyses.

b) Chlorite and clay minerals are often present together and may be difficult to distinguish during the mapping.

c) Clay minerals are almost impossible to identify during the drillcore mapping. It is also probable that clay minerals are partly lost during drilling operations and therefore the frequency of clay minerals in the core mapping can be regarded as an absolute minimum.
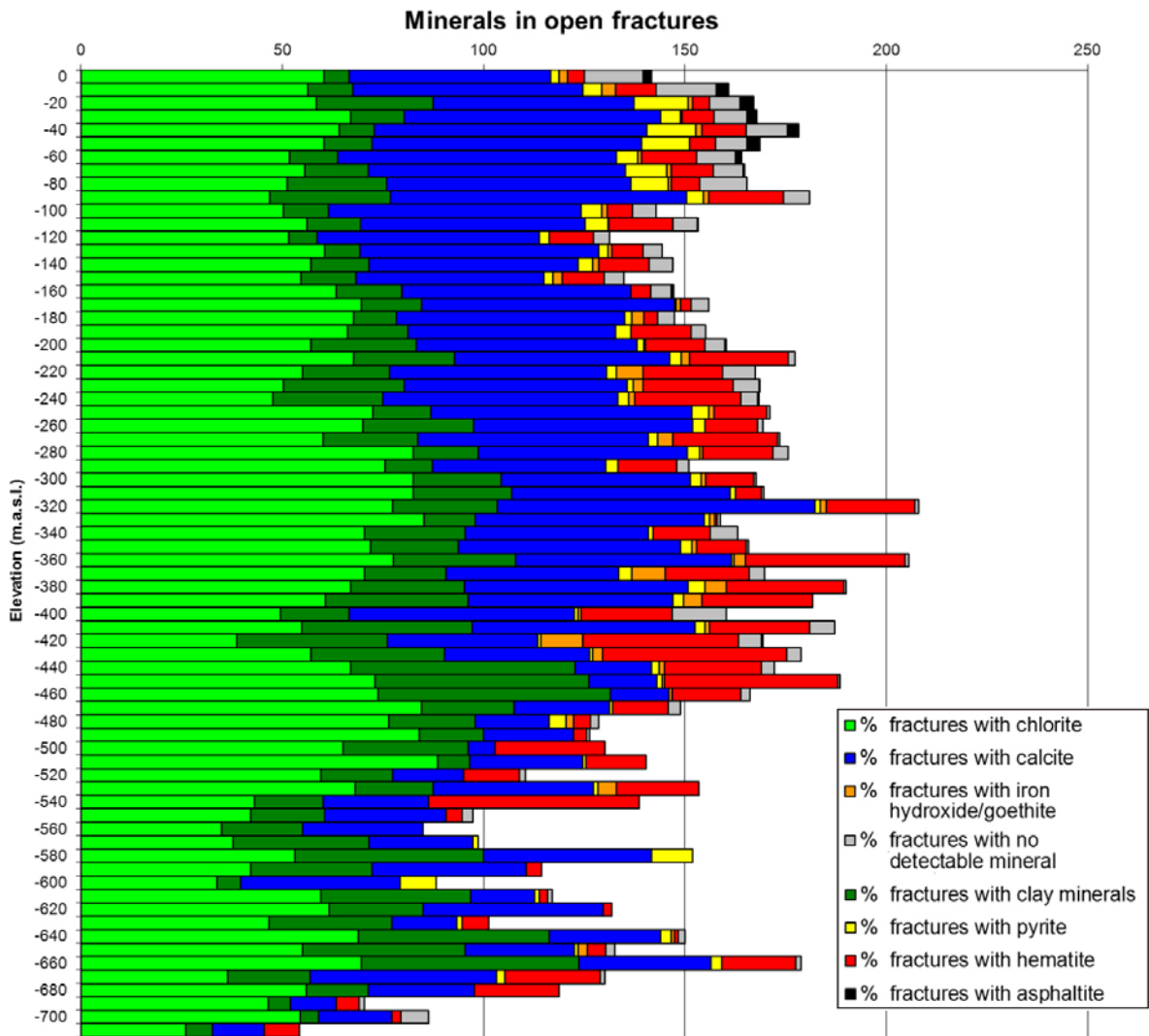
Figure 2-11. *Depth distribution of fracture minerals in all mapped open fractures from the SFR including also KFM11A from the Forsmark site investigation. Note that the distribution only considers frequency and not the amounts of a certain mineral.*

Figure 2-11 shows the frequency of calcite, chlorite, clay minerals, pyrite, hematite, Fe-oxyhydroxides and asphaltite in open fractures versus depth; also shown are the frequency of fractures where no visible fracture fillings are detected. The data represent information from the SFR drillcores and KFM11A. Fractures omitted from the SFR dataset are fractures from KFR24 down to Secup 147.50 metres where no core was available, and also fractures from the remapped drillcores where no BIPS-logging has been carried out (KFR04, KFR08, KFR09, KFR13, KFR35, KFR36, KFR54, KFR55, KFR7A, KFR7B and KFR7C) (Petersson J, personal communication). Data from below 400 m.a.s.l. relate to boreholes KFM11A, KFR27 and KFR102A.

It can be concluded that calcite and chlorite are by far the most frequent minerals, which corresponds to findings from the Forsmark drillcores (Sandström et al. 2008). Asphaltite and pyrite (both of generation 3) and fractures with no visible minerals are more common in the upper 100 metres indicating that organic material emanating in the overlying sediments during the Palaeozoic possibly reached at least 100 m or more into the bedrock. Pyrite, precipitated during the same event, has remained in the fractures indicating that no extensive oxidation has occurred. Despite the larger fracture frequency in the upper part of the bedrock (Curtis et al. 2011), the presence of unmineralised fractures suggests the possiblity that new fractures have been formed, for example as a result of deglaciation(s) (Claesson Liljedahl et al. 2011).

Figures 2-11 and 2-12 show all the open fractures whereas in Section 5.6 only fractures indentified as flowing features are shown and their fracture mineralogy is discussed in terms of redox and pH buffer capacity.
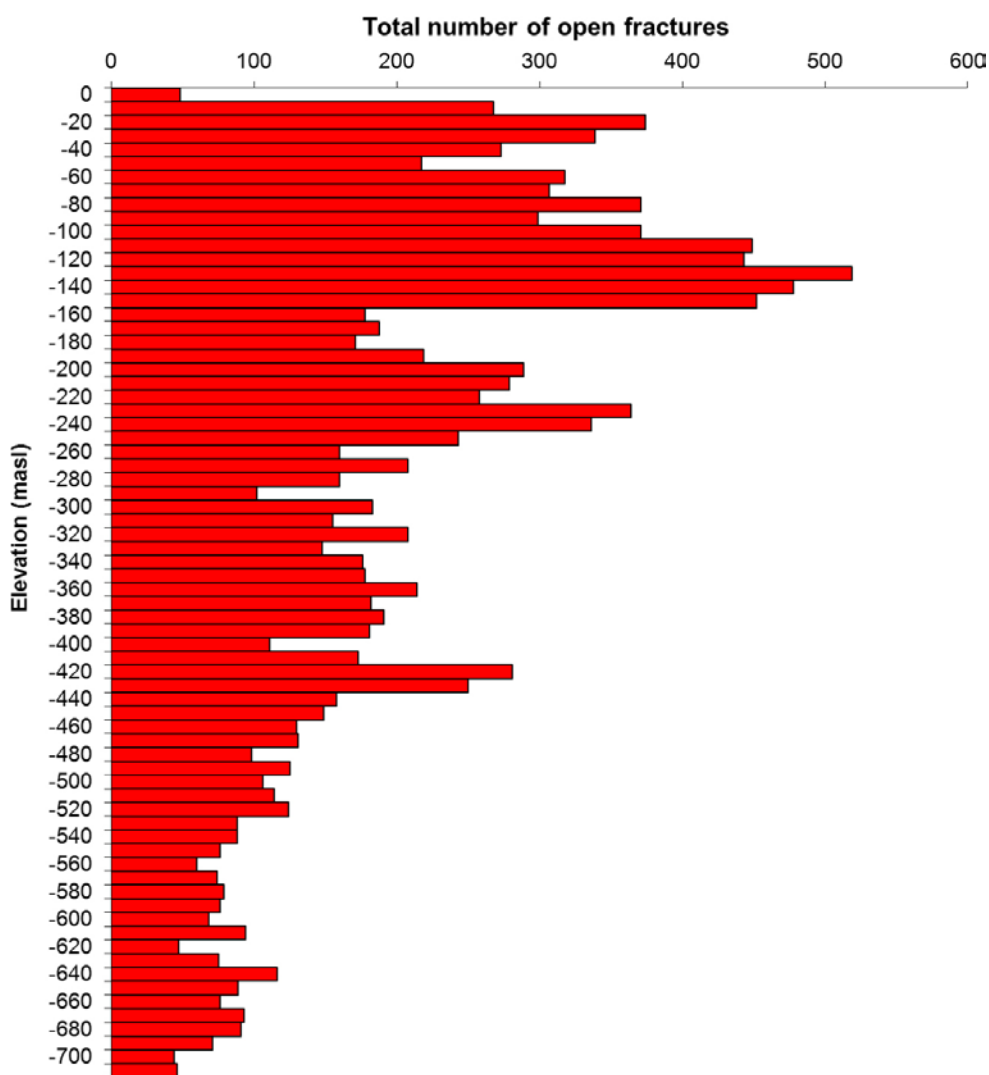
Figure 2-12. Depth distribution of the total number of mapped open fractures.

2.2 Hydrogeological setting

This description of the hydrogeological setting is based mainly on the final Hydrogeological Site Descriptive Model version 1.0 (Öhman et al. 2011).

The SFR local and regional model areas lie within the Baltic Sea area, including only as landmass the surface locality of the SFR radioactive waste facility, the topographic feature of Asphällskulten, and the shallow banks of Grisselgrundet to the northeast (regional model), and the most northeastern extension part of Asphällskulten (local model) (cf. Figure 2-1). Here, the Baltic Sea is shallow with a current depth of about 2–6 metres in the area where the SFR deposition tunnels are located, and the deposition tunnels are about 600 metres off the shoreline. Both regionally and locally the general trend of the topography is a smooth lowering of the topographic elevation towards the northeast. This is shown in Figure 2-13 which presents the topography both above and below the present shoreline.

2.2.1 The regolith

The SFR regional domain is mainly covered by the Baltic Sea and the sea bottom is characterised by recent sea sedimentation and still older Quaternary deposits, both of varying thickness. These sediments potentially have an important role in controlling the hydraulic connection between the
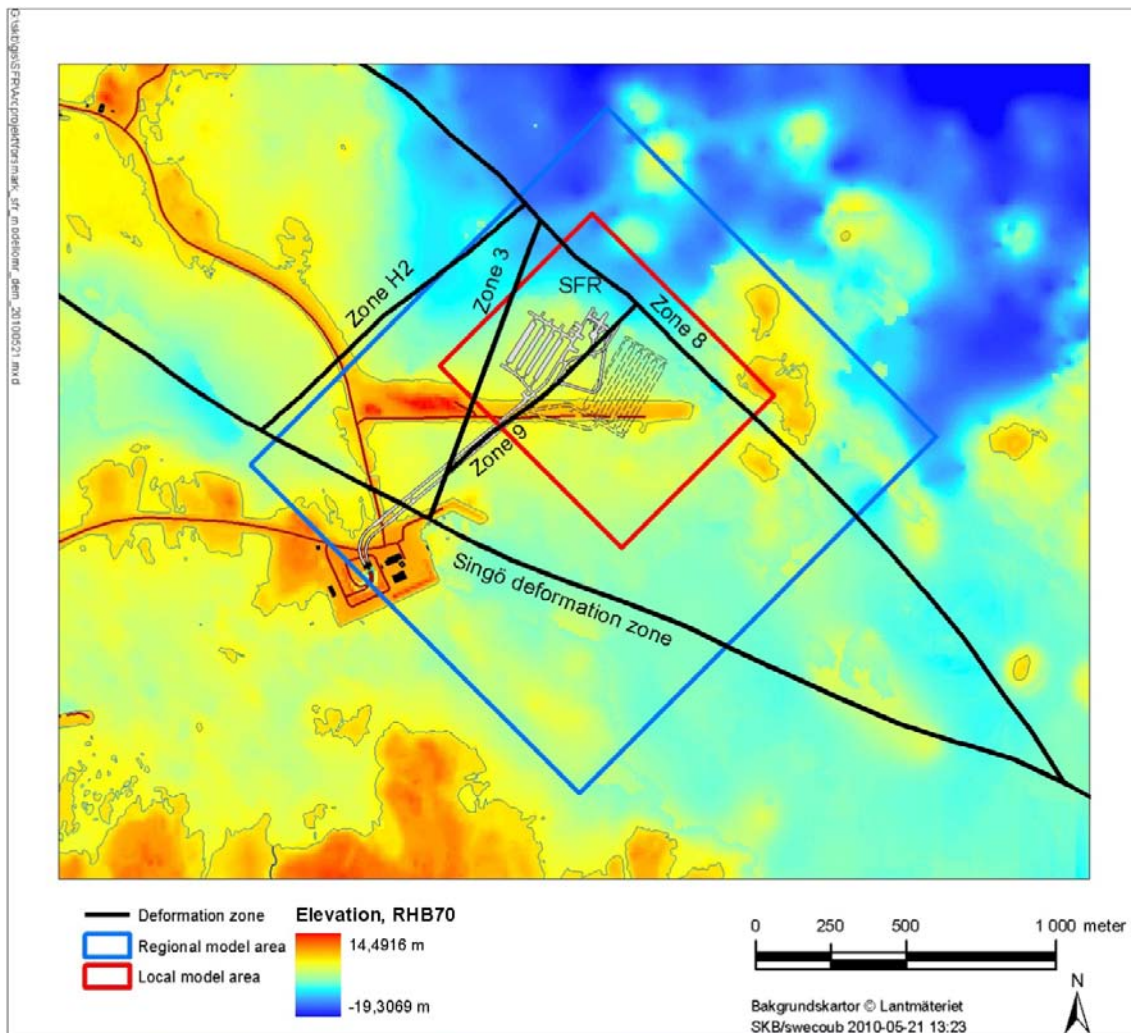
Figure 2-13. *The regional topography denoting the regional model area (blue rectangle), the local model area (red rectangle) and the areas close to and above sea level, as well as showing the central location of the SFR waste facility and the major fracture zones (black). (Zone ZFMWNW0001, formerly Singö zone; ZFMNW0805A and ZFMNW0805B, formerly Zone 8), ZFMNNE0869, formerly Zone 3, ZFM871, formerly Zone H2, and ZFMNE0870B, formerly Zone 9).*

Baltic Sea and the underlying rock mass (Öhman et al. 2011). The nature and thickness of these overlying sediments therefore are probably important to explain past and present hydrogeochemical conditions, for example the presence, or not, of Baltic type groundwater in the underlying bedrock (cf. Section 5.2).

Modelling of the regolith was not conducted as part of the SFR project, but the conceptual model of the distribution of Quaternary deposits that was developed within the Forsmark site investigation Programme covered the Forsmark inland as well as the marine sediments above the SFR (Hedenström et al. 2008). Nine Quaternary deposition layers were identified but their distribution and extent are quite heterogeneous (cf. Figure 2-14). The spatially variable thickness was modelled using a horizontal spatial resolution of 20×20 m with the total thickness of the deposits varying from less than a decimetre to a maximum of 42 m.

Conclusions drawn in Öhman et al. (2011) from the regolith model and the hydraulic observations are:

- The sediment layers are considerably thicker on the south side of the pier due to a combination of wave erosion, the wave breaking function of the pier, and the topographical depression of the Singö deformation zone, and include low conductive glacial clays and a bottom layer of till with vertical calibrated conductivities of $K = 1.5×10^{-8}$ and $K = 7.5×10^{-7}$ m/s, respectively (Bosson et al. 2008). The sediments may act as a constriction to water movement at the contact between the fractured rock and the Baltic Sea floor, at least for fracture transmissivities greater than 10^{-7} m/s.

- On the north side of the pier there are areas with no, or only partial, sediment coverage and this could partly explain the anomalously high transmissivities observed in the vicinity of the Northern boundary belt. For example, the islet location of boreholes KFR106 and HFR106 has virtually no soil/sediment coverage and therefore provides direct contact to the Baltic Sea for zones ZFMWNW3262, ZFMNW0805b (formerly Zone 8) and ZFMNNW1034.

- The pier itself is constructed from a coarse, permeable, blocky material that should facilitate direct hydraulic contact to the underlying bedrock. To what extent the space between the blocks has been filled with fine sediment material, thereby reducing any hydraulic contact is not known. Therefore, potentially the pier is considered to have good contact with the bedrock below.
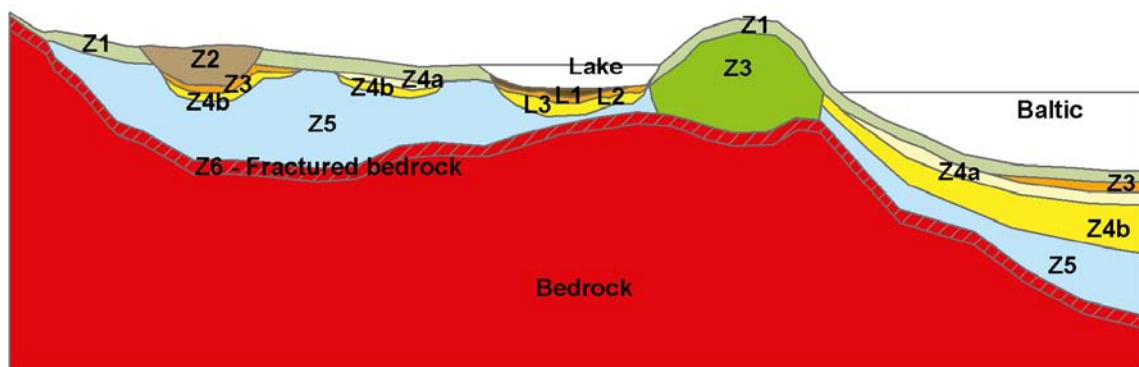
Figure 2-14. Conceptual model for the layering of Quaternary deposits where the different layers are; L1 = Different kinds of gyttja/mud/clay or peat of varying thickness, L2 = Sand and gravel of varying thickness, L3 = Different clays (glacial and postglacial) of varying thickness, Z1 = Surface affected layer present over the full extent of the model, except where peat is found and under lakes with lenses; thickness is 0.10 m on bedrock outcrops, 0.60 m elsewhere; if total regolith thickness is less than 0.60 m, Z1 will have the same thickness as the total, i.e. in those areas only Z1 will exist. Z2 = Surface layer consisting of peat; zero thickness in the sea and always followed by Z3, Z3 = Middle layer of sediment; only found where surface layers are other than till, clay or peat, Z4a and b = Middle layers consisting of postglacial clay followed by glacial clay, Z5 = Till layer; the bottom of layer Z5 corresponds to the bedrock surface, and Z6 = fractured upper part of the bedrock with a constant thickness of 0.5 m (Öhman et al. 2011).

2.2.2 Fracture domains

To facilitate site description and modelling work in the Forsmark site investigations, emphasis was put on the geological subdivision of the bedrock in between deformation zones into fracture domains, mainly based on the frequency of open fractures (Olofsson et al. 2007). These were also shown to be consistent with the hydrogeology (Follin et al. 2007a, b). However, currently there does not exist a fracture domain model for the SFR site mainly due to an absence of geological data (Öhman et al. 2011). As mentioned in Section 2.1, because this concept has not been used in the geological and hydrogeological characterisations, it has not been considered useful for the hydrogeochemical interpretations.

2.2.3 Local model bedrock features

Deformation zone properties

The transmissivity data above –200 m.a.s.l. were not found to be higher inside or close to deformation zone intercepts if no distinction is made to the type of deformation zones. However, the few transmissivity data below –200 m.a.s.l. appear more correlated to deformation zones. Structures of the Northern and Southern boundary belts (cf. Figures 2-3 and 2-5) are interpreted as important vertical conductors; however, they exhibit a distinct hydraulic signature with the high transmissive PFL-f (Descrete groundwater inflow detected by the Posiva Flow Logging method) inside intercepts parallel to the zone. Structures inside the Central Block (cf. Figures 2-6 to 2-9) are generally more inconclusive.

The hydraulic properties of the deformation zones (cf. Figures 2-5 to 2-9) that are likely to have a significant impact on the hydrogeochemical conditions are described below.

* *The Southern boundary belt (dominated by the ZFMWNW0001, formerly the Singö Zone).* In contrast to other deformation zones, the Singö zone (from observations in borehole section KFR01:1) shows a much lower correlation with sea level and atmospheric pressure which indicates that the zone, or at least the hydraulic contact with this borehole section, is confined at the surface. The reason may be the thicker sediment layer on the south side of the pier. The other boreholes within the Singö zone (KFM11A, HFM34, HFM35 and HFR105) show a stronger correlation with the sea level variation. This is also indicated by the intruding Baltic Sea type groundwater sampled in boreholes HFM34, HFM35 and HFR105. The sampled sections in KFM11A are located deep enough to connect with other types of groundwater sources.

* *The Northern boundary belt (including ZFMNW0805A and ZFMNW0805B, formerly Zone 8).* Of the two named deformation zones, ZFMNW0805A is judged to be more transmissive than ZFMNW0805B and it is also better connected to the gently dipping zone ZFM871 (formerly Zone H2).

* *Zone ZFMNNE0869 (formerly Zone 3)* is clearly atypical of the NNE to ENE set of deformation zones which generally have low transmissivities. In the SFR geological model version 1.0 it has a width of 60 m and the transmissivity of the four borehole intercepts ranges between 3×10^{-6} and 4×10^{-5} m^2/s.

* *The gently dipping Zone ZFM871 (formerly Zone H2).* This zone seems to have a central role in the hydraulic connectivity within the SFR. Disturbances in ZFM871 are monitored in the steep deformation zones ZFMNE0870, ZFMNW0805A,B and ZFMNNE0869, and *vice-versa*; in addition, disturbances in the steep deformation zones are also monitored in ZFM871. Furthermore, the zone is better connected to ZFMNW0805A than ZFMNW0805B despite the fact that ZFMNW0805A is located outside ZFMNW0805B. Although ZFM871 is interpreted as highly conductive, it is also proved to be heterogeneous due to a partial lack of internal connectivity within the zone (i.e. discontinuous stairwise pattern).

* *In the new southeastern area investigated in the SFR extension project,* the two most important zones for the hydrogeological and hydrogeochemical interpretations are ZFMNNW1034 and ZFMWNW0835. The highest transmissivity values in this area are found in the vincinity of Zone ZFMNNW1034. The early borehole KFR27 that was extended from –140 to –468 m.a.s.l. within the SFR extension project is located entirely within Zone ZFMWNW0835. The hydraulic observations from this borehole do not, however, differ significantly from those measured in the bedrock inbetween zones at corresponding depths.

Rock stress regimes and hydraulic anisotropy

Both previously at Forsmark and presently at the SFR site there is a good correlation between rock stress anisotropy and hydraulic anisotropy (Glamheden et al. 2007, Follin 2008, Öhman et al. 2011). The largest transmissivities are orientated orthogonally to the minimum principal stress, for example, the gently dipping zone ZFM871 (orthogonal to σ_3) and the steep WNW-striking deformation zones (orthogonal to σ_2) are highly transmissive. This correlation in transmissivity is also found at the fracture scale where steep fractures are predominantly sealed, while horizontal and gently dipping fractures are predominantly open. This condition is likely to obstruct widespread mixing of different types of groundwaters in the vertical direction and may be one of the underlying factors that allow the presence of less saline groundwater (i.e. of glacial origin) to be preserved below more saline groundwater (i.e. Littorina Sea origin) in several boreholes.

Shallow bedrock aquifers

Rock stress release due to glacial cycles of loading/unloading is recognised in the Forsmark area at shallow depths down to about 150 m (Follin et al. 2007a), where the bedrock is considered to be hydraulically anisotropic due to a lattice of intersecting near-surface joints and gently dipping single fractures (i.e. sheet joint; Figure 2-15). The groundwater flow field is considered horizontally aniso-tropic and flow rates are high. When the meteoric recharge waters enter the subhorizontal fractures they mix with existing groundwaters in the fractures and are rapidly transported laterally to be discharged towards the Baltic Sea to the northeast of the Forsmark candidate area, i.e. towards the SFR site.
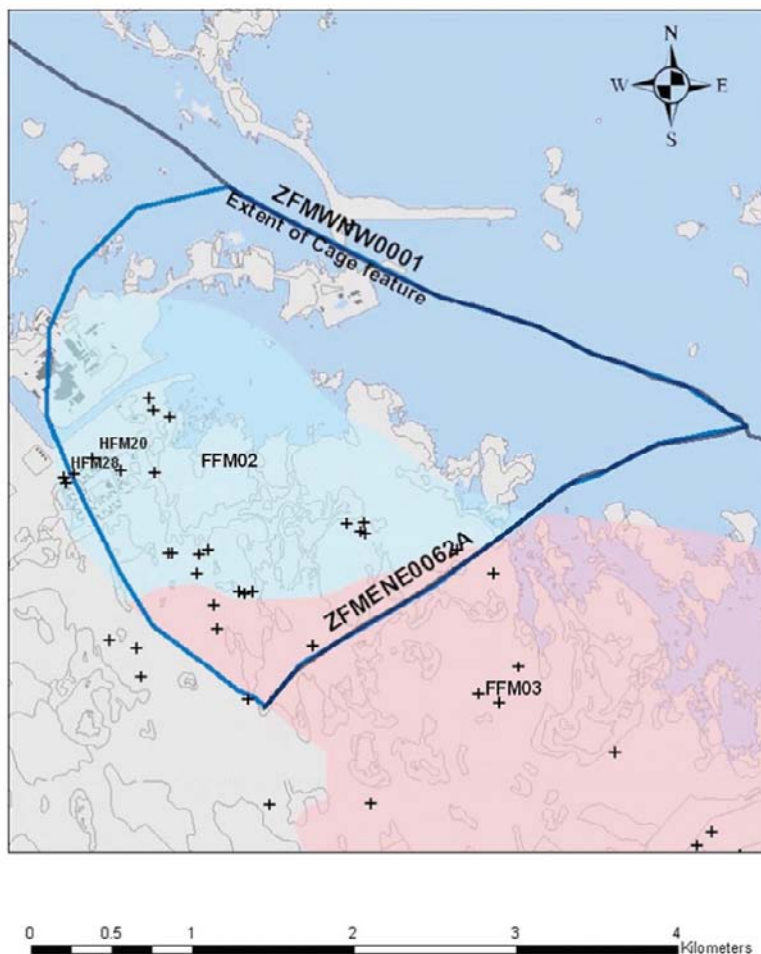
Figure 2-15. The estimated lateral extent of the sheet joint referred to in the figure as the now obsolete 'cage feature' covering the Forsmark target area (Follin et al. 2007b). This sheet joint is interpreted to discharge shallow inland groundwater into the Singö zone or the SFR Southern boundary belt (i.e. deformation zone ZFMWNW0001).

The SFR site appears to share some of these properties with Forsmark and generally it is concluded that the upper approximately 200 m of the bedrock at the SFR facility and the planned extension is hydraulically dominated by a system of connected subhorizontal fractures with high transmissivity (Öhman et al. 2011 and Table 2-3). Accordingly, in the hydrogeological models for the SFR a number of deterministic discrete features (Shallow Bedrock Aquifers or SBAs) have been introduced to represent this transmissive subhorizontal fracture network with heterogeneous channelised flow paths (cf. Figure 2-16). The boreholes having PFL-f information close to the Northern boundary belt provide the most convincing evidence of SBA structures existing north of the Singö deformation zone, although not as well developed as those modelled at Forsmark. However, they are considered to play an important role in the hydraulic connectivity of the rock mass in the vicinity of the Northern boundary belt, but are of less significance further away in the Central Block towards the Southern boundary belt and below –60 m.a.s.l. (Öhman et al. 2011).

Table 2-3. Boreholes and modelled intercepts with the Shallow Bedrock Aquifers SBA1 to SBA6 (modified from Öhman et al. 2011). Modelled intercepts sampled for groundwater are shown in bold font.

Borehole	SBA1 (mbl[1])	SBA2 (mbl[1])	SBA3 (mbl[1])	SBA4 (mbl[1])	SBA5 (mbl[1])	SBA6 (mbl[1])
HFR102	eoh[2]					
KFR27	55	98				193
KFR101						181
KFR102A		72				206[3]
KFR102B						172
KFR103		86	86	182	182	
HFR106			**39**			
KFR106				71	**155**	

[1] Metre borehole length.

[2] End of borehole.

[3] Sampled section 214–219 mbl.
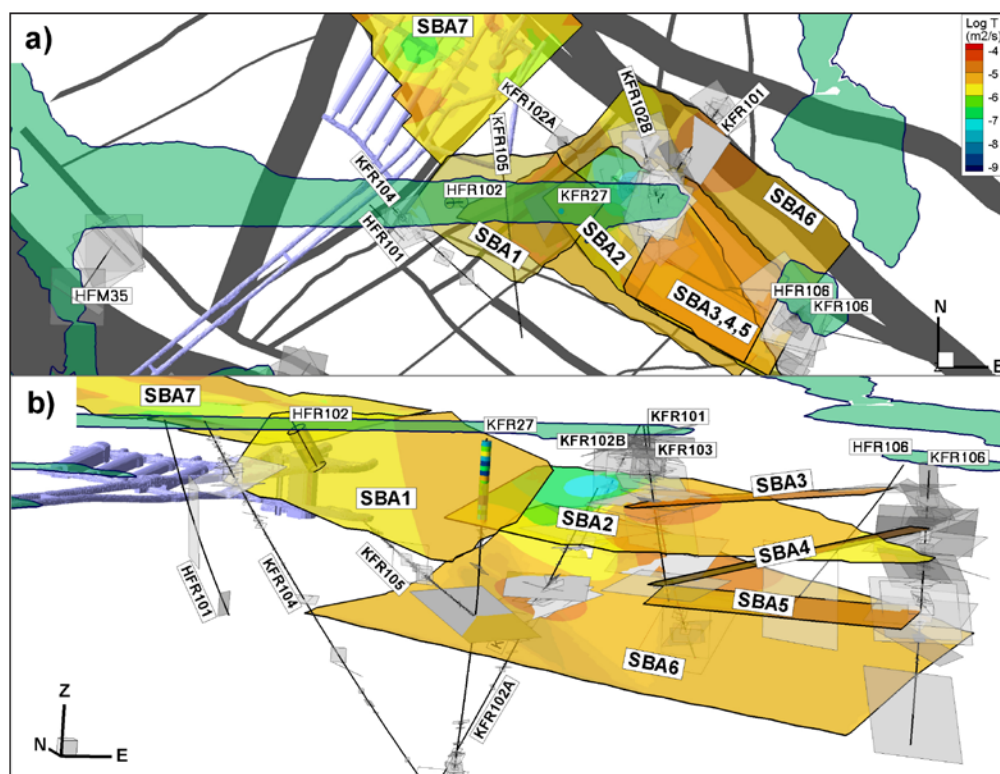
Figure 2-16. *Deterministically modelled Shallow Bedrock Aquifer (SBA) features; a) top view, and b) side view from the southwest (Öhman et al. 2011).*

Still unresolved, however, is the uncertainty of the full extent and therefore connectivity of the SBA feature(s) within the SFR area. For example, in the final geological model SFR version 1.0, the gently dipping deformation zone ZFM871 (formerly Zone H2) lying at approximately 100–250 m depth is inferred to terminate against the vertical zone ZFMENE3115. In the previous model version 0.2, however, it extended beyond this vertical zone and covered also the target area for the SFR extension southeast of the present SFR facility. Furthermore, there is some uncertainty of a connection further southwest to intersect with the major Singö deformation zone. From hydrogeochemical data it is obvious that a number of boreholes show a different groundwater composition at a position corresponding to, or relatively close to the previous model version 0.2 extension of zone ZFM871. This groundwater is more saline and has a somewhat greater marine character compared to the more brackish-glacial type groundwaters above and below. This would suggest a wider distribution of connected SBAs than indicated by the geological and hydrogeological modelling, but there are too few relevant data available at the moment for further interpretation.

Nevertheless, there exist data of ground level transmissivities from a series of crosshole interference tests between zones ZFM871 (formerly Zone H2), ZFMNE0870B (formerly Zone 9), ZFMNNE0869 (formerly Zone 3), ZFMNNW0999, ZFMNW0805A (formerly Zone 8) and ZFMNW0805B (formerly Zone 8) (Öhman and Follin 2010). These data underline the moderately high hydraulic conductivities of especially deformation zones ZFM871 and ZFMNNE0869, and less so for zones ZFMNNW1209 (formerly Zone 6) and ZFMNW0805, and the low hydraulic conductivity which characterises Zone ZFMNE0870B. Zone ZFMNNE0869 is the most permeable zone giving a geometric mean value of the ground level hydraulic transmissivity of $2.2 \cdot 10^{-4}$ m^2/s. These observations, together with the strong hydraulic connection between zones ZFM871 and ZFMNNE0869, are of importance when evaluating the hydrochemical data.

For the rock mass around the tunnels and between the interpreted fracture zones, Holmén (2005) gives a hydraulic conductivity value between about $2 \cdot 10^{-9}$ m/s and about $7 \cdot 10^{-9}$ m/s. For the rock mass nearer the sea floor (from the sea floor to a depth of about 25 m beneath the sea floor), the conductivity is estimated to be an order of magnitude greater.

2.3   Hydrogeological conditions induced by the SFR repository

Crucial to the hydrogeochemical evaluation is to understand the hydraulic changes that may or may not have taken place at the SFR since the initial drilling and site investigation stage, the subsequent excavation and construction stage, the present day operational stage, and predictions of post-closure conditions.

2.3.1   Inflow to the SFR and evidence of time-related changes

The inflow to the SFR facility has been measured regularly since January 1988 (Carlsson and Christiansson 2007). Initially, after the excavation work (1986) the inflow was about 720 L/min. Since then there has been a relatively constant decrease in the inflow for the last 25 years and the average total inflow in 2009 amounted to about 250 L/min (Öhman et al. 2011). The hydraulic head was quickly stabilised in the largest zones ZFMNW0001 and ZFMNW0805A,B (i.e. formerly Singö zone and Zone 8) whilst in the less conductive zones there has been a constant, more gradual decrease with time. The contribution from the open upper part of the ramp (about 20 L/min), i.e. the pump pit in connection to the entrance gates to the SFR tunnel, is not included in these inflows. Furthermore, the inflow figures are not corrected for the contribution from moisture transport associated with the ventilation systems. The location and distribution of inflow to the tunnel system is presented in Figure 2-17.

The Singö zone is estimated to contribute about 30% of the inflow (30% of totally 140 L/min in 2009) to the ramp above the repository level, and the inflow from the subhorizontal deformation zone ZFM871 (formerly Zone H2) in the lower end of the lower construction tunnel, is estimated to be about 30 L/min (Öhman et al. 2011). The proportions of inflow between the different parts of the facility appear to have been constant with time.
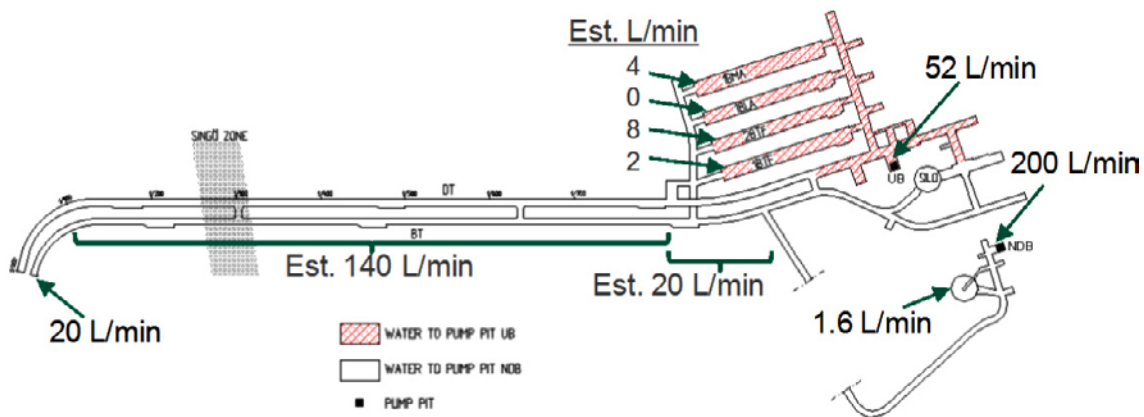
Figure 2-17. *The location and distribution of inflow to the tunnel system in 2009. The pump pits are denoted by UB (upper basin) and NDB (lower basin) (Öhman et al. 2011).*

Two different processes have been suggested in order to explain the declining trend of inflow with time; 1) there may be an ongoing transient drawdown around the facility, i.e. the flow around the facility has not yet reached steady state, and 2) the hydraulic properties of the surrounding bedrock are changing towards an increased flow resistance with time. The first explanation agrees with the observations of an ongoing relatively constant declining trend in heads in many boreholes around the facility (cf. Section 2.3.2). The second possible explanation, on the other hand, should be accompanied by an increased groundwater pressure upstream along the zone of increased resistance, but this has not been observed. On the contrary, the observed decline in heads has been greatest in the less conductive rock, being most pronounced in zone ZFMNE0870 (formerly Zone 9) and in the rock mass east of it (cf. Figure 2-19 b). This suggests that the decreased inflow has been caused by transient drawdown (accompanied by a decreased flow) in the less conductive parts of the rock volume, and not by a decreased flow through the larger zones. The Silo is not grouted and seems to be located in an unusually low conductive rock mass. Inflow to the Silo from the cavern walls and the ceiling originally amounted to 2 L/min and has successively been reduced to 0.7 L /min. This is surprising considering the large exposed area of about 8,000 m^2 and that the location is close to two highly conductive deformation zones (10 m above ZFM871 and 60 m from ZFMWNW805B).

The water composition in samples collected from the two basins/pump pits exhibits the typical Local Baltic type groundwater signature as defined in Section 3.3. Also these water samples show the lower magnesium concentrations compared to the actual seawater and typical for the Baltic type groundwater. A comparison of some concentration values of importance between the water in the pump pits and a typcal Baltic Seawater sample is presented in Table 2-4.

The groundwater inflow has been modelled by Svensson and Follin (2010) based on particle trajectories in a west to east vertical cross section which shows the extent of the area influenced by groundwater inflow to the SFR during the excavation/operation phase (cf. Figure 2-18). As expected, most of the inflow occurs around the excavation site, but some inflow originates at some distance towards the west at shallow depths, possibly corresponding to the shallow horizontal/subhorizontal zone ZFM871 (formerly Zone H2) (cf. Section 2.1.3).
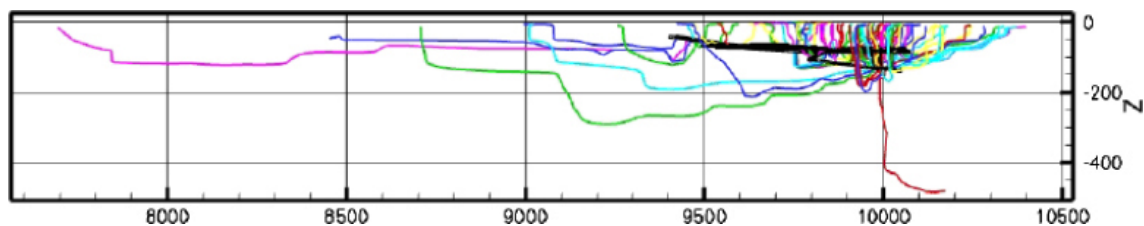
Figure 2-18. *Vertical visualisation along a left to right, W-E cross section showing backward tracking particle trajectories with inflow rates > 0.1 L/min. (y-axis points North and represents vertical depth in metres; x-axis represents horizontal distance in metres) (Svensson and Follin 2010).*

Table 2-4. Some typical concentration values in samples from the upper and lower basins and in Baltic Seawater.

Sampling location	Idcode	Date	Cl	Mg	SOZ	pH	O-18	EC
Upper basin	PFR000121	2007	3,110	144	411	7.84	–8.3	980
Lower basin	PFR000122	2007	2,990	136	381	7.99	–8.7	932
Lower basin	PFR000122	2009	2,960	140	356	7.96	–9.2	935
Baltic Seawater*	–	–	3,025	172	345	8.0	–8.0	–

* Baltic Seawater composition = average value (Pitkänen et al. 2004).

2.3.2 Drawdown around the SFR

The drawdown around the SFR facility since its construction in 1985 can be regarded as a large scale, long term interference test. At a given point, the measured drawdown can be interpreted as an indication of its relative hydraulic connection to the SFR or to the sea floor. A large observed drawdown far from the SFR repository implies a relatively poor connection to the overlying Baltic Sea, while a low drawdown close to the SFR indicates a poor connection to the SFR. Drawdown leads to dispersion and the dominant connection will mask subordinate connections (Öhman et al. 2011).

During and immediately following the construction period there was a rapid decrease in head which was most pronounced in the vicinity of the Silo and associated to zones ZFMNE0870 (formerly Zone 9) and ZFM871 (formerly Zone H2). Zone ZFMNE0870 strikes to the ENE and has an almost vertical dip; it is for most of its length a water bearing gouge filled joint, occasionally with increased fracturing on one or both sides. Zone ZFM871 is a subhorizontal zone which intersects the access tunnels below the Silo; however, the zone does not intersect the access tunnels close to the BMA storage tunnels.

The head stabilised most quickly in the largest, most conductive deformation zones ZFMWNW0001 and ZFMNW0805A,B (formerly the Singö zone and Zone 8); in the less conductive fracture zones there has been a predictably slower, and constant declining trend since 1987–88. Borehole KFR7A, i.e. one of the SFR tunnel boreholes (Figure 2-19), shows the greatest drawdown and also the largest decline and therefore has hydraulic properties clearly different from the other boreholes inside zones ZFMNW0805A,B and is likely to represent a junction with zone ZFM871 (formerly Zone H2). The marked spatially variability recorded in borehole KFR7A indicates that zone ZTM871 is heterogeneous and hydraulically discontinuous. This observation of heterogeneity is supported by the new boreholes drilled within the SFR extension project where the largest drawdown is observed in the vicinity of zone ZFM871 and also decreases with distance away from it, both laterally and vertically (Figure 2-20). The measured heads in 1988 and 2010 are given in Table 2-5 for boreholes that have been sampled for groundwater chemistry.

Seasonal variation in monitored head has only been observed in borehole KFR02 which may be an indication of indirect contact to the overlying pier via zones ZFM871 (formerly Zone H2) and ZFMENE0870 (formerly Zone 9). The correlation with the sea level is strongest in boreholes KFR102A (most sections) and HFR105.
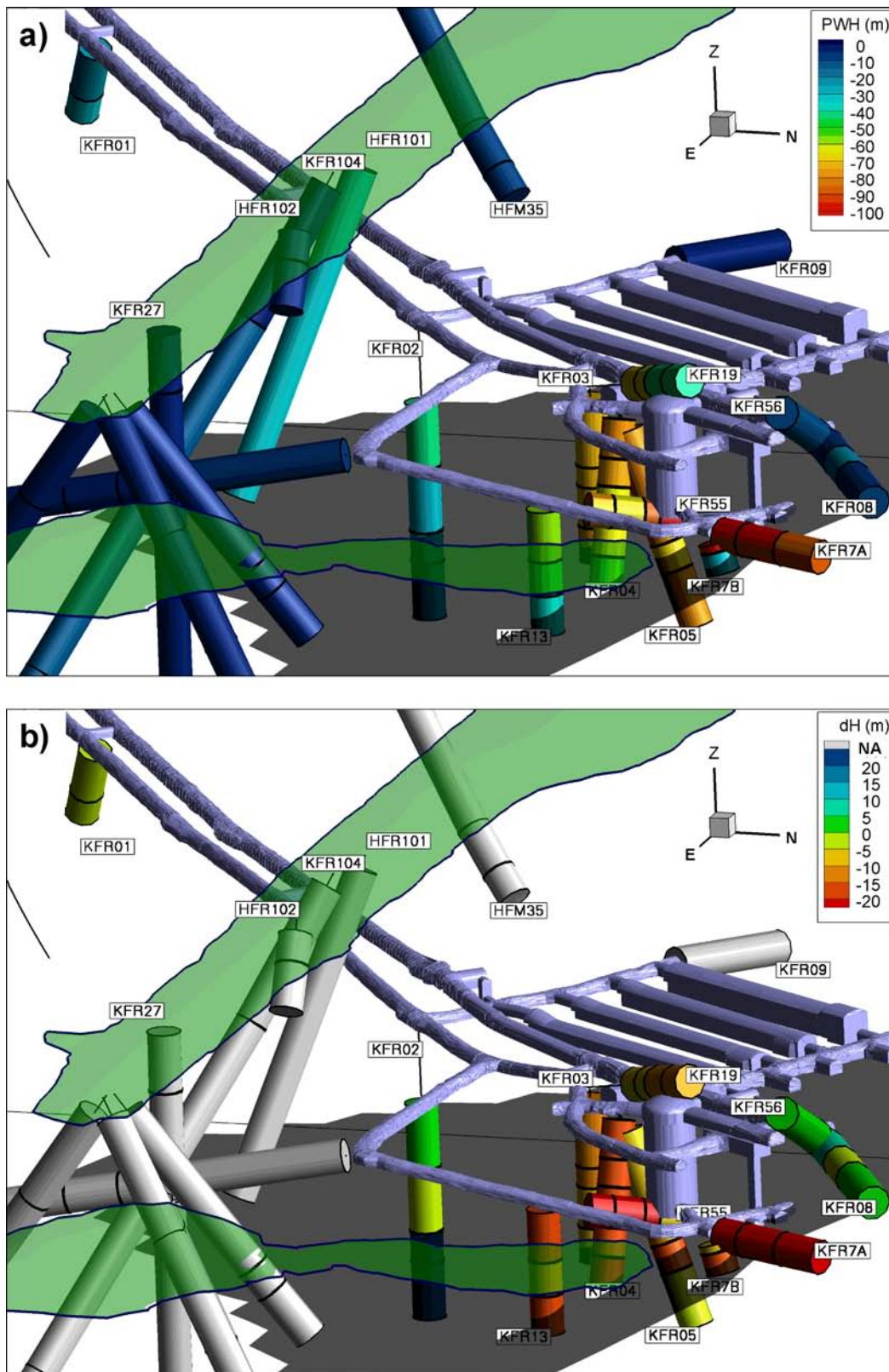
Figure 2-19. Hydraulic head in the SFR tunnel boreholes; a) 2010, and b) change in head between 1988 and 2010. The reference year 1988 was chosen since there has been a relatively constant, declining trend in most borehole sections since then. (Öhman et al. 2011). The land areas are given in green and the gently dipping zone ZFM871 is represented as a grey colour. PWH = point water head, dH = change in head.
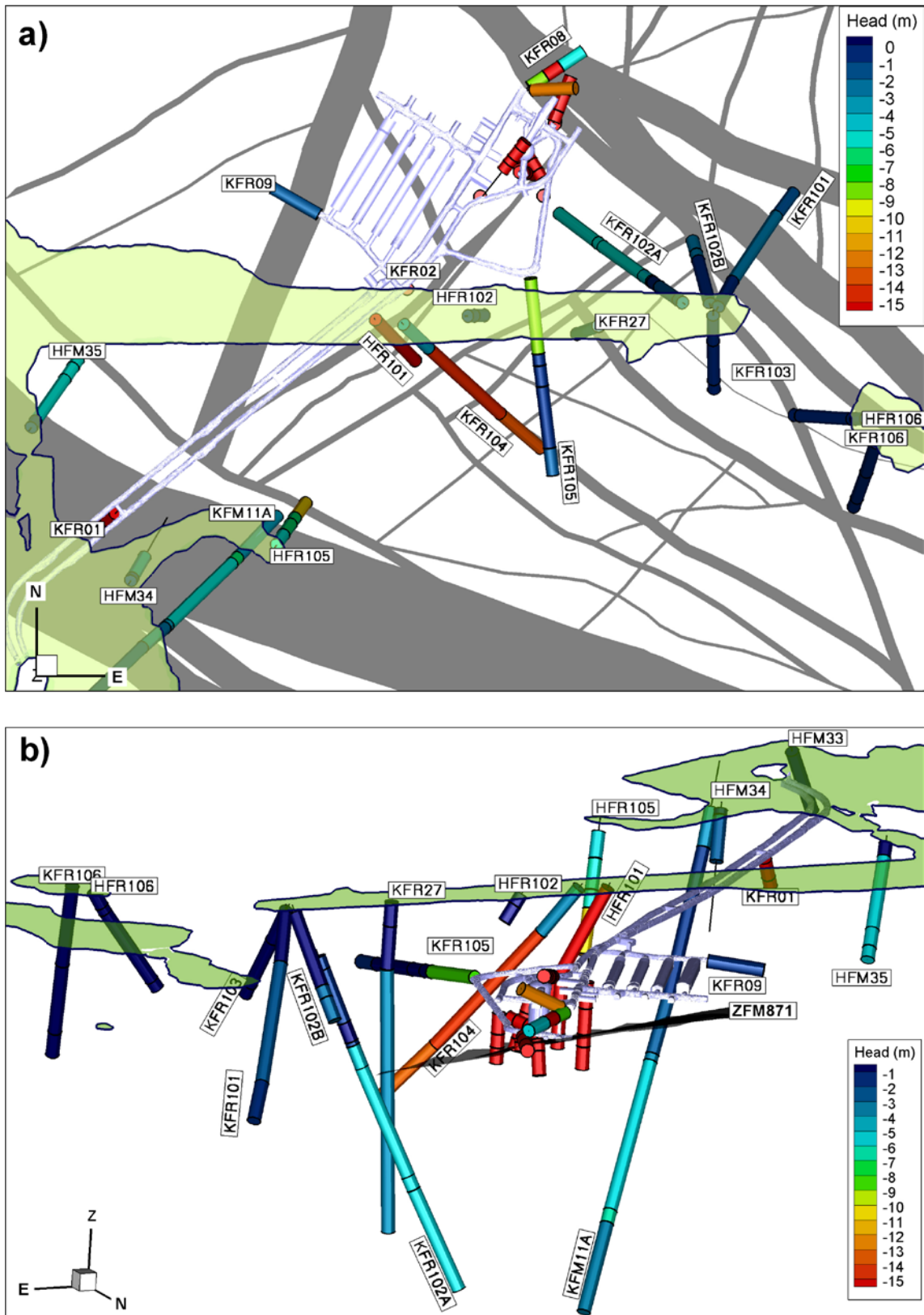
Figure 2-20. *Measured point water head from monitored borehole sections in 2010; a) top view, and b) side view along the dip of zone ZFM871. Fresh water heads in the old data set are generally below –15 m (Öhman et al. 2011).*

Table 2-5. Groundwater head (m) 1988 and 2010 in boreholes and borehole sections sampled for groundwater chemistry.

Idcode: section no	Secup mbl*	Seclow mbl*	Head 1988 (m)	Head 2010 (m)	Comment
HFM34:2	22	90		−2.9	Sinking trend. Seasonal variation, A ≈ 0.5 m.
HFM34:3	11.99	21		−0.5	Sinking trend. Seasonal variation, A ≈ 0.5 m.
HFM35:1	182	200.75		−5.3	Seasonal variation, A ≈ 0.5 m.
HFM35:2	151	181		−5.4	Seasonal variation, A ≈ 0.5 m.
HFM35:3	34	150		−5.4	Seasonal variation, A ≈ 0.5 m.
HFM35:4	12.04	33		−0.6	Sinking trend. Seasonal variation, A ≈ 0.5 m.
HFR101:1	8.04	209.3		−31	Sinking trend to spring 2010.
HFR105:1	134	200.5		−10.9	
HFR105:2	107	133		−6.3	
HFR105:3	61	106		−6.3	
HFR105:4	21.04	60		−5.9	
HFR106:1	175	190.4		−0.6	Rising trend.
HFR106:2	47	174		−0.6	Rising trend.
HFR106:3	36	46		−0.2	Rising trend.
HFR106:4	9.03	35		−0.1	Rising trend.
KFM11A:1	711	851.21		−3.5	
KFM11A:2	690	710		−6.8	
KFM11A:3	457	689		−5.5	
KFM11A:4	446	456		−3.1	
KFM11A:5	361	445		−2.9	
KFM11A:6	131	360		−1.5	
KFM11A:7	70.8	130		−3.0	
KFR01:1	44.65	62.3	−33	−33	Rising trend.
KFR01:2	11.15	43.65	−24	−24	Rising trend.
KFR02:1	137.24	170.3	−53	−15	Jump at reinstrumentation.
KFR02:2	119.24	136.24	−47	−25	Jump at reinstrumentation.
KFR02:3	81.24	118.24	−24	−28	Jump at reinstrumentation.
KFR02:4	43.24	80.24	−44	−40	Jump at reinstrumentation.
KFR03:1	81.16	101.6	−69	−75.1	Absolute level uncertain.
KFR03:2	57.16	80.16	−65	−71.7	
KFR03:3	45.16	56.16	−64	−74.5	Absolute level uncertain.
KFR03:4	5.16	44.16	−60	−73.7	Absolute level uncertain.
KFR04:1	84.09	100.5	−33	−54	Sinking trend.
KFR04:2	44.09	83.09	−44	−63	Sinking trend.
KFR04:3	28.09	43.09	−56	−75	Sinking trend.
KFR04:4	5.09	27.09	−63	−80	Absolute level uncertain. Sinking trend.
KFR05:1	97.15	131	−78	−81.4	Absolute level uncertain.
KFR05:2	80.15	96.15	−49	−65	Sinking trend.
KFR05:3	57.15	79.15	−70	−81.5	Absolute level uncertain.
KFR05:4	12.15	56.15	−72	−81.3	Absolute level uncertain.
KFR08:1	62.95	104	−7	−5.0	
KFR08:2	35.95	61.95	−19	−22	Sinking trend to spring 2010, jump in February 2009 (also in pressure).
KFR08:3	5.95	34.95	−17	−8.0	
KFR09:1	0	80.24		−1.9	Strong correlation with sea level, A ≈ 0.5 m.
KFR101:1	279.5	341.76		−1.6	
KFR101:2	91	278.5		−2.5	
KFR101:3	13.72	90		−0.1	
KFR102A:1	444	600.83		−5.1	
KFR102A:2	423	443		−5.3	

Idcode: section no	Secup mbl*	Seclow mbl*	Head 1988 (m)	Head 2010 (m)	Comment
KFR102A:3	255	422		−5.0	
KFR102A:4	220	254		−4.0	
KFR102A:5	214	219		−1.0	Rising trend.
KFR102A:6	185	213		−0.9	Rising trend.
KFR102A:7	103	184		−1.2	
KFR102A:8	70.38	102		−1.4	
KFR105:1	265	306.81		−1.3	
KFR105:2	170	264		−0.8	
KFR105:3	138	169		−0.7	
KFR105:4	120	137		−0.1	
KFR105:5	4	119		−8.2	
KFR106:1	260	300.13		−0.8	Rising trend.
KFR106:2	143	259		−0.6	Rising trend.
KFR106:3	8.86	142		−0.3	Rising trend.
KFR13:1	53.75	76.6	−23	−39	Sinking trend.
KFR13:2	33.75	52.75	−38	−48	Sinking trend.
KFR13:3	3.75	32.75	−40	−55	Sinking trend.
KFR19:1	95.57	110	−27	−41	Sinking trend.
KFR19:2	77.57	94.57	−30	−43	Sinking trend.
KFR19:3	66.82	76.57	−54	−63.0	
KFR19:4	51.82	65.82	−61	−68.0	
KFR27:1	110	501.64		−3.0	
KFR27:2	47	109		−0.5	
KFR27:3	11.91	46		−0.3	
KFR55:1	48.53	61.89	−113	−121	Absolute level uncertain. Rising trend.
KFR55:2	39.53	47.53	−67	−90	Sinking trend.
KFR55:3	21.53	38.53	−38	−61	Sinking trend.
KFR55:4	7.53	20.53	−57	−79	Sinking trend.
KFR56:1	9.55	81.7	−13	−12.5	Variable change in head with time.
KFR7A:1	48.11	74.7	−38	−85	Sinking trend. Emptying of limited reservoir?
KFR7A:2	20.11	47.11	−89	−113	Sinking trend.
KFR7A:3	2.11	19.11	−91	−113	Sinking trend.
KFR7B:1	8.6	21.1	−10	−27	Sinking trend. Jump in head during 2008.
KFR7B:2	3.4	7.6	−100	−107	Rising trend.

*mbl = metre borehole length.

2.3.3 Initial and future hydraulic conditions at the SFR

The hydrology of the initial 'undisturbed' bedrock conditions prior to the excavation/construction phases has been addressed by (Svensson and Follin 2010). Using post-construction data comprising a total measured inflow rate of 4.8–6.0 L/s and groundwater levels measured at 11 boreholes, simulations were carried out on the preconstruction situation. The simulations agreed with the measured field data suggesting a discharge area once characterised the SFR locality.

Forward predictive modelling may provide some insight into the expected hydraulic (and hydrochemical) conditions following closure and resaturation of the SFR, a key element in the safety case calculations. This modelling has been carried out by e.g. Holmén and Stigsson (2001a, b) and Odén (2009), and showed that in such a scenario, as long as the sea covers the repository area, the regional flow in the surroundings of the SFR as well as the flow in the deposition tunnels will be small. Any flow present will be nearly vertical and directed from depth towards the sea bed, i.e. a return to 'undisturbed' preexcavation/construction conditions. In the event of a retreating shoreline, the general direction of the groundwater flow will change to a more horizontal flow and the magnitude of the groundwater flow will increase.

3 Evolutionary effects

Past climatic changes, which in the Forsmark region has involved both glaciations/deglaciations and marine transgressions/regressions, are the major driving forces for long term hydrogeochemical changes and are therefore of fundamental importance for understanding the palaeohydrogeological, palaeohydrogeochemical and present evolution of the groundwater in the region. This section is devoted to a description of the Quaternary evolution in the area in order to provide the required background to interpret the present groundwater system.

3.1 Quaternary evidence

3.1.1 After the last deglaciation

Quaternary studies have underlined the importance of major crustal movements that have affected and continue to affect northern Europe following the melting of the latest continental ice mass, i.e. the Weichselian glaciation. These show the interplay between isostatic recovery on the one hand and eustatic sea level variations on the other. The net effect of these two processes in terms of elevation is called shore level displacement (Påsse 1997). Detailed descriptions of the development at Forsmark after the last deglaciation, including shore level displacement and the development of the Baltic Sea, is given in Söderbäck (2008), Follin et al. (2008a, b), Smellie et al. (2008) and is summarised below.

In northern Sweden, during the Weichselian glaciation, the heavy continental ice at its maximum depressed the Scandinavian Shield by as much as 800 m below its present altitude. Shortly after this glacial maximum, a marked climatic change occurred about 18,000 years ago, and the ice started to retreat. This was followed by a major standstill and, in some areas, a readvance of the ice front during a cold period ca. 13,000 to 11,500 years ago. The end of this cold period at approximately 10,000 years ago marked the onset of the present interglacial, the Holocene, whereupon the ice retreated more or less continuously during the early part. As soon as the vertical stress decreased after the ice recession, the basement and crustal rocks started to slowly rise (isostatic rebound). This uplift started before the final deglaciation and, importantly, is still an active process in most of Sweden where the current rate of uplift is around 6 to 7 mm per year in the Forsmark region.

Figure 3-1 and Table 3-1 show the aquatic evolution in the Baltic basin since the last deglaciation characterised by a series of brackish and fresh water stages which are related to changes in sea level. This evolution has been divided into four main stages: the Baltic Ice Lake, the Yoldia Sea, the Ancylus Lake and the Littorina Sea (Björck 1995). The most saline period during the Holocene occurred approximately 4500 to 3000 BC, when the surface water salinity in the Littorina Sea was 10 to 15‰ compared with approximately 5‰ today in the Baltic Sea (Westman et al. 1999).

Table 3-1. Evolution of the Baltic Sea basin since the last deglaciation (Follin et al. 2008a).

Baltic stage	Calender year BC	Salinity	Environment in Forsmark
Baltic Ice Lake (not applicable in Forsmark)	13,000 to 9500	Glacio-lacustrine	Covered by inland ice.
Yoldia Sea (perhaps not applicable in Forsmark)	9500 to 8800	Lacustrine/Brackish /Lacustrine	At the rim of the retreating inland ice.
Ancylus Lake	8800 to 7500	Lacustrine	Regressive shoreline from about 140 to 75 m elevation RHB 70 (elevation reference system, see Section 1.4).
Littorina Sea (→ Baltic Sea)	7500-present	Brackish	Regressive shoreline from about 75 to 0 m at SFR. Most saline period 4500 to 3000 BC. Present-day Baltic Sea conditions have prevailed during the last ca. 2,000 years.
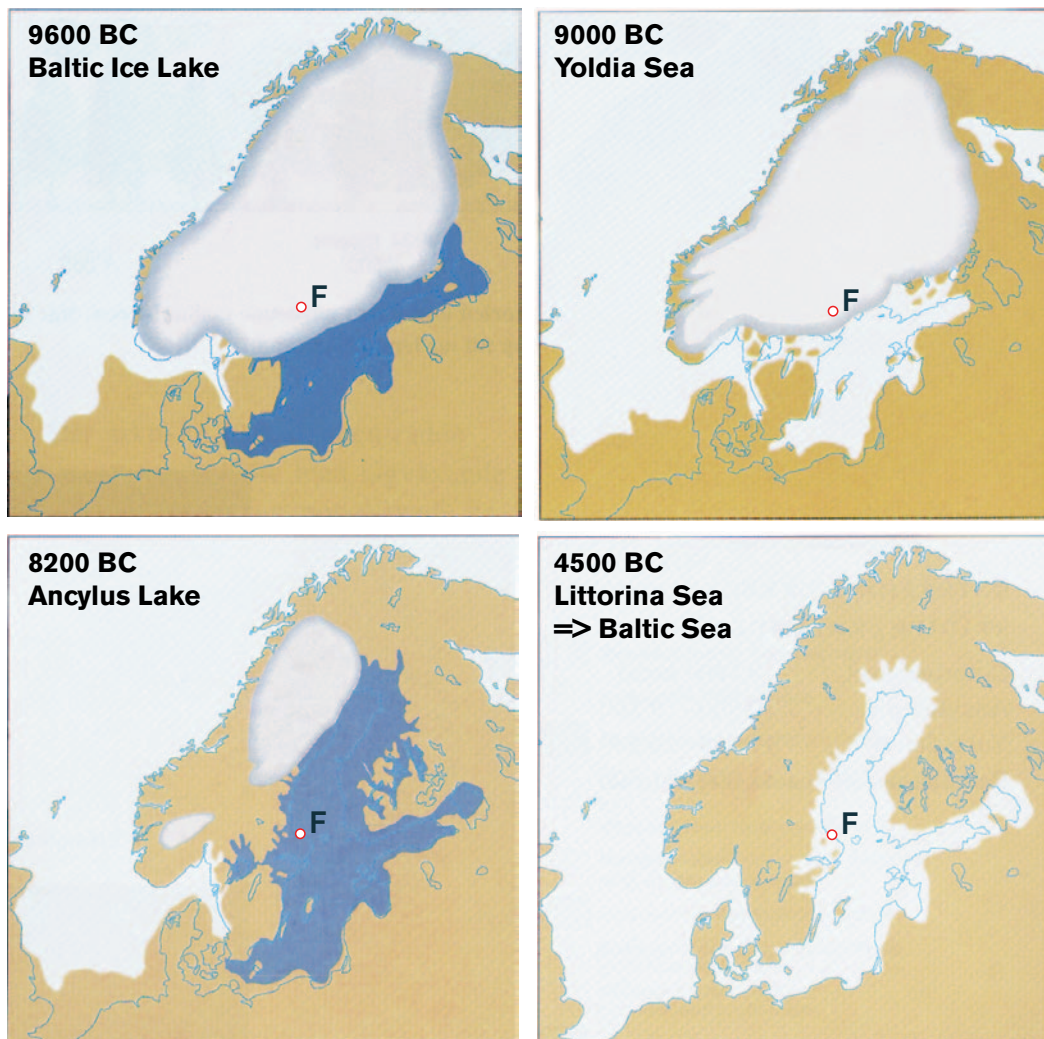
Figure 3-1. *Map of Fennoscandia illustrating some of the important stages during the Holocene period. Four main stages characterise the development of the aquatic systems in the Baltic basin since the last deglaciation: the Baltic Ice Lake (13,000 to 9500 BC), the Yoldia Sea (9500–8800 BC), the Ancylus Lake (8800 to 7500 BC) and the Littorina Sea (7500 BC to present). Fresh water is symbolised with dark blue and marine/brackish water with light blue. The Forsmark region including SFR (notated 'F') was probably at or close to the rim of the retreating ice sheet during the Yoldia Sea stage (from Follin et al. 2008a).*

3.1.2 Permafrost

In general, but not always, the glaciation is preceded by tundra and then permafrost. Permafrost formation is governed by cold and dry climates where an annual ground temperature of between –5 and –2°C is defined as the boundary for extensive discontinuous permafrost (50–90% of landscape covered by permafrost) and –5°C and colder as the boundary for continuous permafrost (90–100%) (Heginbottom et al. 1995). However, it is also stated that a large part of the area with continuous permafrost has a ground temperature warmer than –5°C. Sporadic permafrost (less than 50% of landscape covered), may exist when the annual mean temperature is between 0 and –2°C.

In parts of northern Canada permafrost presently exists to between 400–600 m depth (Ruskeeniemi et al. 2002, 2004, Holden et al. 2009), and most is thought to date back to the Pleistocene period (Tarasov and Peltier 2007). In Siberia permafrost extends to 1,500 m depth and more (e.g. Alexeev and Alexeeva 2003), but this represents a very old accumulative effect incorporating input from several glacial periods far back in time. In northern Fennoscandia some discontinuous remnants of permafrost from the Weichselian and the Holocene are believed to exist (Kukkonen and Šafanda 2001).

Prior to the Weichselian glacial maximum at approximately 18,000 years ago, the ice margin is thought to have been more permanently located across southern Fennoscandia some 30,000 to 50,000 years ago, and to have been subject to fluctuation. There is the possibility, therefore, that the Forsmark site has been subject to variable permafrost conditions for a long period of time until eventually overrun by the advancing continental ice sheet.

The impact of permafrost on groundwaters is largely unknown as most evidence has been removed/modified either during permafrost decay coeval with the advancement of the ice cover, and/or subsequently flushed out during deglaciation (cf. Smellie et al. 2008 for discussion). However, the possibility of preservation of such evidence in the matrix porewaters cannot be ruled out (cf. Waber et al. 2009).

3.2 The scenario for groundwater evolution from before the last deglaciation to the present day

As shown above, the given Quatermary evidence for Holocene evolution is relatively detailed compared with that of glacial and older periods and therefore there is the likelihood that evidence of groundwater evolution can be recognised in the bedrock aquifer in the Forsmark region (cf. Figure 3-2 and Figure 3-1).

When the continental ice melted and retreated (i.e. deglaciation stage approximately 18,000 BC to 8000 BC), glacial meltwater was hydraulically injected under considerable head pressure into the bedrock close to the ice margin. The exact penetration depth is still unknown, but depths exceeding several hundred metres are possible according to hydrodynamic modelling (e.g. Svensson 1996). Any permafrost decay groundwater signatures may have been disturbed or destroyed during this stage.

Several different non-saline and brackish lake/sea stages then transgressed the Baltic Sea basin during the period ca. 9000 BC to 1500 AD. Of these, two periods with brackish water can be recognised; Yoldia Sea (9500 to 8800 BC) and Littorina Sea (from 7500 BC continuing to the present), with the Baltic Sea from 2,000 years ago to the present. The Yoldia period has probably resulted in only minor contributions to the subsurface groundwater since the water was very dilute to brackish in type from the large volumes of glacial meltwater it contained. Furthermore, this period lasted only for 700 years. The Littorina Sea period in contrast had a salinity maximum of about twice the present Baltic Sea and this maximum prevailed at least from 4500 to 3000 BC; during the last 2,000 years the salinity has remained almost equal to the present Baltic Sea values (Westman et al. 1999 and references therein). Dense brackish seawater such as the Littorina Seawater was able to penetrate the bedrock resulting in a density intrusion which affected the groundwater in the more conductive parts of the bedrock. The density of the intruding seawater in relation to the density of the groundwater determined the final penetration depth. As the Littorina Sea stage contained the most saline groundwater, it is assumed to have had the deepest penetration depth eventually mixing with preglacial groundwater mixtures already present in the bedrock.

These different stages have influenced the Forsmark region apart from the Yoldia Sea transgression which was of less importance and may even be not applicable because of its relatively short period of duration and the very dilute nature of the brackish water.

When the Forsmark region was sufficiently raised above sea level 1,000 to 500 years ago to initiate recharge of fresh meteoric water, this formed a lens on the surface of the saline water because of its low density. As the present topography of the Forsmark area is flat and the time elapsed since the area was raised above sea level is short, the flushing out of saline water has been limited and the freshwater lens remains at shallow depths (from the surface down to 25 to 100 m depending on hydraulic conditions). The entire SFR local model volume is situated below the present Baltic Sea with the exception of some small islands and shallow banks and therefore fresh modern water is not to be expected.

As a result of the described sequence of events, saline (non-marine), glacial and marine waters at the SFR are expected to have been mixed in a complex manner at various levels in the bedrock, depending not only on the hydraulic character of the fracture zones and groundwater density variations, but also on anthropogenic activities including hydraulic testing, groundwater sampling and above all the change in hydrogeological conditions caused by the existing SFR repository.

a Deglaciation before Ancylus Lake > 8800 BC

Continental Ice sheet

δ¹⁸O = –22 to –20‰

Dilute glacial melt water transported to depth by strong hydraulic gradients

Brackish to saline water

500 m

25   50 km

b Fresh water Ancylus Lake 8800–7500 BC

Water depth 170–100 m

δ¹⁸O = –11 to –12‰

Mixture of glacial melt water with brackish/saline water types

500 m

25   50 km

c Littorina Sea stage (started 7500 BC) Salinity maximum around 4500–3000 BC (Salinity = 9–14‰)

Water depth 75–50 m

Fresh to Brackish water

δ¹⁸O = –6‰

Density intrusion; saline Littorina Sea waters mixing with older glacial and brackish waters

Saline water

500 m

25   50 km

d Present day situation; the salinity has remained the same for the last 2000 years

Emergence above sea level started around 500 BC

δ¹⁸O = –12 to –11‰

Fresh water

Brackish water

Local discharge pathways

Saline water

500 m

25   50 km

Figure 3-2 a–d. Conceptual model for the Forsmark region following the last deglaciation. The different stages are; a) deglaciation before the Ancylus Lake (> 8800 BC), b) freshwater Ancylus Lake between 8800 to 7500 BC, c) density intrusion of Littorina Seawater between 7500 BC to 0 AD, and d) the present day situation where the SFR is situated below sea-level just outside the coastline. Blue arrows indicate possible groundwater flow patterns (after Laaksoharju et al. 2008).

3.2.1 The possible influence of older waters

The climate changes discussed above and in Söderbäck (2008) and Follin et al. (2008a) affect not only the precipitation and hence the amount of water, but also the type of water infiltrating the bedrock.

The infiltrating water can be glacial meltwater, precipitation, or seawater dependent of the prevailing climatic conditions. The hydraulic driving forces or the density of these water types, together with the hydrogeological properties of the bedrock, determine where and how deep the waters can penetrate. However, climatic change is a cyclic process and tends to flush out earlier water types, but the driving forces and conditions can vary and residuals of earlier climate input can be preserved often in less transmissive fractures and/or rock volumes. Extreme conditions, such as the maximum melting of the inland ice, the most saline seawater, or the longest wet period, provide the best possibility to leave an imprint on the bedrock groundwater. These palaeohydrogeochemical events therefore provide an important framework to understand the hydrogeochemical evolution of the bedrock groundwaters. However, to only consider scenarios occurring after the last deglaciation can be seriously misleading, especially considering hydrochemical input data to establish boundary conditions for hydrodynamic modelling of the Forsmark region. For example, analyses of some of

the groundwaters from the relatively tight and isolated bedrock outside the deformation zones show compositions significantly influenced by glacial meltwater (probably from the last glaciation but may also be older) and brackish non-marine water of unknown age. In other words, there may be an important groundwater component from before the last deglaciation that has influenced to varying degrees the present-day hydrochemistry of the SFR local model volume. This is also supported by evidence of pre-Holocene porewater analysed within the Forsmark site investigations (Waber et al. 2008). Based collectively on the above described observations, the present groundwaters are a result of complex mixing and reactions over a long period of geological time. Mixing will be more important in those parts of the bedrock with dynamic hydrogeological properties, for example, the more conducting fractures and fracture zones in the SFR model volume. In other less dynamic parts, the groundwater chemistry will be more influenced by water/rock interaction processes and diffusion processes. In common with the Foresmark site, diffusion processes also may have preserved an older groundwater type; however no porewater analyses have been carried out within the SFR site investigations.

3.2.2 Working hypothesis

The five key water origins recognised in the Forsmark Site investigations were in chronological order: *Saline Water > Brackish Non-marine Water > Last Deglaciation Meltwater > Brackish Marine (Littorina/Baltic) Water > Fresh Water* (Laaksoharju et al. 2008, Smellie et al. 2008) (Notethat Last Deglaciation refers to the period 18,000 to 8000 BC). These waters are also basically similar to the ones characterising the SFR site but in rather different portions. For example, saline water (Cl > 6,000 mg/L) is not found, probably due to the relatively shallow depth of the groundwaters sampled (i.e. < –400 m.a.s.l.). In addition, fresh groundwater of present meteoric origin is almost absent because the SFR is located under the Baltic Sea. This fact has instead led to intrusion of Baltic Seawater in some of vertical fracture zones due to drawdown related to the present SFR tunnels.

3.2.3 Present conceptual model

In the context of geological time scales, fluid inclusions in calcite of Palaeozoic origin show the presence of very saline (around 20 wt%) mainly Ca-Cl fluids (Sandström et al. 2008). It can be assumed, therefore, that during the Late Palaeozoic when several kilometres of marine and terrestrial sediments covered the Precambrian Shield area of southeast Sweden, brine solutions were formed saturating both the fractures and eventually the interconnected pore spaces in the underlying crystalline bedrock. The present non-marine saline water may still contain components of this original brine water.

Of greater importance for the present groundwater chemistry at the SFR is the evolution during the Weichselian and Holocene times. Figure 3-3 a shows a tentative distribution of groundwater types and salinity gradients in the SFR area before the intrusion of the last deglaciation meltwater just prior to the Holocene. Based on an understanding of the climatic changes that have occurred since the last deglaciation, it is logical to presume that there must have been at this time old meteoric waters comprising components derived from both temperate and cold climate events. These waters would have intruded the bedrock and have had long periods of time to interact with the minerals. Assuming there were favourable gradients, old meteoric waters could have been partially mixed with deeper, more saline groundwaters, but the high density contrast would have prevented further mixing. What can be said with confidence is that the residual old brackish waters in the Forsmark region do not have a marine signature. In the SFR model volume the old non-marine water has been mixed with glacial water from the last deglaciation (Figure 3-3 b); the largest components of glacial waters are found between –100 and –300 m.a.s.l.

During the subsequent Littorina Sea stage (Figure 3-3 c) the SFR area was covered by brackish marine water assumed to be at around 6,500 mg/L Cl (Pitkänen et al. 1999, 2004). This maximum salinity (twice the present salinity of the Baltic Sea) lasted at least between 4500 and 3000 BC. Due to the unstable density situation generated by the higher density Littorina Seawater located over previously infiltrated last deglaciation meltwater of lower density, the Littorina Seawater entered the deformation zones and fractures and mixed/displaced the previously resident fresh water of glacial and old meteoric character.
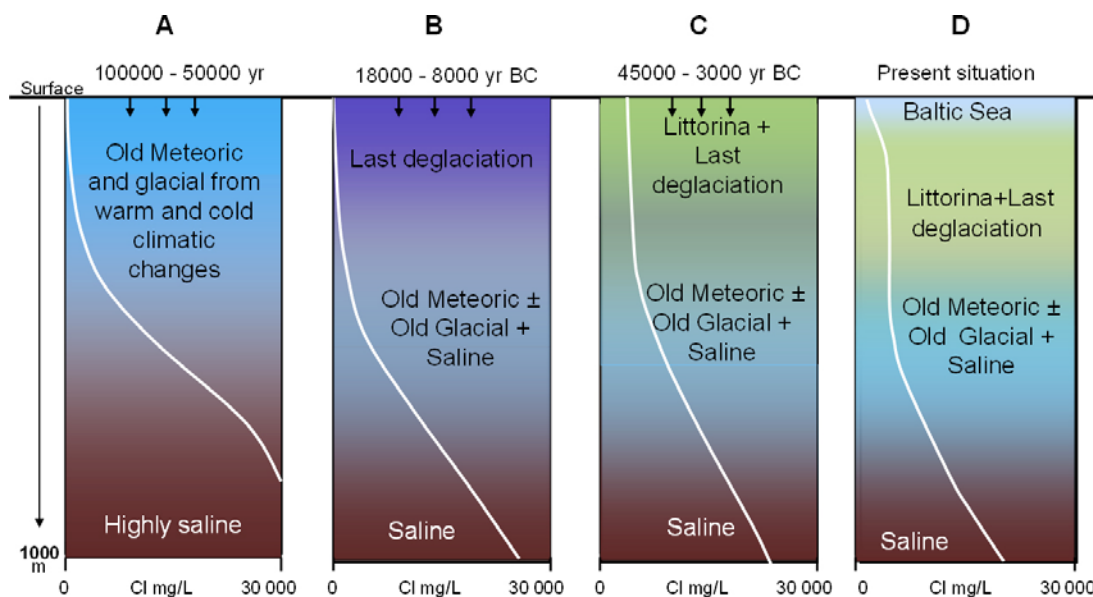
Figure 3-3. *Sketch showing tentative salinities and groundwater-type distributions versus depth for the transmissive deformation zones at the SFR. From left to right: a) situation prior to the last deglaciation, b) last deglaciation and intrusion of Late Weichselian meltwater, c) the Littorina Seawater penetration caused by density intrusion, and d) the present situation with possible penetration of local Baltic Seawater.*

The present situation is shown in Figure 3-3 d, which illustrates the intrusion of present Baltic Seawater in some fractures down to about –100 m.a.s.l. This intrusion is probably to a large extent driven by the hydraulic gradient created by the existing SFR storage facility.

The above description is valid generally for most areas in the Forsmark bedrock where first the last deglaciation meltwater, then later the brackish marine (Littorina Sea) water, and finally present Baltic Seawater, have been introduced. Further conceptual development of the Forsmark area, for example, future land uplift processes, are described in Söderbäck (2008) and Tröjbom et al. (2007).

3.3   Groundwater types used in the SFR modelling

3.3.1   Subdivision into groundwater types

Based on these palaeoclimatic considerations, and in order to facilitate the description and interpretation of figures and diagrams presented in Chapter 5, a subdivision into different water types is preferred. The same approach was used within the site modelling (e.g. Smellie et al. 2008) at Forsmark. However, from a compilation of all available data from the SFR local model volume, and the earlier gained data set from the Forsmark site investigations, it can be concluded that (cf. Figure 3-4 a–d):

1) The range in chloride concentration of the SFR groundwaters is small (1,500 to 5,500 mg/L Cl) compared with the Forsmark site investigation area (50–16,000 mg/L Cl), but the $\delta^{18}O$ values show similar variation (–15.5 to –7.5‰ V-SMOW) compared with Forsmark (–16 to –8‰ V-SMOW).

2) The SFR data set covers depths down to about –250 m.a.s.l. with two single sampling locations at –300 and –400 m.a.s.l. (the late sampling in KFR104 included).

3) Fresh meteoric water components (present precipitation type) are suggested to be minor.

4) Marine indicators, such as Mg/Cl, K/Cl and Br/Cl ratios, show relatively large variations especially considering the limited salinity range and the shallow depth of sampling, and it can be suspected that components of both the more saline Littorina Seawater and the more diluted present Baltic Seawater are present.
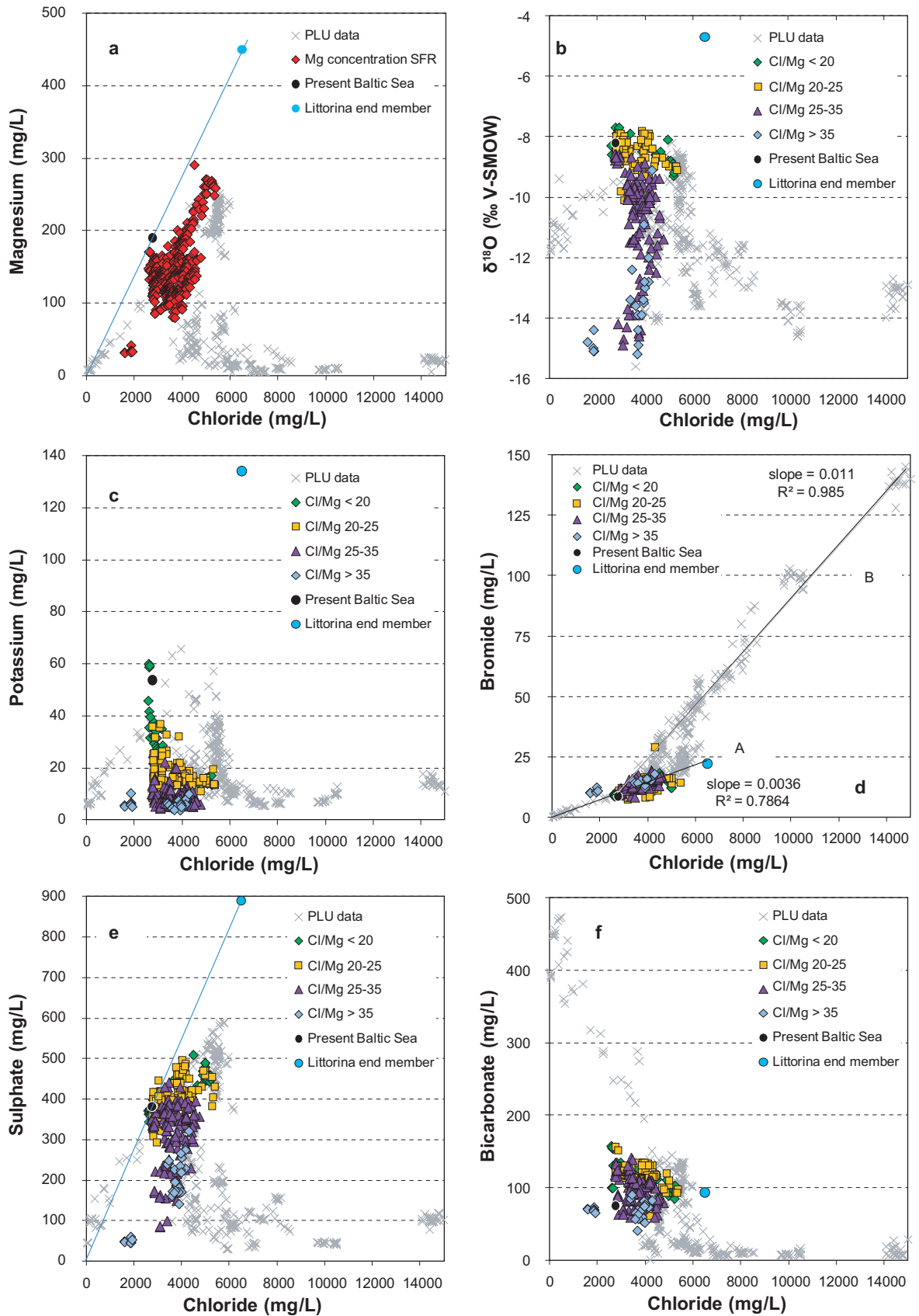
Figure 3-4 a–f. *Distribution of magnesium, δ¹⁸O, potassium, bromide, sulphate and bicarbonate versus chloride concentration in the SFR and Forsmark site groundwaters (PLU data) indicated by grey crosses in the plots. Figures 3-4 b–f show the groundwater samples categorised according to the Cl/Mg weight ratio. Plot (a) show dashed lines representing the marine Mg/Cl ratio, plot (b) includes the typical marine (A) and non-marine (B) Br/Cl ratios, and plot (e) includes the marine SO₄/Cl ratio.*

Based on these observations, coupled to the need to separate groundwaters of different origins and residence times in the bedrock, a subdivision of the groundwaters different from the one applied during the Forsmark Site investigation is nessessary. In contrast to the situation at Forsmark where the aim of the hydrogeochemical programme was to give a description of the undisturbed conditions in the bedrock, the SFR samples cover a time span from 1986 to 2010 during which the entire SFR facility has been constructed and is now in operation. The present groundwater chemistry is influenced by the drawdown to the tunnel which will be important in some of the sampled sections where inflow of Baltic Seawater can be expected. In other bore-hole sections changed hydraulic conditions have led to a significant mixing of different groundwaters, whilst other borehole sections have remained unaffected and show a stable groundwater chemistry throughout the operational phase of the SFR.

From the Forsmark site investigation it was recognised that variation in Cl and Mg contents, together with $\delta^{18}O$, can describe the various grundwater types (Laaksoharju et al. 2008). The observed variations in magnesium ranged from high concentrations close to 300 mg/L for the most saline marine groundwaters, to concentrations around 10 mg/L for non-marine older waters of equal salinity. In Figure 3-4 a, Mg is plotted versus Cl for all samples from the SFR and Forsmark, in addition to values for the present Baltic Sea and suggested values for the Littorina Sea, cf. Pitkänen et al. (2004). From this plot it is evident that the SFR samples, in common with the Forsmark samples, show a large variation in Mg for groundwaters with similar Cl contents. However, almost all of the SFR and Forsmark samples are somewhat depleted in magnesium compared to the initial marine ratios indicated by the line representing the marine Mg/Cl ratio, due primarily to ion exchange reactions lowering the Mg value in the groundwater. Furthermore, all SFR samples contain elevated magnesium concentrations (all are above 25 mg/L and the majority are above 70 mg/L) compared to the Forsmark non-marine groundwaters which indicate that the SFR ground-waters contain at least a minor marine water component. There is no attempt, or any clear evidence, to suggest that these somewhat elevated Mg contents reflect an alternative source(s). Therefore, Mg can be regarded as a useful indicator of marine waters in the Forsmark area including SFR and a set of scatter plots with the samples colour coded according to their Cl/Mg weight ratio were prepared and integrated with plots of Cl versus $\delta^{18}O$, Br, HCO_3, SO_4, and K (cf. Figure 3-4 b–f). From Figure 3-4 e it is evident that SO_4 versus Cl shows the same major trends as Mg versus Cl, which indicates that SO_4 is also an excellent tracer of marine conditions, However, unfortionately in the early analyses there was a larger uncertainty in the SO_4 measurements and therefore the Mg/Cl ratio has been preferred.

None of the plots show a simple two component mixing behaviour. Instead, it is obvious that input from at least three different water sources are needed to explain the measured groundwater chemistry of the SFR samples: 1) Brackish marine water similar to the present Baltic Sea, 2) Brackish marine water with a salinity higher than the present Baltic Sea; based on the conceptual understanding of the area (cf. Section 3.1) this is a component of Littorina Seawater, and 3) Brackish water of partly non–marine origin with a significant glacial meltwater component.

Plotting the two conservative parameters Cl and $\delta^{18}O$ resulted in a separation of the above given three water types and thereby suggested a possible method of subdivision. However, a great number of samples still showed a mixed origin and it was therefore necessary to introduce a fourth water type, here referred to as a Mixed transition groundwater type, and a satisfactory subdivision was obtained (cf. Figure 3-5). See Table 3-2 below where the different groundwater types with given compositions in terms of Cl, Mg and $\delta^{18}O$ are described together with their colour codes.

Whilst the present method to subdivide the SFR groundwaters into different types to achieve better understanding has been broadly successful, the complexity of the hydrogeochemical system has given rise to some anomalies. In Chapter 5 some sample/data points seem to deviate from the other samples representing the same groundwater group. The most common explanations for these anomalies include erroneous analytical concentrations (e.g. especially early on in the sampling during 1986–87) and sudden isolated increases/decreases in components in an otherwise long term stable groundwater environment. In order to further test this groundwater subdivision based on expert judgement, a principal component analysis of the groundwaters was also carried out (cf. Section 3.3.2 below).
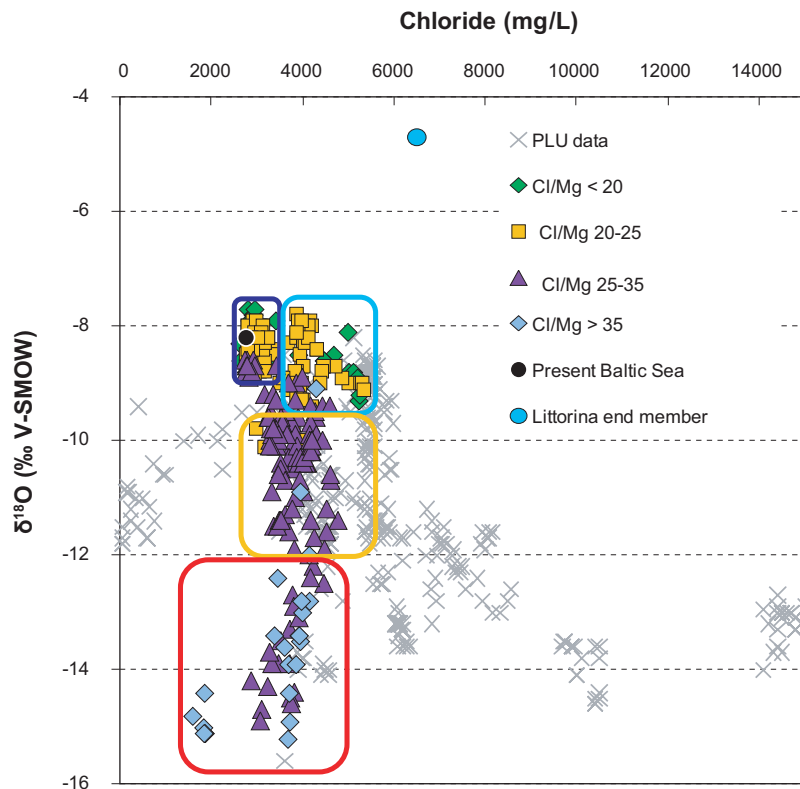
Figure 3-5. *Plot of δ¹⁸O (‰ V-SMOW) versus chloride concentration. PLU data includes data from the Forsmark site only. The figure shows the groundwater samples categorised according to the Cl/Mg weight ratio and the boxed areas signify different groundwater types. There is a continuous mixing line between the Baltic and the Littorina type groundwaters. However, a limit between Local Baltic groundwater type and Littorina type is set at a chloride concentration equal to 3,500 mg/L.*

Table 3-2. Presentation of groundwater types used to categorise groundwater samples from the SFR site.

Local Baltic Sea type groundwater ■

Water type: Brackish marine water with a Cl content of 2,500 to 3,500 mg/L and δ¹⁸O at –9 to –7.5‰ V-SMOW; Na-(Ca)-(Mg)-Cl-SO$_4$ in type. This is a brackish water with a Cl/Mg weight ratio < 27 (with a few exceptions) indicating a marine origin which is further supported by the contents of sulphate and potassium and the Br/Cl ratio. Some modification of this water has occurred caused by ion exchange and microbial reactions which has resulted in the lowering of Mg, K, Na and SO$_4^{2-}$ and enrichment of Ca and HCO$_3^-$ compared with the Baltic Sea. However, the Cl and δ¹⁸O ranges correspond to that of Baltic Seawater sampled off the coast at the SFR. Some samples referred to as the Local Baltic Sea type also contain components of Littorina and glacial water types. The Local Baltic Seawaters are the youngest waters present at the SFR.

Littorina type groundwater with a glacial component ■

Water type: Brackish marine water with a Cl content of 3,500 to 6,000 mg/L and δ¹⁸O at –9.5 to –7.5‰ V-SMOW; Na-Ca-(Mg)-Cl-SO$_4$ in type. This water type has a higher salinity than the present Baltic Sea and is commonly found in the Forsmark area to the west. The Cl/Mg ratio is generally < 27, but exceptions do occur. The sulphate concentration and Br/Cl ratio support a marine origin for the saline component. The potassium concentration is increased but not as high as in the Local Baltic Sea type of groundwater. The Na/Ca ratio is decreased compared with the marine ratio. These changes are due to ion exchange but also to dilution from the contributing glacial meltwater. The Littorina type of groundwater previously observed during the site investigations at Forsmark was often more saline and showed similar potassium concentrations as the Baltic Seawater. The depleted δ¹⁸O values compared to the Littorina end member (–5‰ V-SMOW), indicate a significant component of glacial water probably from the last deglaciation. Some samples may also contain portions of Baltic Seawater.

Brackish-glacial type groundwater ■

Water type: Brackish-glacial water: Na-Ca-Cl groundwater with a Cl content of 1,500 to 5,000 mg/L and $\delta^{18}O$ < –12.0‰ V-SMOW: Na-Ca-Cl in type. This water type has low Mg (Cl/Mg ratio > 32) and K, has higher Br/Cl ratios than marine waters, and is usually relatively low in SO_4 and HCO_3. It is a mixture of glacial (last deglaciation or older) + brackish non-marine water ± Littorina. The marine signature is generally weak and the Br/Cl ratio deviates from that of marine waters. The brackish-glacial waters are the oldest present at the SFR and the amounts of post-glacial components are small.

Mixed brackish transition type groundwater □

Water type: Brackish water with a Cl content of 2,500 to 6,000 mg/L and $\delta^{18}O$ at –12.0 to –9.5‰ V-SMOW: Na-Ca-(Mg)-Cl-(SO_4) in type. The waters in this group result from the mixing of the above three groundwater types (the mixing may either be natural or artificially created by the drawdown caused by the SFR repository or during the drilling and sampling procedures). Most of these waters contain components of brackish marine waters (maybe of different ages but mostly Littorina in type) + glacial waters (from the last deglaciation or older) ± weakly brackish waters.

Note: The groundwater types described above should not be mistaken for the end members (original waters) used in, for example, the M3 calculation representing original compositions (i.e. glacial meltwater, Baltic Seawater etc). Therefore, when using and describing the groundwater types it is important to remember that, for example, the Littorina type groundwater is a mixture of different groundwaters with a significant (dominating) component of Littorina Seawater. However, no groundwater samples with Cl and $\delta^{18}O$ contents typical for the original Littorina Sea (6,500 mg/L and 5‰ V-SMOW) have ever been found in the bedrock. Instead, all the "Littorina type groundwaters" have at least components of both the Littorina Seawater and glacial meltwater and in many cases also small portions of brackish non-marine waters of largely unknown composition, or even of recent Baltic Seawater. This is also the case concerning the other water types.

3.3.2 Principal component analysis of water types

Each sample in the general data table has been assigned by expert judgment to one of the four groundwater types described above, together with Baltic Sea samples from near the SFR (black symbols), and these samples have been used in the Principal component analyses (PCA) (cf. Gimeno et al. 2011 for details).

Figure 3-6 shows three principal component projections of the complete dataset using the same colour code for each sample as in Section 3.3.1, and using Cl, SO_4, δ^2H and $\delta^{18}O$ as input compositional variables (cf. Section 5.3). The first principal component (axis labelled "Component 1" in Figure 3-6) stores information on the "depletion" of the isotopes (isotopically depleted samples plot on the left and enriched samples on the right); the second component carries information on TDS (very dilute samples plot in the lower part of the axis and less dilute ones in the upper part); the third refer to sulphate concentration (with low SO_4 samples plotting in the upper part and high SO_4 samples in the lower part); and finally component 4 carries information on the isotopic ratio (samples with a high $\delta^2H/ \delta^{18}O$ ratio plotting in the lower part of the axis and samples with a low ratio in the upper part).

Lines have been added to these three graphs marking the boundaries between the groundwater groups; they actually represent planes in the three-dimensional volume. The top graph (plotting component 1 against component 2) has three lines; one marks the boundary between the Glacial (red) and Transitional (yellow) water types; other marks the boundary between the Transitional and the Littorina+Baltic water types; and the last one (horizontal) marks the boundary between the Littorina and the Baltic water types. The middle and bottom graphs in Figure 3-6 only have two lines; one marks the boundary between the Glacial and the Transitional water types, and the other marks the boundary between the Transitional and the Littorina+Baltic water types.

These lines have been drawn to minimise the number of colour (i.e. water type) changes with respect to the original grouping. In other words, the position of the lines is such that it separates the groups (by statistical means) matching as close as possible the previous types (defined by expert judgment). As Table 3-3 shows and Figure 3-6 confirms, only a very small number of samples belong to a different groundwater type depending on methods.

Table 3-3. Samples with reassigned water type.

ID Sample	ID code	Sample Number #	Old water type	New water type
22	KFR01	13948	T	B
51	KFR01	17034	L	T
57	KFR01	17074	T	L
61	K FR01	12651	T	B
107	KFR04	13957	T	L
117	KFR08	3219	B	T
135	KFR08	17000	B	T
256	KFR13	12663	L	T
265	KFR55	3204	L	T
314	KFR7A	16585	T	L

B = Local Baltic type, L = Littorina type, T = Mixed transition type, G = Brackish-glacial type.

In addition to the ten samples shown in in Table 3-3, three (ID samples: 216, 254, and 324) are virtually on the line separating two groups and thus their type could be either one (Transition or Littorina) and two other samples (40 and 312) have an anomalous composition (very high SO_4 concentration for their Cl content) and analytical problems may be the explanation (cf. their anomalous position in the middle graph of Figure 3-1). The ten samples (out of 375) with a suggested "reassigned" water category by PCA, confirms the quality of the initial categorisation. After a recheck of these samples it was decided to retain the initially given water types. This was because; 1) most importantly the waters were close to the border between different groundwater types and could as well be one or the other, or 2) deviating values for one of the components used in the PCA (most often sulphate) due to erroneous analysis or uncertain values.

Figure 3-6 identifies several samples with very low Cl contents (ranging from 1,610 to 1,880 mg/L), whereas the next less dilute sample in the dataset has a Cl content of 2,465 mg/L. In fact, as will be seen below, this group of samples can not be easily explained as a mixture of any of the selected end-member waters, and it is therefore indicated that they have been isolated for a very long time.

Figure 3-7 shows again the PC1 vs PC2 projection but now the position of the end members has also been added. Two views of the PC1-PC2 plane are shown; graph (a) shows the complete dataset, with the extended y-axis to include in the plot the Deep Saline end member whose component-2 coordinate (+15) is much larger than that of any sample in the dataset. In this plot, the cloud of sample points has a linear shape which is suggestive of a binary mixing between the Littorina and Glacial end members, or between the Local Baltic and Glacial end members. As will be quantitatively shown in Section 5.4, this is true for a subset of samples in the SFR dataset. However, if the scale of the y-axis is changed (graph b in Figure 3-7), omitting the Deep Saline end member, the picture that emerges is more complex. Now the cloud of sample points is no longer a "line" but an "area". This is suggestive that the chemical composition of the SFR groundwaters is actually the result of a complex mixture of three or more end members. These preliminary observations are fully substantiated in Section 5.4.
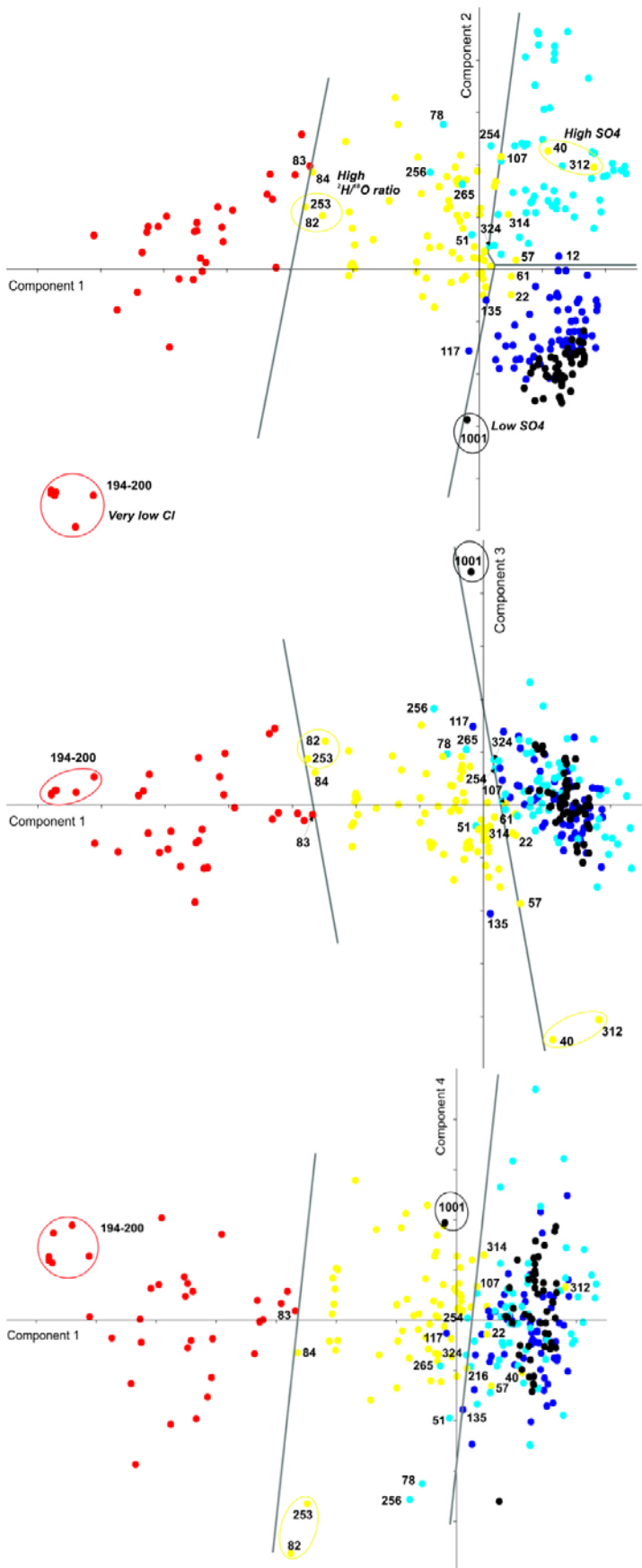
Figure 3-6. *Three PC projections (all with the first principal component as the horizontal axis) showing the boundaries between groundwater types. Samples plotting in the wrong PC area are labelled. Also labelled are several samples with anomalous compositions (encircled). The PCA has been performed with Cl, SO$_4$, δ^2H and $\delta^{18}O$ as input variables.*
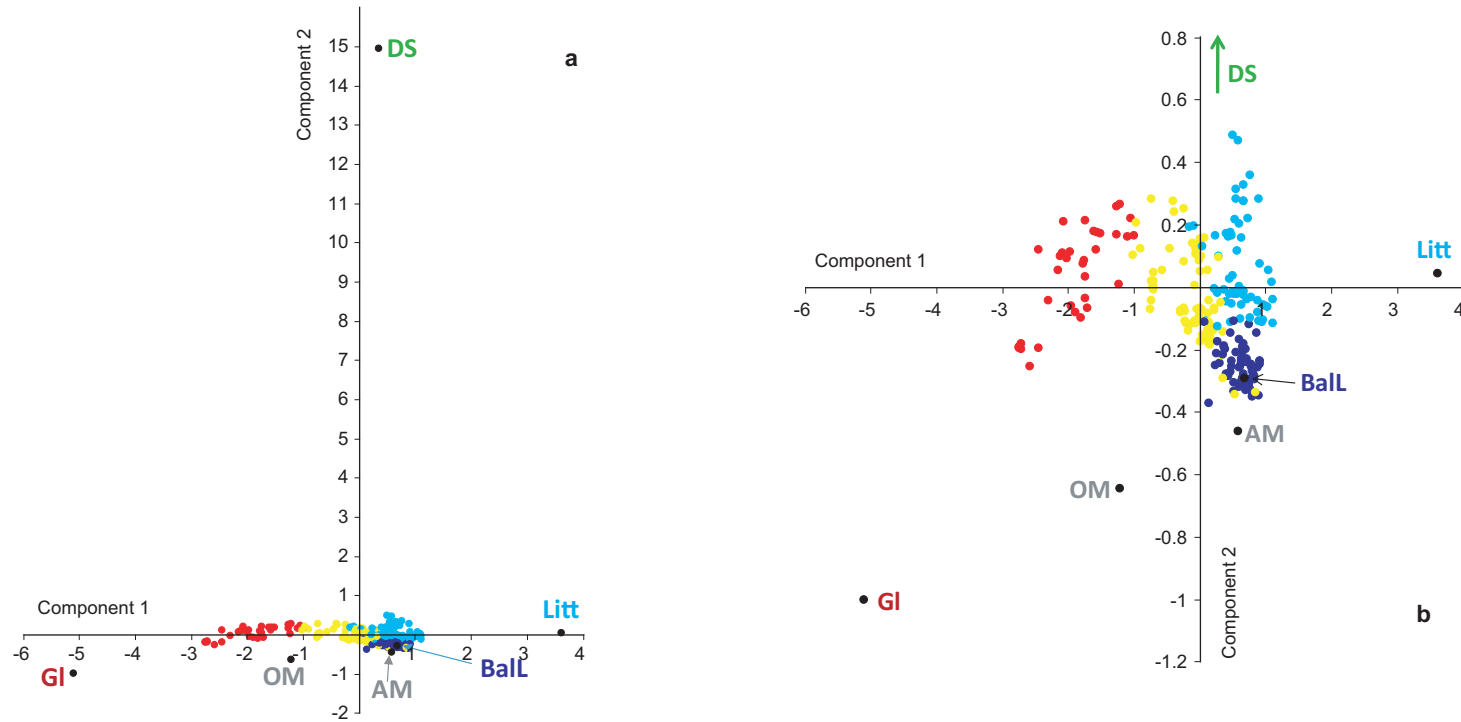
Figure 3-7. *Location of the end members Deep saline (DS), Littorina (Litt), Glacial (Gl) Local Baltic (BL), Altered Meteoric (AM) and Old Meteoric (OM) in the Principal Components plane defined by component 1 (x axis) and component 2 (y axis) for the SFR groundwaters. Plot (a) has an extended y-axis to include the position of the Deep Saline end member whose component-2 coordinate is +15, much larger than any of the water samples. In this graph, the cloud of sample points has a linear shape suggesting a binary mixing between the Littorina and Glacial end members, or between the Local Baltic and Glacial end members. However, if the y-axis scale (plot b) is expanded, omitting from the plot the DS end member, the cloud of sample points adopts a more complex shape, suggestive of a mixture of at least three, and probably more, end members. The difference between this figure and Figure 3-6 is the inclusion of the end members and the exclusion of the Baltic Seawaters; this has slightly changed the position of the samples. The PCA has been performed with Cl, SO_4, $\delta\,^2H$ and $\delta\,^{18}O$ as input variables.*

4 Hydrogeochemical data

4.1 Databases

The dataset forming the basis for the modelling stage version 1.0 in the SFR extension project contains quality assured data from the recent investigation phase in the target area southwest of the repository (Jönsson et al. 2008, Thur and Nilsson 2009a, b, Thur et al. 2009, Lindqvist and Nilsson 2010) as well as from earlier studied boreholes in the present SFR facility (Nilsson A-C 2009), from three Forsmark boreholes (Gustavsson et al. 2006) and from complementary investigations in the present SFR in the autumn of 2010 (Nilsson K 2011). The main part of the data consists of basic groundwater analyses including isotopes, although a few gas, microbe and redox data are also available. Quality assured data were extracted from the Sicada database (Sicada-10-077 (0:1)) and complemented with late data (Sicada-11-056 (0:1)) and compiled to produce the Hydrogeochemistry Data Table version 1.0. This data table, in Excel format, is used for all the interpretation and model-ling work and is stored in the SKB model database SKBDoc for traceability. A general evaluation of hydrogeochemical data from the early SFR boreholes and information on detection limits and measurement uncertainties, is presented in (Nilsson A-C 2009). The consistency checks, in order to establish a reliable set of major constituent concentrations for each of the samples included in the version 0.2 modelling (Dataset I) and also to justify rejection of some of the samples (Dataset II), are presented in (Nilsson et al. 2010a).

The data (values) from Sicada were not changed, only the data structure, during the procedure to compile the table, unless errors or questionable data were discovered. If so, the same changes or comments on data were also introduced in Sicada. Furthermore, complementary informa-tion on deformation zones, flow anomalies and hydraulic transmissivities (approved geological deformation zone model and quality assured data from Sicada) were included in the table and some groundwater samples were commented upon or explained. The samples/records were categorised according to quality (categories 1 to 5) and divided into two sheets; Dataset I (suitable for model-ling, i.e. categories 1 to 4) containing 368 samples and Dataset II (unsuitable for modelling, i.e. cat-egory 5) including 160 samples. Most borehole sections represented in Dataset II have also quality assured data from other sampling occasions in Dataset I. Exceptions are boreholes KFR27 (sampled during drilling) and KFR83 (possibly affected by grouting). These boreholes are not represented in Dataset I. The sample quality assessment into the five categories is presented in Appendix 1 and the contents of Dataset I and II are accounted for in Section 4.3.4.

4.2 Available data

The compiled dataset to be used for the SFR-extension modelling work includes:

1) Groundwater data from the hydrogeochemical investigation programme in the SFR extension project comprising a total of 15 borehole sections in five cored drilled and three percussion boreholes (cf. Table 4-1).

2) Groundwater data extracted from the SKB database Sicada related to the period 1984 to October 2010; altogether a total of 45 borehole sections in 18 early boreholes drilled from the SFR tunnel system (cf. Table 4-2).

3) Data representing three boreholes from the site investigations in Forsmark located within the SFR extension regional model volume (cf. Figure 4-1). NOTE: In this report, data values from one of the three Forsmark boreholes, KFM11A, were omitted from the interpretation and modelling work (cf. Section 1.5.2). However, the identified water type of the groundwater sampled in the upper section has been displayed in 3D visualisations. It is most likely that this groundwater belongs to the brackish groundwater type although the water composition is not stable.

Twelve potentiometric Eh values are available from logs of on-line Eh measurements for seven different borehole sections. Other available redox sensitive data for the SFR include total Fe, Fe(II), S(-II), Mn, N(III), N(V), N(III)+N(V), N(-III) and U concentrations for a limited amount of the groundwater samples in the dataset.

Furthermore, gas data including gas compositions (N_2, H_2, CO_2, O_2, Ar, CH_4, He, CO, C_2H_2, C_2H_4, C_2H_6 and C_3H_8) and the total gas volume are available from boreholes KFR01, KFR10, KFR7A, KFR105, KFR08 and KFR19.

Microbiological data (including in this term the determinations of total number of cells, concentration of ATP, number of cultivable, heterotrophic aerobic bacteria, and most probable number of cultivable metabolic groups, i.e. iron, manganese, sulphate and nitrate reducing bacteria, as well as acetogens and methanogens) are available for two sections in the borehole drilled from the SFR tunnel system (KFR105). For other borehole sections (KFR01 at 44.5–62.3 mbl, KFR10 at 0.0–107.28 mbl and KFR7A at 48.0–74.4 mbl) data from year 2000 on total number of cells are available.

Most of the available pH data were measured in the laboratory and this situation may represent a serious uncertainty in redox pair modelling and speciation-solubility calculations. Field measurements of pH have been conducted only in the recent investigations in the SFR extension project, in the three boreholes from the Forsmark site investigations and during the complementary groundwater sampling in the early SFR boreholes in October 2010. A sensitivity analysis of the effect of pH on the modelling is presented in (Gimeno et al. 2011).

Table 4-1. Available data (2006–2011) from the SFR extension boreholes and the site investigations at Forsmark (Hydrogeochemistry data table version 1.0, Dataset I (cf. Section 4.3)). The number of samples as well as available redox measurements, gas analyses and microbe determinations are indicated.

Idcode	Secup (mbl*)	Seclow (mbl*)	Elev.secmid (m.a.s.l.)**	No. of samples***	Eh (years)	Gas (years)	Microbes (years)
SFR extension project							
HFR101	107.3	197.0	**−136.80**	6			
HFR105	55.6	120.0	**−75.40**	3			
HFR106	36.0	41.0	−31.36	3			
	175.0	190.4	−146.90	3			
KFR101	279.5	341.8	−240.15	8			
KFR102A	214.0	219.0	−194.64	5			
	423.0	443.0	−388.97	5			
KFR104	333.0	454.6	−306.50	3	June 2011		
KFR105	4.0	119.0	−117.42	4			
	120.0	134.0	−128.38	5	2009	2009	2009
	138.0	169.0	−132.73	4			
	170.0	264.0	−142.94	4			
	265.0	306.8	−153.59	10	2009, 2010	2009	2009
KFR106	143.0	259.0	−187.20	3			
	260.0	300.0		3			
Forsmark data							
HFM34	0.0	200.8	−82.92	3			
HFM35	*0.0*	*200.8*	*−78.24*	*3*			
KFM11A	*447.5*	*454.6*	*−389.68*	*7*	Excluded from evaluations and interpretations.		
	446.0	*456.0*	*−389.62*	*4*			
	690.0	*710.0*	*−593.76*	*7*			

*mbl = metre borehole length.

** Elevation for the midpoint of the borehole section (or, in bold font, the flow anomaly position).

***Including laboratory measurements as well as field measurements of pH and EC for samples in the SFR extension project and from the site investigations in Forsmark.

Table 4-2. Available data (November 1986–October 2010) from the early SFR boreholes (Hydrogeo-chemistry data table version 1.0, Dataset I (cf. Section 4.3)). The number of samples as well as available redox measurements, gas analyses and microbe determinations are indicated.

Idcode	Secup (mbl*)	Seclow (mbl*)	Elev.secmid (m.a.s.l.**)	No. of samples***	Eh, pH_F (years)	Gas (years)	Microbes (years)
KFR01	11.0	43.5	−71.58	4			
	44.5	62.3	−94.23	42	1987, 2000	2000	2000
KFR02	43.0	80.0	−146.93	5			
	81.0	118.0	−184.93	6			
	119.0	136.0	−212.93	6			
	137.0	170.3	−239.08	6			
KFR03	5.0	44.0	−106.87	4			
	45.0	56.0	−132.87	4			
	57.0	80.0	−150.87	5			
	81.0	101.6	−173.67	4			
KFR04	28.0	43.0	−111.48	6			
	44.0	83.0	−138.52	4			
	84.0	100.5	−166.29	4			
KFR05	57.0	79.0	−141.06	2			
	80.0	96.0	−159.86	2			
KFR08	6.0	35.0	−87.81	3			
	36.0	62.0	−90.29	5			
	63.0	104.0	−93.31	31	2010	2010	
KFR09	0.0	80.2	−80.94	2			
	63.0	80.2	−83.68	13			
KFR10	0.0	107.3	−116.23	14	1986, 2000	2000	2000
	87.0	107.3	−146.99	19			
KFR11	7.0	24.0	−89.19	1			
	25.0	39.0	−92.06	1			
	40.0	55.0	−94.75	1			
	56.0	98.1	−99.88	2			
KFR12	0.0	50.25	−112.25	1			
	20.0	33.0	−113.62	1			
KFR13	4.0	33.0	−141.84	2			
	34.0	53.0	−166.84	4			
	54.0	76.6	−188.64	4			
KFR19	3.0	50.0	−74.5	1			
	77.0	94.0	−60.43	4			
	95.0	110.0	−56.35	5	2010	2010	–
KFR20	0.0	109.7	−71.24	1			
KFR55	8.0	21.0	−128.34	4			
	22.0	39.0	−131.39	4			
	40.0	48.0	−133.97	4			
KFR56	9.0	81.7	−64.66	5			
KFR7A	2.0	19.0	−132.65	4			
	20.0	47.0	−133.46	1			
	48.0	74.7	−134.43	37	1987, 2000, 2010	2000, 2010	2000
KFR7B	4.0	7.0	−138.85	3			
	8.6	21.1	−147.59	5			
KFR7C	6.0	34.0	−152.19	4			

*mbl = metre borehole length.

** Elevation for the midpoint of the borehole section.

***Including laboratory measurements of pH and EC and pH_F measured 2010.

**** pH_F and Eh measured in a flow through cell at the borehole orifice.

Sampling date yyyy-mm-dd
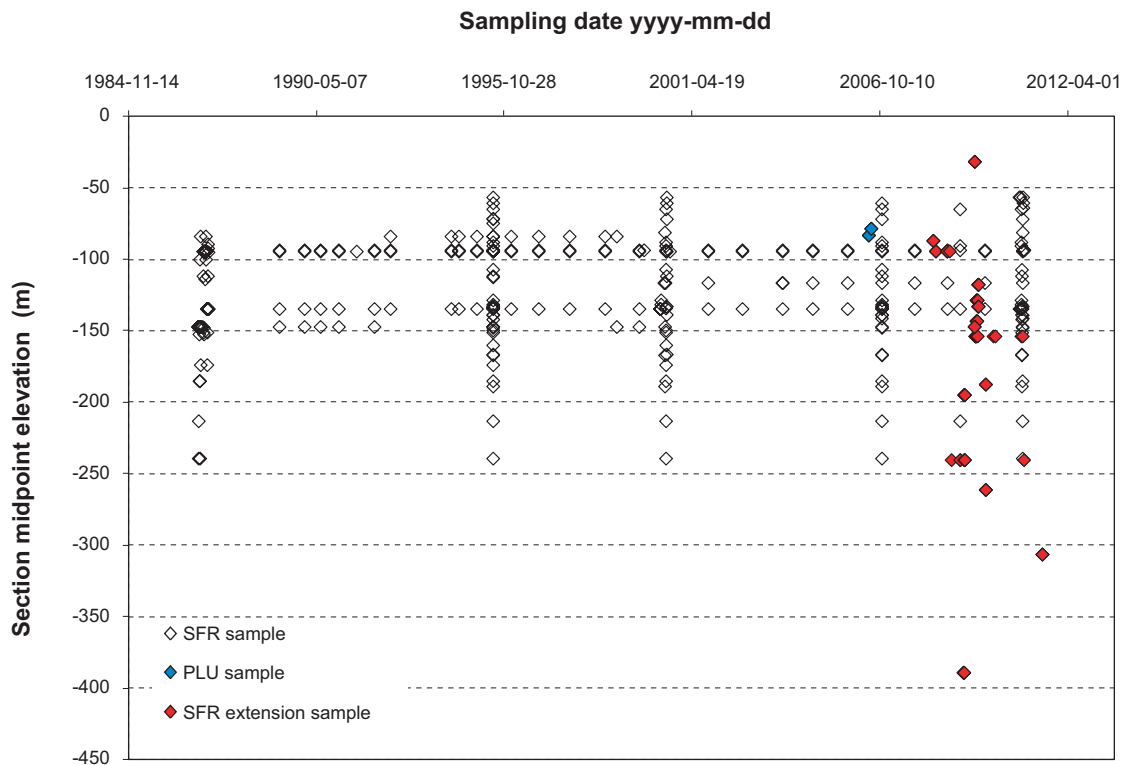
Figure 4-1. Sample distribution versus depth from 1986 to 2010. Samples are from boreholes HFM34 and HFM35 and the site investigation in Forsmark (PLU), together with the early SFR boreholes (SFR) and those within the SFR extension project (SFR Extension sample).

As can be seen from Table 4-2, the number of samples from each borehole section in the early SFR boreholes varies considerably and the sporadic sampling complicates evaluation of changes and trends. Furthermore, these data are obtained over a long period of more than twenty years and therefore relate to different development stages of the SFR. For example:

1. There are no groundwater chemistry data from the first drilling stage (1980–1981) prior to the commencement of the excavation phase, only hydrogeological measurements. These boreholes were drilled mainly from off-shore platforms and a few from shore and harbour locations.

2. Early quality assured data from before the operational stage of the repository (November 1986 to December 1987) are used to represent 'undisturbed conditions', i.e. not affected by the SFR operational phase starting in 1988 but possibly affected by the preceding excavation phase.

3. Data from 2006 and 2010 are used together with recent data from Forsmark and from the SFR extension project to present and describe the present day groundwater situation in the investigation area.

4. Data obtained between 1987 and 2006 as well as between 2006 and 2010. These data are used to support the interpreted groundwater conditions and to verify changes and trends.

4.2.1 Late supplementary data

Late supplementary data implies data obtained in the autumn of 2010 from complementary investigations within the SFR extension project (Nilsson K 2011), as well as from the regular annual control programme in the SFR. The interpretation and modelling work performed to produce the previous hydrogeochemical site description version 0.2 revealed the need for more data related to important issues such as redox conditions and residence times. Therefore, complementary investigations were performed in October–December 2010 which included:

- On line measurements of Eh and pH in three borehole sections in the early boreholes KFR19, KFR08 and KFR7A drilled from the present SFR tunnel system. The borehole sections were selected to represent the Local Baltic groundwater type (KFR19 and KFR08) and the Littorina groundwater type (KFR7A).

- Collection of sample series including a full isotope protocol in the same three borehole sections.

- Fracture mineral studies on drill cores from borehole sections where redox measurements have been conducted (cf. Section 2.1.4).

- Determinations of the isotopes carbon-13, carbon-14 and chlorine-36 in groundwaters from selected borehole sections in early SFR boreholes as well as in some new SFR extension boreholes (KFR101, KFR105).

- In addition, the annual sampling within the running control programme was conducted according to the extensive sampling protocol carried out each fifth year. This implies that all the water yielding early boreholes and borehole sections in the present SFR were sampled and the analytical protocol included basic water analyses, field pH measurements as well as the isotopes tritium, deuterium and oxygen-18.

Hydrochemical sampling in borehole KFR104 has been conducted even later (June–July 2011) and the analytical data were obtained during the review process of this report. These data are discussed in a separate inserted section in the report, Section 5.10.

Figure 4-2. Location of sampled boreholes/borehole sections in the SFR extension project.

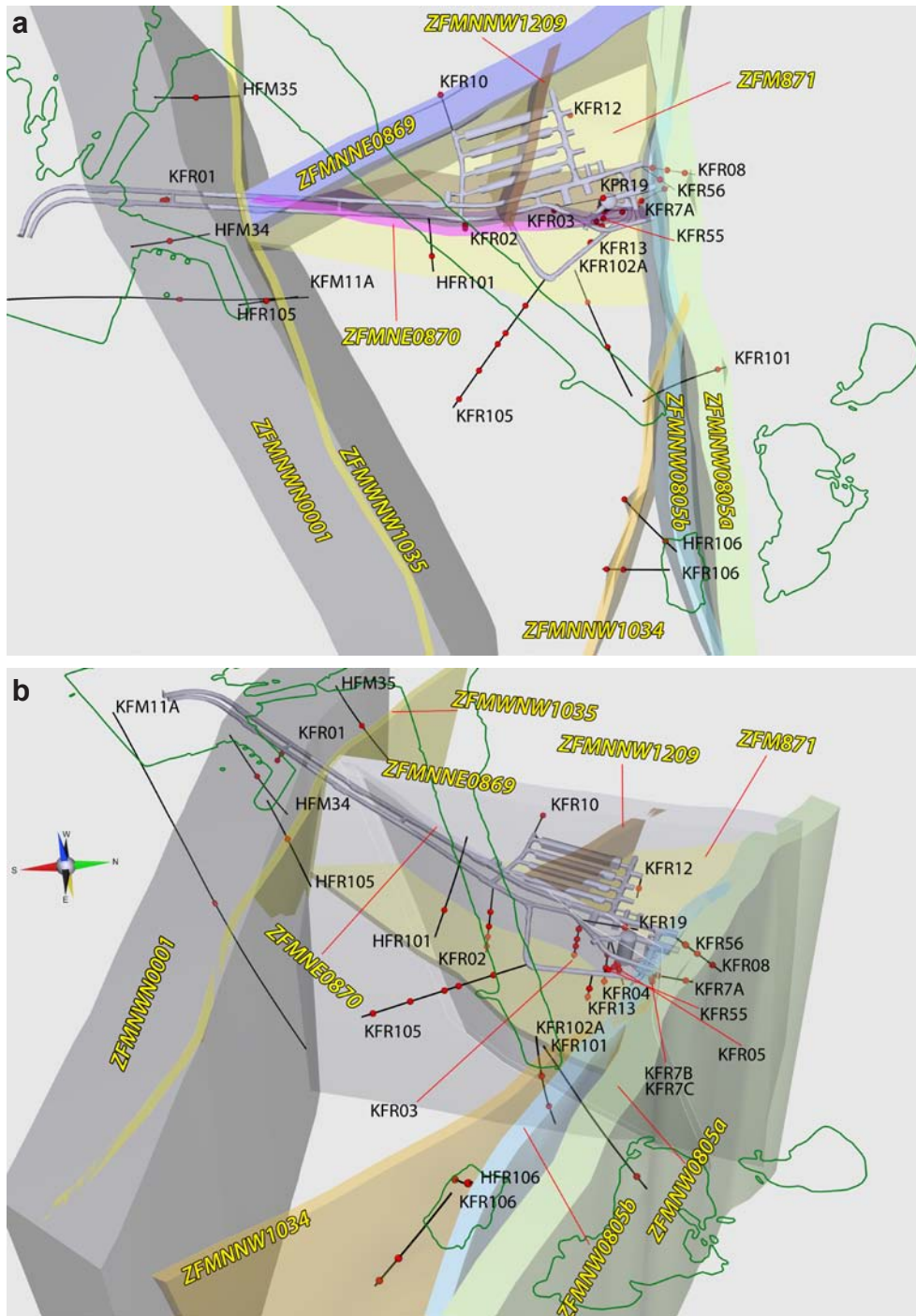***Figure 4-3 a, b.*** *Location of the sampled borehole sections in relation to major deformation zones; a) top view, and b) viewed from above and from the southeast. Three Forsmark boreholes (HFM34, HFM35 and KFM11A) are added to the figure. The centre of each section is given as a red ball and the zones are labelled according to present terminology. The green contour represents the coast line.*

4.3 Sample quality assessment and data selection

The groundwater dataset available for the hydrogeochemical interpretation and modelling work within the SFR SDM is based on more than twenty years of investigations and therefore is understandably inconsistent in several aspects. In addition, to interpret the changes in groundwater composition due to the presence of the SFR facility during this period is a special task not addressed in previous SKB site investigations. The dataset consists of; 1) data from the SFR (and to a minor extent Forsmark) site investigations in recently drilled boreholes, and 2) groundwater data collected during more than twenty years from boreholes drilled in the 1980's from the SFR tunnel system.

The first group of data generally constitute a short time series of three to four samples collected during continuous discharge of water from the borehole section in question, and the analyses were complete and carried out using modern and well documented techniques. The second group of data includes very few time series but numerous single samples collected annually from four borehole sections, and four to five times during the period 1986 to 2010 from the remaining 41 borehole sections. Furthermore, the number of analyses carried out for each sample varies.

The data have been evaluated and categorised into five sample quality categories using a similar approach as previously used for Forsmark and Laxemar (Smellie et al. 2008, Laaksoharju et al. 2008). The background, the criteria for the categorisation and the results from this sample quality assessment are presented in Appendix 1 together with trend plots with time (chloride, magnesium and $\delta^{18}O$ data) for each borehole and borehole section having more then three samples from different years.

The SFR site largely represents an anthropogenic mixing (e.g. by hydraulic drawdown effects) of different groundwater types and therefore, in contrast to the Forsmark SDM, it is not the natural conditions that are being described. In particular, the old SFR boreholes are influenced to different degrees by the present SFR facility. The system has been transient since the SFR construction and the hydraulic impacts from the presence of the SFR facility are expected to be more significant than other anthropogenic disturbances from, for example, groundwater sampling or hydraulic tests. Most of the early SFR borehole sections have been sampled on several occasions over a time period of more than twenty years, and generally show either a quite stable water composition or a clear trend due to changes in hydraulic conditions from the impact of the SFR repository. In addition to information on changes with time, the chloride, magnesium and $\delta^{18}O$ trend plots for each borehole (see Appendix 1) may to some extent verify the quality of the groundwater data (and also of the chemical analyses). From a total of 528 samples collected from the SFR boreholes during more than twenty years (between 1984 and December 2010), 368 samples were considered suitable for modelling (categories 1 to 4) and included in Dataset I, and 160 samples were judged as unsuitable (category 5) and included in Dataset II. In contrast to the Forsmark site investigation, category 4 samples were used also for modelling since it was considered important to include as much data as possible covering the entire time period. Categories 1 to 4 are not distinguished in the following evaluations and plots in this report. The content of Dataset II (mainly category 5 samples) and the reasons for classifying the data as unsuitable for modelling purposes are presented in Table 4-3.

Single questionable analyses and outliers do occur also in Dataset I which is evident from some of the plots in Chapter 5 and from Appendix 1. However, they are possible to identify and disregard and they are too few in number to obstruct the general trends. Since the data represent a long time period, further selection according to date was made in order to describe initial/early conditions as well as present groundwater conditions in Section 5.2.1.

Table 4-3. Content of Dataset II (sample quality category 5) and possible use of the data in this category.

No. of samples	Reason for exclusion	Comments and possible other use of the data
78	Samples collected during the first investigation phase from 1984 to 1986; large charge imbalances and scattered data (Nilsson A-C 2009).	None.
1	Other late samples having charge imbalances exceeding ± 5%.	None.
1	Sample confusion is suspected.	None.
5	Drilling water samples.	Useful for drilling water budget calculations and evaluation of possible contamination from drilling.
4	Samples collected during borehole drilling (KFR101, KFR102A and KFR27).	First strike samples from the three boreholes; however, the drilling water contents are high. One of the drilling samples was collected from borehole KFR27and is the only sample from this borehole.
7	Return water during drilling of KFR105	Useful for drilling water budget calculations and evaluation of possible contamination from drilling.
4	Samples with high pH values which probably reflect concrete grouting in galleries and tunnels (KFR83).	None, which means that useful data are missing from borehole KFR83.
46	Samples with very incomplete analyses.	None, values for several of the major constituents are missing.
12	Sample series from the two investigated sections in borehole KFM11A (Forsmark site) with very unstable water compositions (cf. Section 1.5.2).	Information from the upper section is used in 3D visualisations (Brackish-glacial groundwater type). This was used since it is most likely that representative groundwater from this location belongs to the brackish groundwater type although the water composition is not stable.
2	Samples from the upper and lower basin (note that the lower basin has been used as a drilling water source and three samples are included in the drilling water category above).	Documentation on the chemical composition of the inflow to SFR (cf. Section 2.3.1).
160	**Total number of samples in Dataset II.**	

5 Explorative analyses and modelling

Explorative analysis including initial data evaluation, mixing modelling using the software M3, speciation-solubility calculations and redox modelling as well as evaluations of microorganism, gas and fracture mineral data, where performed in order to describe the data and construct the conceptual model for the area presented in Chapter 6 (cf. also Section 3.3).

Since the approved dataset comprises a long time period (November 1986 –December 2010), the data in this chapter are used somewhat differently. The 3D presentations include new data from the SFR extension boreholes together with data from 2006 representing the early SFR boreholes. The selection of the complete dataset from 2006 to represent present conditions seems justified since most of the changes in the groundwater composition occurred prior to 2000 (cf. Nilsson A-C 2009 for time series of data). Furthermore, the conditions were proved to have been more or less stable since then by data obtained from sampling late in 2010. The x-y scatter plots, on the other hand, present all data in Dataset I from the entire time period 1986–2010, if not stated otherwise, and often data from Forsmark are included for comparison. Changes in groundwater composition with time are treated in Section 5.2.

5.1 Explorative data evaluation

5.1.1 Salinity distribution

The spatial distribution of the salinity was examined to provide an initial basic understanding of the hydrogeochemical conditions in the model volume. The electrical conductivity (EC) is a direct measure of the salinity in the groundwaters in the different boreholes/borehole sections. A three dimensional visualisation of the boreholes is presented in Figures 5-1 (a, b) showing the distribution of EC in groundwaters as viewed from above (a) as well as a side view (b) in relation to some of the major deformation zones. The displayed EC data were measured at two different occasions in each borehole using two different methods; 1) borehole measurements during PFL logging and pumping from a specific fracture, and 2) measurements in groundwater samples from investigated borehole sections. The EC data from the PFL logging were included to obtain a better data coverage of the model volume and a more complete picture. Some caution is needed in the interpretation since the values do not represent exactly the same conditions. However, in those cases where both measurements are available for the same part of the borehole, the values agree fairly well (within 15%). Some observations from the salinity distribution in the 3D Figure 5-1 (a, b) are listed below.

- The overall EC range at the SFR site (600–1,600 mS/m) corresponds to a chloride concentration of 1,500–5,500 mg/L down to a depth of about –400 m.a.s.l. In four boreholes, KFR101, KFR102A, KFR106, and KFR02, groundwaters with lower EC/Cl concentrations are found at greater depth than groundwaters with higher EC/Cl concentrations; this contrasts with the more common increase in salinity with depth normally recorded in bedrock groundwater environments. An extremly low EC value was measured in borehole KFR27 (110 mS/m); however, it is likely that this value is an artefact. Drinking water was used when enlarging the upper part of the borehole and most probably this water has contaminated the bottom part due to the drawdown/ lowered pressure caused by the SFR. The present hypothesis for the mechanism behind this contamination is presented in Öhman et al. (2011).

- The highest EC values are found in early samples from boreholes KFR7A and KFR10 which intersect deformation zones ZFMNW0805A,B and ZFMNNE0869 (formerly Zone 8 and Zone 3), respectively. It is possible that these boreholes and the two zones also connect to zone ZFM871 (formerly Zone H2). At present the EC reaches a maximum of about 1,300 mS/m, although early samples from the two mentioned boreholes recorded EC values up to about 1,600 mS/m corresponding to about 5,500 mg/L Cl.

- The lowest EC value of 600 mS/m, corresponding to about 1,600 mg/L Cl (i.e. significantly lower than the present Baltic Sea), is found in borehole KFR101 at a depth interval of –240 to –262 m.a.s.l. associated with zone ZFMNW0805A (formerly Zone 8a). Chemical and isotope analyses from KFR101 confirmed a significant glacial meltwater contribution in this groundwater and contamination from meteoric water can be excluded in the borehole. A second late observation of this dilute groundwater was made in KFR104.
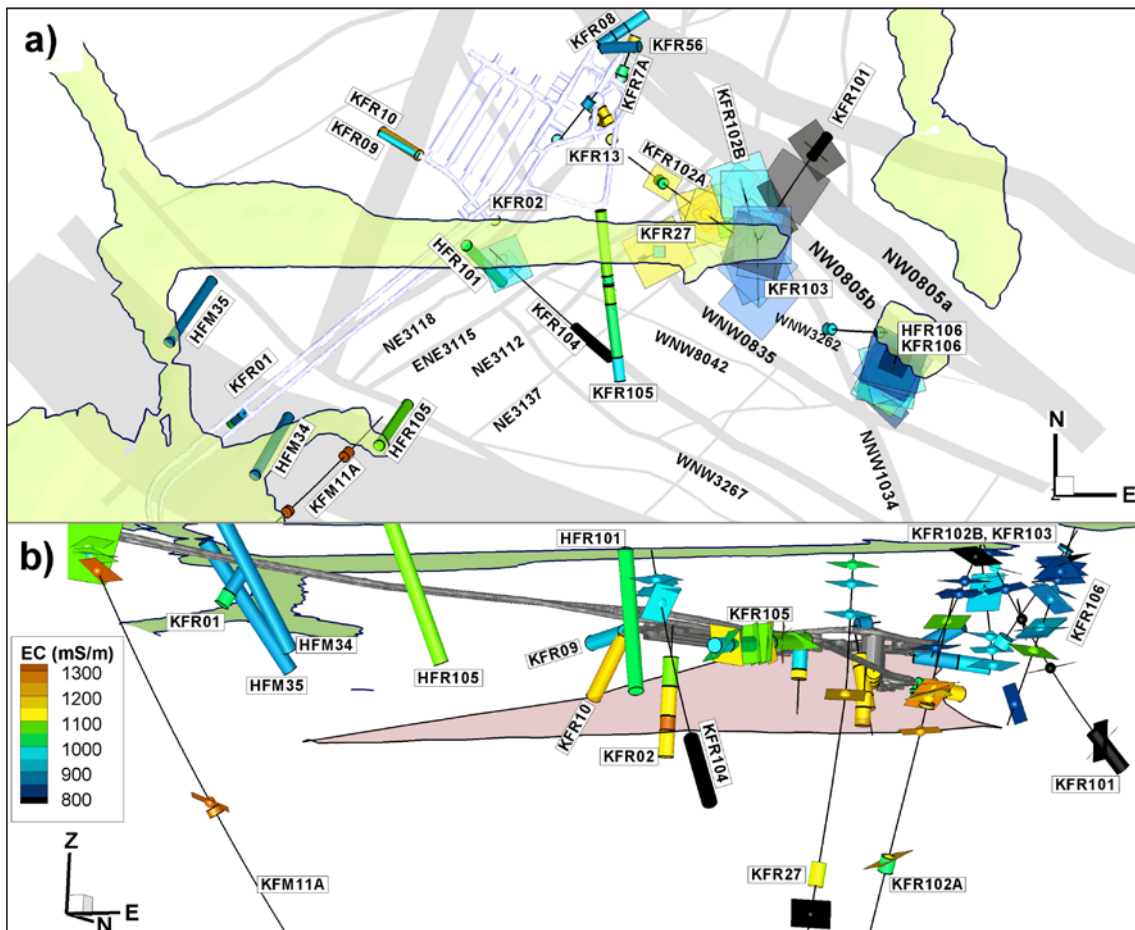
Figure 5-1. Electrical conductivity (EC) measurements; a) view from above, and b) side view. EC from PFL flow logging is shown as planes and EC from monitored borehole sections is represented as cylinders. A deep PFL logged interval in KFR27 (409.6 to 435.6 m borehole length) is also represented by a cylinder (Öhman et al. 2011). In Figure 5-1 a the deformation zones are indicated in grey, and in Figure 5-1 b the extension of the gently dipping zone ZFM871 is represented by a greyish pink colour.

5.1.2 Depth trends of selected major ions

Three important hydrochemical indicators (Cl, Mg and $\delta^{18}O$) were used for the subdivision of the groundwaters into different groundwater types (cf. Section 3.3). Plots of the dataset from 1986 to 2010 against elevation (two elevation ranges), showing also the groundwater types (colour coded), are given in Figure 5-2 (a–f).

Chloride (Figure 5-2 a, b) is one of the main components in these groundwaters and it is directly correlated with their salinity (cf. also Figure 5-1). The main hydrogeochemical data included in the SFR 1.0 version represent the depth range –20 to –400 m.a.s.l. (most data from shallow depths above –250 m.a.s.l.) where the chloride concentration varies between 1,600 and 5,500 mg/L. However, only a few data points are below 2,800 mg/L Cl (equal to the concentration of the present Baltic Sea) or exceeding 4,500 mg/L Cl (the typical Littorina type composition identified from the Forsmark Site investigation). All of the latter were observed prior to 1995 since impacts from the SFR facility have caused dilution with time. The chloride concentrations do not show any clear depth trend, but rather reflect consequences of groundwater type and association to different deformation zones. The groundwater type coding reveals that more dilute brackish groundwater of the local Baltic type is found at shallow depths down to 100 m while the groundwater with the lowest salinity (1,600 mg/L Cl) is of the Brackish-glacial type and found at approximately 240 m depth. The most saline groundwater is generally found at intermediate depths (100–200 m) and represents the brackish marine Littorina type.
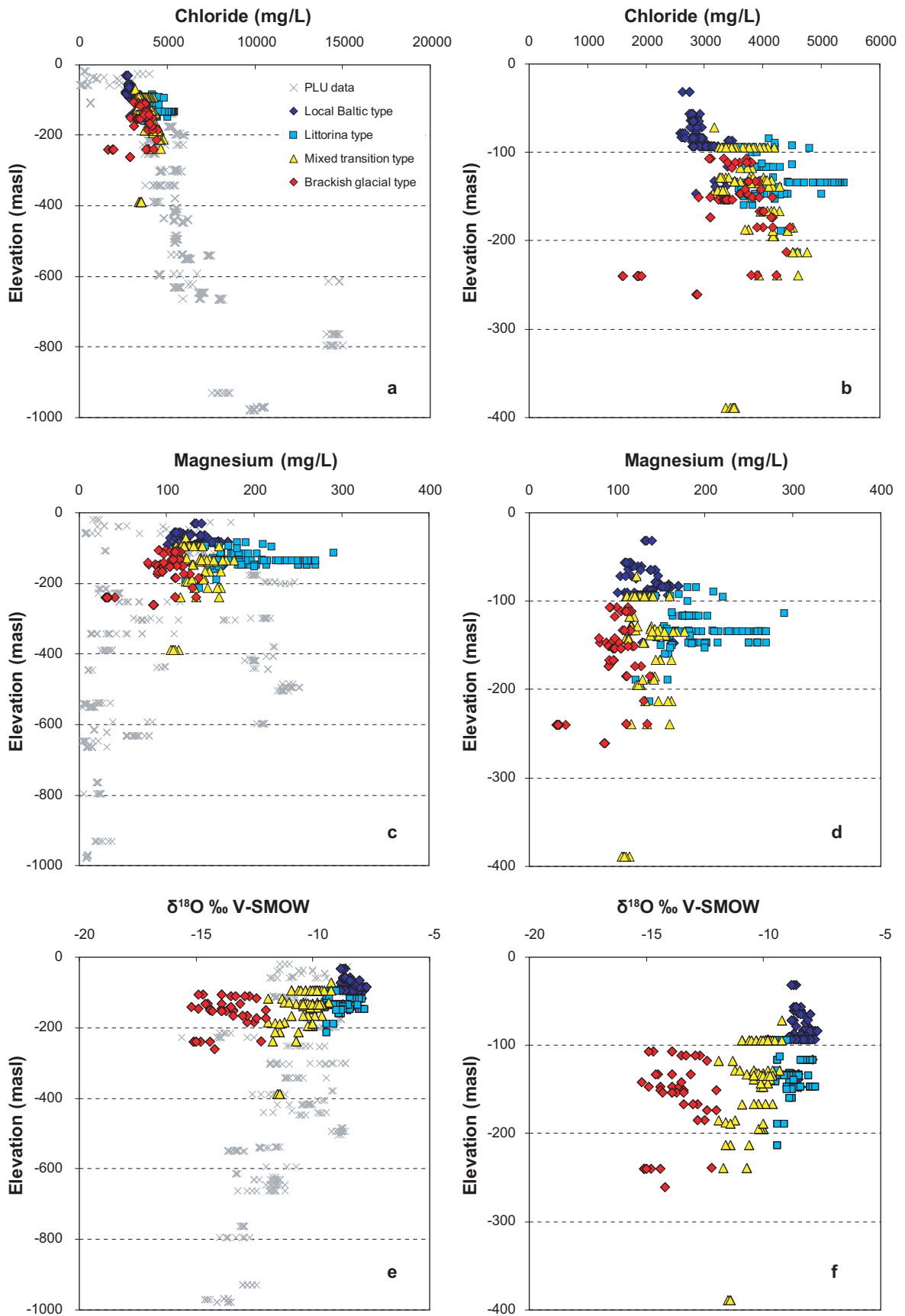
Figure 5-2 a–f. *Distribution of chloride, magnesium and $\delta^{18}O$ with depth (1986–2010) related to the different groundwater types defined for the SFR Site in Section 3.3. The diagrams to the left include PLU data (Forsmark) down to 1,000 m while the diagrams to the right are restricted to 400 metres depth which is more relevant to the SFR extension data.*

The magnesium concentration (Figure 5-2 c, d) emphasises the marine influence in most ground-waters within the SFR model volume. The magnesium concentration varies between approximately 30 to 300 mg/L and the lowest concentrations (< 10 mg/L) observed from the site investigations in Forsmark are absent in samples from the SFR site. This implies that even the mainly non-marine groundwaters contain a minor marine component. The younger marine groundwaters of the local Baltic type generally show magnesium concentrations between 90 and 150 mg/L and are found down to depths of about 100 m, while the older marine groundwaters of the Littorina groundwater type show magnesium concentrations between 150 and 280 mg/L and are found at depths between 100 and 200 m. Both these groundwater types are preferably encountered in, or adjacent to, deformation zones (cf. Figures 5-8 and 5-10). The magnesium concentrations in groundwaters of the two mainly non-marine water types are still relatively high, although the Mg/Cl ratio decreases and the marine components are less conspicuous.

With respect to oxygen-18 (Figure 5-2 e, f), three ranges are distinguished; a) enriched values rang-ing from $\delta^{18}O = -9.5$ to $-7.5‰$ V-SMOW representing groundwaters of marine origin (local Baltic and Littorina type), b) values in the intermediate range between $\delta^{18}O = -12$ and $-9.5‰$ V-SMOW representing mixed brackish groundwater of the transition type, and finally c) depleted values of $\delta^{18}O = -16$ to $-12‰$ V-SMOW with a significant glacial component giving a low $\delta^{18}O$ signature. The enriched values are found at shallow (local Baltic type) and intermediate depths (Littorina type) and in connection to deformation zones, while the most depleted values are found above and below zone ZFM871 (formerly Zone H2) and also relatively deep in zone 8 (KFR101) (cf. Figure 5-10).

Figure 5-3 (a–f) shows the variation of the potassium, sulphate and bromide with depth. In most cases, the groundwater types are reflected in these major elements. By comparing the brackish marine and the brackish non-marine groundwaters at similar depths, the marine groundwaters gener-ally show higher potassium and sulphate concentrations as well as Na/Ca weight ratios (Figure 5-4 c) than the non-marine groundwaters. This is more or less true also for bicarbonate (Figure 5-4 a) due to the residence times reflected in the groundwater types. Bromide (Figure 5-3 e, f) shows a somewhat increasing trend with depth but, except for the comparatively low concentrations in the local Baltic groundwater type, the relation with groundwater types is rather weak. This was also the case for the samples from the equivalent depth range in the Forsmark site investigation.

Some observations of special interest from the plotted depth distributions are listed below:

- The highest chloride and magnesium concentrations, and also some of the most enriched $\delta^{18}O$ values, are observed in early samples from the SFR boreholes, i.e. KFR7A and KFR10 at depths of -134.43 and -116.23 m.a.s.l., respectively. None of the groundwaters sampled in the recent boreholes, representing the SFR extension phase, show these high salinities. Both of the early sampled borehole sections are located at depth in two different vertical deformation zones, Zone ZFMNW0805A,B (Zone 8) and Zone ZFMNNE0869 (Zone 3) where they possibly connect to Zone ZFM871 (formerly Zone H2), cf. Figures 2-5, 2-7 and 2-9. Furthermore, the salinity has decreased with time at both locations following the first sampling in 1986 due to the drawdown of Baltic Seawater resulting from the presence of the SFR repository. However, samples from both boreholes still retain the Littorina type signature today.

- The lowest chloride and magnesium concentrations and also the most depleted $\delta^{18}O$ values are observed in the recently drilled borehole KFR101 at -240.15 m.a.s.l. The chloride concentration is significantly lower than Baltic Sea and varies between 1,600 and 1,800 mg/L. The other investigated boreholes don't show concentrations in this low range.

- Four boreholes, KFR101, KFR102A, KFR106 and KFR02 (cf. Figure 5-1), show a decreasing salinity trend with depth, and this salinity difference is most striking in KFR101. These condi-tions are due to the presence of Littorina or Mixed transition type groundwaters located above the Brackish-glacial type groundwater of lower salinity.

- The local Baltic type water is typically found at relatively shallow depths and in localities such as zone ZFMNNE0869 (Zone 3), zone ZFMNW0805A, B (Zone 8) and zone ZFMWNW0001 (the Singö zone), where the Baltic intrusion goes somewhat deeper than in bedrock between zones. Borehole KFR08 penetrating zone ZFMNW0805A, B (Zone 8) has been frequently sampled and is considered typically representative for marine water of local Baltic type. However, it is unclear if the Baltic Seawater was present in the bedrock fracture system before the excavations of the SFR facility. The boreholes were drilled from the tunnels and the drawdown effect in the meantime may have caused the intrusion of this water between excavation and the first sampling occasion.

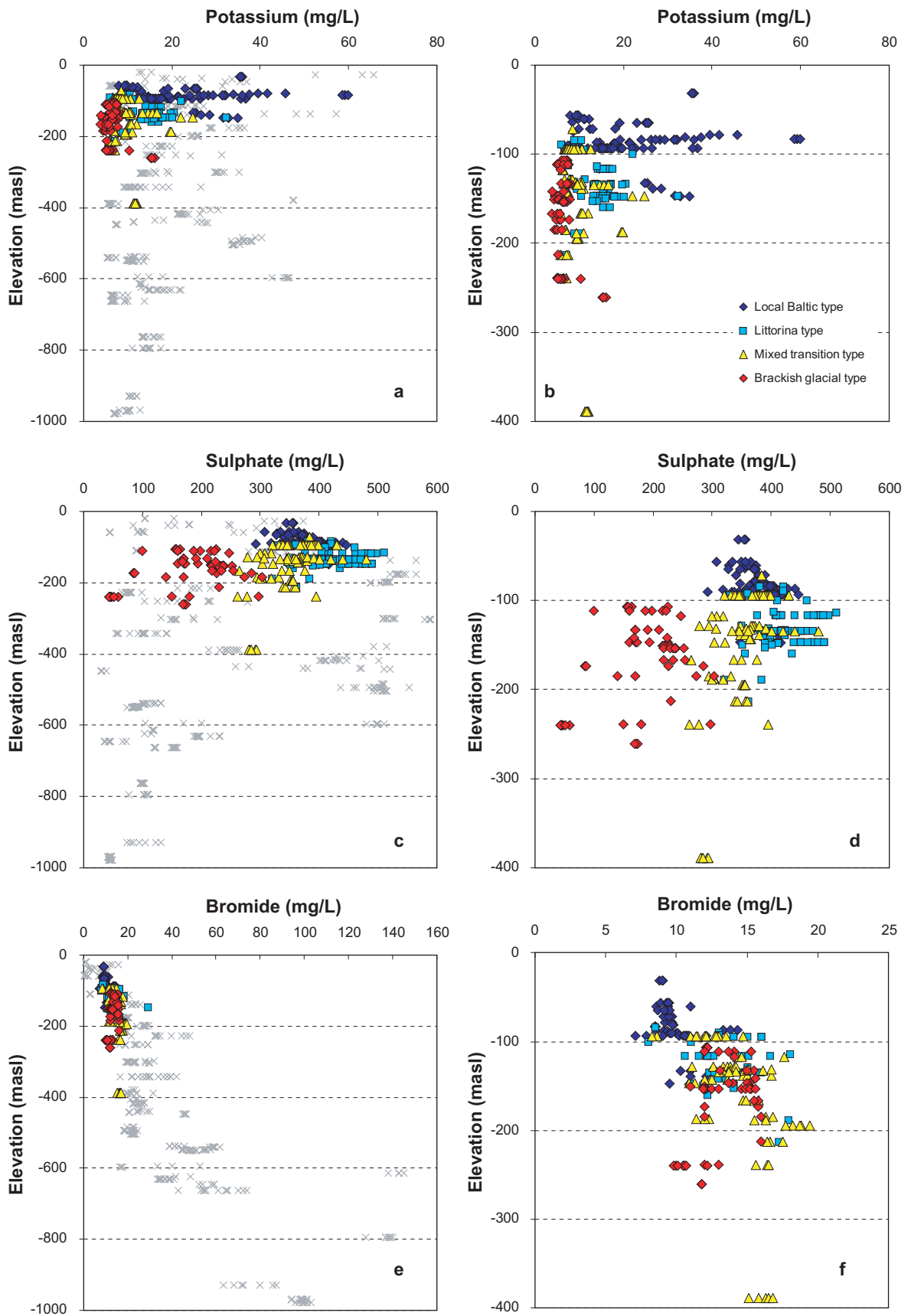**Figure 5-3 a–f.** *Distribution of; a,b) potassium concentration, c,d) sulphate concentration, and e,f) bromide concentration with depth (1986–2010) related to the different groundwater types defined for the SFR Site in Section 3-3. The diagrams to the left include PLU data (Forsmark) down to 1,000 m while the diagrams to the right are restricted to 400 metres depth which is more relevant to the SFR extension data.*

- A few samples of local Baltic type groundwater have been collected at a deeper level than the other data representing this groundwater type (at 130–150 m depth). These data points represent single samples from boreholes HFR106, KFR7A, KFR7B and KFR10. These samples represent outliers in the time series measurements from these boreholes where the dominant groundwater is of Littorina type in all cases except for the bottom section of HFR106. The series of samples collected from this section show a trend from a more diluted Baltic type to a more saline Brackish-glacial type groundwater. This is most likely due to a decreasing contribution of shallower groundwater to the samples. A pressure gradient between the two sections may have caused a downward water flow and supplied the lower section with groundwater of a more shallow type prior to sampling (cf. Section 1.5.2).

5.1.3 Depth trends of selected minor ions

Trace metals and rare earth element (REE) components generally occur in groundwaters at concentrations of less than 1 mg/L (Drever 1997). The following elements have been regularly analysed within the present SFR site investigation programme: Al, B, Ba, U, Th, Fe, Mn, Li, Sr, Sc, Rb, Y, Zr, In, Sb, Cs, La, Ce, Pr, Nd, Sm, Eu, Gd, Tb, Dy, Ho, Er, Tm, Yb and Lu. Also included are
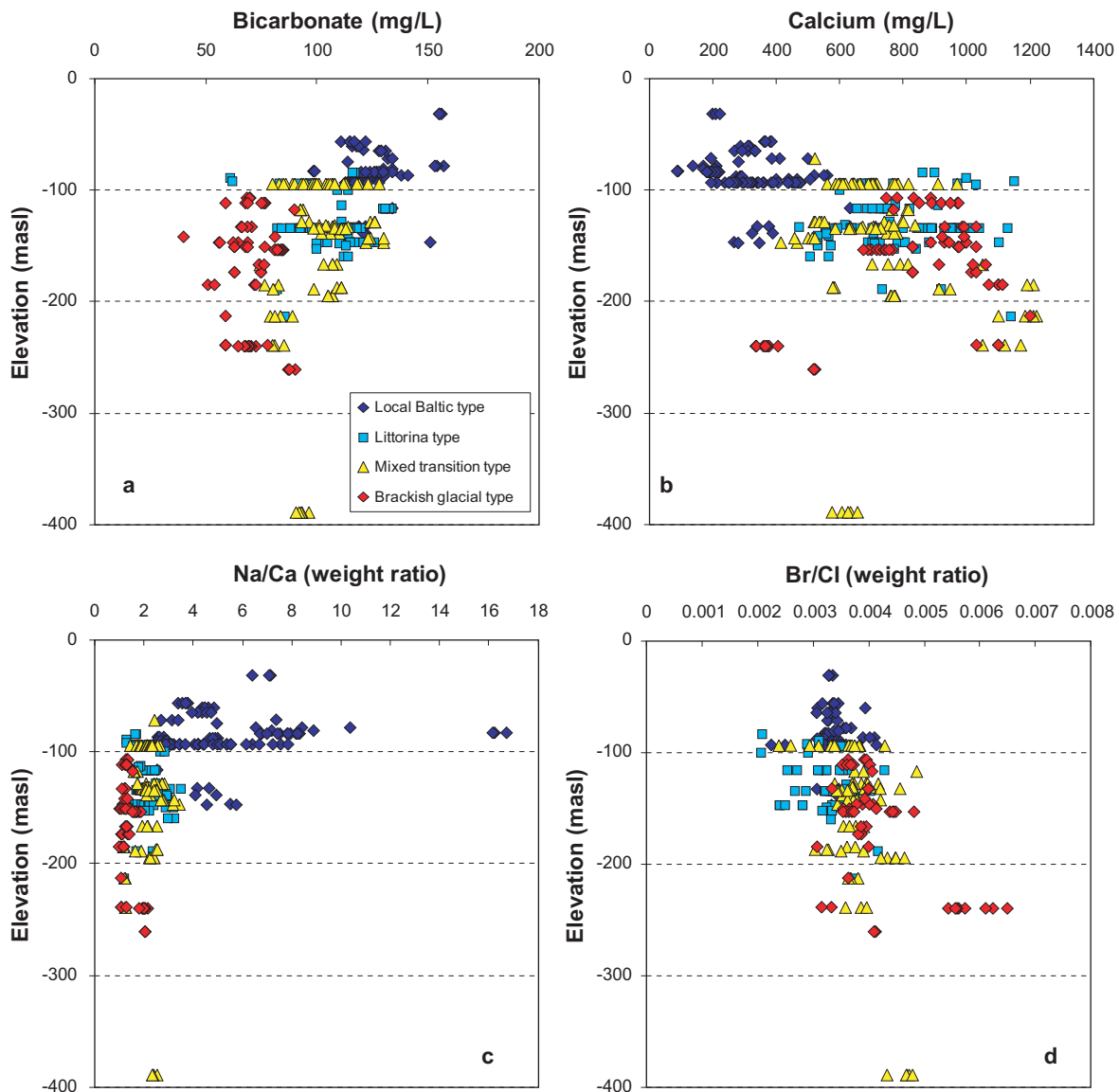

Figure 5-4 a–d. Distribution of; a) bicarbonate concentration, b) calcium concentration, c) Na/Ca weight ratio, and d) Br/Cl weight ratio with depth (1986–2010) related to the different groundwater types defined for the SFR Site in Section 3.3.

commonly occurring heavy trace metals such as Cu, Ni, Cr, Zn, Pb and Mo, even though these may be influenced by contamination related to borehole activities. The risk of contamination is large also for aluminium and the usefulness of the analytical results can be questioned. However, the trace metals and REE data from previous investigations in the early SFR boreholes are few and patchy for the model volume which limits interpretation. This report is restricted to short discussions about the redox sensitive elements, iron, sulphide, manganese and nitrogen compounds in Section 5.6 and uranium in Section 5.8.

5.1.4　Major ion-ion/isotope plots

Figures 5-5 to 5-7 show a collection of ion-ion/isotope cross plots, including data from the period 1986 to 2010, which can provide additional insight to the origin and evolution of the groundwaters. Typically, they may reveal whether the groundwater composition is affected by processes other than mixing (e.g. precipitation/dissolution of mineral phases or ion exchange). Two chloride ranges are given covering the entire PLU-Forsmark range to the left, and the more narrow range relevant for the SFR site to the right. In Figure 5-5, magnesium, $\delta^{18}O$ and potassium are plotted versus chloride, and Figures 5-6 and 5-7 display bicarbonate, bromide and sulphate, as well as Na/Ca weight ratios versus chloride.

Magnesium and $\delta^{18}O$ are the determining indicators for the different groundwater types together with chloride and, therefore, they show a clear contrast between the pre-Littorina brackish non-marine groundwaters and the more recent marine groundwaters (local Baltic and Littorina types). Magnesium (Figure 5-5 a and b) is susceptible to ion-exchange reactions and consequently the brackish marine groundwaters do not follow strictly the mixing line between pure end member waters, i.e. Littorina Sea, Baltic Sea and fresh meteoric water (cf. Figure 3-4 a). However, despite the effect of reactions, the Mg content in the brackish marine groundwaters is still sufficient to serve as a distinct marine indicator. Data on $\delta^{18}O$ ratios are scarce before 1995; Figure 5-5 c and d display the narrow chloride concentration range and at the same time the large variation in $\delta^{18}O$.

Potassium (Figure 5-5 e, f) and also bicarbonate, bromide, sulphate and Na/Ca weight ratio (Figures 5-6 a–f and 5-7 a,b) show a more or less clear distinction between the different groundwater types. As expected, most of the overlap is by the mixed transition type with the other groundwater types. The potassium concentration is high in both types of brackish marine groundwaters as demonstrated by the two peaks (Figure 5-5 e) at chloride concentrations close to 3,000 mg/L and at above 5,500 mg/L for the local Baltic and the Littorina type groundwaters, respectively. The fact that none of the samples in the SFR dataset reflects the strongest Littorina signatures from the site investigations in Forsmark is very obvious from this plot since few of the SFR data points plot at the second potassium peek which reflects the PLU data. The Littorina-glacial meltwater mixture found at the SFR site plots more towards the glacial meltwater side than the typical Littorina type groundwater sample from the site investigations at Forsmark.

The bicarbonate concentrations (Figure 5-6 a, b) are related to the microbial breakdown of organic material and are, as expected, highest in the shallow brackish marine groundwaters of the local Baltic type (usually higher than the original 70–90 mg/L found in the Baltic Seawater at the surface). Also, the Mixed transition type groundwaters and the Brackish-glacial type groundwaters have concentrations well above 50 mg/L and the extremely low values encountered in the Forsmark dataset do not occur in the SFR groundwaters. Furthermore, if the depth distribution is taken into account the SFR samples are generally higher in bicarbonate compared with Forsmark data from the same depth. Finally, the bicarbonate concentrations were high enough (> 30 mg/L) to allow ^{14}C dating of all the recent SFR samples. The carbonate system is presented in more detail in Section 5.4.1.

The bromide versus chloride plots (Figure 5-6 c, d) indicate two somewhat diffuse mixing trends for the brackish non-marine and brackish marine groundwaters, respectively. Marine waters should have a bromide/chloride ratio of approximately 0.0035 whereas higher ratios (around 0.01) are more typical of water/rock interaction. The bromide/chloride ratio is usually a reliable marine indicator in this system, but since the overall differences are not large enough, together with the associated sampling and analytical uncertainties which may obscure the details especially for the early samples in the sample series, the magnesium signature is still more informative when differentiating between a marine and non-marine origin.
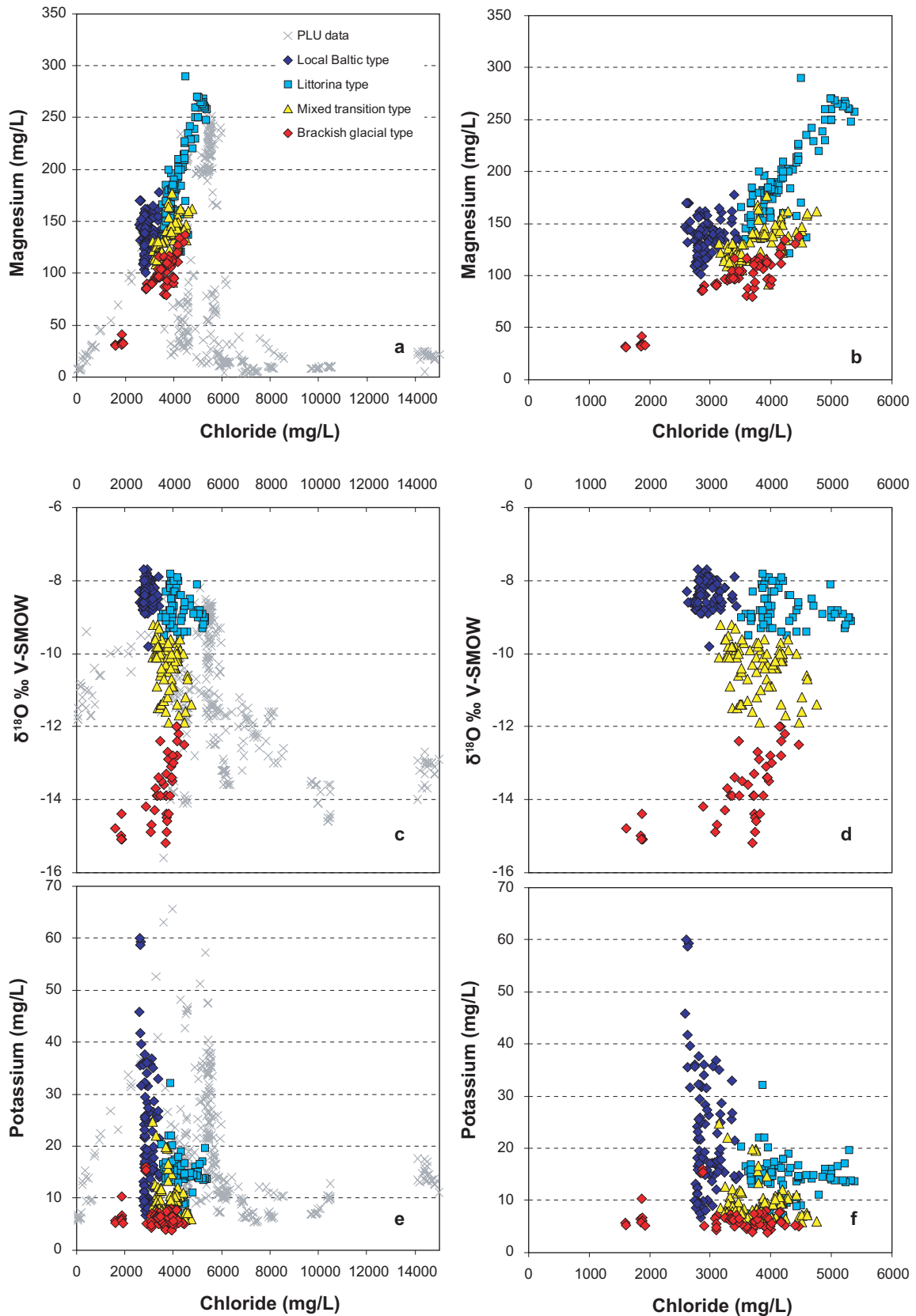
Figure 5-5 a–f. *Plots of magnesium, δ¹⁸O and potassium versus chloride concentration (1986–2010). The two different chloride scales refer to the Forsmark site investigation data and SFR data, respectively. The groundwater samples are colour coded according to the different groundwater types defined for the SFR Site in Section 3.3.*
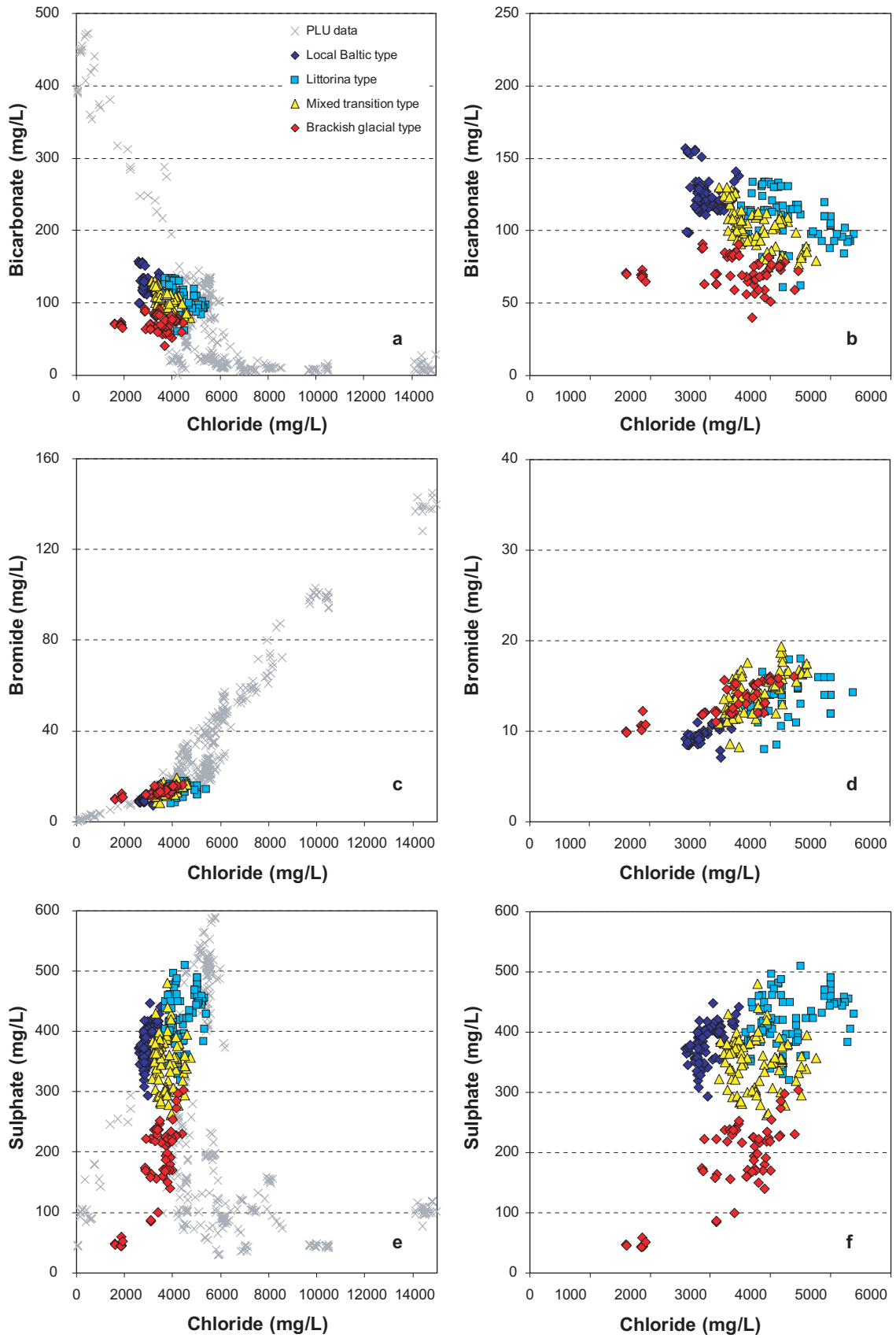
Figure 5-6 a–f. *Plots of bicarbonate, bromide and sulphate versus chloride concentration (1986–2010). The plots use two different chloride scales referring to the Forsmark site investigations data and SFR data, respectively. The groundwater samples are colour coded according to the different groundwater types defined for the SFR Site in Section 3.3.*

From Figure 5-6 e,f it is clear that the major source of sulphate in the SFR groundwaters is of marine origin and correspondingly high sulphate contents are associated with both the local Baltic and the Littorina type groundwaters. The sulphate system is presented in more detail in Section 5.4.2.

The Na/Ca weight ratio (Figure 5-7 a, b) shows a clear relation to groundwater types with the highest values corresponding to the two marine groundwater types. However, the Littorina type values are significantly lower than the Baltic type which is probably the result of more intense water/rock reactions (ion exchange) and mixing with a non-marine saline component. Most of the Brackish-glacial groundwater type samples show a ratio close to one and are clearly influenced by a deeper non-marine saline component.

The lowest calcium concentrations (and highest Na/Ca ratios) in the SFR groundwaters are associated with Local Baltic type groundwaters. Some of these groundwaters show calcium contents only slightly higher (87–90 mg/L in the HFM34: –82.9 m.a.s.l.) than the present Baltic Sea (around 75–80 mg/L), which can be attributed to their dominant Baltic signature slightly modified by water-rock interaction processes (calcite dissolution, mainly). However, most of the Baltic type ground-waters show calcium concentrations clearly higher than the Baltic seawaters (mostly between 200 and 600 mg/L), showing a rough positive correlation with chloride contents (Figures 5-7 c and d). Thus, although modified by heterogeneous reactions (e.g. calcite dissolution-precipitation, cation exchange), a mixing control seems to be still noticeable.

Figure 5-7 a–d. *Plots of Na/Ca weight ratio and calcium concentration versus chloride concentration (1986–2010). The plots use two different chloride scales referring to Forsmark site investigation data and SFR data, respectively. The groundwater samples are colour coded according to the different groundwater types defined for the SFR Site in Section 3.3.*
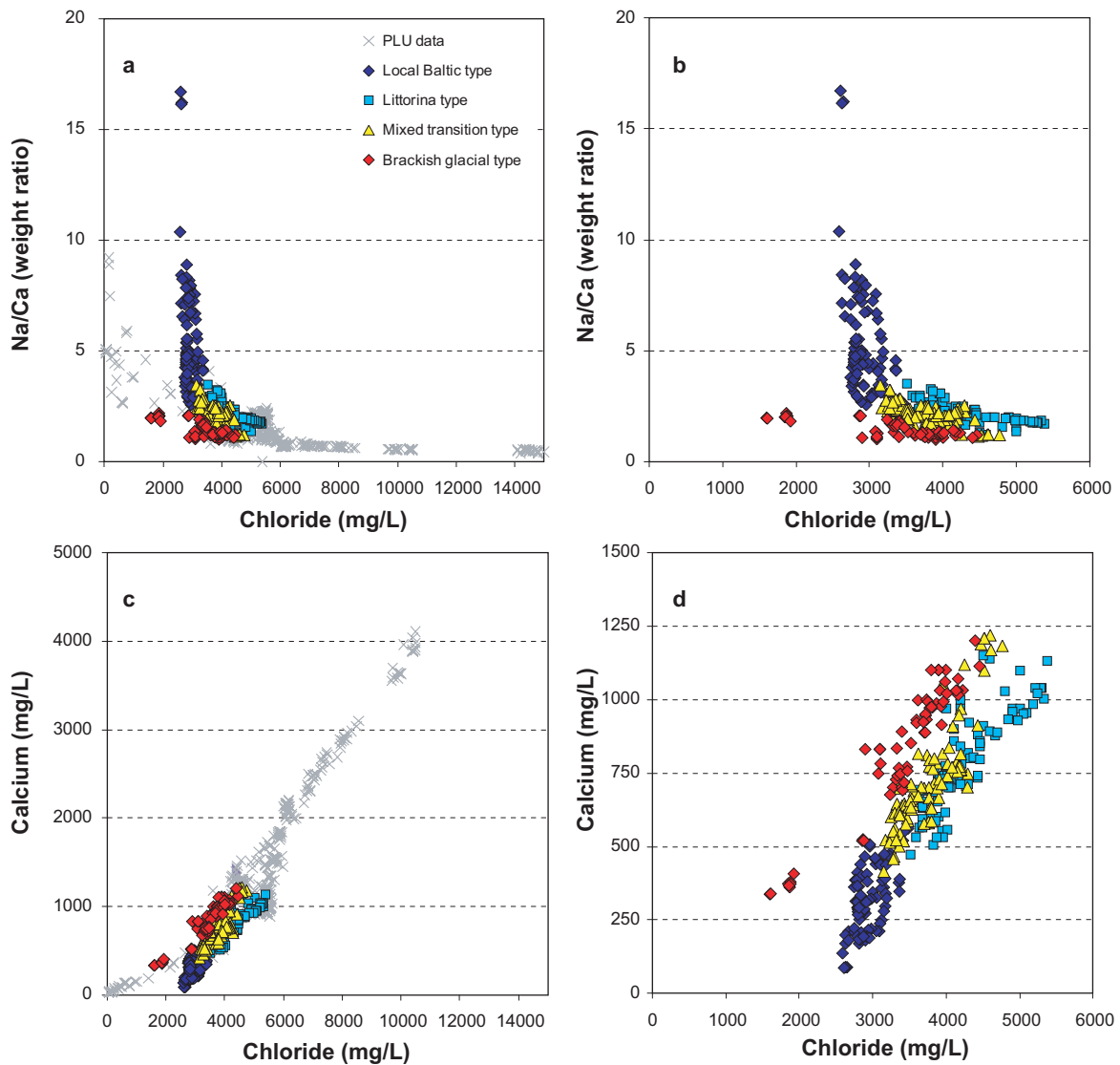
5.2 The influence of the SFR on groundwater chemistry

The impact of changes in flow paths and groundwater drawdown effects during and following construction of the SFR tunnel system has influenced the groundwater composition in the investigated boreholes. In the early drilled SFR boreholes, which penetrate several major transmissive fracture zones, the effects of changes in groundwater composition are observed from long term trends measured over periods of years (1987–2006) and implying generally slow but systematic alterations in chemistry (Laaksoharju and Gurban 2003, Nilsson A-C 2009). These changes are addressed below based on sample series data from 1987 to 2010.

Changes in groundwater composition may be observed at several sampling locations since the first samples were collected in 1986/87. Where and how the changes occur provide valuable information about the hydraulic conditions at the site and especially in the different major deformation zones. However, it is possible that some changes were sufficiently rapid and had already occurred before the first sampling occasion, which could explain, for example, the occurrence of the Baltic type of groundwater in boreholes KFR19, KFR08 and KFR56 already from the first sampling occasions in 1989–95 (the sampling started later in these boreholes). An attempt to visualise the changes in water types with time is presented in Figure 5-8 and in Table 5-1 the changes in groundwater types have been listed and related to the different deformation zones described and discussed above in Section 2.1.3.
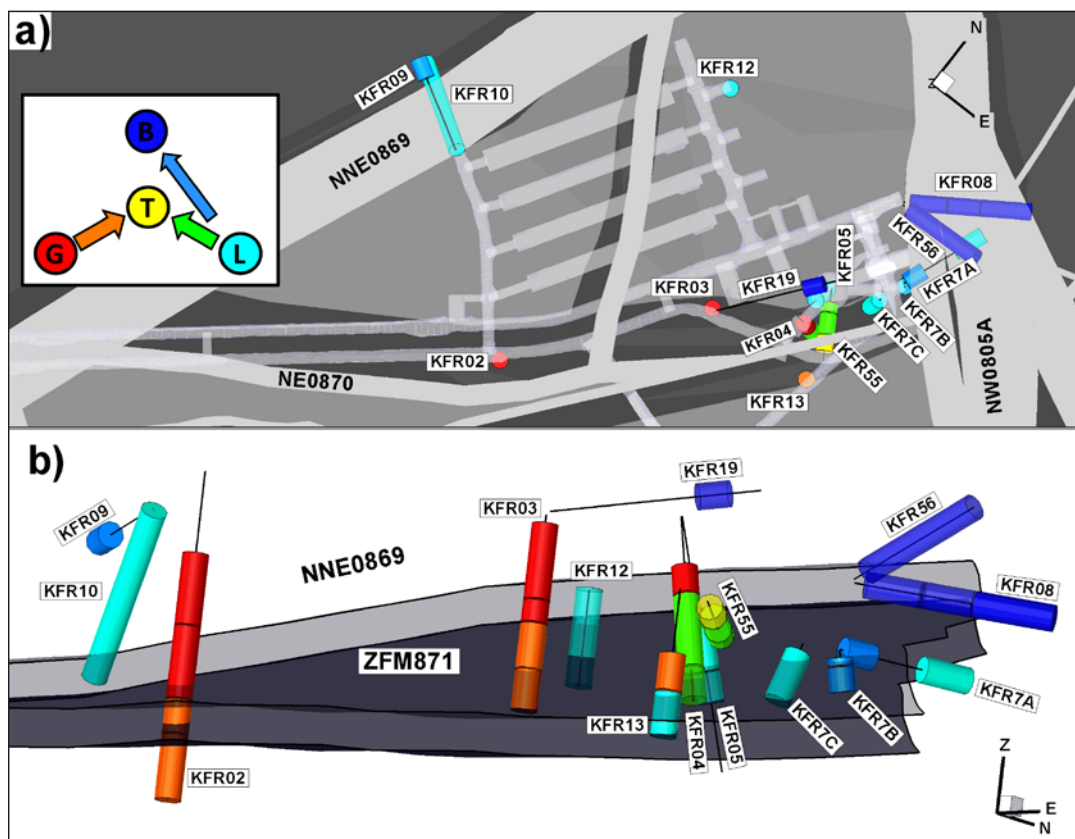
Figure 5-8. *Change of groundwater types between 1987 and 2006; a) top view, and b) side view towards the northwest The defined groundwater types are Local Baltic (B; blue), Littorina (L; cyan), Brackish-glacial (G; red), and Mixed transition (T; yellow). The transient changes are: Brackish-glacial towards Mixed transition (G → T; orange), Littorina towards Mixed transition (L → T; green), and Littorina towards Baltic (L → B; light blue). Incomplete ongoing changes are not resolved. Sections with poor coverage of the chosen time interval are shown as translucent. Deformation zones are coloured grey. The grey plane in Figure 5-8 b represents the gently dipping zone ZFM871 (formerly zone H2).*

Table 5-1. Changes in water chemistry in borehole sections and intersected major zones. Shadowed borehole sections are sampled annually.

Borehole	Section (mbl)	Elev. Secmid (m.a.s.l.)	Year; Cl (mg/L)	Year; Cl (mg/L)	Change in chemistry*	Zone
The Southern boundary belt						
KFR01	11.0–43.5	–71.58	95; 3,170	10; 2,760	T → B	ZFMWNW0001 Singö
KFR01	44.5–62.3	–94.23	87; 4,200	10; 3,370	T → T(B)	ZFMWNW0001 Singö
The Northern boundary belt						
KFR56	9.0–81.73	–64.66	95; 2,910	10; 2,810	B → B	ZFMNW0805b, ZFMNW0805a
KFR08	6.0–35.0	–87.81	95; 2,900	10; 2,790	B → B	ZFMNW0805b
KFR08	36.0–62.0	–90.29	95; 3,040	10; 2,830	B → B	ZFMNW0805a, ZFMWNW0836
KFR08	63.0–104.4	–93.31	89; 3,170	10; 3,100	B → B	ZFMNW0805a, ZFMWNW0836
KFR7A	48.0–74.7	–134.43	87; 4,900	10; 3,680	L → L(B)	ZFMNW0805a[1]
The Northern boundary belt at junction to ZFM871 (Zone H2)						
KFR7A	2.0–19.0	–132.65	95; 3,950	10; 3,180	L → B	ZFMNW0805b, ZFM871(H2)
Zone ZFMNNE0869 (Zone 3)						
KFR09	0.0–80.24	–83.68	86; 4,100	10; 2,815	L → B	ZFMNNE0869
KFR10	0.0–107.28	–116.23	00; 3,850	10; 4,290	L → L	ZFMNNE0869[2]
KFR10	87.0–107.28	–146.99	86; 5,000	99; 3,860	L → L(B)	ZFMNNE0869[2]
Zone ZFM871 (Zone H2)						
KFR02	81.0 –118.0	–184.93	86; 4,000	10; 4,470	G → T	ZFM871
KFR02	119.0–136.0	–212.93	86; 4,400	10; 4,520	T → T	ZFM871
KFR04	84.0–100.5	–166.29	95; 4,290	10; 4,080	T → T	ZFM871
KFR13	54.0–76.6	–188.64	95; 4,430	10; 4,180	L → T	ZFMNE3118, ZFM871
Zone ZFM871 (Zone H2) at junction to zone ZFMNE0870 (Zone 9)						
KFR03	57.0–80.0	–150.87	87; 3,100	10; 3,930	G → G(T)	ZFMNE0870, ZFM871
KFR03	81.0–101.6	–173.67	86; 3,100	00; 4,140	G → G(T)	ZFMNE0870, ZFM871
KFR7B	8.6 –21.1	–147.59	86; 4,300	10; 3,160	L → B	ZFM871, ZFMNE0870
Zone ZFMNE0870 (Zone 9) and zone ZFMNE3118 and bedrock mass between zones						
KFR03	5.0–44.0	–106.87	95; 3,720	10; 3,080	G → G$^+$	ZFMNE0870
KFR03	45.0–56.0	–132.87	95; 3,740	10; 3,760	G+→ G	ZFMNE0870
KFR04	28.0–43.0	–111.48	87; 3,400	10; 3,720	G → G	ZFMNE0870
KFR04	44.0–83.0	–138.52	95; 4,270	10; 4,100	L → T	ZFMNE0870
KFR55	8.0–21.0	–128.34	95; 4,020	10; 3,840	T → T	ZFMNE3118, ZFMNE0870
KFR55	22.0–39.0	–131.39	95; 3,990	10; 4,080	L → T	ZFMNE0870
KFR55	40.0–48.0	–133.97	95; 3,860	10; 3,910	L → T	ZFMNE0870
KFR13	34.0–53.0	–166.84	95; 3,940	10; 4,110	G → G(T)	ZFMNE3118
KFR19	77.0–94.0	–60.43	95; 2,890	10; 2.790	B → B	–
KFR02	43.0–80.0	–146.93	86; 3,600	10; 3,740	G → G$^+$	–
KFR02	137.0–170.3	–239.08	86; 3,900	10; 4,610	G → T	–

* Explanation: mbl = metres borehole length. B = Present local Baltic, L = Littorina type, T = Mixed Transition type, G = Brackish-glacial type. Groundwater types indicated in brackets (e.g. L(B)) means that the groundwater type is still Littorina but is changed towards the local Baltic type. G → G$^+$ means that the original groundwater type was glacial and the last sample showed an even lower δ^{18}O glacial signature.

[1] and [2] According to the geological deformation zone model version 1.0, these sections do not intersect zone ZFM871 as is indicated by hydrogeological and hydrogeochemical data.

Comments to Figure 5-8 and Table 5-1 and the observed changes can be summarised as follows:

- Changes from the Littorina type to local Baltic type groundwaters occur in or close to the shallow parts of the major vertical zones, i.e. in the Northern boundary belt and zone ZFMNNE0869 (formerly Zone 3) as well as in the Southern boundary belt (not included in Figure 5-8).

- Changes from Brackish-glacial type to the Mixed transition type occur to the west at some distance from the Northern boundary belt at the intercept with zone ZFM871 (formerly Zone H2; boreholes KFR02 and KFR03) and above the intercept (KFR04) in one case.

- Changes from the Littorina type to the Mixed transition type occur at or close to the intercept with zone ZFM871 in two boreholes (KFR04 and KFR55) at an intermediate distance from the Northern boundary belt.

Most of the changes occurred before year 2000 and since then the groundwater composition has remained rather stable. As expected, the greatest changes in groundwater pressure and inflow to the boreholes and the tunnel system occurred soon after construction. Since then, conditions have slowly stabilised to reach a close to equilibrium situation around year 2000; this naturally effects also the groundwater composition. The somewhat decreasing or close to stable chloride and magnesium concentration trends between 1986 and 2010 (associated with the different groundwater types) are displayed in Figures 5-9 and 5-10 and the $\delta^{18}O$ trend is given in Figure 5-11. The Figures include the annually sampled boreholes KFR01, KFR08, KFR10 and KFR7A as well as a selected typical bore-hole section (KFR04:3 at 28.0 to 33.0 m borehole length) showing the Brackish-glacial groundwater type; this latter borehole section was sampled more seldom. Corresponding diagrams for bicarbonate and pH are presented in Section 5.5.1 and more trend plots with time (chloride, magnesium and $\delta^{18}O$) for all boreholes having enough data are displayed in Appendix 1 where values and water types that deviate in the plots are commented on.

Figure 5-9. *Chloride concentration plotted versus sampling date; groundwaters from annually sampled borehole sections (bottom sections) in KFR01, KFR08, KFR10 and KFR7A as well as from KFR04 at 28.0 to 43.0 m borehole length. Note that KFR10 had packers installed (section 87.0–107.28 m borehole length) probably until year 1987, and after that date the entire borehole was sampled. The single Baltic groundwater type sample from KFR10, collected year 2001, is probably due to an erroneously too low chloride value. Furthermore, this borehole lacks data for a period during the 1990's.*

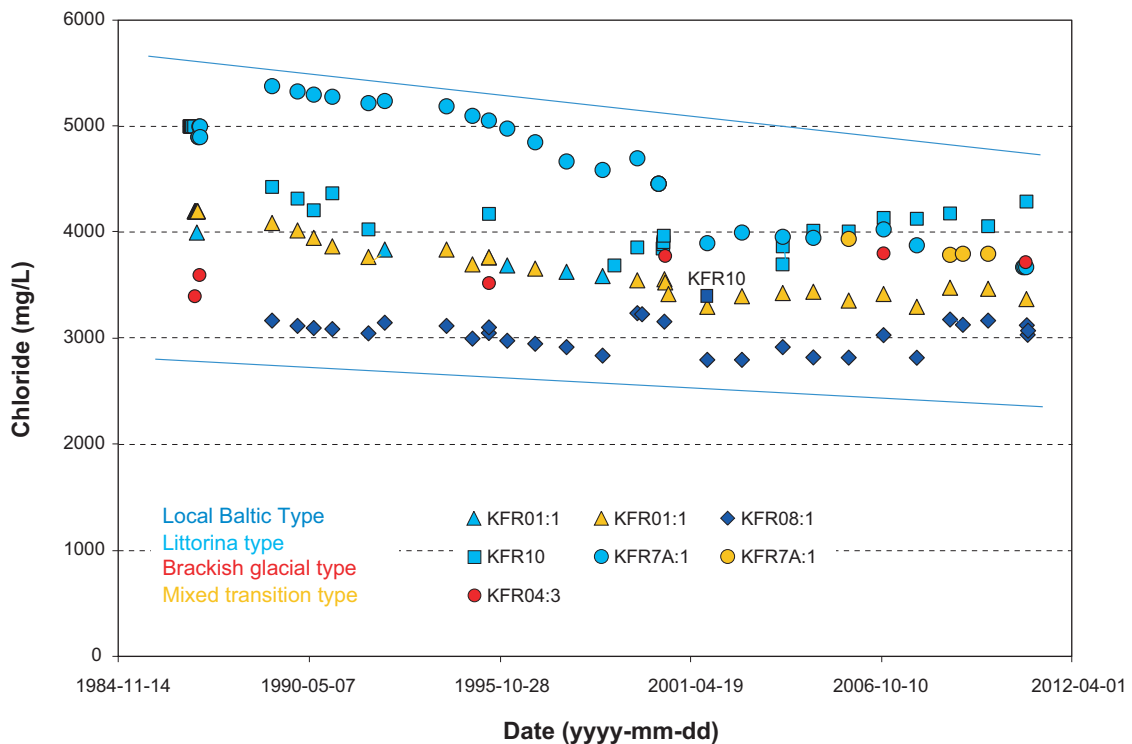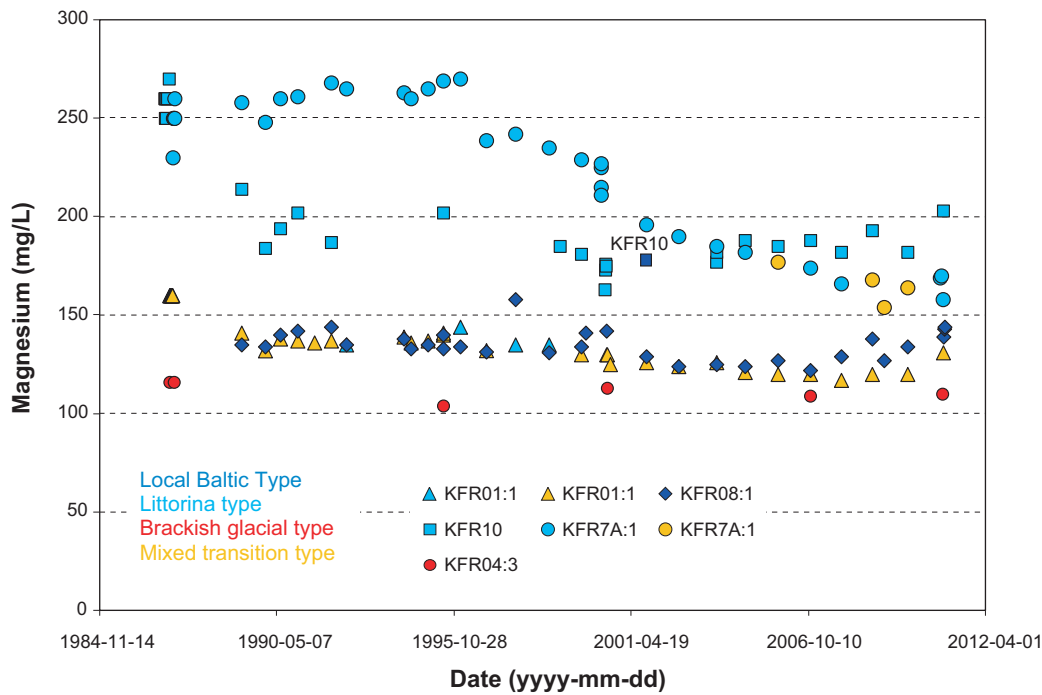***Figure 5-10.*** *Magnesium concentration plotted versus sampling date; groundwaters from annually sampled borehole sections (bottom sections) in KFR01, KFR08, KFR10 and KFR7A as well as from KFR04 at 28.0 to 43.0 m borehole length. KFR10 had packers installed (section 87.0–107.28 m borehole length) probably until 1987. After that date the entire borehole was sampled. The sample from KFR10 collected in 2001 is interpreted to be of a Baltic groundwater type due to a low and probably erroneous chloride value. The borehole lacks data for a period during the 1990's.*
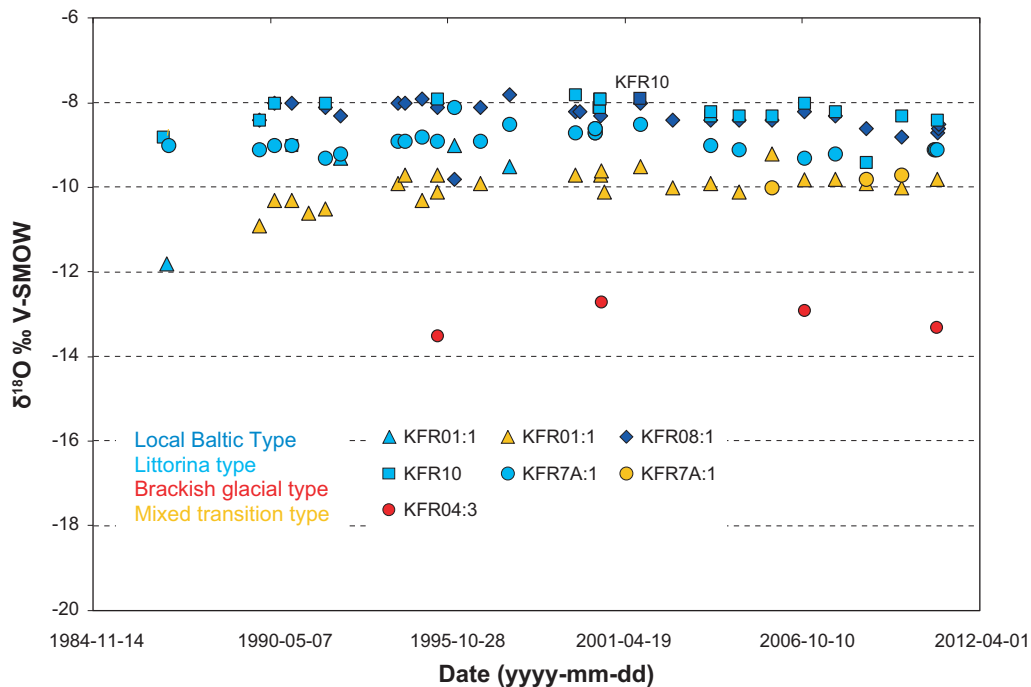
Figure 5-11. *$\delta^{18}O$ (‰ V-SMOW) plotted versus sampling date; groundwaters from annually sampled borehole sections (bottom sections) in KFR01, KFR08, KFR10 and KFR7A as well as from KFR04 at 28.0 to 43.0 m borehole length. KFR10 had packers installed (section 87.0–107.28 m borehole length) probably until 1987. After that date the entire borehole was sampled. The borehole lacks data for a period during the 1990's. The samples from 1996 are likely to be confused and KFR08 is interpreted to be of a Baltic groundwater type inspite of the low and probably erroneous $\delta^{18}O$ value.*

5.3 Groundwater composition of different bedrock features

Most of the hydrogeochemical data from the SFR site originates from deformation zones or possibly shallow bedrock aquifer (SBA) features and only a limited amount comes from discrete single fractures in the bedrock mass between zones. Moreover, these latter data also may have been influenced to a varying extent by nearby deformation zones since sampling is possible only in fractures with sufficient groundwater flow. In the previous site investigations in Forsmark, a clear difference was observed between the types of groundwater sampled in major deformation zones and those in single fractures in the bedrock mass between major zones (Olofsson et al. 2007). For example, the system of repeated gently dipping zones in the southeastern part of the target area showed a younger, more marine Littorina influenced groundwater present down to about –600 m.a.s.l., compared to the very old non-marine groundwater in single fractures from depths of about –400 m.a.s.l. in the low transmissive bedrock which characterises the northwestern target area. The variation in groundwater composition related particularly to differences in transmissivity is even more obvious from the SFR data (cf. Figure 5-12), partly due to the greater concentration of sampling locations (i.e. hydraulically active structures) within a small area. Deformation zone and SBA properties, as well as sea sediment thickness, play important roles in explaining the distribution of different water types, including the Baltic Sea intrusion. The similarities and differences between contrasting bedrock features are described below.
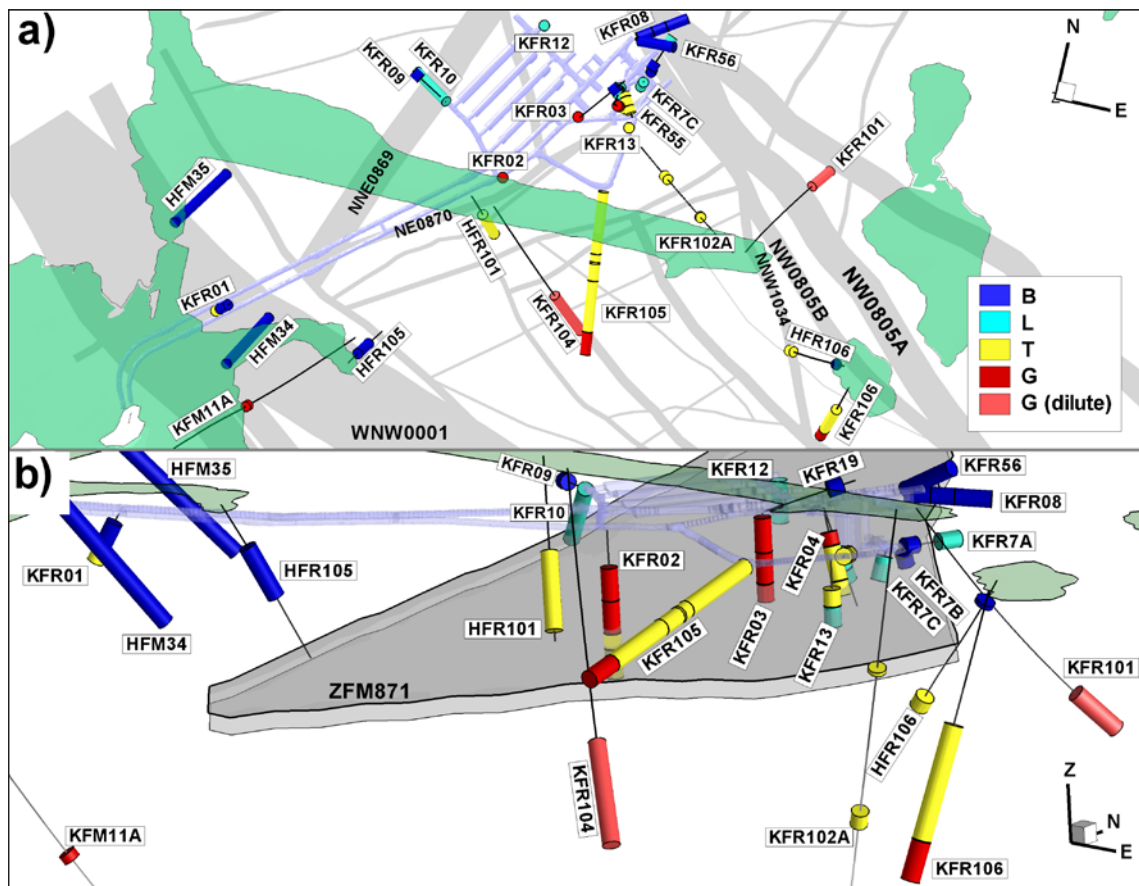
Figure 5-12. 3D presentation viewed from the top a) and from soutwest b) of the groundwater type distribution in relation to the major zones ZFMNW0805a, b and ZFM871 (grey) respectively in the regional model volume. The green areas at the surface indicate land (with the pier). Note that the recently sampled borehole KFR104 is included. Note also the decrease in colour intensity along the boreholes when viewed through a penetrated rock/deformation zone volume.

5.3.1 Comparison between the Southern and Northern boundary belts

The boreholes associated with the Southern boundary belt are HFR105, HFM34, HFM35, KFR01 and, at greater depth, KFM11A, while the Northern boundary belt is intersected by KFR56, KFR08, KFR7A and to the southeast at depth the new borehole KFR101. The elevations (m.a.s.l.) of the investigated sections are given in Table 5-2.

The groundwater composition of all samples collected down to an elevation of –150 m.a.s.l. in the Southern and Northern boundary belts, as well as the inland groundwater compositions in the depth range –19 to –139 m.a.s.l. from the site investigations in Forsmark (i.e. the shallow bedrock aquifer), are compared in Figure 5-11 a–d. The plots demonstrate not only some similarities but also different trends between the two belts. However, the different trends are based on only one borehole at each location (Belt) and therefore caution must be excercised.

Table 5-2. Borehole (Idcodes), sections (elevation secmid) and groundwater types in the Southern and Northern boundary belts.

Southern boundary belt				Northern boundary belt			
Idcode	Elevation secmid (m.a.s.l.)	Init. water type[1]	Present water type	Idcode	Elevation secmid (m.a.s.l.)	Init. water type[1]	Present water type
KFR01	–71.58	B	B	KFR56	–64.67	B	B
HFM35	–78.24	–	B	KFR08	–87.81	B	B
HFM34	–82.92	–	B	KFR08	–90.29	B	B
HFR105	–86.73	–	B	KFR08	–93.31	B	B
KFR01	–94.23	L	T	KFR7A	–132.65	L	B
KFM11A	–389.62	–	G	KFR7A	–134.43	L	L
KFM11A	–	–	PLU	KFR101	–240.15	–	G

[1] Initial water type = the groundwater type of early samples collected from 1986–87. It is likely that the true initial groundwater types before the excavation of the SFR repository did not include the local Baltic groundwater type. B = Present local Baltic, L = Littorina type, T = Mixed Transition type, G = Brackish-glacial type.

The observations are summarised as follows:

- The local Baltic type of groundwater is present in several investigated shallow borehole sections in both the Northern and Southern boundary belts.

- Long time series samples without Baltic character are available from one borehole section at shallow to intermediate depth in each structure; however, the concentration trends provided by these two time series differ. The Southern boundary belt trend shows a less marine signature although the initial samples belong to the Littorina type (i.e. close to the border line between Littorina type and Mixed transition type groundwaters). The Northern boundary belt trend, on the other hand, follows strictly the mixing line between the Littorina and Local Baltic type groundwaters.

- One reason for the different trends may be the thicker sediment cover constricting intrusion of first Littorina water and later Baltic Seawater via the Southern boundary belt, compared to the Northern boundary belt characterised by a very thin (or lack of) sediment cover. Furthermore, discharge of shallow groundwater from the inland via the upper conductive shallow bedrock aquifer may supply a groundwater mixture of young meteoric and Littorina origin to this depth interval in the Singö zone (cf. Section 2.2.3 and Figure 5-12). It is not clear at the moment whether this mixture could progress further to the northeast beyond the Singö zone.

- As can be observed from the plots in Figure 5-13, the mixing line between young meteoric water and Littorina water in groundwaters from the site investigations in Forsmark corresponds closely to the composition of the Local Baltic type of groundwater for most components. Therefore, the trend with time in the Southern boundary belt may be due to intruding Baltic Seawater or due to intruding shallow inland groundwater or a mixture of both.

- The different trends in the Southern and Northern boundary belts therefore may be an indication of discharge of shallow inland groundwater (i.e. via the shallow bedrock aquifer) to the Southern boundary belt and/or restricted intrusion of Baltic Seawater. However, due to the few observed borehole sections it may also be explained by hydrogeological heterogeneity and/or hydrochemical heterogeneity due to varying conditions in different boreholes.

Possible interpretations of such flow paths at the access tunnel passage through the Southern boundary belt are conceptualised below in Figure 5-14 (Öhman J 2011, personal communication).
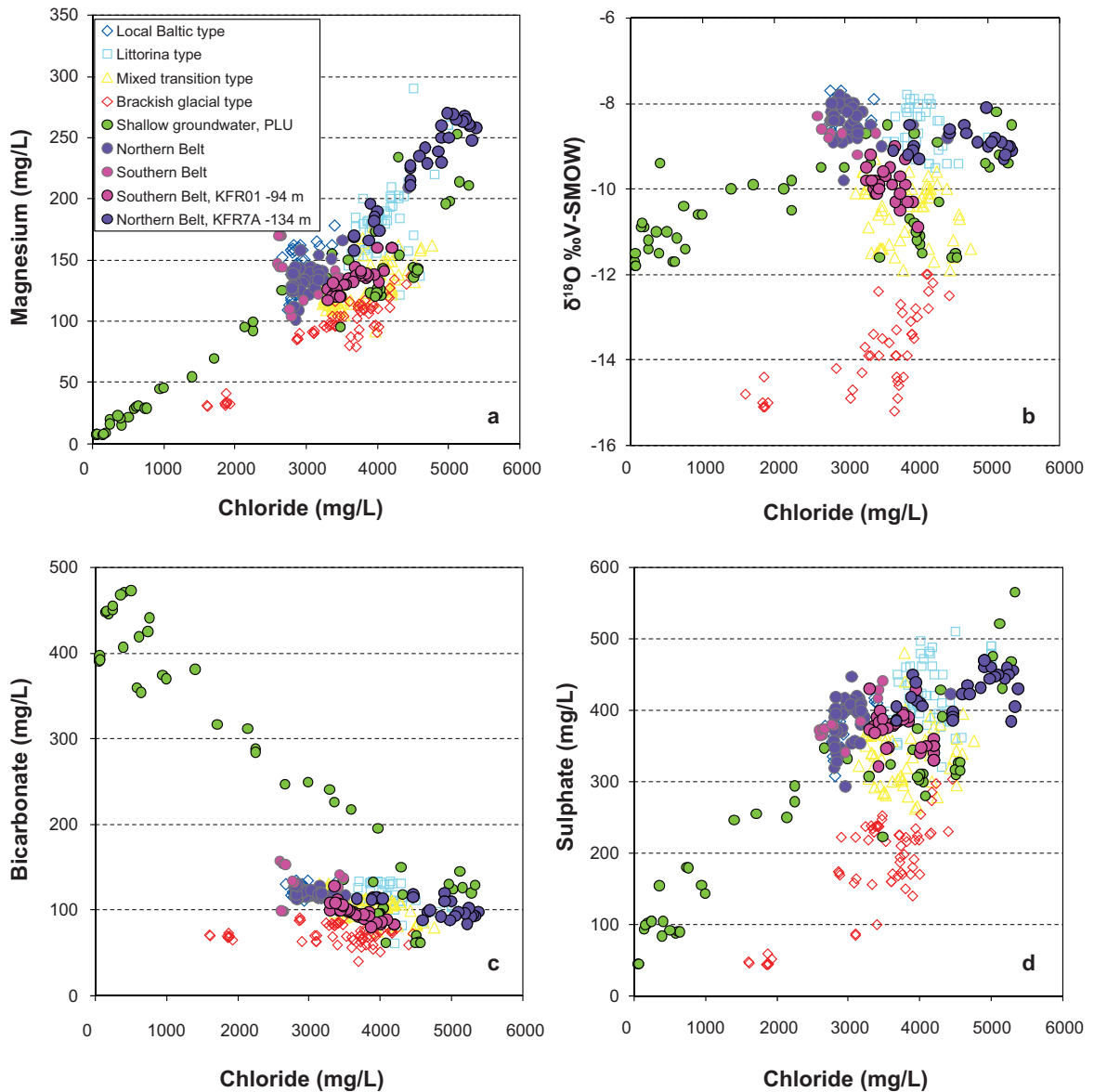
Figure 5-13 a-d. *Comparison of groundwater composition in boreholes that represent the Southern and Northern boundary belts as well as shallow borehole sections (i.e. shallow bedrock aquifer – SBA) representing the depth interval –19 to –137 m in inland boreholes (Forsmark site investigation). The dots representing sample series (1986 to 2010) from KFR01: –94 m.a.s.l. and KFR7A: –134 m.a.s.l. are given with symbols outlined in black. The concentration trends with time can be compared in Figures 5-9 to 5-11.*
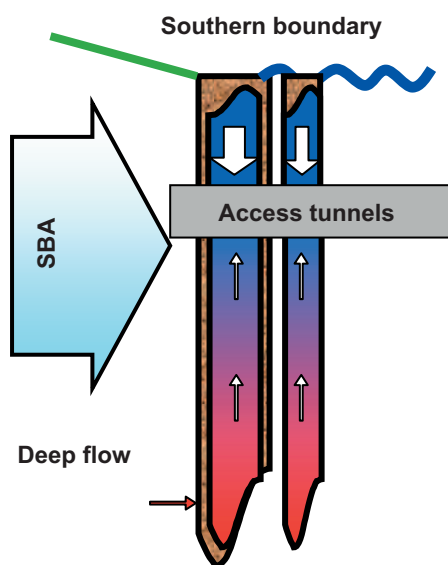
The intersection of the SFR access tunnels BT and DT causes drawdown in the Southern boundary belt resulting in a downward gradient above the tunnel and an upward gradient from below; hydrochemical data are very limited above the access tunnels and are absent below.

There exist 3 possible sources of inflow:

a) From the overlying Baltic Sea; this flow path may be partly impeded by the thick sedimentary cover.

b) Horizontal, shallow bedrock aquifer (sheet joint) groundwater flow inland from the Forsmark area towards the Singö zone; mixture of young meteoric and Littorina type groundwaters. However, the connectivity between SBA structures and the Singö zone is uncertain due to the possibility of clay filled rim zones.

c) Deep upward flow of saline non-marine groundwaters.

The meteoric-Littorina mixed groundwater types are linearly dependent with Baltic; therefore, sources a) and b) cannot be differentiated. Source c) is a minor component masked by the strong SFR Baltic signature inflow from above. In conclusion, whilst source a) is most probable, there are very few hydrochemical data, the extent of the sedimentary cover impediment to groundwater flow is not known, and the potential importance of source b) is hindered by a lack of hydrogeological data. Furthermore, the degree of hydrogeological heterogeneity probably plays an important role, but again there are insufficient data available.

Figure 5-14. Possible interpretations of flow paths at the access tunnel passage through the Southern boundary belt (Öhman J 2011, personal communication).

5.3.2 Similarities between zone ZFMNNE0869 and the Northern boundary belt

The boreholes associated with zone ZFMNNE0869 (formerly Zone 3) are KFR09 and KFR10. The elevations (m.a.s.l.) of the sampled borehole sections as well as groundwater types are compared to the Northern boundary belt in Table 5-3.

The groundwater composition of all samples collected down to an elevation of −150 m.a.s.l. in zone ZFMNNE0869 are presented in Figure 5-15 a–d. The groundwater composition strictly follows the Littorina to Baltic type mixing line and shows a similar pattern to the corresponding groundwaters associated with the Northern boundary belt. Both zones have been interpreted as having generally high hydraulic transmissivity values and the sediment thickness on the bedrock over both these zones is very thin.

- Baltic type groundwater is present at shallow depths also in zone ZFMNNE0869 (formerly Zone 3).

- Long time series data are available from one borehole section at shallow to intermediate depth and the groundwater composition strictly follows the mixing line between the Littorina type and the Local Baltic type groundwaters. The last samples in the time series still belong to the diluted Littorina type groundwater in common with the Northern boundary belt.

- The strongest Littorina signatures in the area have been observed at the junctions between both vertical zones ZFMNNE0869 (formerly Zone 3) and ZFMNW0805A, B (formerly Zone 8) and the gently dipping zone ZFM871 (formerly Zone H2). However, the interpretation of flow paths at the junctions is uncertain (cf. Figure 5-16).

- Also in the case of zone ZFMNNE0869, the similarities may be due to few observation points and more observation points might reveal more heterogeneous groundwater conditions.

Table 5-3. Borehole (Idcodes), sections (elevation secmid) and water types in zone ZFMNNE0869 and the Northern boundary belt.

Zone ZFMNNE0869 (formerly zone 3)				Northern boundary belt			
Idcode	Elevation secmid (m.a.s.l.)	Init. water type[1]	Present water type	Idcode	Elevation secmid (m.a.s.l.)	Init. water type[1]	Present water type
KFR09	−80.94	–	B	KFR56	−64.67	B	B
KFR09	−83.68	L	B	KFR08	−87.81	B	B
KFR10	−146.99	L	L	KFR08	−90.29	B	B
				KFR08	−93.31	B	B
				KFR7A	−132.65	L	B
				KFR7A	−134.43	L	L
				KFR101	−240.15	–	G

[1] Initial water type = the groundwater type of early samples collected from 1986–87. It is likely that the true initial groundwater types before the excavation of the SFR repository did not include the local Baltic groundwater type. B = Present Local Baltic, L = Littorina type, T = Mixed transition type, G = Brackish-glacial type.

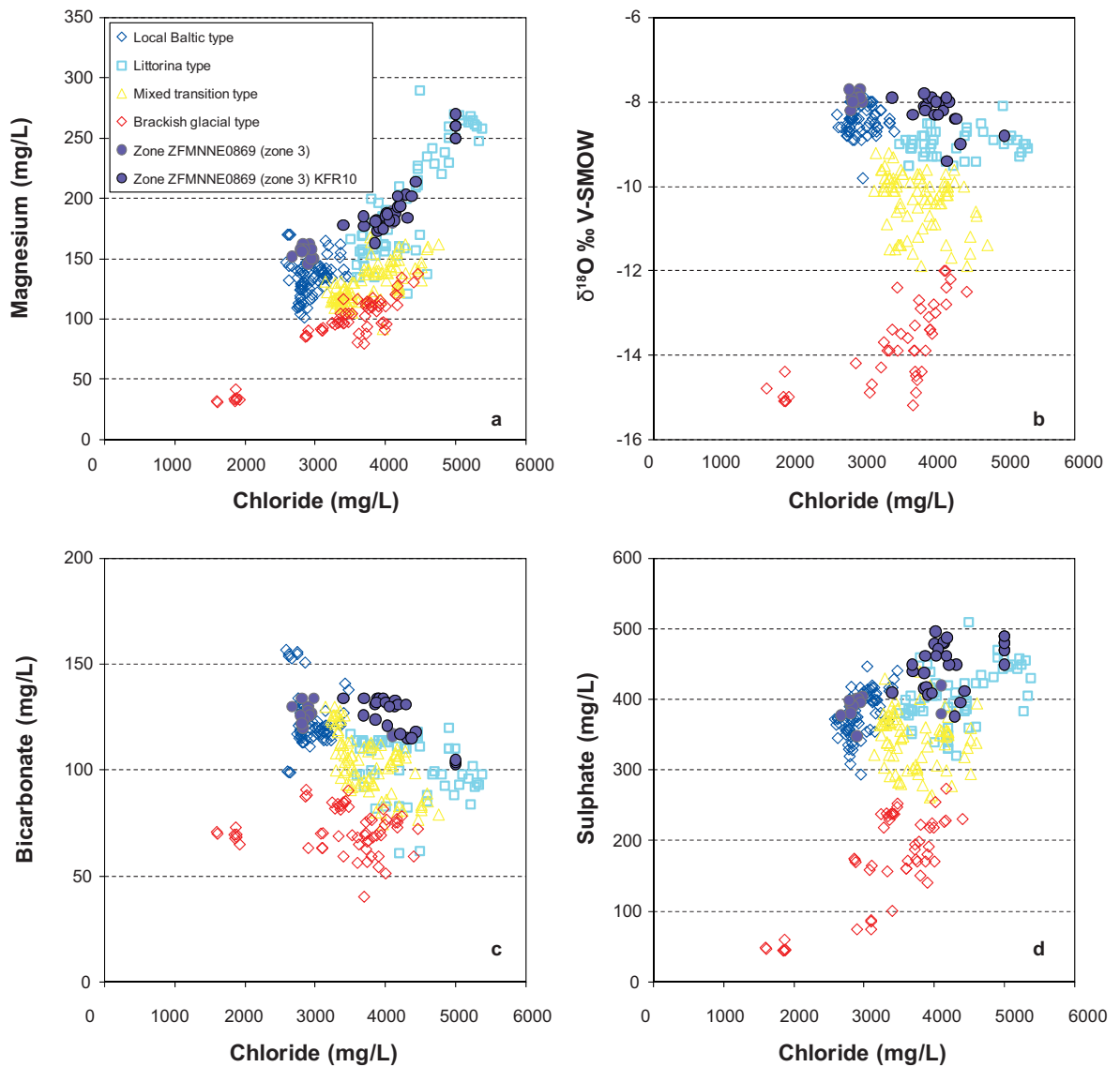
Figure 5-15 a–d. Presentation of groundwater composition in two boreholes representing zone ZFMNNE 0869 (formerly Zone 3) in relation to other borehole data. The purple plots represent KFR10: –147 m.a.s.l. and KFR09: –84 m.a.s.l. both in ZFMNNE 0869. The sample time series (1986 to 2010) from borehole KFR10 are encircled in black in order to distinguish them from borehole KFR09: –84 m.a.s.l.

ZFMNNE0869 and ZFMNW0805A,B
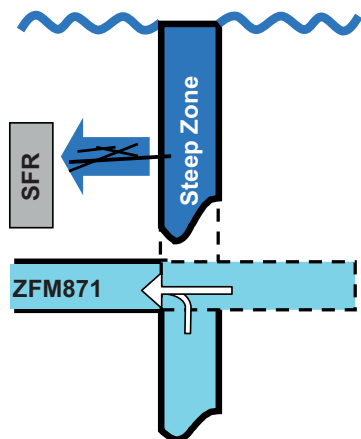
Zones ZFMNNE0869 (formerly Zone 3) and ZFMNW0805A,B (formerly Zone 8) show similar characteristics. They are both steep, transmissive and intersect the subhorizontal zone ZFM871 (formerly Zone H2). Their Baltic signatures at the SFR level imply hydraulic flow from the sea towards the SFR facility. Note also that the western part of ZFMNNE0869 intersects the access tunnels which are also expected to cause Baltic type water intrusion.

However, below the SFR (e.g., Borehole KFR7A), the preservation of Littorina type waters requires altern ative interpretations. These include:

a) Vertical hydraulic discontinuity in the steep zone.
b) Stratified, horizontal flow paths, without mixing (arrows).
c) Stagnant water or minor flow through ZFM871.
d) Supply of Littorina type water from below, or beyond the steep zone.

Figure 5-16. Possible interpretations of flow paths at the junction between zone ZFM871 and the steep zones ZFMNNE0869 or ZFMNW0805A,B. (Öhman J 2011, personal communication).

5.3.3 The heterogenic zone ZFM871

The boreholes associated with the gently dipping zone ZFM871 (formerly Zone H2) are KFR02, KFR03, KFR04, KFR05, KFR12, KFR13, KFR7A, KFR7B and KFR7C. Several borehole sections are investigated in most of the boreholes. None of the sections that are interpreted to intercept the zone were included in the annual sampling programme and therefore the available data represent many boreholes and sections, but few sampling occasions, in contrast to the previous zones (i.e. Southern and Northern boundary belts and ZFMNNE0869). Especially, the two bottom sections of KFR7B are worth mentioning since they show initial Littorina signatures deviating from the other data points, but change to Local Baltic with time. The elevations (m.a.s.l.) of the investigated sections are given in Table 5-4.

Table 5-4. Borehole (Idcodes), sections (elevation secmid) and groundwater types in zone ZFM871 (formerly zone H2).

The Littorina – Baltic trend				The Glacial – Transition trend			
Idcode	Elevation secmid (m.a.s.l.)	Init. water type[1]	Present water type	Idcode	Elevation secmid (m.a.s.l.)	Init. water type[1]	Present water type
KFR7A	−132.65	L	B	KFR02	−184.93	G	T
KFR7B	−138.85	L	B	KFR02	−212.93	G	T
KFR7B	−147.59	L	B	KFR03	−150.87	G	G
KFR7C	−149.37	L	–	KFR03	−173.67	G	G
KFR7C	−152.19	L	–	KFR04	−166.29	–	T
KFR05	−141.06	L	L				
KFR05	−159.86	L	–				
KFR12	−112.25	L	–				
KFR12	−113.62	L	–				
KFR13?	−188.64	L	L				

[1] Initial water type = the groundwater type of early samples collected from 1986–87. It is likely that the true initial groundwater type before the excavation of the SFR repository did not include the local Baltic groundwater type.

B = Present Local Baltic, L = Littorina type, T = Mixed transition type, G = Brackish-glacial type.

The plots in Figure 5-17 a–d reveal two separate groups of data, i.e. the Littorina-transition type borderline group towards the Baltic type, and the brackish-glacial-transition type group. It is obvious from Table 5-4 and Figure 5-8 (change of water types) that borehole sections close to the Northern boundary belt show a more marine character while locations further away (i.e. KFR02, KFR03 and KFR04) show more of a non-marine character.

Possible interpretations of flow paths at the junction between ZFMNE0870 (formerly Zone 9) and ZFM871 (formerly Zone 3) are outlined in Figure 5-18. Brackish-glacial type groundwater is observed below the SFR access tunnel in KFR02, KFR03, and KFR04. The Mixed transition type or a change from Littorina type to Mixed transition type is observed in KFR04 and KFR55. A large drawdown is observed (–31 m) at z = –31 in HFR101, –40 to –75 m towards the Silo. Draining of Littorina type water may have occurred during tunnel constructions although the glacial component is still present. No data exist above BT or below zone ZFM871 in zone ZFMNE0870.
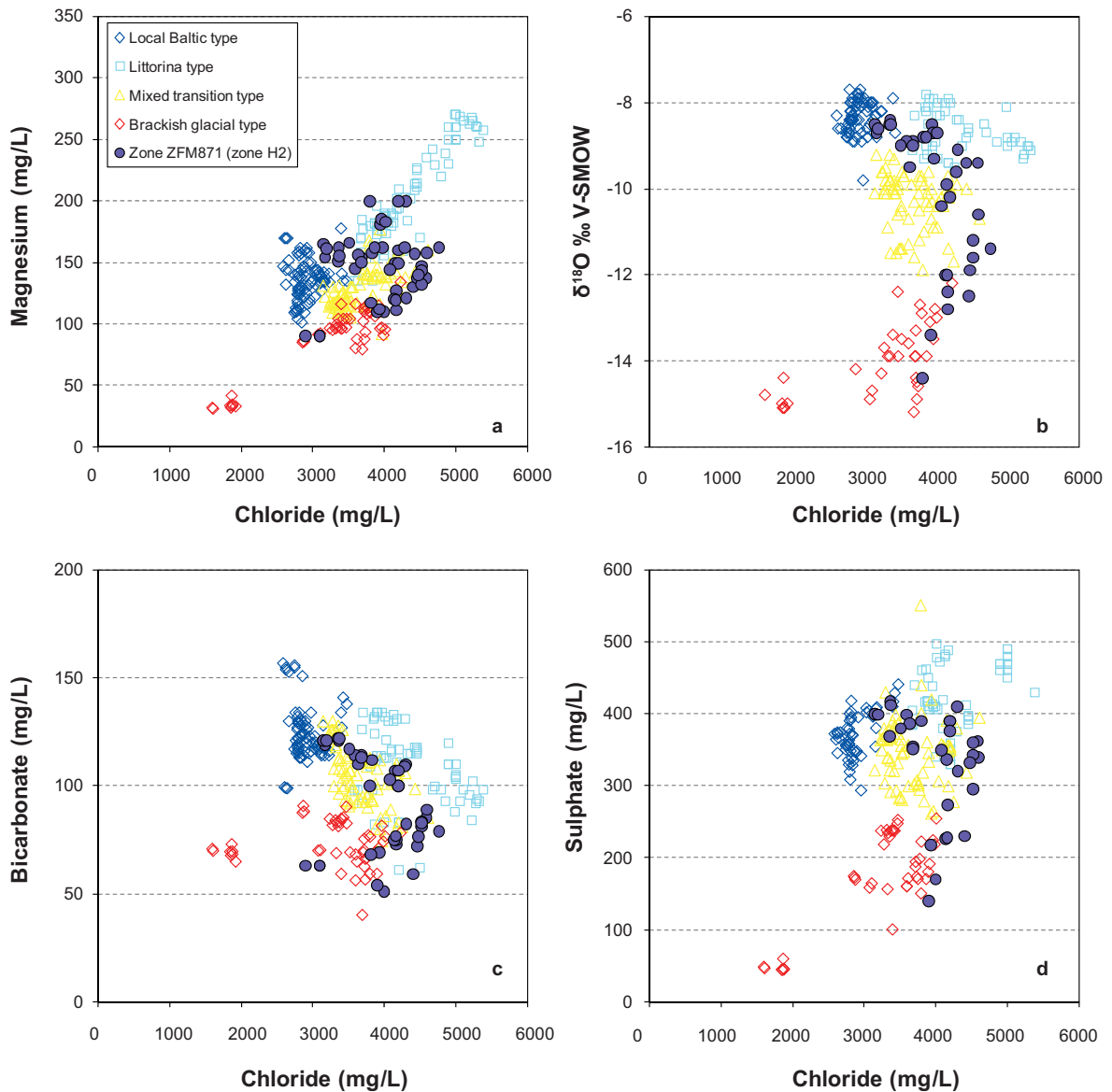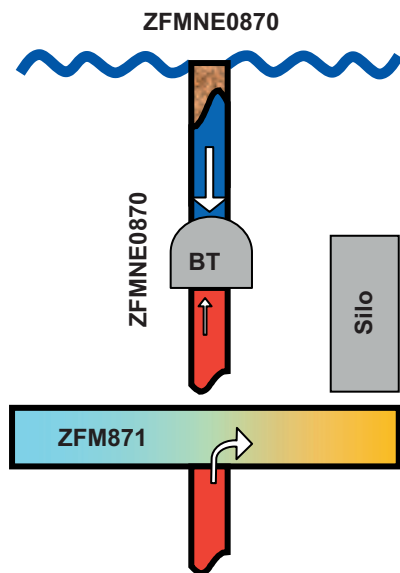

Figure 5-17 a–d. Groundwater composition in boreholes representing zone ZFM871 compared to other borehole data. ZFM871 data are given with purple symbols enclosed in a black line.

ZFMNE0870

The western part of ZFMNE0870 (formerly Zone 9) has a long intersection with the access tunnels which are expected to cause Baltic type intrusion in its upper part; however no hydro-chemical data are available. In addition, there are no data from above the BT access tunnel and none below zone ZFM871 (formerly Zone H2).

Above the SFR no hydrochemical data are available but the groundwater is assumed to be Baltic in type.

A large drawdown suggests relative poor connectivity to the Baltic Sea, e.g. KFR101 has no detectable tritium at a ground-water level = –31 m coinciding with the intercept elevation.

Between tunnel BT and zone ZFM871 the Brackish-glacial type signature increases with time (KFR02-04), probably due to an upward directed deep flow. Zone ZFM871 has a different development, suggesting poor connectivity.

Closer to ZFM0805A,B, the irregular patterns reflect converging flow paths at junctions with ZFM871/ZFM0805A,B.

Figure 5-18. Possible interpretations of flow paths at the junction between zones ZFMNE0870 and ZFM871 (Öhman J 2011, personal communication).

5.3.4 The Central Block and zones southeast of zone ZFMENE3115

The boreholes within the Central Block and southeast of zone ZFMENE3115 have been all drilled recently within the SFR extension project. The boreholes included are KFR102A, KFR105, KFR106 and HFR106 and several of the sampled borehole sections intersect different deformation zones. The elevations (m.a.s.l.) of the investigated sections, the deformation zones and the general water types are given in Table 5-5.

The groundwater compositions of samples collected in this recently investigated area are compared in Figure 5-19 a–d. The plots demonstrate the following:

- The Littorina component is less abundant in these samples and very few samples, all of them from a single very shallow location (–31 m.a.s.l.), showed the Local Baltic groundwater type.

- The most saline samples, deviating from the other samples and closest to the Littorina cluster in the oxygen-18 plot, where collected in a single borehole section situated close to one of the interpreted shallow bedrock aquifer (SBA) features.

- Groundwaters from borehole sections intersecting zone ZFMNNW1034 show the largest spread in water composition which may reflect intersecting the same zone at different depths.

Table 5-5. Borehole (Idcodes), sections (elevation secmid) and water types in the Central Block and intersected zones.

Idcode	Elevation secmid (m.a.s.l.)	Intersected zone	Present water type	Comment
KFR102A	–194.64	–	T	SBA intercept.
KFR102A	–338.97	ZFMENE3115	T	Less saline than the upper section.
KFR105	–117.42	ZFMENE3115, ZFMNE3112	T	4 samples, first (G).
KFR105	–128.38	–	T	
KFR105	–132.73	–	T	
KFR105	–142.94	ZFMWNW8042, ZFMWNW3267, ZFMNE3137	T	
KFR105	–153.59	ZFMWNW3267	G	
KFR106	–187.26	ZFMNNW1034	T	
KFR106	–261.03	ZFMNNW1034	G	
HFR106	–31.36	ZFMNNW1034	B	
HFR106	–146.90	ZFMNNW1034	T	3 samples, first (B).

B = Present Local Baltic, L = Littorina type, T = Mixed transition type, G = Brackish-glacial type.
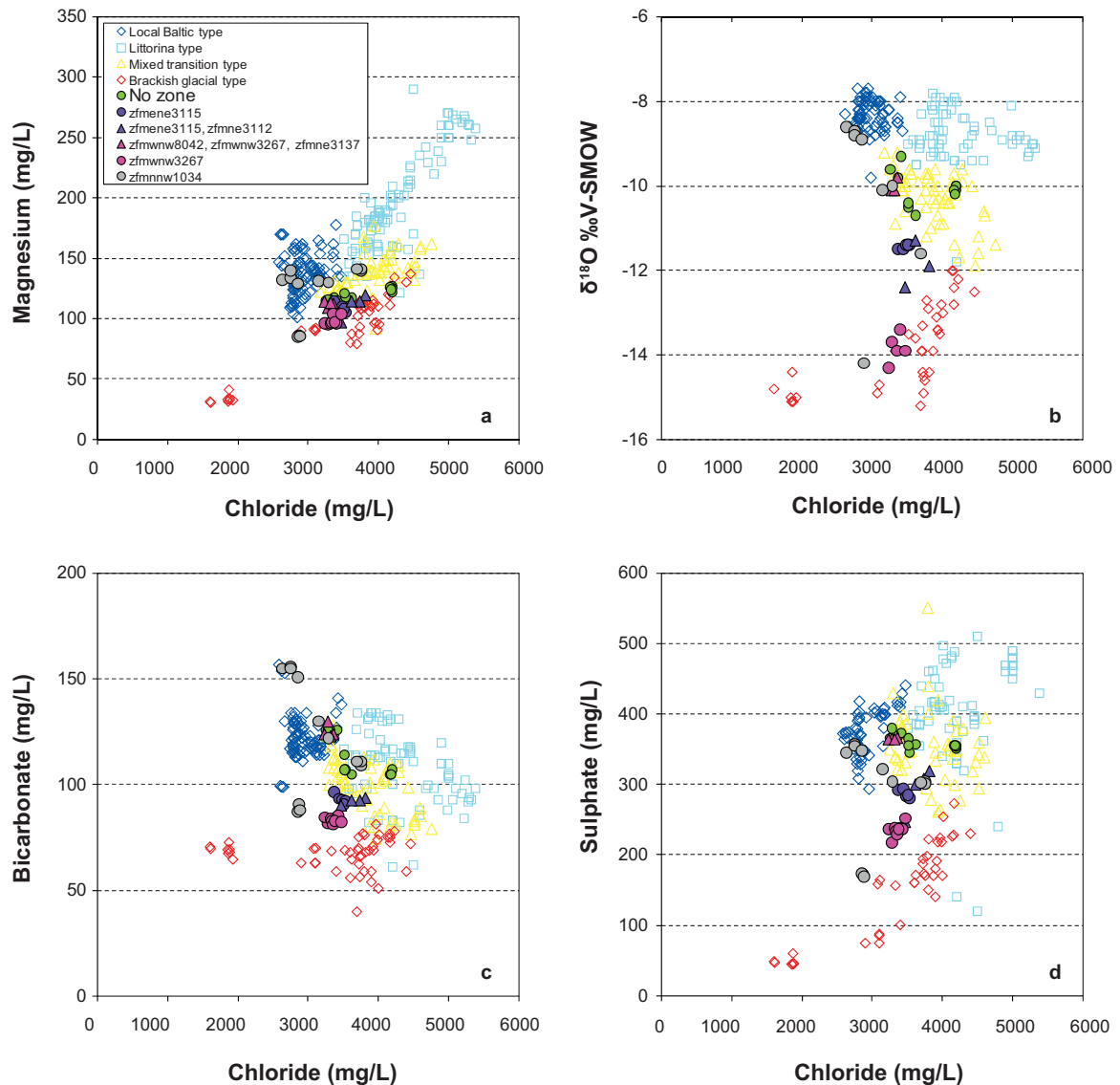
Figure 5-19 a–d. *Groundwater composition in borehole sections representing zone ZFMENE3115 and the area southeast of this zone including zones ZFMNE3112, ZFMWNW8042, ZFMWNW3267,ZFMNE3137 and ZFMNNW1034, as well as "no zone" implying the bedrock mass between the zones (symbols outlined in black) compared to the entire SFR data set (Dataset I).*

5.4   Mixing calculations (M3 analysis)

M3 is a Principal Component Analysis code that approaches the modelling of mixing and mass balance from a purely geometrical perspective (Laaksoharju et al. 1999, Gómez et al. 2006, 2009). This is done by performing a Principal Component rotation of an $n \times n$ covariance matrix, where n is the number of chemical and physicochemical variables (e.g. Gershenfeld 1999). Graphically this is equivalent to the rotation of a reference frame composed of n orthogonal axes until one axis, the first principal component (a variable or a set of correlated chemical variables), points in the direction of the maximum variability of the data set; the second principal component, points in the perpendicular direction with the second largest variability; and so on for the other principal components. Once the samples and the end members have been expressed in the Principal Component coordinates, mixing proportions are calculated in a straightforward way as the local coordinates of each sample in a k–1 dimensional hyper-tetrahedron whose vertices are the k end-member waters (Gómez et al. 2006). Because there is one coordinate (i.e. one axis) for each input variable, at least as many input variables as end members minus one are needed to obtain the mixing proportions (note that this case only works in ideal conditions).

Once the mixing proportions are calculated, the constituents that cannot be described by mixing are described using reactions by simple elemental mass balance supported by independent knowledge of the system. Reactions are inferred heuristically (by inspection) from the difference, for each sample, between the actual value of an input compositional variable and the value computed by M3 assuming pure mixing.

5.4.1 Selection of input compositional variables

As thoroughly explained in Gómez et al. (2006) and Gimeno et al. (2011) mixing results are only meaningful if the Input Compositional Variables (ICVs) are mostly controlled by mixing. Any element can be used as long as its concentration in the mixed water is to first order controlled by the mixing process and not by subsequent reactions; it is the relative intensity of the two processes (mixing and reaction) that matters.

In the case of the SFR dataset, Cl, Br, ^{2}H, ^{18}O, and SO_4 can be considered, after a preliminary exploratory analysis, as elements not affected to first order by reactions. So, the following sets of ICVs have been used:

Set 1: Cl+Br+D+O^{18}

Set 2: Cl+SO$_4$+D+O^{18}

Set 3: Cl+SO$_4$+Br+D+O^{18}

Apart from these three sets, additional sets where analysed, including some non-conservative elements, in order to test; (1) the resolution of the first three sets, and (2) the effect of including non-conservative elements among the input variables in the predicted concentrations for the *conservative* elements. Results obtained with these extra sets will be commented when necessary.

5.4.2 Selection of end-member waters

The selection of the end members to be used has been based on the hydrogeochemical and palaeo-geographical knowledge of the system. Although thoroughly indicated above, in order to under-stand the selection process it is worth indicating here again that the main objective of the study of this system is to describe the disturbed conditions resulting from the SFR activities, and therefore, groundwaters studied at the SFR reach maximum depths concentrated in the upper bedrock regions (0–400 m), the most fractured and potentially transmissive part. Due to this, the hydrochemistry at the SFR is strongly influenced by anthropogenic mixing of resident *in situ* groundwater types of similar palaeohydrogeochemical orgin to those described at Forsmark. The major groundwater groups identified as representing the SFR area comprise Local Baltic Sea type water, Littorina type water with a glacial component, Brackish-glacial water type and Mixed brackish water (Mixed transition type; see Note to Table 3-2). Therefore, the end members considered to have had any possible influence in this system are, in principle, the same ones used for Forsmark (Table 5-6). Some of these end-member waters are represented by real samples from natural systems and some others are estimated from diverse geological sources (for more detailed information cf. Gimeno et al. 2008, 2009).

Table 5-6. Potential end-member waters used in the M3 analysis of the SFR groundwaters.

End-member	Abbr	Na	K	Ca	Mg	HCO$_3$	Cl	SO$_4$	Br	δ^2H	δ^{18}O	Tr
Deep Saline	DS	8,500	45.5	19,300	2.12	14.1	47,200	10	323.6	−44.9	−8.9	0
Glacial meltwater	Gl	0.17	0.4	0.18	0.1	0.12	0.5	0.5	0.001	−158	−21	0
Littorina Sea	Lit	3,674	134	151	448	93	6,500	890	22.2	−38.0	−4.7	0
Altered Meteoric (Forsmark)	AM	274	5.6	41.1	7.5	466	181	85.1	0.572	−80.6	−11.1	12.1
Old Meteoric (Forsmark)	OM	–	–	–	7.5	–	181	85.1	0.572	−50.0	−5.0	0
Baltic Sea (average)	BalP	1,760	66	82	219	78.7	3,025	450	10.3	−60.8	−7.55	15.4
Baltic Sea Local (sample #4330; PFM000064)	BalL	1,410	48.6	69.5	172.0	80.5	2,494.6	345.2	9.42	−60.2	−8.0	14.2

The **Deep Saline end member (DS)** corresponds to the deepest and most saline water sampled in Laxemar. It has a Ca-Na-Cl composition and a significant deviation from the MWL (Meteoric Water Line in $\delta^{18}O$ vs $\delta^2 H$ plots) due to its long interaction with the bedrock in a near-stagnant environment. For Forsmark, the sulphate content of this end member has been changed to a very low value of 10 mg/L (Gimeno et al. 2008).

The **Old Meteoric end member (OM)** corresponds to an old, warm climate derived meteoric water component whose composition is similar to the Altered Meteoric end member but with a longer residence time and different isotopic composition (Laaksoharju et al. 2008). Some concentrations are omitted for this endmember since they are not used in the M3 and they are difficult to estimate.

Glacial end member (Gl) represents the chemical composition of surface meltwaters prior to the water-rock interaction processes undergone during their infiltration into the bedrock. The composition corresponds to present meltwaters from one of the largest glaciers in Europe, the Josterdalsbreen in Norway (Laaksoharju and Wallin 1997). It has a very low content of dissolved solids and an isotopically light signature ($\delta^{18}O = -21‰$ (V-SMOW), $\delta^2 H = -158‰$ (V-SMOW)).

Littorina end member (Lit). The chemical composition of the Littorina end member is based on the maximum salinity estimation of 12‰ or 6,500 mg/L Cl$^-$ for the Littorina stage, while the concentration of other main elements were obtained by diluting the global mean ocean water (Pitkänen et al. 2004).

The **Altered Meteoric end member (AM)** corresponds to a real sample from Forsmark (Gimeno et al. 2008, 2009) which represents a typical shallow dilute groundwater (less than 100 m depth) of recent meteoric origin and, therefore, it should reflect the chemical characteristics of meteoric waters after a short interaction with soils, overburden and granite. Its tritium content and low chloride concentrations are representative of its recent meteoric origin and the absence of mixing processes with more saline waters.

The **Baltic Sea (average) end member (BalP)** corresponds to the average Baltic Seawater defined by Pitkanen et al. (2004). It is a good compromise for the Baltic Sea end member as it gives a spatial (and, in some way, a temporal) average which eliminates short lived and local variations. However, due to the fact that infiltration of Baltic Seawater into the SFR bedrock has increased during the construction and operation of the SFR, it seems also reasonable to use a local Baltic Sea sample as an end member.

The **Baltic Sea (local) end member (BalL)** is a real water sample collected in the Baltic Sea near the SFR site (sample #4330, PFM000064). The selection of the most appropriate local Baltic Sea sample (among the 51 samples in the dataset) was carried out with the help of M3's End-member Variability Module (Gómez et al. 2006). A summary of the procedure can be found in Gimeno et al. (2011).

5.4.3 PCA and mixing calculations with M3

Once the ICVs needed to create the PCA, and the extreme compositions to be used as potential end members have been selected, M3 performs a systematic search of combinations. For the 7 potential end members used here (Table 5-6), the total number of combinations is 127. In other words, M3 solves the mixing problem for all the samples in the dataset a total of 127 times for each set of ICVs (the three sets indicated above and some other alternative options (Gimeno et al. 2011)), selecting each time a different combination of potential end members and computing the percentage of samples (coverage) that can be explained by mixing the chosen end members. The "best" combinations of end member waters are *a priori*, those with higher coverage, i.e the maximum number of samples in the dataset inside the mixing volume (whose corners are occupied by the end members). A complete description of these results can be found in Gimeno et al. (2011).

As a summary, only mixing models with three and four end-member waters have coverage > 80%. The best combination of 5 end members (with 5 ICVs, Cl, SO$_4$, ^{2}H, ^{18}O, Br and Cl, SO$_4$, ^{2}H, ^{18}O and Na) have low maximum coverages of 52.7% and 68.6% respectively, thus casting serious doubts on the possibility of more than four end-member waters being responsible for the chemistry of the whole set of SFR groundwaters.

Apart from other interesting conclusions obtained from this analysis (cf. Gimeno et al. 2011), the following three can be highlighted here; (1) only mixing models that include both the Glacial and the Deep Saline end members can be considered capable of explaining the SFR groundwaters, (2) both Baltic Sea end members (BalP and BalL) are equally good *a priori*, and (3) the Old Meteoric (OM) end member only appears in sets of conservative ICVs, whereas the Altered Meteoric (AM) only appears in sets of non-conservative ICVs.

Without any *a priori* knowledge of the site, three end-member and four end-member combinations are equally possible, and no one can be eliminated. Also, no set of ICVs can be eliminated beforehand without a more detailed analysis of each mixing model. This is the topic of the next section.

Test of mixing models

Coverage is not the only attribute of a "good" mixing model. Obviously, a key aspect for classifying a mixing model as good or bad is how well the chemical composition of conservative elements (in this study Cl, ^{2}H, ^{18}O, SO_4^{2-} and Br) can be reproduced. This is easily performed once the mixing proportions have been computed. Then the values obtained for each sample are compared with the measured values by plotting them in an X-Y plot with the measured values in the horizontal axis and the calculated ones in the vertical axis (some examples will be shown next). The analysis of all the mixing models can be found in Gimeno et al. (2011) and are briefly described below.

Apart from a simple visual inspection, a more quantitative assessment of the quality of each mixing model was performed. The reduced chi-square statistics, χ_r^2, have been used as a measure of suitability (i.e. good or bad fit) because it is useful for assessing relative deviations (Gimeno et al. 2011). The values obtained have been very useful therefore to categorise the suitability of the models and also to discard many of them:

- Sets of ICVs with only conservative elements are superior to sets with conservative and non-conservative elements; therefore, the models obtained with the sets of ICVs containing all the variables have been eliminated.

- Four end-member combinations are superior to three end-member ones; therefore, models obtained with Set 1 (Cl+Br+D+O^{18}) have also been eliminated as they only give combinations with 3 end members.

- Sets 2 and 3 (S2: Cl+SO$_4$+D+O^{18}, S3: Cl+SO$_4$+Br+D+O^{18}) with different combinations of 4 end members give the best results; but the suitability of the fit is much better in the case of using Set 2 (4 ICVs) than Set 3 (5 ICVs).

- Finally, there are two models far superior to the rest from a chi-square point of view: [DS Gl Lit OM] with a reduced χ^2 of 0.6 and a coverage of 100% and [DS Gl Lit BalL] with a reduced χ^2 of 1.1 (the third model in suitability has reduced χ^2 of 14.2, more than ten times bigger (Gimeno et al. 2011)) and a coverage of 94.5%. The comparison between the measured and the calculated values for the conservative elements in these two models is shown in Figure 5-20.

Figure 5-22 plots deviations with respect to the conservative elements chloride, sulphate, deuterium and oxygen-18 for the selected mixing model. Sulphate is reproduced even better than chloride, which can be a little surprising as its behaviour is not usually as conservative as that of chloride. The isotopes are also well reproduced, although the scatter is slightly larger than for chloride. Overall, the match between the predicted and measured concentrations of chloride, sulphate, deuterium and oxygen-18 can be considered as excellent from a chi-square point of view. Thus, it could be concluded that only the first two mixing models reproduce in a quantitatively satisfactory way the mixing behaviour of SFR groundwaters. The question is which of them is better?

Mixing proportions

The two selected mixing models are based on four conservative input compositional variables (Cl, SO$_4$, δ^2H, and δ^{18}O) and have four end members: Model 1 consisting of Deep Saline, Glacial, Littorina, and Baltic Sea (local), and Model 2 including Old Meteoric instead of Baltic Sea. Figure 5-21 summarises in a graphical way the mixing proportions predicted by the 2 mixing models. Samples are separated in four groups according to water type, and within each group they have been sorted by increasing sample number, but the labels shown are not the sample IDs, only a numeric order. Gaps in the graph correspond to samples that cannot be explained by the selected mixing model ($\approx$ 10 samples). Mixing proportions for all samples in the dataset using the two models are tabulated in Gimeno et al. (2011).
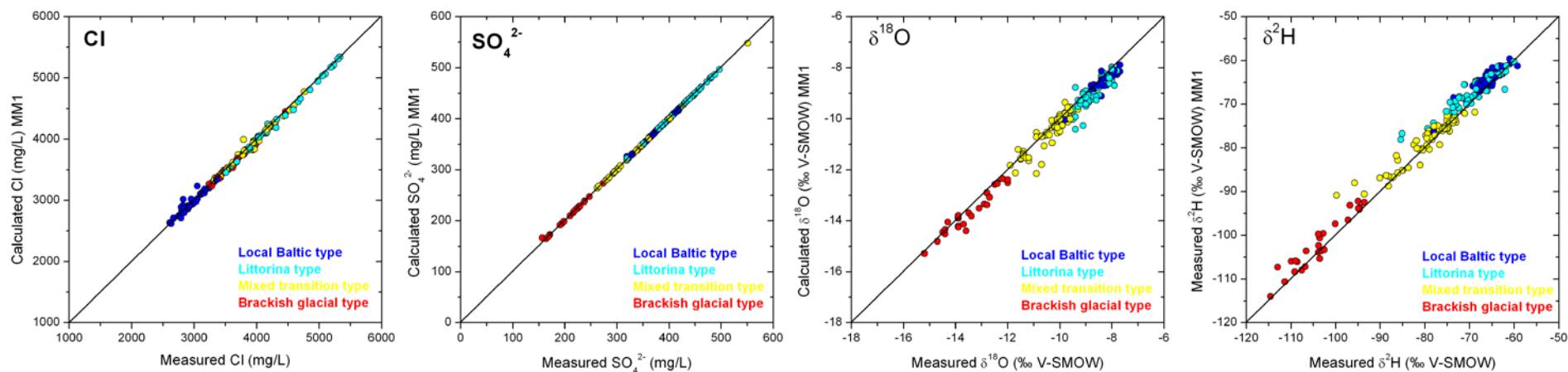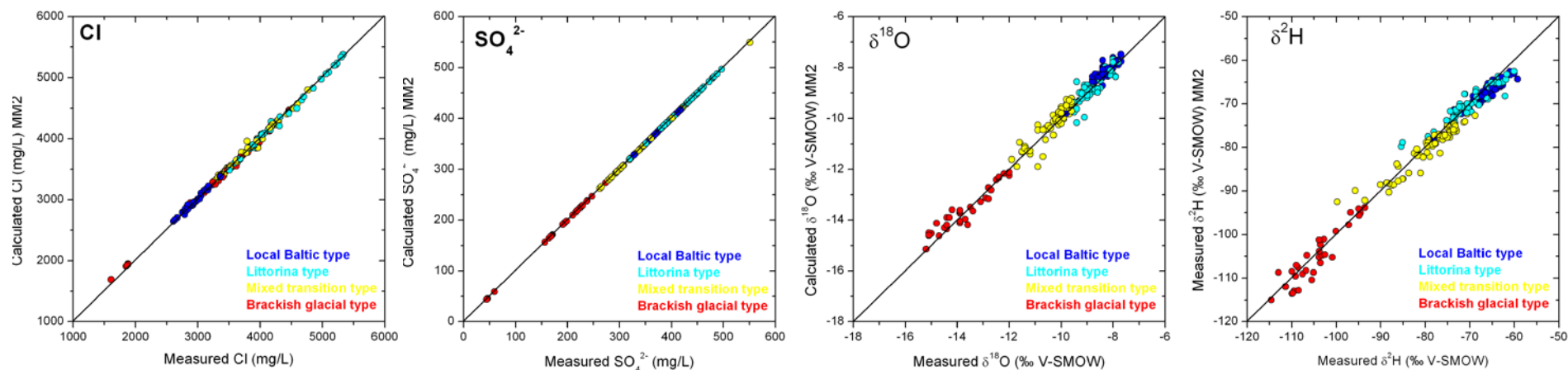
Figure 5-20. *Measured and calculated chloride, sulphate, deuterium and oxygen-18 values in the finally selected 2 mixing models, with the measured concentration in the vertical axis and the calculated one in the horizontal axis. The closer to the diagonal line the better the reproducibility of the measured values. Both models have $Cl+SO_4+^2H+^{18}O$ as input compositional variables. Apart from Cl and the isotopes, sulphate behaves as a conservative element in this system, as clearly shown in the corresponding plots.*
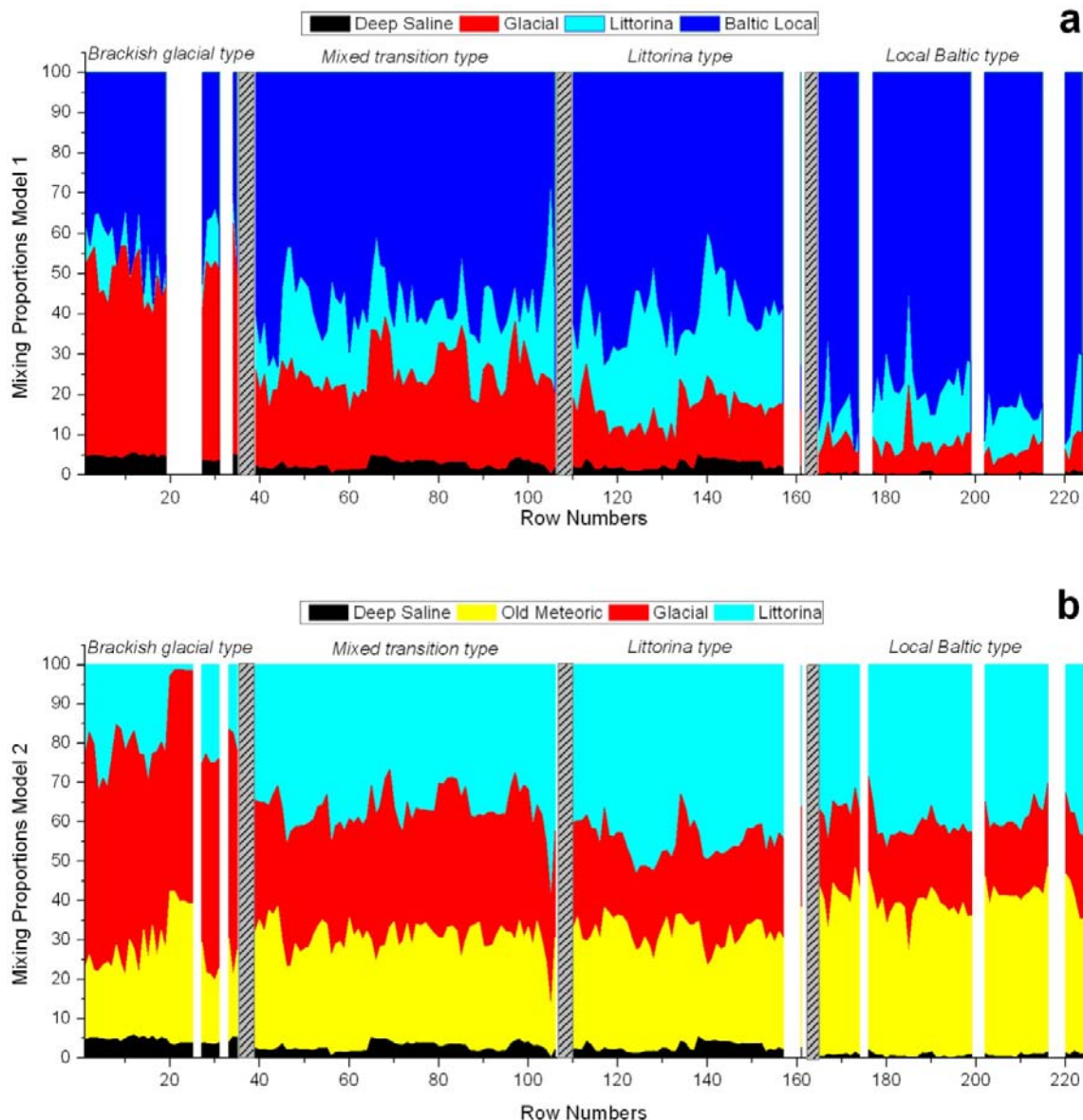
Figure 5-21. Mixing proportions predicted by the selected mixing models. Samples are ordered in four groups according to the water type, and within each group they have been sorted by increasing sample number but the labels shown do not represent the sample ID, only a numeric order. White gaps in the graph correspond to samples that can not be explained by the selected mixing model (≈10 samples).

As shown in the plots, Model 1 (with the BalL end member) predicts that the most abundant component in the SFR groundwaters is BalL, followed by the Gl (only dominant in some of the waters of the Brackish-Glacial type) and Lit components; the DS component is, by far, the less abundant (this is clearly seen in the PCA plots, where the DS end member plots very far from the locations of the set of samples, Figure 3-7). This could be correct for many samples (mainly those affected by the hydraulic drawdown effects resulting from the SFR) but it is clearly inaccurate for most of the Brackish-glacial type waters, where the influence of the local Baltic Seawaters is negligible.

Model 2, with the Old Meteoric end member, predicts similar abundances, in general, for the Litt and the OM components which increase as the proportion of Gl decreases. Gl is clearly dominant, even more than in Model 1, in the case of the Brackish-glacial type groundwaters. The DS component is exactly the same as in Model 1. This model looks acceptable for the samples that were not well explained with Model 1 (the ones with the highest glacial signature) but is unacceptable for the set of samples at the right side of the plot, i.e. those with a clear Baltic seawater component in them.

An alternative way of viewing these results is by means of x-y graphs where the mixing proportions of one end member are plotted against the mixing proportions of another end member for each of the selected mixing models (Figures 5-22 and 5-23). For Model 1 (Figure 5-22), the BalL end member is plotted against the other three end members in the first column. For Model 2 (Figure 5-23), the OM end member is the one that is plotted against the other three. For both models (Figures 5-22 and 5-23), the Lit end member is plotted against the two remaining end members (Gl and DS) in the second column; and in the third column the Gl end member is plotted against DS.

Samples that can be explained as a mixture of only two end-member waters will plot on the diagonal line when the two end members contributing to its composition define the axes of the graph. A sample plotted on one axis has a zero contribution from the end member occupying the other axis; a sample near the origin of coordinates has zero contribution from the two end members that define the axes in the corresponding graph; and a sample located in the interior of the triangular area defined by the two axes and the diagonal line has contributions from at least three (possibly four) different end member waters (the two end members defining the axis plus, at least, one end member more).

Figure 5-22. Mixing proportions for mixing Model 1. Colours refer to the water types defined in Section 3.3.1 (red: Brackish-glacial water type; blue: local Baltic water type; cyan: Littorina water type; yellow: Mixed transitional water type). The Gl versus DS mixing plot is also shown in an expanded view. The slanted line ending in 100% Gl is the same diagonal line shown in the rest of the graphs.

Apart from the visualisation of the mixing proportions corresponding to the different groundwater types (colour codes in the plots), these plots show the relative distribution of these groups. One of the first observations to highlight is that here the meaning of "transitional" is made clear; these waters are basically a complex mixture with contributions from the Gl, Lit and BalL end members (for Model 1) or Gl, Lit and OM end members (for Model 2), although basically their position in the graphs fills the gap between groundwaters dominated by the Gl and the Lit end members.

Baltic and Littorina water types follow a clear trend that starts with the BalL end member (lower left corner in the upper right graph in Figure 5-22) and evolves towards the Lit end member by increasing at the same time as the Lit and Gl contributions. On the other hand, neither the brackish-glacial nor the transitional water types follow any clear trend. A final interesting observation is the trend followed by all groundwater types when glacial proportions are plotted against DS. To better appreciate this trend, these graphs have been plotted again in the corresponding figures with the vertical axis (DS mixing proportions) expanded.

There is an obvious continuous increasing trend starting at the origin of coordinates in Figure 5-22, and slightly displaced to the right (higher Gl proportion) in Figure 5-23. In both cases, Baltic type waters are the first ones in the trend, followed by Littorina waters, then by the mixed transitional
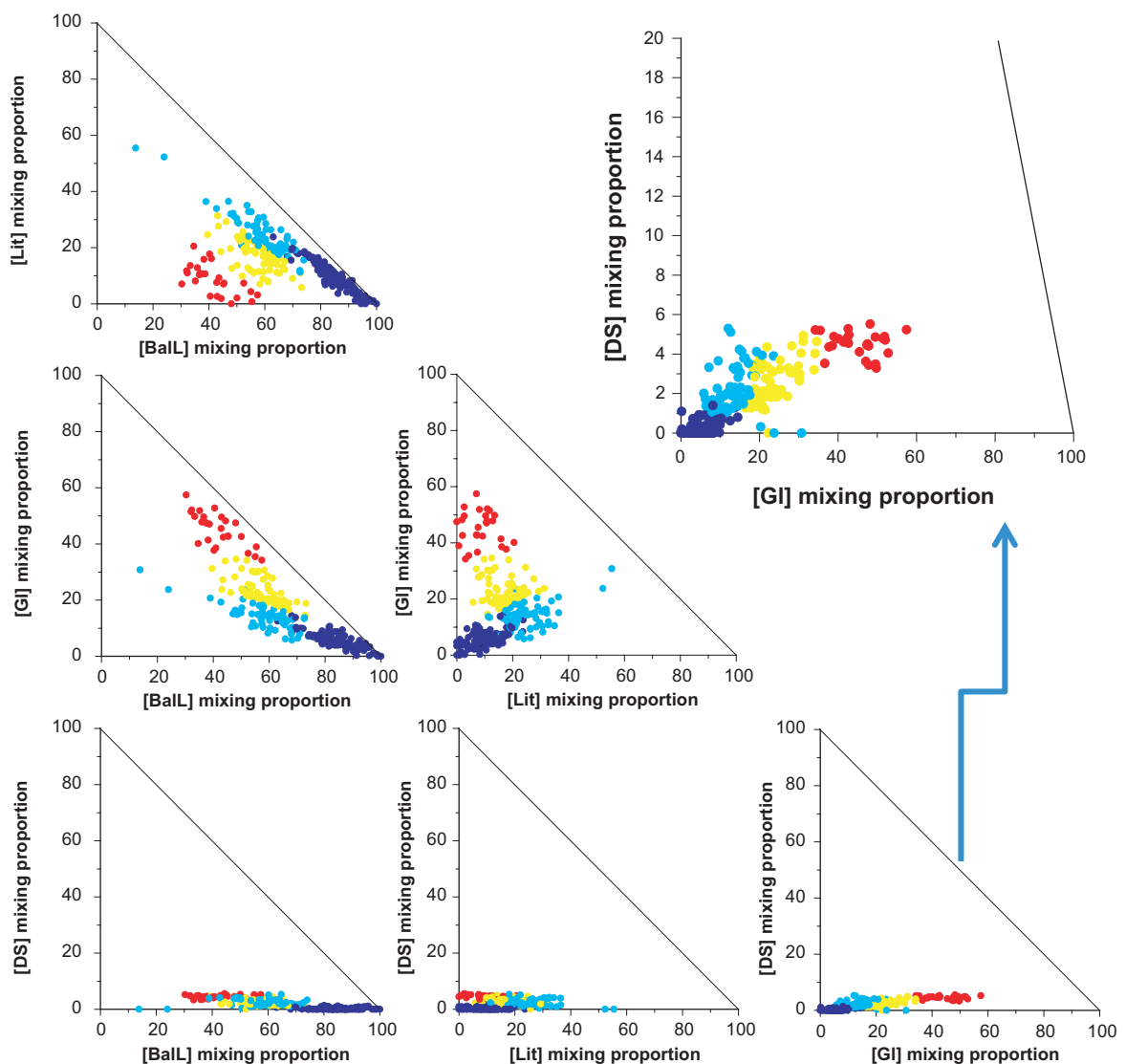

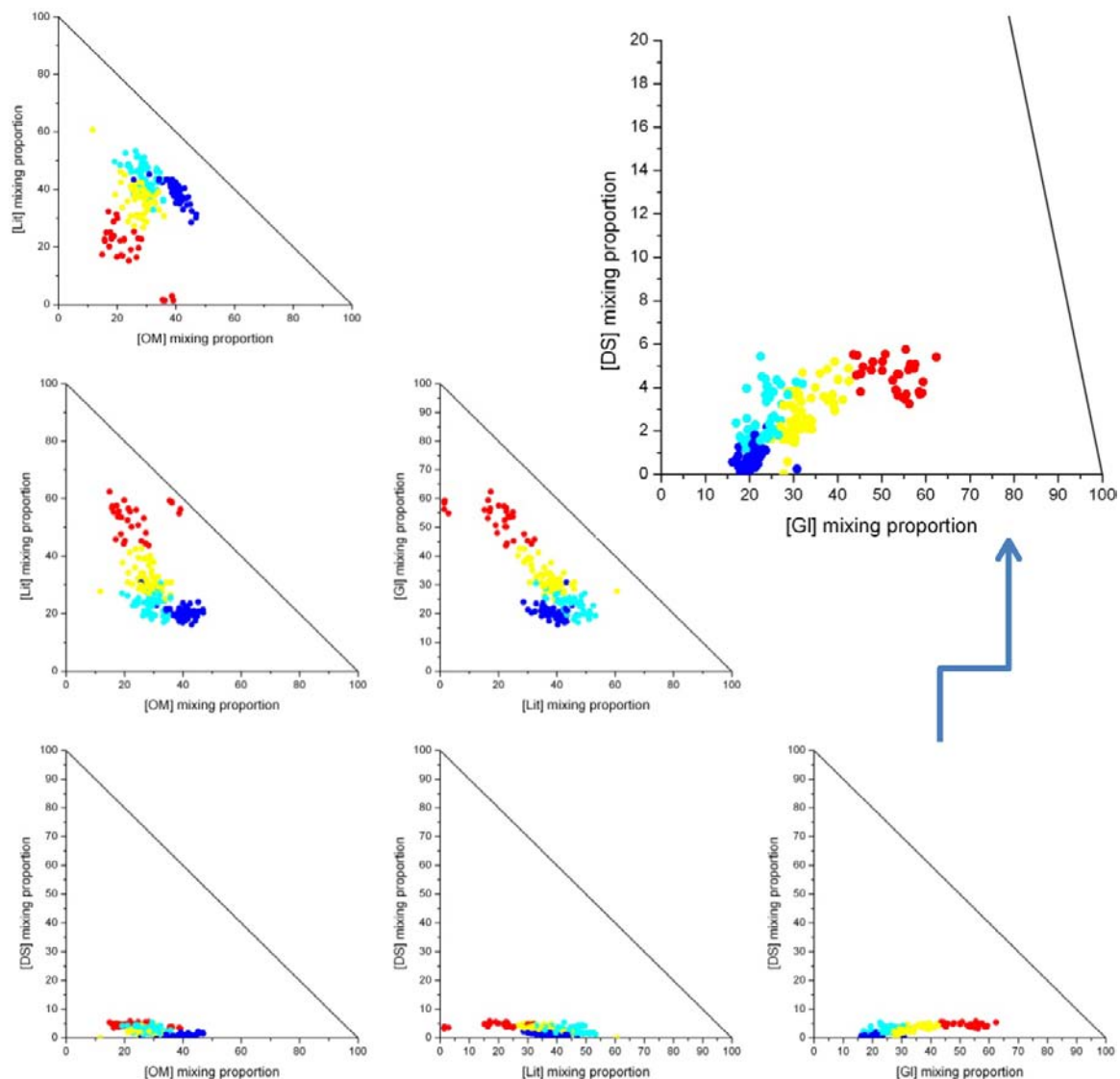*Figure 5-23. Mixing proportions for mixing Model 2. Colours refer to the water types defined in Section 3.3.1. (red: Brackish-glacial water type; blue: local Baltic water type; cyan: Littorina water type; yellow: Mixed transitional water type). The Gl versus DS mixing plot is also shown in an expanded view. The slanted line ending in 100% Gl is the same diagonal line shown in the rest of the graphs.*

waters and finally by the brackish-glacial ones. This trend implies a parallel increase in the contribution of both the Glacial and the Deep Saline end members (and a decrease in the contribution of the Lit end member). In other words, those samples with the strongest glacial signature are, at the same time, those with the largest percentage of the Deep Saline end member, in agreement with what could be expected from an original salinity gradient established between glacial waters and deep saline waters occupying the lower reaches of the groundwater system. Here, the "transitional" character of the transitional groundwater type is also evident, filling the gap between the Glacial and the Littorina groundwater types.

A thorough analysis of the difference in the mixing proportions between models 1 and 2 is presented in Gimeno et al. (2011). The key results are that the Deep Saline proportions obtained with both models are almost the same, and the proportion of the Baltic Local end member of Model 1 is converted in Old Meteoric plus additional Littorina and Glacial proportions in Model 2, i.e. the Littorina and Glacial have higher mixing proportions in Model 2 (cf. Figure 5-24).
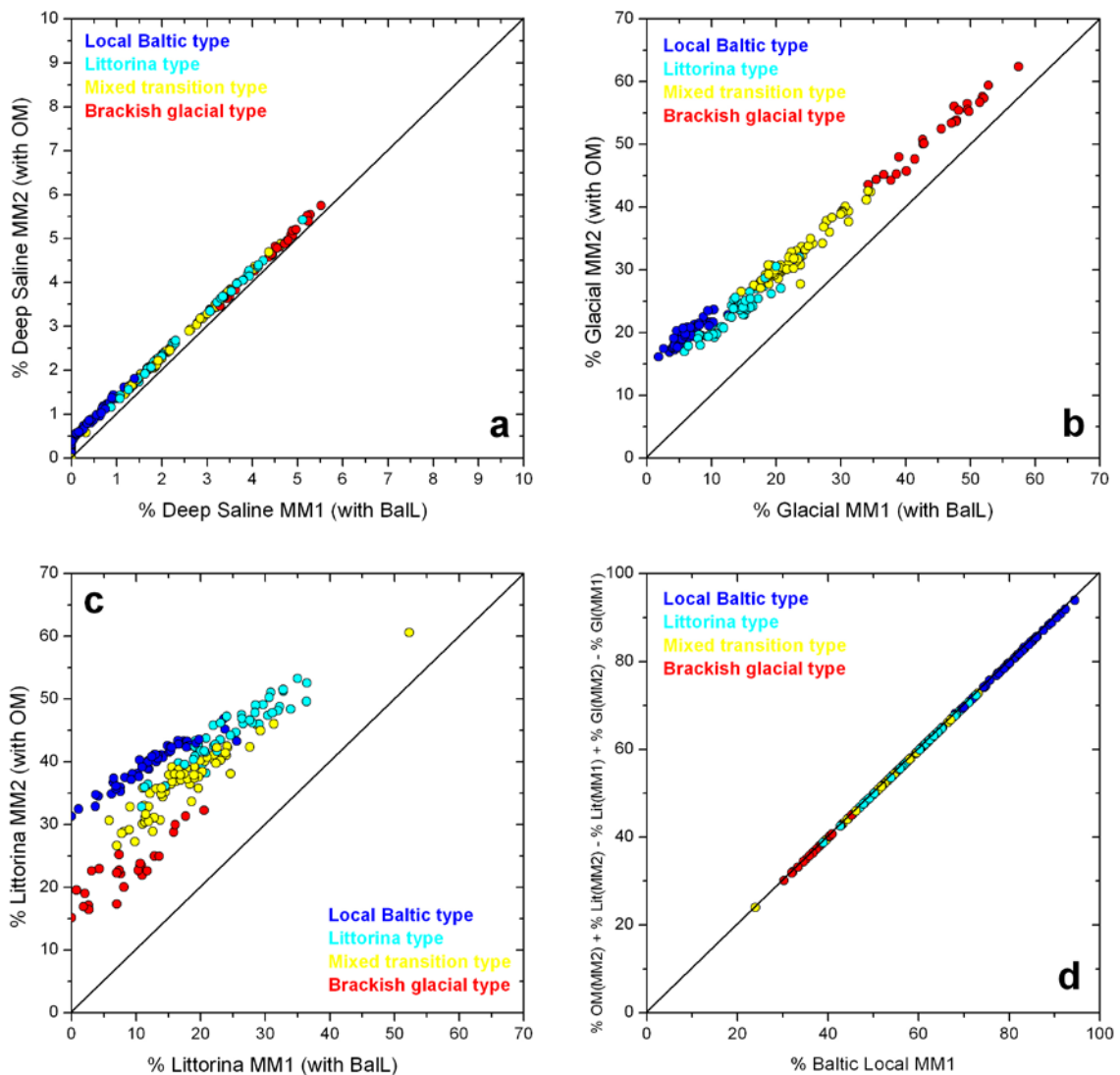
Figure 5-24. Comparison of the mixing proportions obtained for the end members in models 1 (x axis) and 2 (y axis). Deep Saline, Glacial and Littorina are easily compared as they are present in both models. The two remaining end members BalL and OM can not be compared directly, but figure 'd' shows that the BalL proportion obtained with Model 1 is translated as a combination of OM and an excess of Litt and Gl proportions in Model 2, with respect to their proportions in Model 1.

Discussion

As presented above, both models are very good at predicting the concentration of conservative elements (Figure 5-20), but they are less successful when comparing mixing proportions, as the set of end members is not unique.

Therefore, a multivariate statistical approach alone does not seem to be enough to discriminate which mixing model is best. However, statistics are not the only consideration that should be used here; the hydrogeochemical history of the site is also of utmost importance. Based on the hydrogeochemical and palaeohydrogeological knowledge of the system (Nilsson et al. 2010a), old meteoric water components, represented by the Old Meteoric end member, are thought to have been present at shallow to intermediate depths. However, the effects of a Baltic Seawater component are also evident in some parts of the system, either because it was present in the fracture zones before construction of the SFR tunnels, or, mainly, as a result of the recent drawdown as a consequence of its construction. Therefore, both models are equally suitable and reasonable from a hydrogeochemical point of view, but they are applicable to different sets of samples. Having more data on the system, a more specific analysis could be done applying the same procedure but to two different sets of data.

Nevertheless, from a hydrogeological point of view, there is a very interesting piece of information that could be extracted from this otherwise not very conclusive analysis. Despite the different end members and mixing proportions obtained with these two mixing models, it is quite a remarkable fact that the predicted chemical composition as a result of mixing (without reaction) is very similar irrespective of the model used. This is shown in Figure 5-25, where the composition calculated from mixing model MM1 is plotted against the one calculated from mixing model MM2. Except for bicarbonate, whose results are completely different when computed with Model 1 or Model 2, all the other main chemical variables give almost exactly the same value in both models.

This fact would allow a hypothetical composition due to mixing (without the influence of reactions) to be calculated for the whole set of samples, including not only the conservative elements, but also other more reactive ones such as magnesium, sodium, calcium or potassium. These compositions could then be used to calibrate the hydrogeological models of mixing over time, which would add a very important additional constraint that cannot be included in this statistical analysis.

The alternative possibility that is being presently analysed is to try and work with five end members. Had good mixing models with five end members (including always OM and BalL) been found, mixing proportions for the five end-member waters could have been obtained for all the explained samples. However, as thoroughly explained in Gimeno et al. (2011), the best five end member combination represented by DS+Gl+BalL+Lit+OM, was obtained with two different sets of 5 ICVs; $Cl+SO_4+^2H+^{18}O+ Br$ and $Cl+SO_4+^2H+^{18}O+Na$, but the coverage was very low in both cases, 52.7 and 68.6%, respectively, and therefore the results were not very promising. These results are shown in Figure 5-26 using the same type of plots used for models 1 and 2 in Figures 5-22 and 5-23. It is clear that even in this case, mixing proportions obtained for the Baltic end member exceed what would be reasonable for most of the groundwaters of the Brackish-glacial type, although the percentage of the Baltic end member is much lower than in Model 1.

Additional analysis were performed (Gimeno et al. 2011) in order to test the somehow unusual behaviour of the results. Considering that the most uncertain end member used in the models was the old meteoric water, a search for the most appropriate old meteoric composition was carried out with the help of M3's End-member Variability Module (Gómez et al. 2006). Unfortunately, the final result didn't improve what had been found with the original one except in the coverage which could be increased only to 90%.

Though not very conclusive, the improvement found when adding an element like sodium, to the set of ICVs (improving the coverage and still predicting well the concentrations of the conservative elements), indicates that more M3 work must be done in order to systematically analyse which is the best set of ICVs that, being as much conservative as possible to maintain the good fit with the measured values, is also able to resolve the contribution of more end member waters.
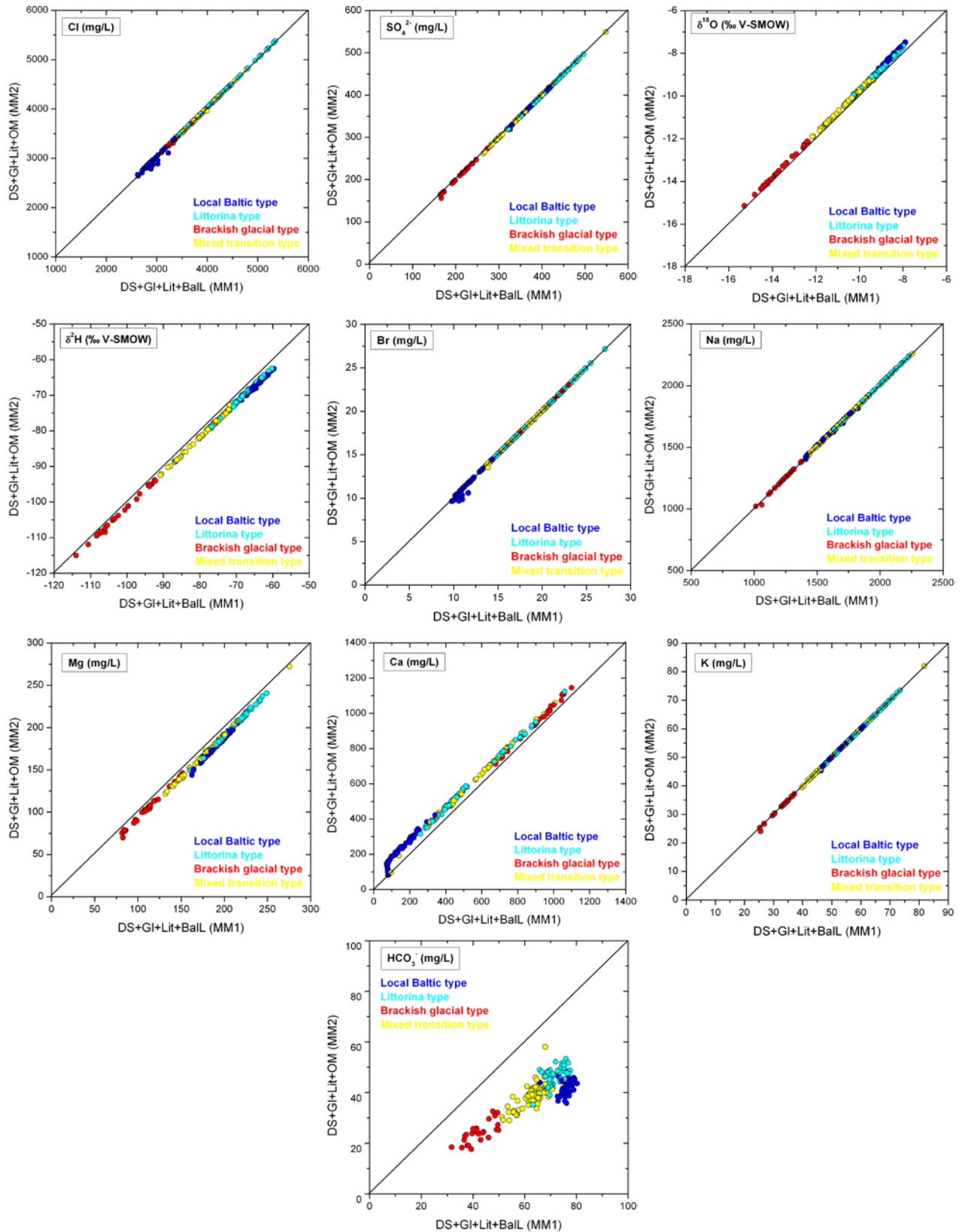
Figure 5-25. *Comparison of the values for the main chemical components calculated with models 1 (x axis) and 2 (y axis). Except for the bicarbonate, the values obtained for all the others are almost the same.*
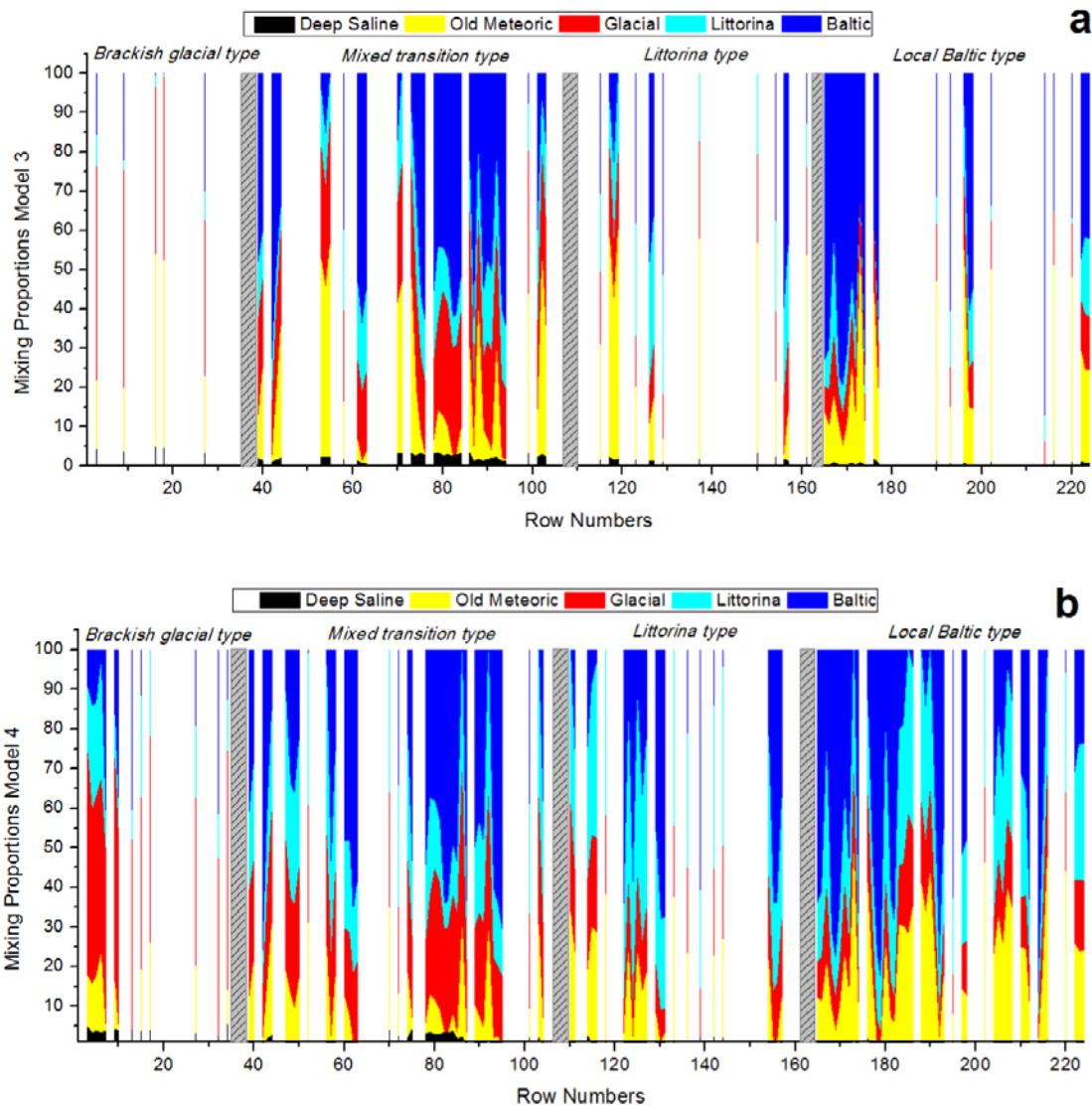
Figure 5-26. *Mixing proportions predicted by the mixing Models 3 and 4. White gaps in the graphs correspond to samples whose composition cannot be explained by them. Samples are ordered in four groups according to the water type, and inside each group they have been sorted by increasing sample number but the labels shown do not represent the sample ID, only a numeric order.*

5.5 Description of groundwater-mineral systems

5.5.1 The carbonate system and pH

The carbonate system is fundamental in understanding the evolution of groundwater parameters such as alkalinity, dissolved calcium and pH in groundwaters representing granitic systems. Calcite is one of the most abundant minerals in fracture fillings (cf. Section 2.1.4) and plays a fundamental role in the pH buffering (cf. Section 5.7) of the recharge groundwaters. Moreover, at the SFR site carbonates are present in the seabed sediments and therefore have been in contact with marine waters during percolation down to the bedrock (cf. Lundin et al. 2004).

The bicarbonate concentrations in the SFR groundwaters range from 40 to 190 mg/L (0.65 to 3.11 mmol/L) and their trends with respect to depth and chloride contents correspond to those of the Forsmark groundwaters (Figures 5-4 a and 5-27). The highest bicarbonate contents in the SFR are found in the brackish marine groundwaters of Littorina and, mainly, Local Baltic types (Figure 5-4 a). These high and variable HCO_3^- values are the result of the biological activity during infiltration of marine waters through the seabed sediments.

Figure 5-27. Bicarbonate concentration plotted versus sampling date; groundwaters from annually sampled borehole sections (bottom sections) in KFR01, KFR08, KFR10 and KFR7A as well as from KFR04 at 28.0 to 43.0 m borehole length. KFR10 had packers installed (section 87.0–107.28 m borehole length) probably until year 1987. After that date the entire borehole was sampled. The sample from KFR10 in 2001 is interpreted to be of a Local Baltic groundwater type due to a low and probably erroneous chloride value. The borehole lacks data for a period during the 1990's.
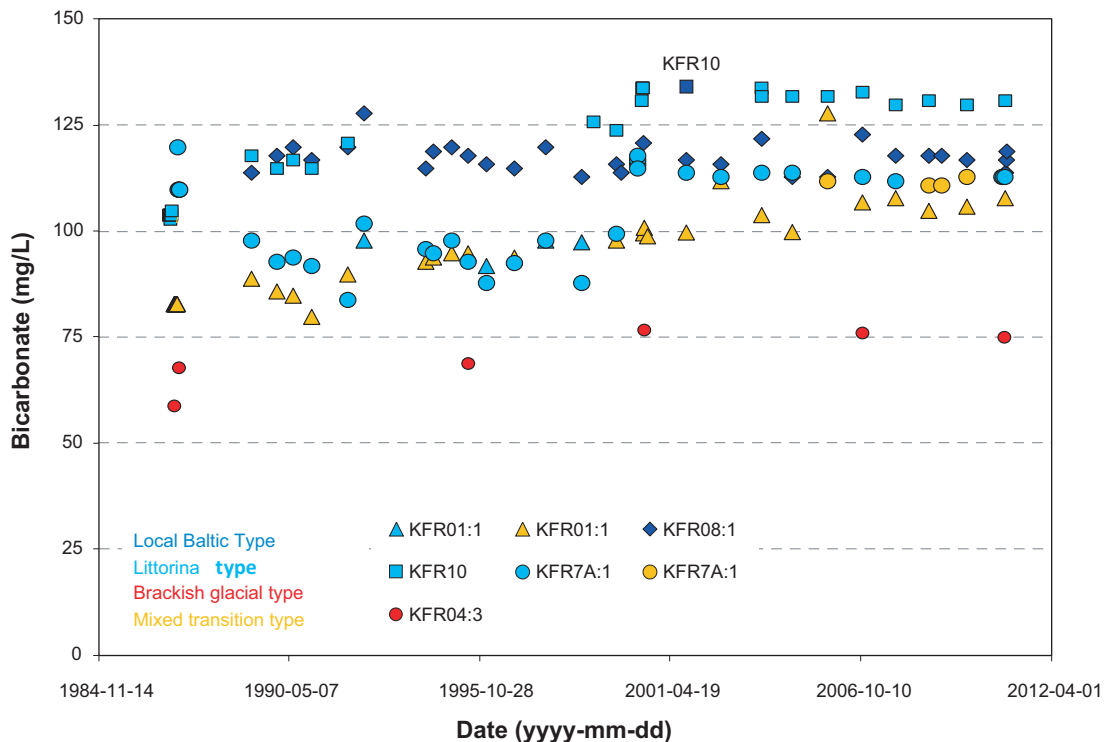
Dissolved calcium concentrations range from 87 to 1,220 mg/L (2.17 to 30.5 mmol/L) and their trends with respect to depth are shown in (Figure 5-4 b). The plot shown in Figure 5-27 indicates a weak increase in bicarbonate content (and also in pH, Figure 5-28) with time which is mainly attributed to increased inflow of Baltic Seawater during the operational phase of the SFR. It is also evident that the Brackish-glacial type groundwater has the lowest bicarbonate values, whereas the brackish marine waters (both Littorina and present Local Baltic type groundwaters) are highest in bicarbonate.

Most of the pH values for the SFR groundwaters are laboratory measurements and show a larger spread than those measured in the field or *in situ* using Chemmac. In Figure 5-28 the measured pH values are plotted versus sampling date and show a weak increase with time. Whether this reflects real conditions or not is difficult to judge because field or *in situ* Chemmac measurements (which usually are regarded as more representative than the laboratory measurements) are only available from 2009 and onwards. It is also noted that the lowest pH values from laboratory are all restricted to measurements prior to 2000 possibly indicating some problems related to the laboratory routines. Most importantly, despite the possibility that the routine procedures for pH measurements may have been changed and that the quality of the values may differ over time, it can be concluded that the pH in the groundwaters at SFR are, with a few exceptions, all between 7 and 8 which is within the pH range for the Forsmark samples (cf. Laaksoharju et al. 2008).

Because most of the pH values for the SFR groundwaters are measured in the laboratory, theoretical pH values assuming calcite equilibrium are useful for comparison (a thorough sensitivity analysis to the pH values is presented in Gimeno et al. (2011)). Measured pH in the SFR groundwaters ranges from 6.6 to 8.0 and the calculated values (assuming calcite equilibrium) fall within a narrower range, between 7 and 7.7 (cf. Gimeno et al. 2011). There is no clear correlation with depth for measured or calculated pH values (Figure 5-29 a and b), which might reflect the heterogeneity of the system and also the frequent horizontal dispersion of this parameter in the examined sections.
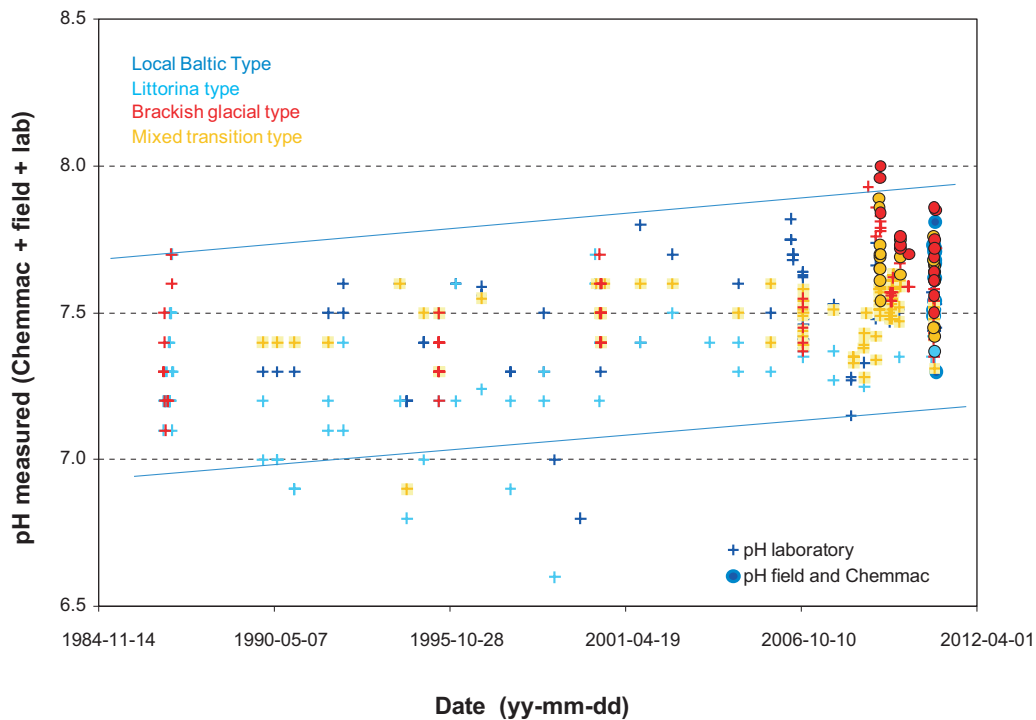
Figure 5-28. *Measured pH in groundwaters from the SFR area plotted versus sampling date.*
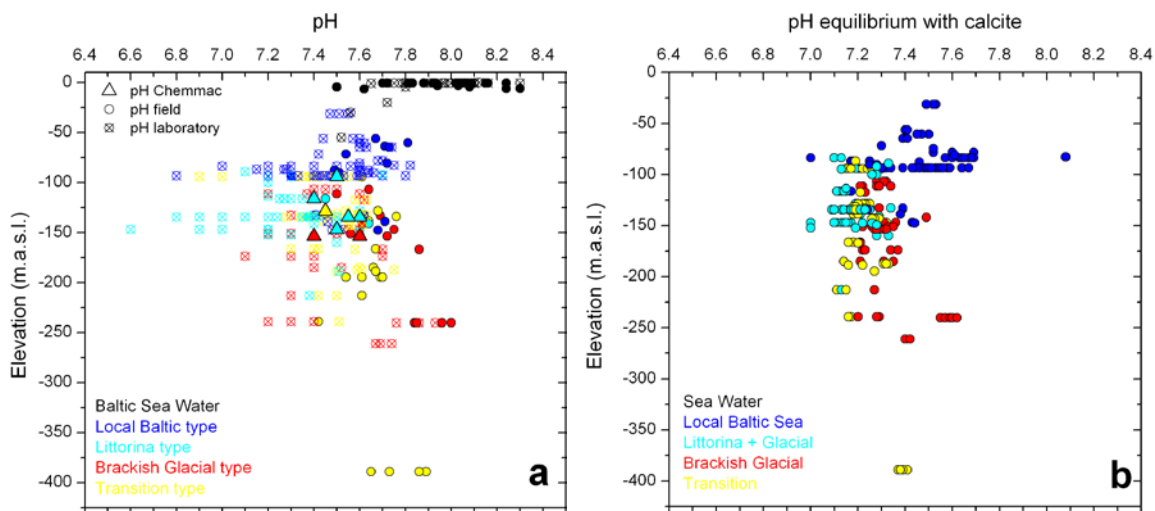
Figure 5-29. *Measured pH values (a) and pH values calculated in equilibrium with calcite (b) with respect to depth in the SRF groundwaters.*

Speciation-solubility calculations performed with available data for the SFR area, using both the measured pH values or those calculated assuming calcite equilibrium, indicate that all the sampled groundwaters are equilibrated with higher pCO_2 than the atmospheric value (Gimeno et al. 2011).

With the measured pH values, groundwaters in general are in equilibrium or slightly oversaturated with respect to calcite; 17 of the 24 samples with pH field data show SI values higher than +0.3 units (cf. Figure 5-30 and Gimeno et al. 2011). These oversaturation values may be either "real" (due to kinetic effects, retarded precipitation of calcite, or microbiological activity; cf. Gimeno et al. 2009) or resulting from CO_2 outgassing during sampling in groundwaters originally equilibrated with respect to calcite.
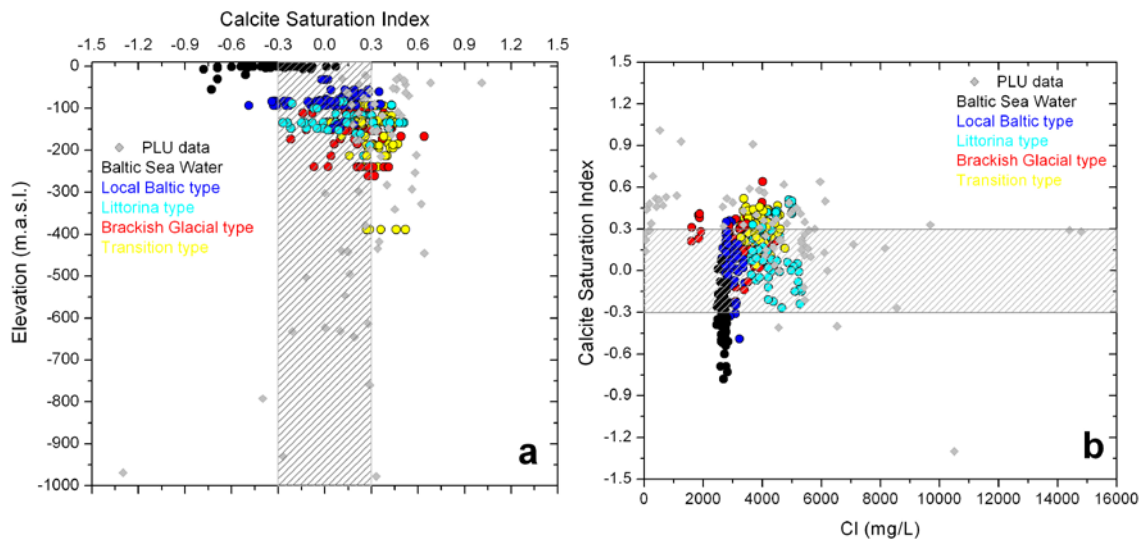
Figure 5-30. Calculated saturation indices for calcite versus depth (a) and chloride content for the SFR ground-waters (colour coded by groundwater types, including the Baltic Seawater samples in black) integrated in the general distribution of the PLU-Forsmark (grey diamonds). Rastered area corresponds to the uncertainty range (± 0.3 units) associated to the calcite saturation index calculations.

A small subset of the groundwater samples seems to be undersaturated with respect to calcite. The most undersaturated values correspond to Baltic and Littorina type groundwaters (SI values of –0.52 and –0.55, respectively; Figure 5-30) in KFR08 (section 63–83.7 m) and KFR10 (section 87–97 m) boreholes. These samples show especially "anomalous" and low pH values compared with those obtained during the long term monitoring of these sections (with differences of at least 0.3 pH units). A few additional Baltic type groundwaters are (slightly) undersaturated with respect to calcite. This could be attributed to a very fast infiltration process with respect to the present Baltic seawaters (undersaturated in this mineral with values reaching SI = −0.44) which prevented attainment of equilibrium with respect to calcite, but probably they are related to uncertainties associated to the pH measurements which were performed in the laboratory.

Conclusion

In summary, most of the parameters related to the carbonate system in the SFR groundwaters show similar trends to those observed during the site investigations at Forsmark (cf. Laaksoharju et al. 2008) especially if only groundwaters with marine contributions are compared. Dissolved calcium and bicarbonate and pH values do not show clear correlations with depth. Although heterogeneous reactions (calcite reequilibrium, cation exchange) may have noticeably modified the dissolved calcium concentrations, mixing control is still evident (Gimeno et al. 2011). High and variable HCO_3^- values are found in groundwaters with a marine signature (both Littorina and especially present Baltic Sea) as a result of the biological activity during infiltration of marine waters through the seabed sediments.

Overall, most of the SFR groundwaters seem to be in equilibrium or slightly oversaturated with respect to calcite, which can either represent a real situation or a result of CO_2 outgassing during pH measurements. Although some calcite dissolution may occur during infiltration of Baltic seawaters, the intensity of this process must be low due to the high alkalinity content and near neutral pH in seawaters. No major shift in bicarbonate content or pH over time can be seen although a weak increase in bicarbonate is indicated.

5.5.2   Sulphate system

Dissolved sulphate in crystalline rock systems is affected by multiple processes such as weathering reactions (e.g. pyrite), microbial sulphate reduction activity or equilibrium situations with respect to different mineral phases (e.g. gypsum or barite). Mixing processes active throughout the palaeo-

hydrological history of the host rock may also exert a fundamental control on dissolved sulphate, especially if marine waters are involved. This is very obvious in the Forsmark and SFR areas where the main sulphate pool is marine and related to input of Littorina or Baltic Seawaters. In this section, the dissolved sulphate trends and controlling processes in the SFR groundwaters are presented and discussed. Barium and strontium trends, commonly coupled to the sulphate system, have been examined and discussed by Gimeno et al. (2011), whereas mineral equilibria (saturation indices) for gypsum, celestite and barite, are addressed in this section.

Dissolved sulphate contents in the SFR groundwaters show a wide variation, ranging from 44 to 551 mg/L (0.46 to 5.74 mmol/L) and their trends with respect to depth and chloride contents are similar to those of the Forsmark groundwaters (Figure 5-31). The highest sulphate concentrations are associated with groundwaters with a clear Littorina Seawater component and with chloride contents about 5,000–5,500 mg/L (141–155.1 mmol/L). Groundwaters of present Local Baltic type appear in the shallow, upper 150 m of the bedrock (Figure 5-31 a, b). The Local Baltic type groundwater has SO_4/Cl ratios similar or slightly lower than the present Baltic Sea, whereas in the Littorina type groundwaters the SO_4/Cl ratio varies considerably and all waters have ratios lower than the original marine signature. This indicates that different processes have influenced (i.e. lowered) the sulphate content in the Littorina type groundwaters or that the Littorina Seawaters have mixed with brackish/saline groundwaters low in dissolved sulphate (e.g. Brackish-glacial type groundwater).

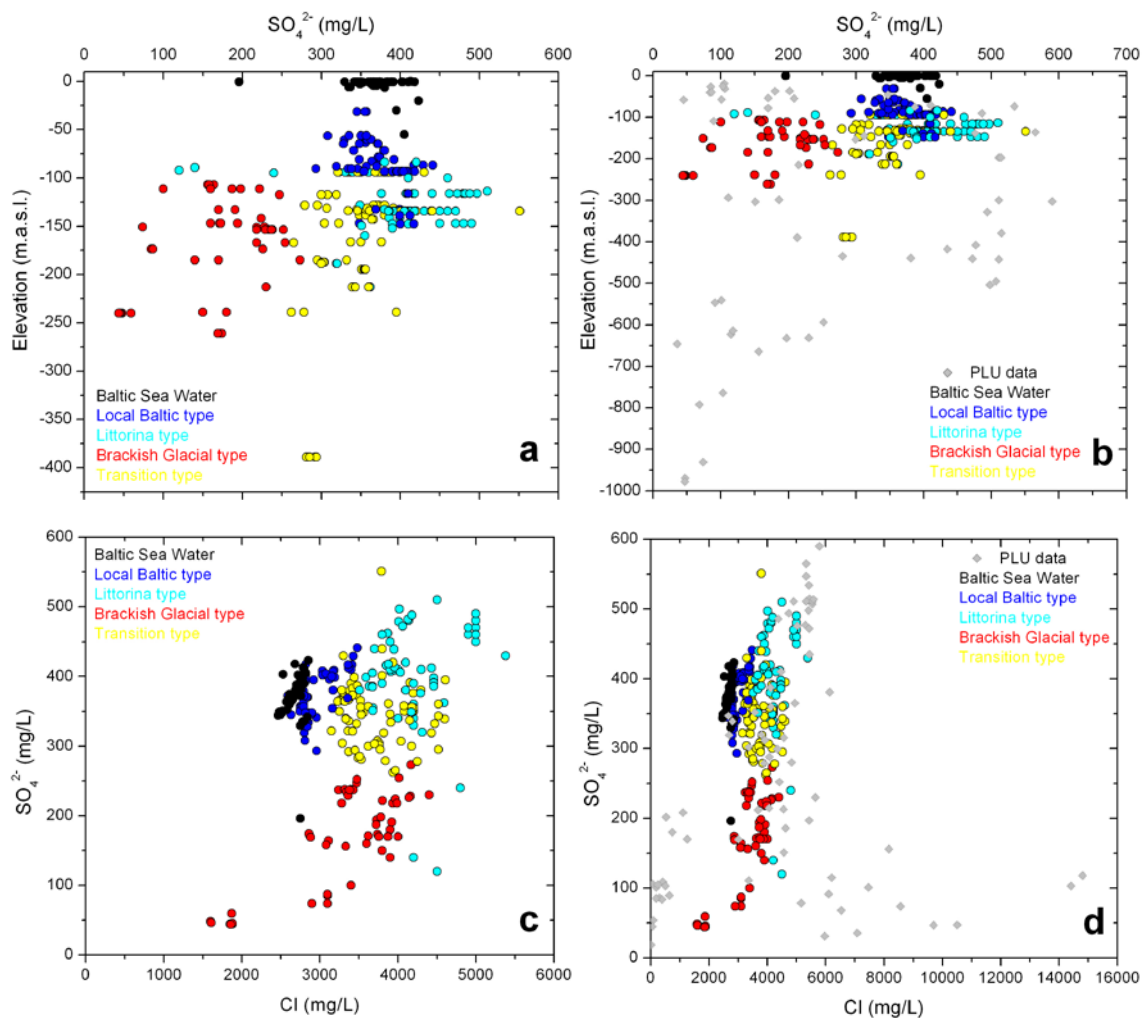*Figure 5-31. Sulphate concentrations versus depth (a, b) and chloride contents (c, d) in the SFR ground-waters colour coded by groundwater type. The plots to the left (a and c) show the SFR data and the respective scales are restricted to those relevant to the SFR extension data. The plots to the right show these data integrated with the Forsmark data down to 1,000 m (b), and at expanded concentration scales (d).*

Despite some deviation in SO_4/Cl ratios, sulphate is still regarded as a good indicator for marine signatures in these groundwaters because the addition from meteoric or glacial meltwater sources is very low. Furthermore, the possible addition of sulphate from deep saline groundwater sources of the area can be excluded as their sulphate content is very lμow, in contrast, for example, to the situation at Laxemar (Laaksoharju et al. 2009).

The marine origin of the sulphate is also supported by the good correlation between dissolved sulphate and other marine derived components in the SFR groundwaters such as Mg ($R^2 = 0.52$) or HCO_3^- ($R^2 = 0.51$).

Microbial sulphate reduction is the most important reaction that reduces the sulphate content in groundwater. Despite that SRB (sulphate reducing bacteria) have not been identified in the few analysed samples, modification of the groundwaters at the SFR by SRB is supported by measureable sulphide contents in most groundwaters analysed for sulphide, and by $\delta^{34}S$ values higher than present marine values in most of the groundwater analyses (i.e. SRB tends to enrich sulphur ^{32}S in the sulphide and therefore a larger portion of the heavy isotope will remain in the sulphate; e.g. Clark and Fritz 1997). Available $\delta^{34}S$ values *versus* depth and dissolved sulphate contents are plotted in Figure 5-32 for the SFR and Forsmark sites. Most of the SFR data show similar trends to Forsmark and values higher than marine ($\delta^{34}S$ ~21‰ CDT; Clark and Fritz 1997) are common.

The highest $\delta^{34}S$ values (+37.5 and 44.6‰ CDT) are observed in samples from KFR101: –240.15 m.a.s.l. with low chloride (1,870 mg/L) and sulphate (22.4 mg/L) contents. Such high $\delta^{34}S$ values are strong indicators of sulphate reducing activity under closed system conditions. This behaviour is also supported by the presence of a glacial meltwater component in these samples ($\delta^{18}O$ values between –14.4 and –15.1‰ V-SMOW in two samples), indicative of long term hydraulic isolation in common with groundwaters of similar character from the Forsmark and Laxemar areas (Smellie et al. 2008, Gimeno et al. 2009). Sulphur isotope ($\delta^{34}S$) values between 22.4 and 24.4‰ CDT, also indicative of sulphate reduction activity, can be observed in other groundwaters with glacial signatures, as well as in the Littorina and transition type.

The available $\delta^{34}S$ data on the Local Baltic type groundwaters (four analyses, ranging from 20.8 to 21.4‰ CDT) fall within the usual range for seawaters (compare the black and the blue circles in Figure 5-32), which excludes inferring the existence of sulphate reducing activity. However, the molal Cl/SO_4 ratio for seawaters is around 19 whereas the values for this Local Baltic type groundwater range from 18.9 to 23.5 (with an average value of 21), suggesting that some sulphate could have been consumed by SRB activity. The presence of sulphate reduction activity during the intrusion of present Baltic Seawaters is also supported by the existence of dissolved S(−II) in some Local Baltic type groundwaters (cf. Section 5.6.3).
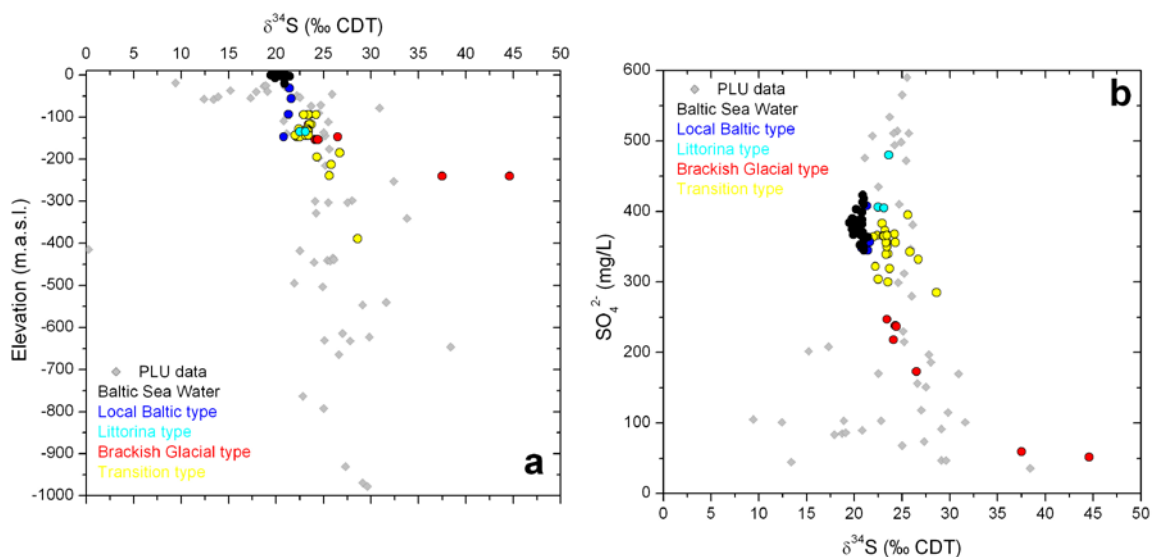

Figure 5-32. $\delta^{34}S$ values (‰ CDT) versus depth (a) and sulphate contents (b) in the SFR groundwaters integrated with the Forsmark data.

Speciation-solubility calculations

The concentrations of many dissolved elements, such as calcium, strontium and barium, may be controlled or regulated by equilibrium with sulphate minerals such as gypsum, celestite and barite (Nordstrom et al. 1989); consequently, the saturation states with respect to these minerals have been calculated. The uncertainty ranges considered for these saturation indices are ± 0.2 SI units for gypsum, ± 0.3 SI units for celestite and ± 0.5 SI units for barite (Langmuir and Melchior 1985, Deutsch 1997). Groundwaters from the SFR area are always undersaturated with respect to gypsum and the SI trends with depth are similar to those observed for the Forsmark site groundwaters (Figure 5-33). Littorina type waters are closest to equilibrium although still clearly undersaturated. The SFR samples show similar overall undersaturation with respect to celestite (cf. Gimeno et al. 2011).

Even though there are no data relative to SFR groundwaters deeper than 400 m and with dissolved chloride contents higher than 5,000 mg/L, the general trends observed for the gypsum saturation states, or the sulphate contents with respect to dissolved chloride concentrations, suggest that the expected trends may be similar to the ones observed for the Forsmark groundwaters.

Overall, these results indicate that, gypsum and celestite do not participate in the control of dissolved sulphate in the SFR groundwaters, and therefore are in agreement with the Forsmark observations (Gimeno et al. 2008). Accordingly, none of these minerals have been identified at the SFR site (Döse et al. 2009a, b, Winell 2009, Winell et al. 2009a, b, Sandström and Tullborg 2011) or following thorough studies focussed on fracture filling minerals from the Forsmark site down to 1,000 m depth (e.g. Sandström et al. 2008). On the contrary, most of the SFR groundwaters are in equilibrium with respect to barite (Figure 5-34), also in agreement with observations from Forsmark (Gimeno et al. 2008).

Mineralogical studies indicate that barite is even more common in SFR than in the Forsmark drillcores (Sandström and Tullborg 2011). However, some of the groundwaters below 150 m depth with the highest barium concentrations, including those from the KFR101 borehole, are clearly oversaturated with respect to barite. The same degree of oversaturation is present in some groundwaters from the Forsmark site (Figure 5-34 b). More studies are needed to assess the influence of other barium rich mineral phases, such as harmotome, a soluble Ba-zeolite locally detected in the fracture fillings from the Simpevarp and Laxemar subareas down to 300–400 m depth and also locally found at the SFR (Drake and Tullborg 2009, Gimeno et al. 2009, Sandström and Tullborg 2011).

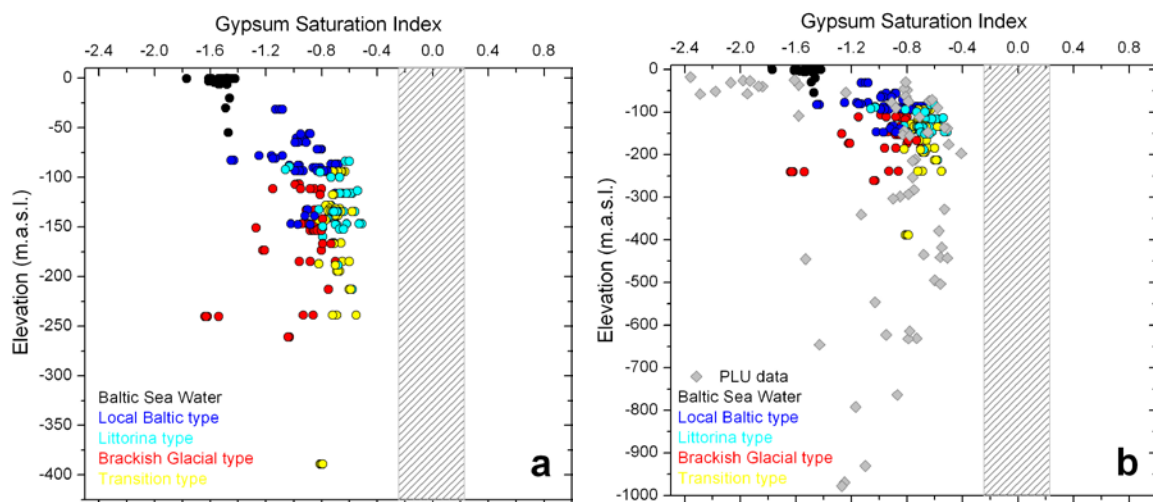***Figure 5-33.*** *Gyspum saturation index versus depth for the SFR groundwaters colour coded by groundwater type. The plot to the left (a) shows the SFR data down to 400 m depth. The plot to the right (b) shows these data integrated with the Forsmark data down to 1,000 m. Rastered areas correspond to the uncertainty range (± 0.2 units) associated with the calculated gypsum saturation indices.*
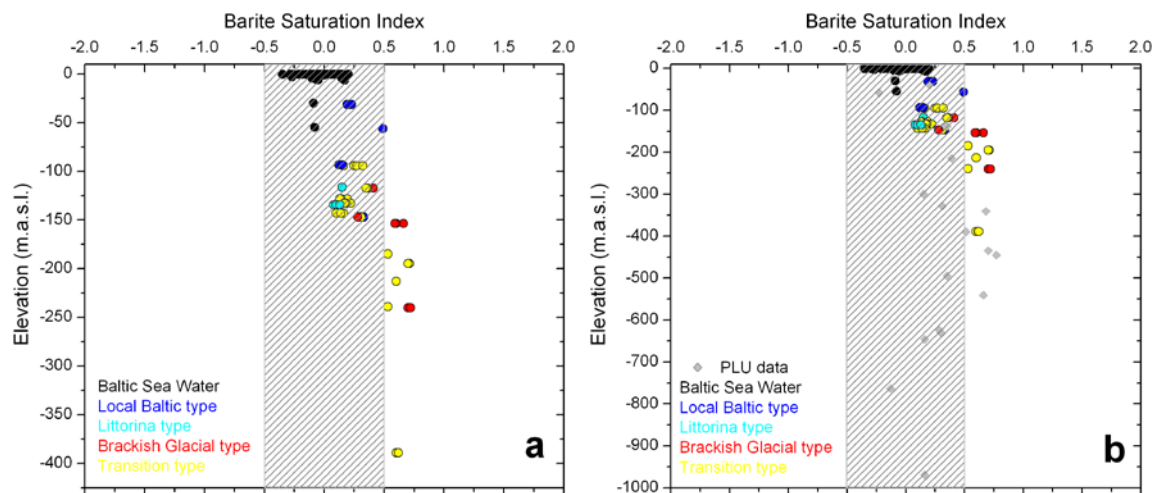
Figure 5-34. Barite saturation index versus depth (a, b) for the SFR groundwaters colour coded by groundwater type. The plot to the left (a) shows the SFR data down to 400 m depth. The plot to the right (b) shows these data integrated with the Forsmark data down to 1,000 m (b). Rastered areas correspond to the uncertainty range (± 0.5 units) associated with the calculated barite saturation indices.

Conclusion

In summary, the main source of sulphur in the SFR groundwaters is the intrusion of past (Littorina) and present (Baltic) seawaters, which have mixed with the earlier resident groundwaters. Apart from these mixing processes and according to the available isotopic data ($\delta^{34}S$), sulphate reducing microbial activity seems to have played a minor role in controlling dissolved sulphate concentrations, except in some of the Brackish-glacial type groundwaters with low sulphate content and high $\delta^{34}S$ values. Moreover, some of the groundwaters with large portions of present Baltic Seawaters show SO_4/Cl ratios which point towards the existence of active sulphate reducing processes, although the effect is small.

In common with the Forsmark groundwaters, all the SFR groundwaters are undersaturated with respect to gypsum and celestite and in equilibrium with respect to barite. However, none of these minerals appear to have appreciably affected the dissolved sulphate contents derived from mixing processes in the studied groundwaters, but the fact that the waters are saturated with respect of barite suggests that not only barium but also radium is related to the sulphate contents in the groundwaters (Gimeno et al. 2011).

5.5.3 Silica and fluoride systems

Both the silica and fluoride systems are discussed in detail in Gimeno et al. (2011) and below is only given a very brief description extracted from their report.

Silica

It is well known that dissolved silica in the near surface and shallow groundwaters is mainly controlled by mineral reactions with no clear limiting equilibrium situations. On the contrary, dissolved silica in deeper groundwaters seems to be generally controlled by equilibrium with respect to a silica phase (quartz or chalcedony), although the influence of seawater intrusion and mixing on the silica content in both systems has also been detected (Gimeno et al. 2009 and references therein).

In the case of the SFR groundwaters, silica concentrations range from 2.4 to 17.5 mg/L (0.04 to 0.29 mmol/L), with the lowest values in one of the Baltic type groundwaters and the highest in some Baltic and Littorina type groundwaters. However, more than 98% of the samples display silica contents between 7 and 14 mg/L (0.12 and 0.23 mmol/L) (cf. Figure 5-35).
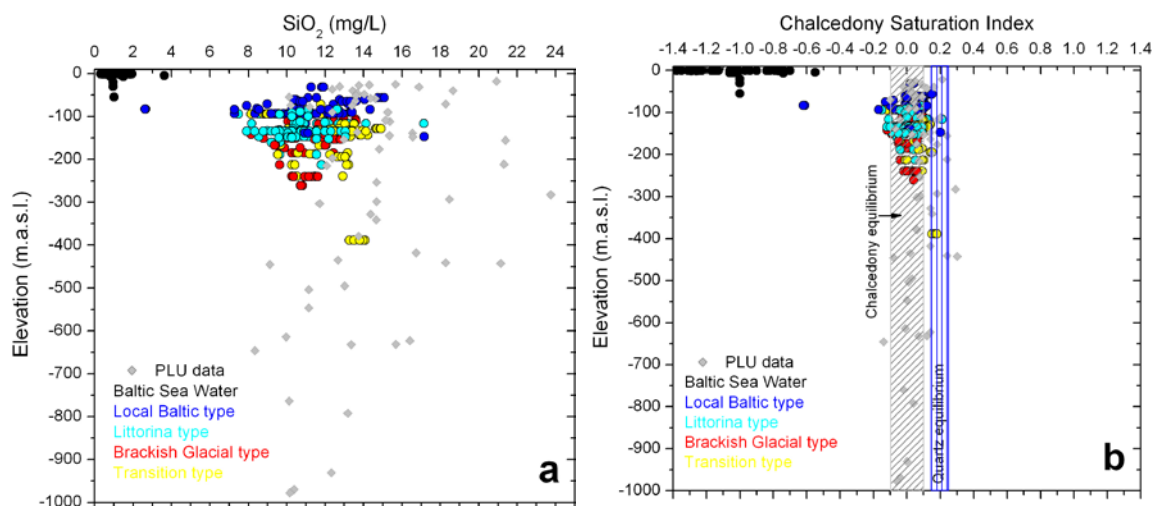
Figure 5-35. *Dissolved silica contents (a) and chalcedony saturation index (b) versus depth in the SFR and PLU (Forsmark) groundwaters. The SFR groundwaters are colour coded by groundwater types. Rastered area in grey corresponds to the uncertainty range (± 0.1 units) associated with the chalcedony saturation index calculations; the area in blue corresponds to the uncertainty range (± 0.05 units) for quartz.*

Despite the potential marine influences on the SFR groundwaters, dissolved silica contents are not correlated with dissolved chloride. Thus, a mineralogical control as source or as limiting phase of this element appears to be clearly superimposed to the mixing effects. The speciation-solubility results are focussed on the saturation indices of chalcedony, as the most frequent silica phase involved in the control of dissolved silica in the groundwaters of this type of crystalline systems, and quartz. Results are presented in Figure 5-35 b. Overall, most groundwaters in the SFR area are closer to equilibrium with chalcedony than with quartz, irrespective of their depth and salinity in common with the samples from Forsmark.

Only the recent Baltic type groundwaters from the HFM34 borehole (together with the proper Baltic Seawaters) are clearly undersaturated with respect to both phases, which suggests that water-rock interaction processes have not had time (these waters have 13.5 TU) to impose the dissolved silica contents found in other groundwaters.

Another observation is the slightly broader range of saturation indices in the shallower and less saline samples compared with the deeper and more saline samples both in the SFR and Forsmark groundwaters (Figure 5-35 b).This may be related to the superposition of other processes controlling the dissolved silica (e.g. aluminosilicate reactions and/or mixing processes, possibly related to the intrusion of the marine waters). In these cases, dissolved silica concentrations might not be controlled by chalcedony equilibrium but by incongruent dissolution reactions or surface processes involving clay minerals in fracture fillings (cf. Gimeno et al. 2009 for further discussion).

Groundwaters from the KFR101: –240.15 m.a.s.l., with long term hydraulic isolation, high δ^{34}S values and presence of an important glacial meltwater component are close to chalcedony equilibrium. The long residence times of these groundwaters, devoid of marine mixing, would favour an effective equilibrium control of dissolved silica as is the case, in the glacial derived groundwaters or in the deepest and more saline groundwaters from the Forsmark and Laxemar-Simpevarp areas (Gimeno et al. 2008, 2009).

Fluoride

Fluoride concentrations in waters from crystalline environments are usually strongly controlled by dissolution-precipitation or exchange processes involving fluoride-bearing minerals (e.g. biotite, hornblende, micas, fluorite, clays with exchangeable fluoride, etc). Amongst these minerals, fluorite is the most usual mineral-limiting phase in crystalline groundwaters (cf. Gimeno et al. 2008, 2009).
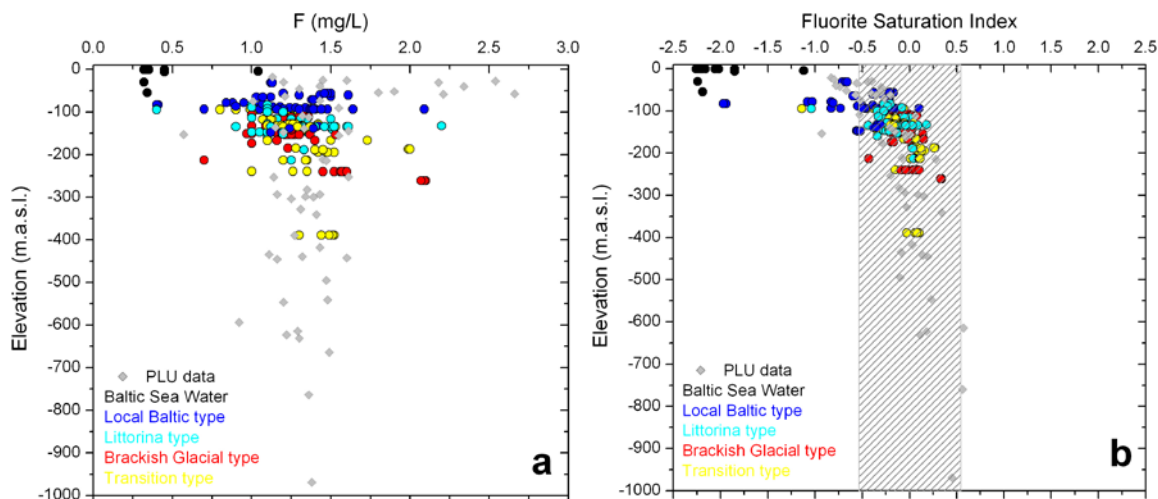
Figure 5-36. *Fluoride contents (a) and fluorite saturation indices (b) vs. depth in the SFR and Forsmark groundwaters colour coded by groundwater types and the PLU (Forsmark groundwaters). Rastered area corresponds to the uncertainty range (± 0.5 units) associated with the fluorite saturation index calculations.*

Moreover, fluorite has been detected in the fracture fillings from the SFR (Sandström and Tullborg 2011). For these reasons, special attention has been paid in this section to the evaluation of equilibrium or disequilibrium situations with respect to this mineral. Fluoride concentrations in the SFR groundwaters range from 0.4 to 2.2 mg/L (0.02 to 0.11 mmol/L), with most values being between 1 and 2 mg/L (0.05 and 0.1 mmol/L; Figure 5-36 a). These ranges are within those reported for the Forsmark groundwaters, with fluoride contents always lower than 2.6 mg/L (0.14 mmol/L).

Some of the lowest fluoride contents (below 1 mg/L or 0.05 mmol/L in the HFM34 borehole) have been measured in groundwaters derived exclusively from present Baltic Seawater, for which similar values have also been reported in the vicinity from Forsmark (usually below 0.45 mg/L or 0.024 mmol/L) or from the SFR area (below 0.3 mg/L or 0.016 mmol/L). However, the overall narrow range of dissolved fluoride in most of the SFR groundwaters, together with the lack of correlation between fluoride and chloride, would suggest the existence of a *"mineral solubility control"* on dissolved fluoride in the groundwaters of the SFR.

According to speciation-solubility calculations, most of the analysed groundwaters at the SFR are equilibrated with respect to fluorite and a similar behaviour was observed also for the Forsmark and Laxemar groundwaters (Gimeno et al. 2008, 2009). This behaviour is especially the case for the groundwaters with longer residence times, which have remained isolated from present or past marine intrusion events. It is noteworthy that this fluoride solubility control becomes superimposed onto the control that calcite exerts on dissolved calcium, thus giving rise to a relationship between pH, alkalinity, calcium contents and fluoride contents. Some groundwaters are undersaturated with respect of fluorite and these correspond mostly to shallow groundwaters affected by the dilution effect associated with the intrusion of present Baltic Seawaters with very low fluoride contents. Moreover, the short residence time of these shallow groundwaters would have prevented their reequilibration with respect to fluoride minerals.

5.6 Descriptions of redox geochemical systems

The understanding of redox systems in crystalline environments needs the integration of all related information, including hydrochemical, mineralogical and microbiological data. This type of integration has been extremely useful for the identification of the main problems during the study of effective redox processes in the target sites during the Site Characterisation Programme and the same methodology is used also for the SFR Site below (Gimeno et al. 2008, 2009, 2011).

5.6.1 Measured Eh data

The selection of the representative pH and Eh values for each specific borehole section from the SFR area has been based on a careful analysis of the data delivered by SICADA and data available in the methodological P-reports. The whole selection procedure, similar to that used in the Site Characterisation Programmes from the Forsmark and Laxemar-Simpevarp areas (Gimeno et al. 2008, 2009), is described in Gimeno et al. (2011).

Twelve Eh logs in seven SFR borehole sections from depths between 94 and 154 m are available. The selected Eh values for these sections are presented in Table 5-7. Six of the twelve revised Eh values show a mildly reducing character whereas the rest indicate slightly oxidising conditions. The sections with reducing values correspond to Littorina and Local Baltic-type groundwaters except the one with the most reducing value (–190 mV), which is a glacial-type groundwater from KFR105: –154 m.a.s.l. These negative values are in line with the measured Eh values from the Forsmark site investigation, mainly, those of Littorina type brackish marine groundwaters (Figure 5-37). However, positive Eh values, similar to those measured in the SFR, have not been reported in the Forsmark groundwaters. These oxidising values do not show a similar evolution in the time series as the rest of the measurements. Eh measured in KFR01 shifts from initially reducing values to oxidant values, while in KFR105: –153.59 m.a.s.l. the opposite has been found. Eh measured in KFR7A changes from reducing to oxidising and back to reducing conditions with time (Table 5-7).

Several possibilities exist to explain these oxidising values:

a) Oxygen diffusion into the tubes connecting the borehole outlet and the measurement cell (e.g. due to long tube lengths or a poor choice of tube material) cannot be entirely discarded for the Eh measurements carried out from 1986–1987 and in 2000 (Nilsson A-C 2009).

b) The intrusion of modern Baltic Seawaters via favourable fracture or deformation zones due to, the drawdown and altered hydraulic conditions caused by the repository.

c) The potential influence of oxidation effects in the old boreholes within the open SFR tunnel system during more than 20 years in an otherwise reducing natural system, could be also responsible for some of the oxidising measured values.

Of these possibilities, the most important one could be the possible intrusion of oxygenated seawaters as it could represent an important modification of the redox environment. Oxidising conditions related to the intrusion of modern oxygenated Baltic Seawaters could be feasible since there are zones in the SFR seabed (on the north side of the pier) with no, or only partial, sediment coverage. Thus, marine waters may penetrate rapidly or, even, infiltrate directly into the bedrock fractures too quickly to become reducing due to, for example, degradation reactions of organic matter which could favour the development of a reducing environment. These possibilities are evaluated in the next section.

Table 5-7. Selected Eh values (mV) for borehole sections in the SFR where the SKB methodology (Chemmac) has been used. The value measured during 1986–87 in KFR10: –146.99 m.a.s.l. (in italics) does not perfectly fulfill the quality criteria, but it has been included for discussion purposes.

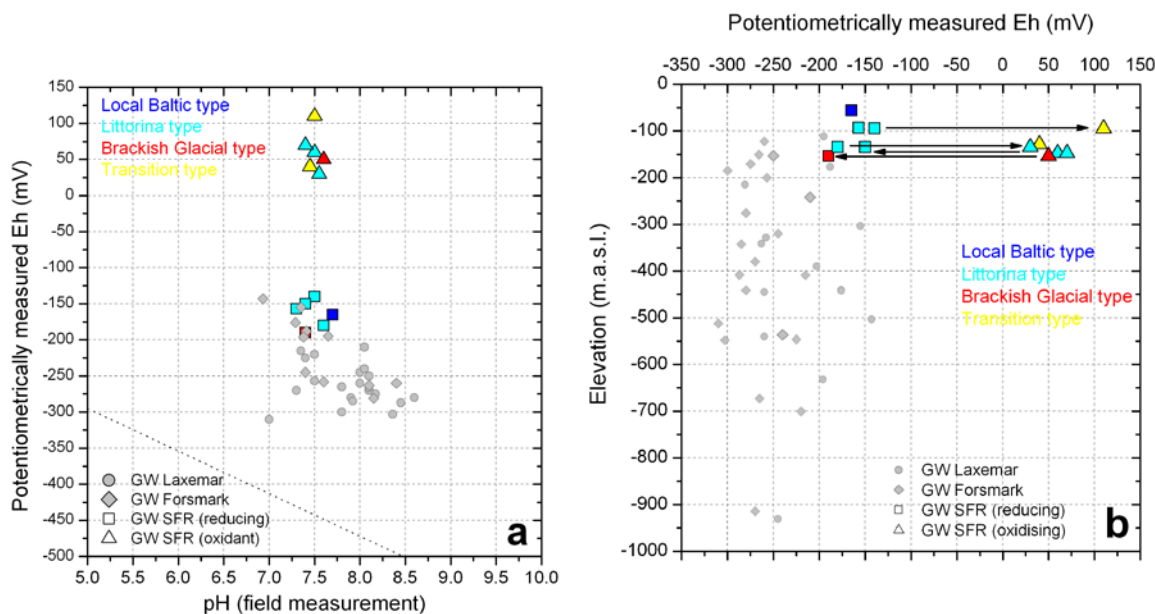|	KFR01: −94.23 m.a.s.l.	KFR7A: −134.43 m.a.s.l.	KFR10: −146.99 m.a.s.l.	KFR105: −128.38 m.a.s.l.	KFR105: −153.59 m.a.s.l.	KFR08: −93.30 m.a.s.l.	KFR19: −56.30 m.a.s.l.
1986–87	−140.0	−180.0	*+60.0*				
2000	+110.0	+30.0	+70				
2009				+40.0	+50.0		
2010		−150.0			−190.0	−157.0	−165.0

Figure 5-37. *Potentiometrically measured Eh values versus pH (a) and depth (b) for the SFR and the Forsmark and Laxemar groundwaters.*

5.6.2 Redox pair modeling

The redox pairs that have been analysed at the SFR are similar to those measured in the Site Descriptive Models for Forsmark and Laxemar-Simpevarp (i.e. the dissolved homogeneous SO_4^{2-}/HS^- and CO_2/CH_4 redox pairs, and the heterogeneous couples Fe^{2+}/$Fe(OH)_3$, $S_{(c)}$/HS^-, SO_4^{2-}/FeS_{am}, SO_4^{2-}/pyrite and Fe^{3+}-clay/Fe^{2+}-clay. These are the most suitable redox pairs for the reducing conditions encountered in the present groundwaters and have performed best in similar systems elsewhere in the Scandinavian Shield (cf. Gimeno et al. 2008, 2009 and references therein). Also included are those particular redox pairs that can be participating in the control of the potentiometrically measured Eh at the values (both reducing and oxidising) encountered in the target system. The PHREEQC code (Parkhurst and Appelo 1999) and the WATEQ4F thermodynamic database (Ball and Nordstrom 2001), with the modifications described in Gimeno et al. (2009) have been used for the calculations. The overall methodological approach is further described in Gimeno et al. (2011).

Redox pairs and potentiometric measured Eh values

The comparison between potentiometrically measured Eh values and those obtained by different redox couples may allow the identification of the redox couples most probably involved in the control of measured Eh (e.g. Langmuir 1997, Nordstrom 2005). Moreover, such measurements can be used to deduce the type of oxyhydroxide that may control these measured values (oxyhydroxides/ Fe^{2+} are clearly electroactive redox pairs) and this methodology has been successfully used in previous studies (e.g. Grenthe et al. 1992, Banwart 1999, Trotignon et al. 2002, Gimeno et al. 2008, 2009)). Thus, some deductions on the redox environment can be made based on this information.

Reducing potentiometric Eh values measured in the SFR groundwaters are compared with the redox potential obtained from the different redox couples using the available pH field measurements (some of them measured with the Chemmac probe) for the groundwater samples (Table 5-8). The Eh values calculated with the Fe^{2+}/$Fe(OH)_3$ redox pair using the equilibrium constant proposed by Grenthe et al. (1992) are too reducing to be consistent with the measured ones. However, the Eh calculated with the same redox pair, but using the equilibrium constant for the oxyhydroxide proposed by Banwart (1999) are in agreement with the measured values within the uncertainty range for Eh measurements considered acceptable to the SKB methodology and generally in the scientific literature, which is around ± 50 mV (Kölling 2000, SKB 2001). This was also found during the studies performed in Forsmark and the Laxemar-Simpevarp Site characterisations (Gimeno et al. 2008, 2009).

Table 5-8. Comparison of the reducing Eh values potentiometrically measured with the Chemmac probe and the Eh values calculated using different redox pairs. For the $Fe^{2+}/Fe(OH)_3$ redox pair, the equilibrium constant for the hematite defined by Grenthe et al. (1992) and the equilibrium constant for the solid phase defined by Banwart (1999) are used.

| | Sample | Meas. Eh (mV) | Fe^{2+} (mg/L) | S^{2-} (mg/L) | pH | Fe^{3+}-clay/ Fe^{2+}-clay | $Fe^{2+}/Fe(OH)_3$ | | SO_4^{2-}/HS^- |
							Banwart 1999	Grenthe et al. 1992	
KFR01	1321	−140	0.46	–	7.5	−140	−139	−270	
KFR105	16651	−190	0.76	0.01	7.70	−152	−187	−318	−210
KFR7A (1987)	1334	−181	5.17	Bdl	7.58	−145	−212	−343	
KFR7A (2010)	16917	−153	2.55	Bdl	7.4	−134	−184.5	−320	
KFR08	16943	−157	1.93	0.02	7.3	−129	−160	−296	−184
KFR19	16937	−167	0.932	0.03	7.7	−151	−213	−349	−211

The Fe^{3+}-clay/ Fe^{2+}-clay redox couple proposed by Banwart (1999) also provides a good agreement with the potentiometric Eh values for the reducing samples (cf. Table 5-8) which was not observed in Forsmark nor Laxemar. Thus, the observed agreement between the $Fe^{2+}/Fe(OH)_3$ and the Fe^{3+}-clay/ Fe^{2+}-clay redox couples in the SFR groundwaters would suggest a closer situation to the one reported for the Large-Scale Redox Experiment carried out at Äspö than to the one in the candidate sites.

Dissolved sulphide was not analysed or was below the reporting limit in most cases for the monitoring sections. Only in the KFR19 borehole was a concentration of 0.03 mg/L analysed and the SO_4^{2-}/HS^- redox pair provided a potential of −211 mV. In the KFR105 and KFR08 boreholes concentrations of 0.01 and 0.02 mg/L were determined but are below the accepted reporting limit (0.03 mg/L) in this work, was measured. Accepting the single value, the SO_4^{2-}/HS^- redox pair would provide a potential of −210 and −184 mV, respectively, which is also in agreement with the potentiometrically measured ones.

For the oxidising values potentiometrically measured in some of the analysed sections, the redox pair calculations would support a control by amorphous Fe(III)-oxyhydroxides (Table 5-9). The potentiometric value obtained for the $Fe^{2+}/Fe(OH)_3$ redox pair using the equilibrium constant for a microcrystalline phase, or for the phases proposed by Grenthe et al. (1992) and Banwart (1999) whould result in too low (reducing) values, as it also occurs for the Fe^{3+}-clay/ Fe^{2+}-clay redox couple. This possible control by an amorphous Fe(III)-oxyhydroxide would imply the existence of present or very recent oxic environments associated with the studied sections. Oxygen intrusion in reducing media usually induces the precipitation of amorphous Fe(III)-oxyhydroxides (ferrihydrite or hydrous ferric oxides (Langmuir 1997)). In addition, this result is not affected by the pH uncertainties (Table 5-9) and therefore it would support the reliability of the oxidising Eh measurement; the $Fe^{2+}/Fe(OH)_3$ heterogeneous redox pair is the most clearly electroactive (especially with amorphous phases) and, therefore, one of the most feasible to control the Eh measurements in natural systems (cf. Gimeno et al. 2008, 2009 and references therein). In this context, the key point is to identify and explain the possible oxygen source (s):

Table 5-9. Selected Eh values for different boreholes and sections and results of the $Fe^{2+}/Fe(OH)_3$ redox pair considering an amorphous and a microcrystalline phase. Redox pair results using both measured and calculated pH are shown.

| Borehole and Elevation of SecMid | | Eh meas. | With measured pH | | With calculated pH | |
			$Fe^{2+}/Fe(OH)_3$ microcrystalline	$Fe^{2+}/Fe(OH)_3$ amorphous	$Fe^{2+}/Fe(OH)_3$ microcrystalline	$Fe^{2+}/Fe(OH)_3$ amorphous
KFR01: −94.23 m.a.s.l.	1987	−140	−37	+77	+16	+130
	2000	+110	−30 to −54	+60 to + 84	+4 to +13	+118 to +126
KFR7A: −134.43 m.a.s.l.	1987	−180	−109	+5	−32	+82
	2000	+30	−87 to −125	−11 to −27	−29 to −33	+81 to +85
KFR10: −146.99 m.a.s.l.	1986	+60	−28 to −99	+15 to +86	−29 to −34	+80 to +87
	2000	+70	−28 to −69	+45 to +86	−17 to −21	+93 to +97

- Contamination problems during the Eh measurements cannot be excluded and this could explain the apparent existence of oxidising environments in the SFR groundwaters.

- Oxidising conditions could also be related to the intrusion of modern oxygenated Baltic Seawaters via favourable fracture or deformation zones. As stated above, (Section 5.6.1) the rapid penetration of oxidising Baltic waters is feasible. However, the most recent measurements performed in preferential "Baltic type" groundwater paths (KFR08 and KFR19 boreholes) indicate that this type of "recent" marine groundwaters is anoxic and clearly reducing. Moreover, oxygen consumption in saturated soils and sediments is well documented (e.g. Drew 1983, Silver et al. 1999, Pedersen 2006) and the Äspö Redox Zone experiment (Banwart 1999, Molinero-Huguet et al. 2004) also showed that microbial respiration, in the upper metres of a fracture zone, effectively consumes the oxygen in infiltrating waters.

- Oxidising values controlled by the precipitation of amorphous Fe(III) oxyhydroxides can also be related to the influence of the oxic environment created by the presence of the SFR tunnels over the old boreholes with fixed equipment installed in the 1980's. Failures in the sealing capacity or oxygen diffusion into tubes, joints and valves might have produced the precipitation of this type of phases. In fact, this was also observed in the Äspö Underground Laboratory when reducing groundwaters came in contact with the oxygen-rich atmosphere of the tunnel. Moreover, in some experiments also performed in the Äspö Underground Laboratory, it was found that microbes (e.g. *Gallionella ferruginea,* an iron-oxidising chemolithotrophic microbe species adapted to low-oxygen conditions) may catalyse the formation of iron oxides from dissolved ferrous iron in groundwaters exposed to an oxidising environment. The formation of these *bacteriogenic iron oxides* (BIOS), constituted by ferrihydrite (Ferris et al. 1999) was significant for groundwaters with dissolved oxygen concentrations between 0.3 mg/L and 1.5 mg/L, pH between 7.4 and 7.7 and Eh values above approximately 100 mV (Anderson and Pedersen 2003, Laaksoharju et al. 2009). These ranges are very similar to the ones found in the SFR groundwaters with oxidising potentials. Thus, these types of "alterations" in the monitored sections could justify the measurement of stable oxidising values during the measurement periods and would highlight the need for longer pumping and measurement periods in order to obtain the Eh values corresponding to pristine and undisturbed conditions.

Redox pairs and overall redox conditions at the SFR

As the available Eh measurements for the SFR are scarce, redox potentials from the redox couples have been calculated for the whole set of groundwater samples comprising suitable data. Redox potentials calculated from redox couples are usually considered the only way to approach meaningful Eh values in natural waters (Thorstenson 1984, Langmuir 1997, Drever 1997, Nordstrom 2005 etc).

The selected redox couples are those of sulphur and iron (including the Fe^{3+}-clay/ Fe^{2+}-clay redox pair), which have provided meaningful results in this and in previous studies. Calculations have been performed with both the measured pH values and the ones calculated in equilibrium with calcite and the results are presented in Figure 5-38. Sulphur redox pairs would provide reducing values for the SFR groundwaters. Values from the SO_4^{2-}/HS^- and SO_4^{2-}/FeS_{am} redox couples, which have generally shown a good agreement with the potentiometrically measured Eh values in the Site Characterisation Programmes (Gimeno et al. 2008, 2009), would be around −200 mV. The Fe^{3+}-clay/ Fe^{2+}-clay redox pair would lead to less reducing values (mean around −120 mV).

From the scarce data available for methane (four samples) values for the CO_2/CH_4 redox pair can be obtained. Redox potential results for this pair are very similar to the ones obtained with the sulphur couples (from −208 to −233 mV) even taking into account the possible impact of pH uncertainty on the calculated values (11 mV of Eh uncertainty in the worst case). A similar agreement has also been reported for the Forsmark and the Laxemar-Simpevarp groundwaters.

The redox potential defined by the $Fe^{2+}/Fe(OH)_3$ heterogeneous redox pair depends on the mineral phase characters (solubility, particle size, etc) of the specific ferric oxyhydroxide included in the calculations. For a crystalline Fe(III)-oxyhydroxide (like hematites, frequently found in the facture fillings of the SFR), the results obtained using the Grenthe`s solubility value would be between −100 and −350 mV. Only the calculations considering microcrystalline or amorphous phases, representative of oxic or post-oxic environments, provide oxidising values.
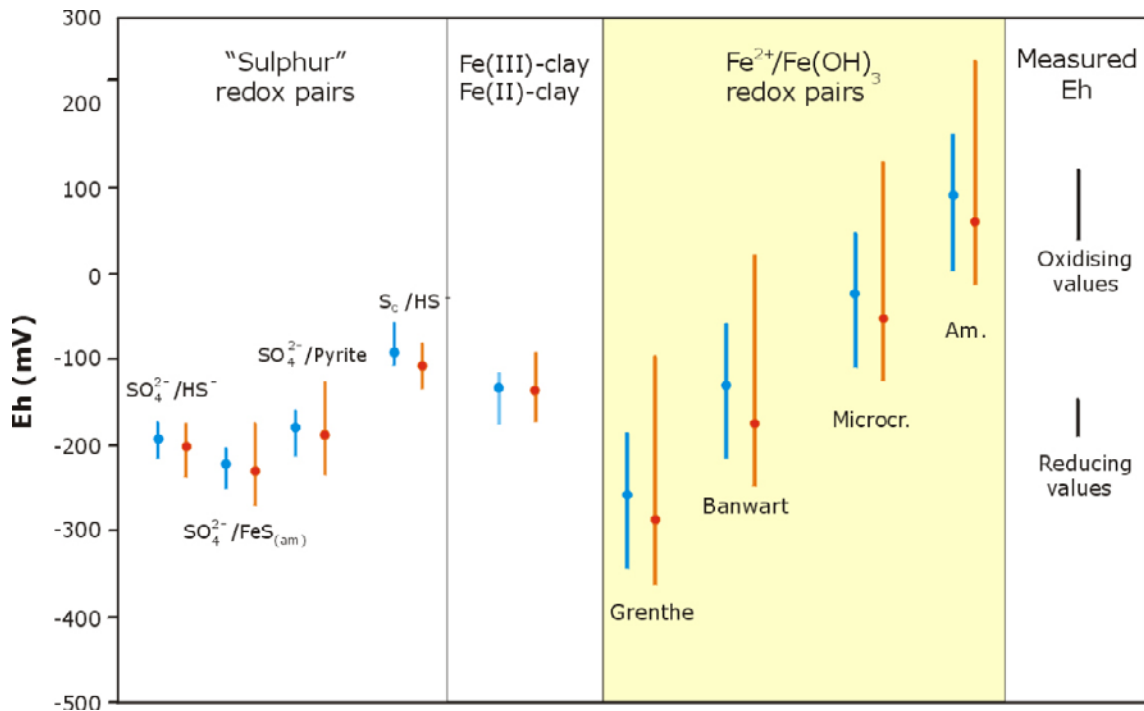
Figure 5-38. *Eh values calculated from different redox couples for the whole suitable set of SFR groundwaters, compared with the potentiometrically measured Eh values. Red lines represent the range of values obtained with the measured pH and blue lines the range of Eh values obtained with the calculated pH. Circles represent the mean value for each case.*

Overall, most of the selected redox pairs suggest the existence of reducing Eh values for the SFR groundwaters. For sulphidic and methanic groundwaters, Eh values between -200 and -220 mV could be proposed. For the rest, values below -100 mV could be feasible considering the redox couples usually active in the studied systems.

Conclusions

The potentiometric Eh measurements in the SFR groundwaters provide oxidising and reducing values. Reducing values (from -140 to -190 mV) are in line with those measured in the PLU-Forsmark groundwaters. They are apparently controlled by the occurrence of an iron phase with an intermediate crystallinity and/or by ferrous clay minerals. The coincidence in the results of the $Fe^{2+}/Fe(OH)_3$ and the Fe^{3+}-clay/Fe^{2+}-clay redox pairs would be similar to that observed in the Large-Scale Redox Experiment (Banwart 1999) where the effects of the intrusion of meteoric waters in the Äspö tunnels were studied.

Moreover, the mineralogical studies in the fracture fillings at the SFR indicate that mixed layer clays (poorly ordered smectite-illite) are the most abundant minerals in the fracture fillings from water conducting fractures. Also, the presence of hematite and other unclassified iron oxyhydroxides has been identified at almost all examined depths (Sandström and Tullborg 2011). These characters would probably support the satisfactory results obtained with the $Fe^{2+}/Fe(OH)_3$ and the Fe^{3+}-clay/Fe^{2+}-clay redox pairs. However, more data are needed on these mineral phases and, especially, on the type and particle size (crystallinity) of the iron oxyhydroxides.

The measured oxidising Eh values in the SFR groundwaters (from $+30$ to $+110$ mV) appear to be controlled by amorphous Fe(III)-oxyhydroxides. They would represent the existence of present or recent oxic environments, since these phases quickly recrystallise (e.g. months) to less soluble and more stable phases under reducing conditions. Chemical characters (e.g. pH and Eh values) for these groundwaters are very similar to those observed in some experiments at the Äspö Underground Laboratory where microbes catalyse the formation of amorphous Fe(III)-oxyhydroxides even al low O_2 contents.

Thus, these oxidising conditions could be representative of groundwaters affected by some artefact (failures in the sealing capacity of the equipment) related to the oxic environment in the tunnels and they would change towards more reducing ones in case of pumping. The gradual removal of the groundwater from the tunnel section and the progressive input of pristine formation water may have caused a disequilibrium and the observed long stabilisation periods towards reducing conditions (cf. Gimeno et al. 2011). The results in the more recent measurements performed in the KFR19 and KFR7A boreholes, also displaying long stabilisation periods, would support this interpretation. In any case, with the available data, local disturbing effects related to the intrusion of modern oxygenated Baltic Seawaters, via favourable fracture or deformation zones, does not appear very probable but it can not be entirely ruled out. More detailed study of the redox evolution of the intruding Baltic Seawaters at the SFR is needed.

The Eh calculation results for the suitable redox pairs in the SFR groundwaters point also towards the existence of overall reducing conditions (below −100 mV), especially in the case of sulphidic and methanic groundwaters (below −200 mV).

5.6.3 Redox sensitive elements

Sulphur and iron systems

Iron and sulphur represent two very important redox systems for the understanding of the redox processes in groundwaters of crystalline rocks. The evolution and behaviour of these elements are frequently linked to bacterial activity (iron reducing bacteria –IRB- and sulphate reducing bacteria –SRB-). Moreover, they are interrelated through inorganic processes, such as sulphide precipitation and reductive dissolution of ferric oxyhydroxides by hydrogen sulphide (cf. Gimeno et al. 2009 and references therein), which may exert an important control on the dissolved $Fe(II)$ and $S(-II)$ contents.

Dissolved iron and sulphide contents in the SFR groundwaters show patterns with respect to depth and chloride contents very similar to those observed in the Forsmark groundwaters. $Fe(II)$ contents are always above the detection limit, ranging between 0.25 and 7.5 mg/L ($4.5 \cdot 10^{-3}$ and 0.13 mmol/L) for groundwaters at depths between 100 and 150 m (Figure 5-39 a). The highest and more variable dissolved $Fe(II)$ contents appear in Littorina-type groundwaters with chloride contents between 3,500 and 5,000 mg/L (Figure 5-39 b) but also Baltic type groundwaters show large variation (between 0.25 and 4.5 mg/L; $4.5 \cdot 10^{-3}$ and 0.08 mmol/L).

Dissolved sulphide contents range between 0.03 and 2.2 mg/L ($9.4 \cdot 10^{-4}$ and 0.069 mmol/L), being mostly below 0.5 mg/L (0.016 mmol/L) and very frequently even below the detection (0.01 or 0.006 mg/L; $3.1 \cdot 10^{-4}$ or $1.9 \cdot 10^{-4}$ mmol/L depending on the date of the analysis) or reporting limits (0.03 mg/L or $9.4 \cdot 10^{-4}$ mmol/L) in SICADA. The values corresponding to these limits, 0.006 and 0.03 mg/L are indicated in the plots as dashed lines. Unless other situation is expressed, calculations and interpretations have always considered samples with sulphide values above the reporting limit.

The highest $S(-II)$ content is associated with a Littorina type groundwater with chloride concentrations about 5,000 mg/L at a depth around 100 m (Figure 5-39 c, d). However, in general most of the waters with sulphide values higher than 0.03 mg/L are of Brackish-glacial or Littorina type, but also some Local Baltic type groundwaters have detectable values (cf. Figure 5-3). The latter could be due to the existence of sulphate-reduction processes during the inflow of Baltic Seawaters either through the marine seabed sediments or along the bedrock fractures receiving recent and continuous input of organic matter associated with the marine intrusion.

Overall, the concentration ranges and distribution of dissolved $Fe(II)$ and $S(-II)$ are very similar to those observed for Forsmark groundwaters, which is apparently related to the presence of similar controlling factors. Inorganic or biotically-induced reductive dissolution of Fe-silicates (e.g. Fe^{3+}-bearing clay minerals or ferric oxyhydroxides in the fracture fillings) appear to be the main sources of dissolved $Fe(II)$. Moreover, some equilibrium situations (e.g. with respect to siderite or ferrous iron monosulphides; cf. below) may participate in the control of dissolved $Fe(II)$ and $S(-II)$. However, the highest $Fe(II)$ contents and their larger variability are associated with Littorina type groundwaters, as also described for Forsmark groundwaters. This could indicate a participation of Littorina intrusion in the control of the $Fe(II)$ dissolved contents.
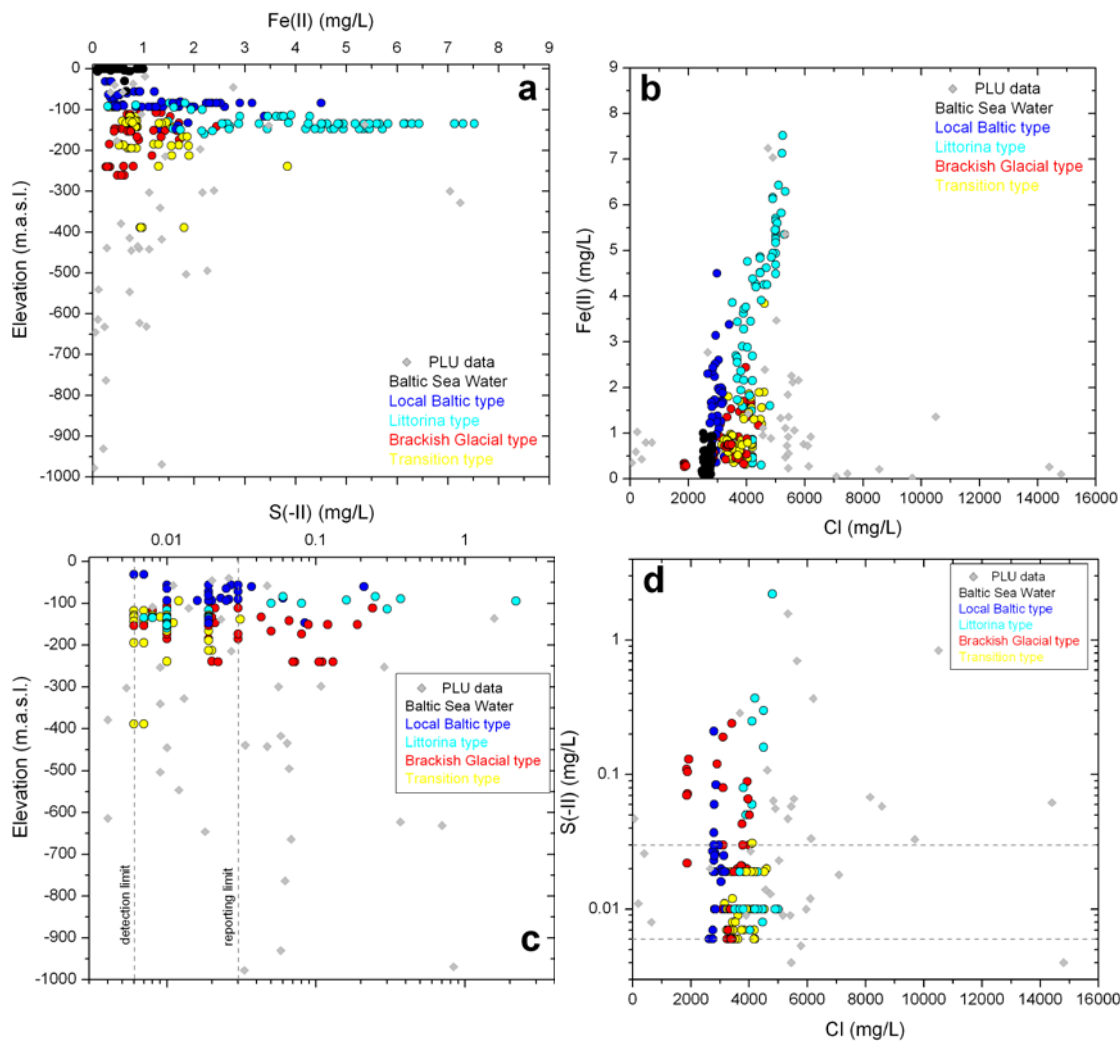
Figure 5-39. Dissolved Fe(II) and S(-II) concentrations versus depth (a, c, respectively) and chloride contents (b, d, respectively) in the SFR groundwaters colour coded by groundwater types and integrated in the general distribution of the Forsmark data.

The existence of sulphate reducing activity (from the presence of detectable dissolved sulphide contents) appears to be distributed from 60 to 240 m depth although the scarce microbiological analyses (only two) have failed to identify the presence of SRB.

Equilibrium situations with respect to amorphous Fe(II)-monosulphides have been reached only in a few groundwaters (of Baltic, Littorina or Glacial type; Figure 5-40). Moreover, some of these results are affected by pH uncertainties, reducing even more the number of samples in equilibrium with respect to this phase.

More groundwaters are in equilibrium with respect to mackinawite (a crystalline and less soluble iron monosulphide; Figure 5-40). These situations could correspond either to a low SRB activity, whose H_2S production would not be high enough to reach the amorphous monosulphide solubility product (but large enough to reach mackinawite equilibrium) or to the presence of environments with an important SRB activity in the past that is no longer existent but which produced the original amorphous phase that has been recrystalised (cf. discussion in Gimeno et al. 2011). This might be the case for the long term hydraulically isolated groundwaters from the KFR101: –240.15 m.a.s.l. (with chloride contents around 1,900 mg/L; Figure 5-40 b) which are equilibrated with respect to mackinawite and which display isotopic $\delta^{34}S$ values (reaching +44.6‰ CDT) strongly indicative of SRB activity under closed system conditions.

Figure 5-40. Saturation indices for amorphous ferrous iron monosulphide (FeSam) versus depth (a) and chloride contents (b) in the SFR groundwaters colour coded by groundwater types integrated in the general distribution of the Forsmark data. Rastered areas correspond to the uncertainty range (± 0.36 units) associated with the FeS(am) (grey inclined lines) and Mackinawite (blue vertical lines) saturation index calculations.

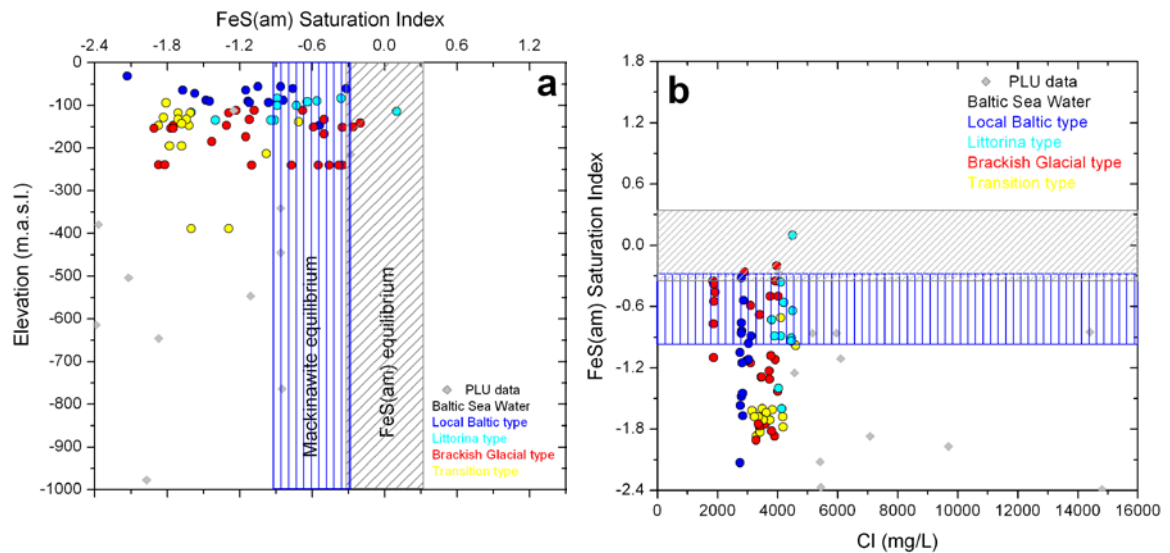In any case, these results must be considered with caution as dissolved sulphide contents may be affected by uncertainties related to the sampling conditions. More data and further studies are needed to clarify the importance of sulphate reduction processes in the SFR groundwaters.

Additionally, siderite could also participate on the control of dissolved Fe(II) in groundwaters with a marine component (i.e. Local Baltic and Littorina types), since most of these groundwaters are in equilibrium with respect to this mineral. However, it is uncertain whether this equilibrium is effective in the bedrock or if it is only an inherited feature from the inflow of marine waters through seabed sediments (cf. Gimeno et al. 2011 for further discussion). All the described features would be indicative of anoxic and reducing environments in the SFR groundwaters. Mineralogy would support this situation as no definite indications of a significant inflow of oxygenated waters, such as oxidation and/or dissolution of sulphides (pyrite is only absent in water conductive fractures in the upper 10 metres) have been identified in the SFR fracture system (Sandström and Tullborg 2011).

From a hydrostructural point of view, some preliminary remarks on the distribution of S(−II) and Fe (II) concentrations can be made. Groundwaters associated with the Southern boundary belt are clearly undersaturated with respect to siderite, do not show meaningful dissolved sulphide concentrations and dissolved iron contents are low and constant (between 0.3 and 0.5 mg/L). Groundwaters associated with the rest of the hydrostructural domains, and especially those related to the Northern boundary belt, are usully in equilibrium with siderite, show a wider range and higher concentrations of dissolved Fe(II), and more samples show sulphidic characters.

High contents of dissolved iron (and, even, of dissolved sulphide) and siderite equilibrium situations are usually related to the Littorina marine intrusion in the Forsmark groundwaters. Therefore, the differences observed in the Southern boundary belt groundwaters could possibly be associated with the presence of a thicker sediment cover in that area, constricting the intrusion of Littorina and Baltic Seawaters.

Manganese system

Manganese contents show variable but high values in the SFR groundwaters (around 4 mg/L; ≈ 0.07 mmol/L); Figure 5-41). The highest manganese concentrations are related to groundwaters with Cl contents around 4,000–5,000 mg/L and with a clear Littorina signature (Figure 5-41 b), as also reported for the Forsmark groundwaters or for other crystalline systems also affected by a Littorina recharge period (e.g. Laxemar-Simpevarp, Forsmark, Olkiluoto and Finnsjön; cf. reviews by Gimeno et al. 2008, 2009).

As expected from their oxic conditions, present Baltic Seawaters in the surroundings of Forsmark and the SFR area display extremely low Mn contents (below 0.05 mg/L or $9.1 \cdot 10^{-4}$ mmol/L) and frequently below the detection limit). However, the Mn contents in groundwaters with a clear component of present Baltic Seawaters are notably higher (between 0.5 and 2.3 mg/L; 0.01 and 0.042 mmol/L), which seems to be related to an evolution towards anoxic and more reducing conditions during their infiltration and/or mixing in the bedrock. This is consistent with the clear sulphidic character of some of these groundwaters.

Different inorganic reactions and microbial processes could participate in the control of dissolved manganese in the SFR groundwaters. The dissolution of Mn(II)-bearing minerals and the reductive dissolution of manganese oxyhydroxides may increase dissolved manganese concentrations in the present marine sediments above the SFR. Depending on the groundwater residence time in these sediments and on the degree of development of a redox sequence in them, manganese oxyhydroxides may also quickly react with dissolved S(−II) and Fe(II). All these processes could justify the observed increase in Mn dissolved contents in the Local Baltic type groundwaters.

The influence of manganese reducing bacteria (MRB) on dissolved Mn contents in the rest of groundwaters is supported neither by the mineralogical results, which do not show the presence of Mn-oxyhydroxides (Sandström and Tullborg 2011) nor by the observed hydrochemical trends (Gimeno et al. 2011). Additional controls on dissolved manganese contents in the groundwaters may involve surface processes or solubility constraints.
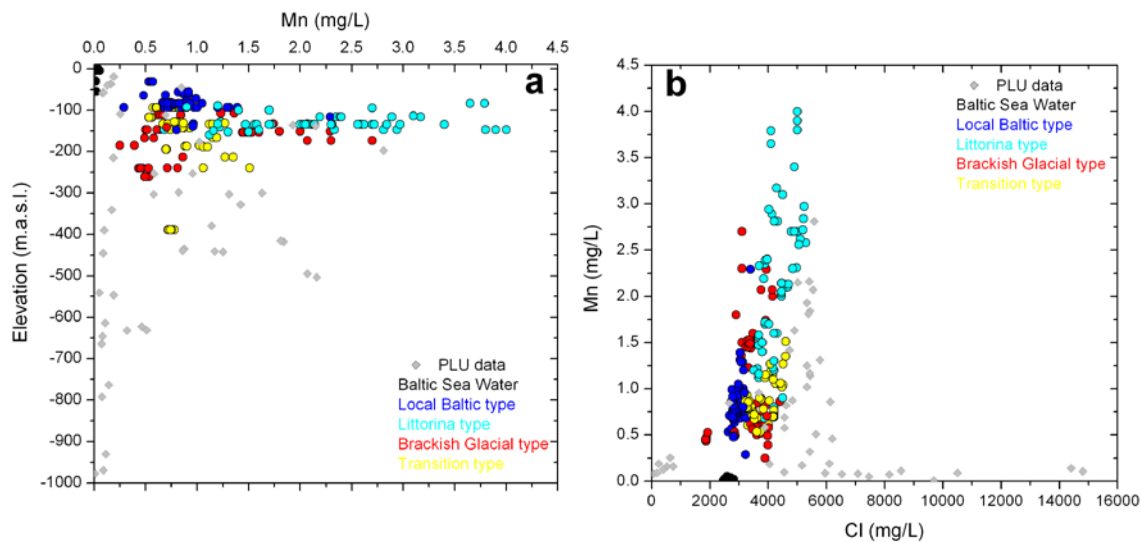

Figure 5-41. Dissolved Mn(II) concentrations versus depth (a) and chloride contents (b) in the SFR groundwaters colour coded by groundwater types and integrated in the general distribution of the Forsmark data.

Overall, dissolved manganese correlates with dissolved Fe(II) contents, mainly in Littorina type groundwaters. The contribution of this old marine component through mixing processes may partially explain this correlation, although the "simultaneous" control by iron phases with traces of manganese (oxyhydroxides, clays) or by the operation of surface processes between dissolved manganese and iron oxyhydroxides may also be effective.

Solubility controls may be also effective as most of the groundwaters are in equilibrium with respect to rhodochrosite and this result is not significantly affected by the pH uncertainty (cf. Gimeno et al. 2011). Littorina type groundwaters may have inherited this character from their infiltration stage through the marine sediments since authigenesis of Mn-carbonates has been an active process in the Baltic Sea since 7000–8000 years ago (Kulik et al. 2000, Neumann et al. 2002 and references therein). The same possibility has already been proposed by Gimeno et al. (2006, 2008, 2009) for these types of groundwaters in the Forsmark and Laxemar-Simpervap areas.

Groundwaters related to the Southern boundary belt show homogeneous dissolved manganese values (between 0.6 and 0.9 mg/L; 0.011 and 0.016 mmol/L), in the lower range of those observed in the rest of the hydrostructural domains, and most of them are clearly undersaturated with respect to rhodochrosite, supporting less influence of marine waters in this zone.

Different inorganic reactions and microbial processes could participate in the control of dissolved manganese in the SFR groundwaters. However, there is a clear link between manganese concentrations and equilibrium with rhodochrosite and Littorina signatures, as also reported for the Forsmark groundwaters. These relationships can be interpreted as an inheritance of the hydrochemical conditions imposed by rhodochrosite formation during the infiltration of Littorina waters through the marine sediments. Thus, an "old" mixing control on manganese contents is still evident in the SFR groundwaters.

The Nitrogen system (nitrate, nitrite and ammonium)

Available analytical data for dissolved nitrogen species in the groundwater samples from the SFR include NO_2^-, NO_3^-, and NH_4^+. Nitrate and nitrite contents in the SFR groundwaters are low (Figure 5-42) and, in many cases, below the detection limit. Mixed transition type and Local Baltic type groundwaters tend to display the highest nitrate concentrations. Nitrite concentrations are similar to the Baltic Seawater contents which could be entering the SFR area (Figure 5-42). However, groundwaters with the clearest Baltic signature (Local Baltic type groundwaters) show the lowest nitrite contents, whereas groundwaters with Littorina or Glacial signatures display the highest concentrations. Thus, the highest nitrite contents in the SFR groundwaters are probably related to *in situ* bacterial denitrification. The available microbiological analyses for the SFR groundwaters indicate that nitrate reducing bacteria (NRB) show the highest MPN (3.3 and 70 cells/mL) of all analysed metabolic groups. The active presence of this metabolic activity would imply the existence of anoxic environments.

Ammonium contents are always clearly detectable (except in a few glacial and Mixed transition type groundwaters) and, in fact, it is the most common analysed nitrogen component in the SFR groundwaters. This would support the existence of generalised reducing conditions in the SFR groundwaters. Overall, the main characters of the nitrogen system would support the existence of anoxic-reducing conditions in the groundwaters from the SFR. The higher concentrations of nitrate detected in some SFR groundwaters compared to those found in Forsmark or Laxemar may be related to anthropic disturbances associated with the SFR facility. But the nitrate contents in most of the SFR groundwaters are generally in the usual range for uncontaminated groundwaters and, furthermore, they are similar or even lower than those found in other crystalline systems. Thus, the possible influence of blasting residues is minimal, if any, in the present SFR groundwaters, some twenty years after excavation and construction of the SFR.
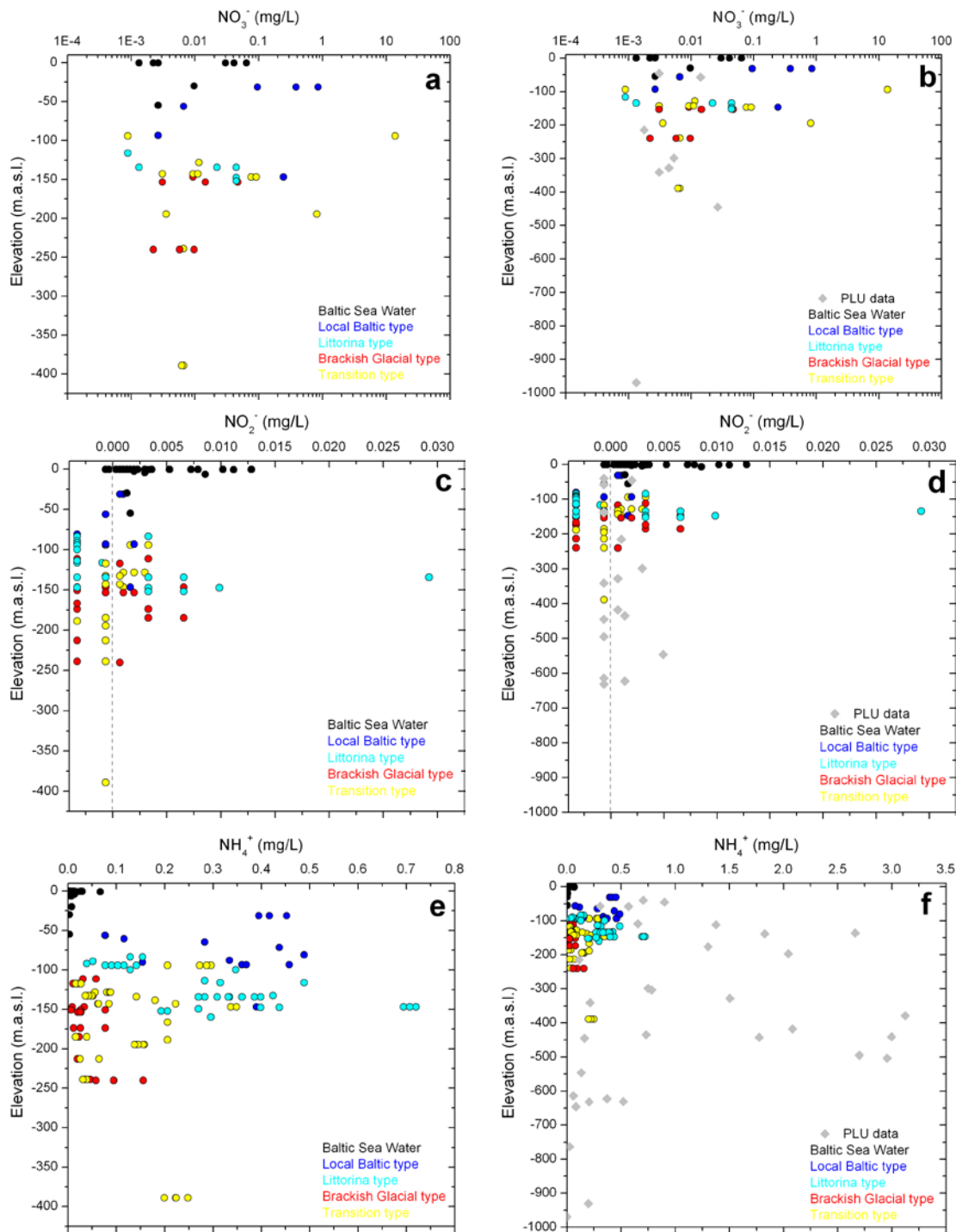
Figure 5-42. *Distribution of NO_3^- (a, b), NO_2^- (c, d) and NH_4^+ concentrations (e, f) versus depth in the SFR groundwaters colour coded by groundwater types. The plots to the left (a, c, e) show the SFR data and the scales are restricted to the ones relevant to the SFR extension data. The plots to the right show the data integrated in the general distribution of the Forsmark data down to 1,000 m (b), and wider concentrations scales (d, f).*

5.7 Buffering capacity for pH and redox provided by the host rock and fracture minerals

Fracture minerals constitute the primary reaction surface in the contact between groundwater and bedrock. These mineral coatings are often fine-grained (e.g. clay minerals), have large specific reactive surface and many of them are more reactive than the crystalline rock matrix minerals (such as carbonates and sulphides precipitated on the fracture walls). Therefore, even though their quantity compared to the rock forming minerals is small, their contribution to the buffer capacity in the bedrock is important. The fracture mineralogy and its variation with depth provide information not only on past redox reactions, but also on the available pH and redox buffer capacity.

5.7.1 Fracture minerals as indicators of pH and redox conditions

Two kinds of boundaries between mainly oxidised to reduced conditions are often present within the bedrock. The terminology used to describe the two different boundaries varies between different authors, but used here are the same definitions as those described in Sidborn et al. (2010):

1. A redox front: A spatially steep gradient of redox conditions within the rock matrix. This type of redox front is generally sharp and can be seen often as a change in colour of the rock due to redox reactions.

1. A redox transition zone: A zone where oxidised conditions in the fracture system close to the surface gradually change to reduced conditions at depth. In contrast, the rock matrix will remain largely anoxic with only very limited impact close to oxic fractures. The groundwater will mainly be in contact with the already oxidised parts. In the oxidised zone above the transition zone, all open parts of the fracture system are largely under oxidised conditions whereas in the redox transition zone, oxidised and reduced conditions may occur contemporaneously at the same depth, but in different channels (or even in the same channel) within the fracture system. Or the condition may vary, for example, annually. Below the lower limit of the transition zone, all parts of the fracture system are under reduced conditions. The position of the transition zone may vary in time, (e.g. seasonally).

Direct measurements of Eh (potentiometric) in the near surface groundwater is associated with both technical and conceptual problems (e.g. Auqué et al. 2008). Therefore, secondary evidence such as the spatial distribution of redox sensitive minerals and elements in the fracture system minerals can be used to detect the depth to which oxidised waters have penetrated (Tullborg et al. 2008, Drake et al. 2009). Redox processes occurring in the water-rock system which are expected to leave detectable mineralogical and/or or geochemical traces include mineral precipitation/dissolution and oxidation/reduction of redox sensitive elements (e.g. Fe, Mn, S, U and Ce). The presence of these processes can be indicated by the spatial distribution of fracture minerals and geochemical analyses of fracture filling material.

It should be emphasised that an observed redox transition zone recorded in fracture minerals may represent the present situation or represent a fossil transition zone where redox reactions occurred at some period during their hydrogeochemical evolution. Uranium-series disequilibrium analyses (USD) can be applied to indicate if oxidised events have occurred during the last 1Ma (Ivanovich and Harmon 1992). In addition, dissolution of calcite, which *sensu stricto* is not a redox sensitive mineral, has been showed to be indicative of intrusion of oxidised waters due to their often higher acidity in these systems (Tullborg et al. 2008, Drake et al. 2009).

Some general conclusions of the intrusion of oxidised water into Precambrian crystalline bedrock based on a review of natural analogue studies made both globally and within the Fennoscandian Shield have been presented in Sidborn et al. (2010) who concluded that the redox transition zone is mainly controlled by fracture zones and the depth rarely exceeds 100 m. However, along major water conductive fracture zones (hydraulic conductivity $> 10^{-7}$ m/s), indications of infiltration of oxidised waters have been found at greater depths. The hydraulic gradient, fracture frequency and thickness off sedimentary cover are controlling factors.

5.7.2 Possible intrusion of oxic waters in the bedrock at SFR

The available fracture mineral data relevant for redox and pH conditions from the SFR site investigation are limited to the spatial distribution of fracture minerals obtained during drillcore mapping and a more detailed study of the mineralogy and geochemistry of borehole sections sampled for groundwater chemistry and measured for Eh (Sandström and Tullborg 2011). In addition, the general conclusions made during the Forsmark site investigation are also considered valid for the SFR area, although there are hydrogeological differences between the two areas. For example, the SFR area is covered by the Baltic Sea and therefore there is no inflow of meteoric water to the upper part of the bedrock. The SFR area is also located outside the tectonic lens which gives a more open hydrogeological system than within the Forsmark area (cf. Stephens et al. 2007, Follin 2008, Curtis et al. 2011, Öhman et al. 2011). In addition, the operational phase of the SFR has also influenced the area. The observations listed below regarding the pH and redox conditions at the SFR is based both on information from the SFR and the Forsmark site investigations.

- The two earliest events of fracture mineralisations (generation 1 and 2 of Proterozoic age) are characterised by the presence of oxidised ferric iron in the form of hematite. The hematite occurs finely disseminated in fracture minerals such as adularia, albite, chlorite and laumontite. The conditions prevailing during precipitation of these fracture minerals were hydrothermal and oxidised. However, the Proterozoic chlorites also contain significant amounts of ferrous iron, suggesting variable redox conditions in both space and time.

- Hydrothermal alteration (red staining) of the wall rock is also associated with the Proterozoic fracture mineral generations. The alteration often extends a few centimetres out from discrete fractures into the host rock matrix but can extend over several metres in deformation zones. It is characterised by saussuritisation of plagioclase, chloritisation of biotite and to some extent hematitisation of magnetite. The red staining is due to hematite dissemination, but the degree of oxidation in the altered red-stained rock is small and the increase in Fe(III)/Fe(total) is generally insignificant (Sandström et al. 2010).

- Asphaltite is only found in the upper 70 m of the bedrock and pyrite occurs in a larger fraction of the open fractures in the upper 100 m (Figure 5-43 and 5-44). This is in agreement with the inferred downward migration of fluids rich in organic material under reduced conditions during the Palaeozoic based on data from the Forsmark site investigation (Sandström and Tullborg 2009).

- No occurrences of sulphide have been recorded in hydraulically conductive fractures in the upper 30 m of the bedrock at SFR (Figure 5-43), and no significant oxidation and/or dissolution of sulphide due to inflow of oxidised waters have been identified in the drill cores below 30 m.

- Fe oxyhydroxides are present in hydraulically conductive fractures and fracture zones, suggesting that oxidised conditions have prevailed at some period of time in parts of the fracture system. It is noteworthy that Fe-oxyhydroxide occurs down to an elevation of –650 m.a.s.l. as indicated by the drillcore mapping at SFR (Figure 5-43). However, if only best choice PFL anomalies are considered, the occurrence of Fe-oxyhydroxide is restricted to –190 m.a.s.l. (Figure 5-43). The age of these occurrences is not known and it is also possible that at least some of them are Fe-oxides (e.g. hematite) that can be difficult to distinguish from Fe-oxyhydroxides by visual inspection. This issue needs to be addressed in future studies.

- The presence of Fe-oxyhydroxide and sulphide in the same zones suggests that circulation of oxidised fluids have been concentrated along channels in which different redox micro environments may have formed.

5.7.3 pH buffering capacity in rock matrix and fracture coatings

Calcite quickly responds to changes in pH by dissolution or precipitation and provides an important buffering capacity against acidification. Calcite occurs abundantly at all levels as a fracture filling mineral at the SFR (Figure 5-43) whereas in the rock matrix it is only present as trace amounts.

No evidence of calcite dissolution in fractures in the upper part of the bedrock can be seen based in the drillcore mapping (Figure 5-43 and Figure 5-44). However, the mineralogical data from the uppermost 10 m of the bedrock beneath the Baltic Sea is limited (Figure 5-43) and it cannot be
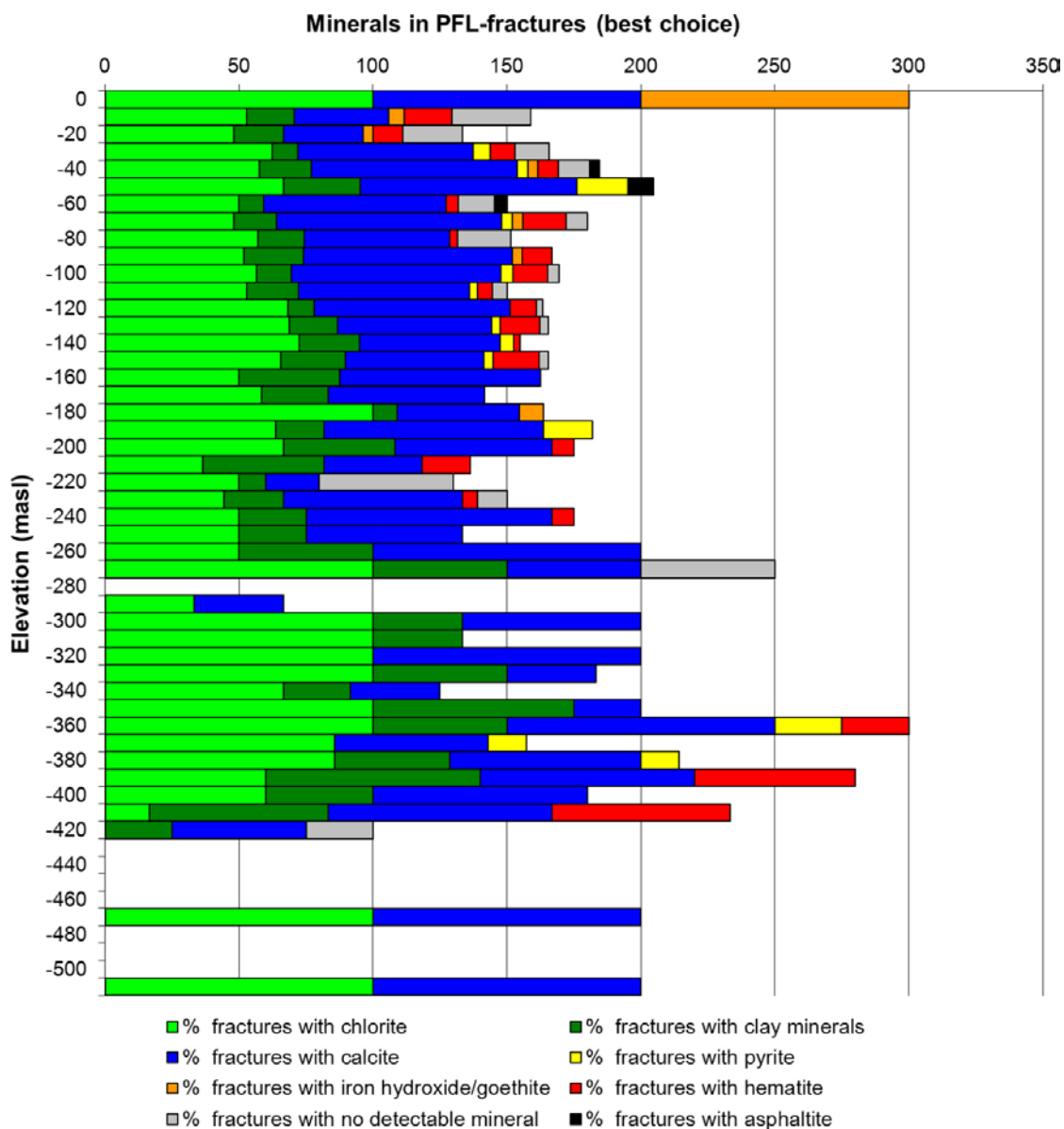
Figure 5-43. *Depth distribution of the fracture mineralogy in all mapped fractures classified as a PFL-anomaly (best choice) from the SFR. Only one best choice PFL-fracture has been identified in the uppermost 10 m (Figure 5-44). The data represent data from the SFR drill cores and KFM11A. Fractures omitted from the SFR data set are fractures from KFR24 down to Secup 147.50 m, where no core was available, and fractures from the remapped drillcores where no BIPS logging has been carried out (KFR04, KFR08, KFR09, KFR13, KFR35, KFR36, KFR54, KFR55, KFR7A, KFR7B and KFR7C) (Petersson J 2011, personal communication).*

excluded that dissolution processes occur in the very uppermost part of the bedrock due to intrusion of Baltic type groundwater undersaturated with respect to calcite without further investigations. However, the till covering both the SFR and Forsmark site investigation areas is rich in limestone (calcite) (Hedenström and Sohlenius 2008, Hedenström et al. 2008), thus increasing the pH buffering capacity. Therefore, calcite dissolution in the bedrock is not to be expected under present conditions. In order to obtain quantitative data of the amount of calcite available as a pH buffer in the fracture system, quantitative mapping such as that carried out during the Forsmark site investigation (Eklund and Mattson 2009) would be required. Then, calcite was quantitatively estimated in 32% of the mapped fractures (Löfgren and Sidborn 2010). The data suggested for modelling purposes for the SR-Site safety analysis at Forsmark are presented in Table 5-10.
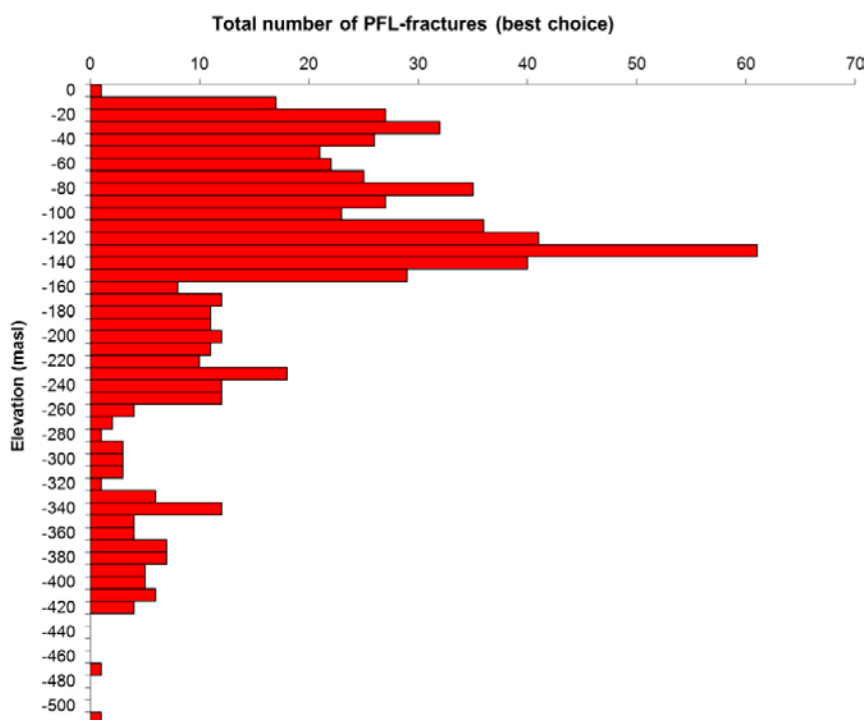
Figure 5-44. *Total number of best choice PFL-fractures at the SFR.*

Table 5-10. Normal distributions of $\log_{10}$ (d_{mean}) of calcite, suggested for use in SR-Site (Löfgren and Sidborn 2010). Data from the Forsmark site investigation. d = fracture mineral thickness.

μ of $\log_{10}$ (d_{mean} [mm])	−1.47
σ of $\log_{10}$ (d_{mean}[mm])	0.70

5.7.4 Reducing capacity in fracture coatings and rock matrix

In the absence of organic material of surface origin, the reducing capacity is dominated by ferrous iron hosted in fracture minerals and in the rock matrix of the SFR host rock, and Fe(II)-bearing minerals serve as a redox buffer in the case of recharging of oxic waters (Tullborg et al. 2008, Drake et al. 2009, Sidborn et al. 2010).

The most important minerals available for redox reactions are the Fe(II)-bearing minerals coating the water conductive fractures, and at the SFR they comprise mainly chlorite, clay minerals and pyrite; pyrite also contains S^- and is therefore a highly potent reductant. Based on the data from the quantitative mapping of fracture minerals during the Forsmark site investigation (Eklund and Mattson 2009, Löfgren and Sidborn 2010) and from geochemical data of fracture filling minerals (Sandström et al. 2008), the amount of Fe(II) available in the fracture system at the Forsmark site investigation area was calculated and presented in Sidborn et al. (2010) (cf. Table 5-11).

Table 5-11. Fe(II) content in bulk fracture fillings on fracture surfaces from the Forsmark site investigation area; E(x) = expected value or mean. Parameters μ and σ are the mean and the standard deviation of the natural logarithm of the content obtained from the lognormal distribution. Data from Sidborn et al. (2010).

E(Fe(II)$_{mean}$)	3.7 wt%
μ of ln(Fe(II)$_{mean}$)	0.84
σ of ln(Fe(II)$_{mean}$)	0.97
E(Fe(II))	23 g/m^2
μ of ln(Fe(II)/m^2)	2.10
σ of ln(Fe(II)/m^2)	1.44

As mentioned above, no quantitative mapping has been carried out on the SFR drillcores but the Forsmark data is expected to be largely similar. One possibility is, however, that the amounts of fracture minerals are less in the Forsmark lens due to restrictions in fluid circulation in this relatively tight part of the bedrock. On the other hand, the higher relative abundance of illite-smectite mixed layer clay at the SFR, instead of chlorite/corrensite which dominated in the Forsmark drillcores (Sandström and Tullborg 2011), may suggest that the amount of available Fe(II) is somewhat lower within fracture systems at the SFR compared to the Forsmark site investigation area. Furthermore, since no analyses of the Fe(II)/Fe(total) in fracture fillings have been carried out during the SFR site investigation, the amount of available Fe(II) in the clay minerals is not known and this will be addressed during future investigations.

The proportions of different rock types in cored boreholes from the SFR have been compiled by Curtis et al. (2011) and are presented in Figure 5-45. The two dominating rock types are metamorphic granodiorite (to granite), SKB code 101057, and pegmatitic granite and pegmatite, SKB rock code 101061 (Curtis et al. 2011). No modal or geochemical analyses of the rock types have been carried out within the investigation programme for the extension of the SFR. However, the same rock types are present within the area investigated during the Forsmark site studies and, based on ocular inspection of the rock types, the mineralogical and geochemical data from the Forsmark site investigation are considered representative also for the SFR area (Curtis el al. 2011).

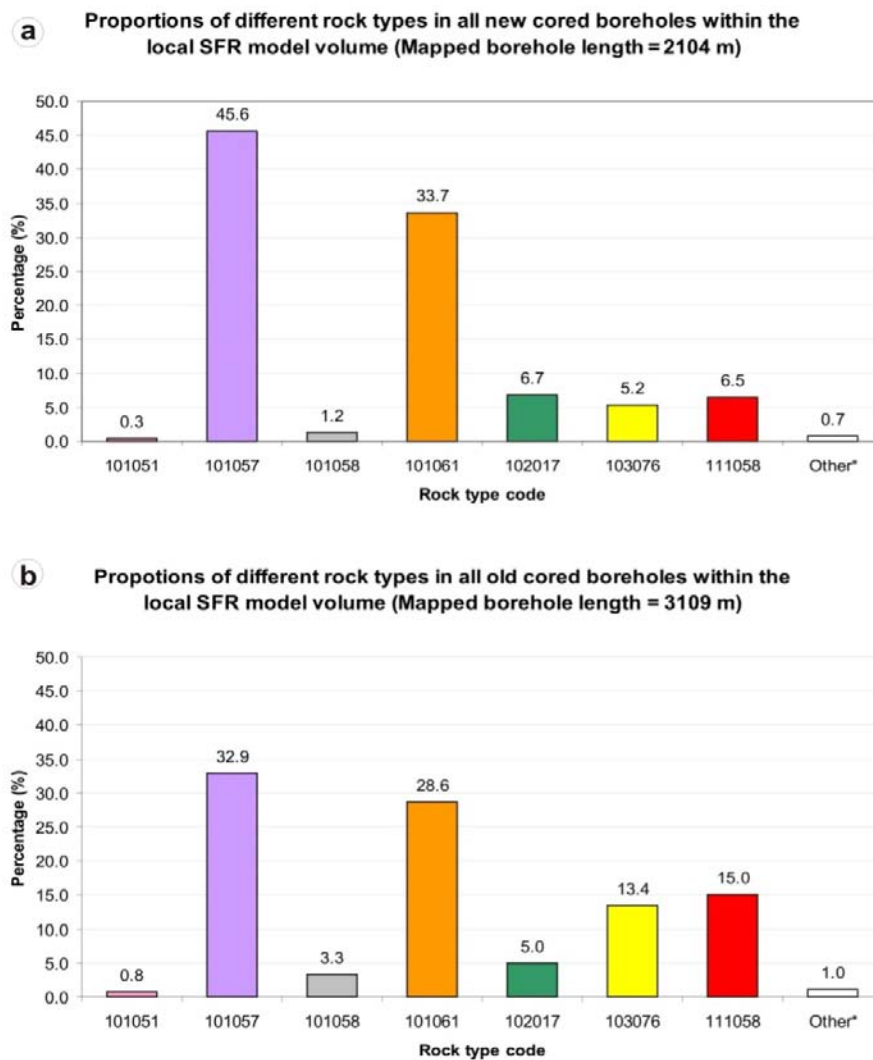
Figure 5-45. Histograms showing the proportions of different rock types in; (a) the cored boreholes from the drilling campaign for the SFR extension, and (b) old cored boreholes from the construction of the SFR. Only data from the local SFR model volume as well as boreholes KFR106 and HFR106 outside this volume are included (Curtis et al. 2011).Translation of codes is provided in Table 5-12.

Biotite is the dominating Fe(II)-bearing mineral in all these rock types, except for amphibolite where amphibole is the dominating Fe(II)-bearing mineral (Sandström and Stephens 2009). The amount of Fe(II) in the main rock types within the Forsmark regional model area was evaluated and presented in Sidborn et al. (2010) and data relevant for the SFR area is presented in Sandström and Tullborg (2011). At the SFR, pegmatite with a low Fe(II) content is one of the more abundant rock types, thus, the overall reducing capacity in the rock matrix is expected to be somewhat lower at the SFR than at Forsmark.

Table 5-12. Fe(II) content (wt%) in rock matrix for different rock types obtained during the Forsmark site investigation (PLU) (Sidborn et al. 2010). Parameters μ_e and σ_e are the mean and standard deviation of the natural logarithm of the content obtained from the lognormal distribution.

SKB code	101057	101051	101058	101061	102017	111058	103076
Name	Granodiorite (to granite), metamorphic	Granite, granodiorite and tonalite, metamorphic	Granite, metamorphic	Pegmatitic granite, pegmatite	Amphibolite	Granite	Felsic to intermediate volcanic rock, metamorphic
μ_e	0.28	0.76	–0.11	–0.35	1.70	–0.03	0.76
σ_e	0.20	0.55	0.18	0.16	0.18	0.20	0.65
Median	1.33	2.14	0.90	0.71	5.49	0.97	2.13
Mean	1.36	2.49	0.91	0.72	5.58	0.99	2.63
Std	0.28	1.49	0.17	0.12	1.01	0.20	1.91

5.8 Uranium, radium and radon

5.8.1 Uranium

Uranium in groundwaters commonly shows a trend of decreasing concentration with depth. The higher concentrations at and close to the surface are mainly due to the chemical reactivity of recharging waters (rich in CO_2 and O_2) which are the factors promoting uranium mobility by oxidising U(IV) to U(VI) and facilitating uranium mobilisation by carbonate complexation. Towards greater depth, the uranium becomes increasingly reduced to the more insoluble U(IV) form as the redox potential drops and therefore concentrations decrease. However, dissolved uranium is stabilised by carbonate complexation (or Ca-carbonate-complexes, cf. Noseck et al. 2012), which not only further stabilises U(VI) at surface/near-surface depths were dissolved bicarbonate is normally high, but may result in U(VI) existing to greater depths even at mildly reducing conditions and depending on the presence and amount of bicarbonate still dissolved in the groundwater. This was demonstrated by the results from the investigations at Forsmark where elevated uranium concentrations (> 10 μg/L) were found in several borehole sections representing depths down to 600 metres. These elevated concentrations were generally associated with Littorina type groundwaters which were not oxidising but had Eh values > –190 mV and bicarbonate contents > 30 mg/L. It was however pointed out already during the site investigations at Forsmark that uranium was not brought into the bedrock aquifer by the Littorina groundwater, but rather these brackish marine waters, under suitable conditions, served to mobilise U if coming into contact with an easily dissolvable uranium phase(s) present along water conducting fracture pathways (Smellie et al. 2008).

The uranium concentrations in the groundwaters in the early SFR boreholes as well as in the new SFR extension boreholes show large variations from a few μg/L up to 140 μg/L, but generally most concentrations are higher than 10 μg/L (Figure 5-46 a). These elevated concentrations, however, seem to have no connection to any specific groundwater type at the SFR. The highest values (> 100 μg/L) are found in groundwaters with a large component of Baltic Seawater, but other samples of the same groundwater type show values < 10 μg/L; furthermore, the plot does not indicate any clear depth dependence (the latter in similarity with the Forsmark samples). However, it is important to note that the sampling locations below about 200 m depth in the SFR extension project are very few. It can also be concluded that all the groundwaters analysed from the SFR show bicarbonate contents > 50 mg/L and the redox potential in the seven sections measured all show Eh

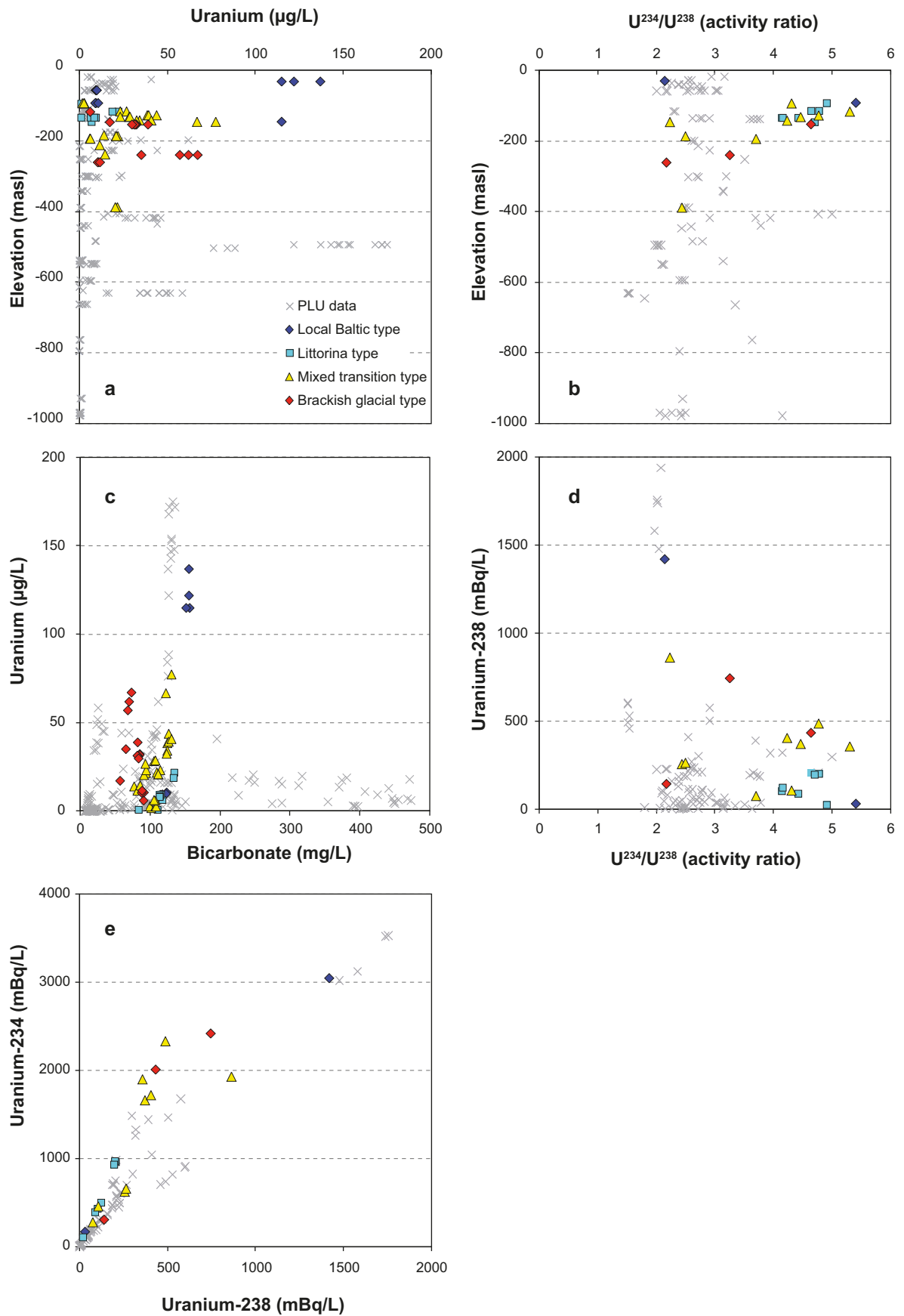**Figure 5-46.** *a) uranium versus elevation (m.a.s.l.), b) $^{234}U/^{238}U$ activity ratio versus elevation (m.a.s.l.), c) uranium versus bicarbonate, d) $^{234}U/^{238}U$ ratio versus ^{238}U (mBq/L), and e)^{234}U versus ^{238}U (mBq/L).*

values $\geq$ –190 mV (cf. Section 5.6.1). Because the hydrogeological situation around the SFR has been changed following the excavation and construction phases (i.e. drawdown to the tunnels, possibly increasing Eh etc), and thereby also altering the groundwater chemistry in many sampled sections, variations in uranium content most likely could be expected. The extent of possible alteration has not really been possible to study due to the very small time series dataset in which uranium values were included. Only two sections have been sampled on several occasions from 1987 to 2010 (KFR 01: –94.23 m.a.s.l. and KFR07A:134.43 m.a.s.l.) from the start of sampling. The uranium content has increased in both borehole sections (from 0.9 to 2.8 µg/L in KFR01 and from 0.9 to 8.2 µg/L in KFR07A). In KFR01 a slight increase in bicarbonate content is observed but in KFR07A the bicarbonate has been stable at around 110 mg/L.

Analyses of uranium isotopes (Alpha-spectrometry) in groundwaters (mainly ^{238}U and ^{234}U) have been carried out on a subset of samples. These data can be used to shed some light on the processes responsible for the elevated uranium contents in some of the groundwater samples. Variation in ^{234}U/^{238}U activity ratios (AR) in groundwaters are well known and the reason can be multifold, for example, marine water intruding the bedrock has originally a low activity ratio (^{234}U/^{238}U AR in the Baltic is close to 1). One reason for high activity ratios may be high groundwater flow rates (short water contact time) which may enhance the contribution of the more mobile ^{234}U.

The ^{234}U/^{238}U activity ratios are within the range 2 to 5.5 and there is no significant correlation with elevated uranium contents or groundwater types (Figure 5-46 b, d); however, in common with the Forsmark samples the groundwaters with the highest uranium contents tend to show the lowest ^{234}U/ ^{238}U activity ratios ($\leq$ 3), and *vice-versa*. In the SFR samples, however, the Littorina type groundwaters are not amongst the waters with the highest uranium contents or the lowest activity ratios in contrast to the observations from Forsmark (Smellie et al. 2008) . This underlines the fact that the high uranium content is not primarily related to the Littorina type groundwaters, i.e, they were not transported into the bedrock by the Littorina Seawater. Instead, as mentioned above and previously suggested in Smellie et al. (2008), the uranium in the groundwater seems to be related to dissolvable uranium phases present in some of the fractures.

Generally it can be concluded that there is a very good correlation between the total uranium content (µg/L) measured with ICP and the isotopic amount of ^{238}U (mBq/L) supporting good analytical quality of the uranium analyses of the groundwater.

The limited fracture mineral studies carried out within the SFR site (Sandström and Tullborg 2011) concentrated on seven borehole sections also sampled for groundwater chemistry during 2010; no uranium decay series data are available for these fracture mineral phases. Several occurrences of poorly crystallised uranium phases were identified on these fracture surfaces, the most common of which being a uranium phosphate occurring as small (< 1 mm), unevenly distributed precipitates on the fracture surfaces (Figure 5-47). Chemical analyses of bulk filling material scraped from the fracture surfaces show Th/U ratios below 2 in all but one of the analysed bulk samples, i.e. significantly lower than the Th/U ratio in all rock types analysed in the area (Sandström and Stephens 2009), indicating uranium deposition at some period(s) in the geological past. Despite the indicated deposition, the uranium contents of the bulk fillings are not exceptionally high (4.9 to 44.2 mg/kg). Many of the uranium precipitates found are cogenetic with the Palaeozoic generation 3 pyrite and asphaltite, cf. Sandström et al. (2008) when an organic-rich alum shale covered the area and fluids emanating in these sediments migrated downward into the crystalline bedrock (Sandström and Tullborg 2009). These sediments have today been eroded in the Forsmark area, but where preserved they often show high uranium contents (Andersson et al. 1995). However, analysed asphaltite samples from bedrock fractures in the Forsmark investigation area, inferred to have emanated in these organic-rich sediments, show low uranium contents (Sandström et al. 2006), although it is possible that the Palaeozoic sediments locally were more uranium rich. During the Forsmark site investigations, uranium oxide was found associated with older chlorite and hematite (Sandström et al. 2008). The presence of uranium phases associated with different fracture mineral generations suggests that uranium has been remobilised and precipitated during several events during the geological evolution of the Forsmark area, probably as far back as the Precambrian (cf. Welin 1964, Sandström et al. 2008, Sandström and Tullborg 2011).
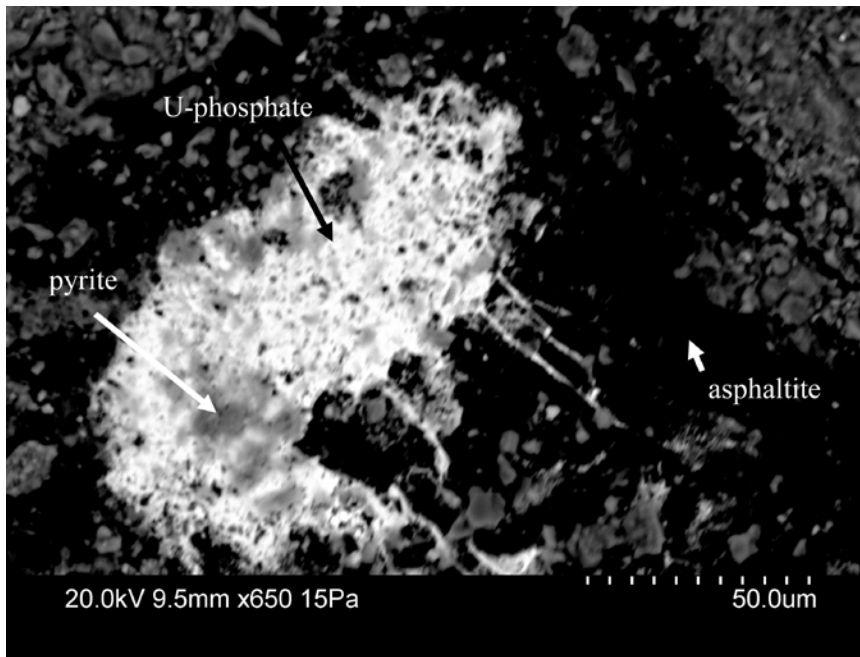
Figure 5-47. *Back scattered electron image of a uranium phosphate mineral cogenetic with pyrite and asphaltite in sample KFR01at 47.09–47.46 m borehole length (Sandström and Tullborg 2011).*

When the uranium content in fracture filling material is compared to the groundwater uranium content in the corresponding borehole sections no direct correlation can be seen. However, in the sampled borehole sections with uranium concentrations in the groundwater above 10 µg/L, analyses of fracture coatings in contact with the groundwater also show elevated uranium contents (> 20 mg/kg).
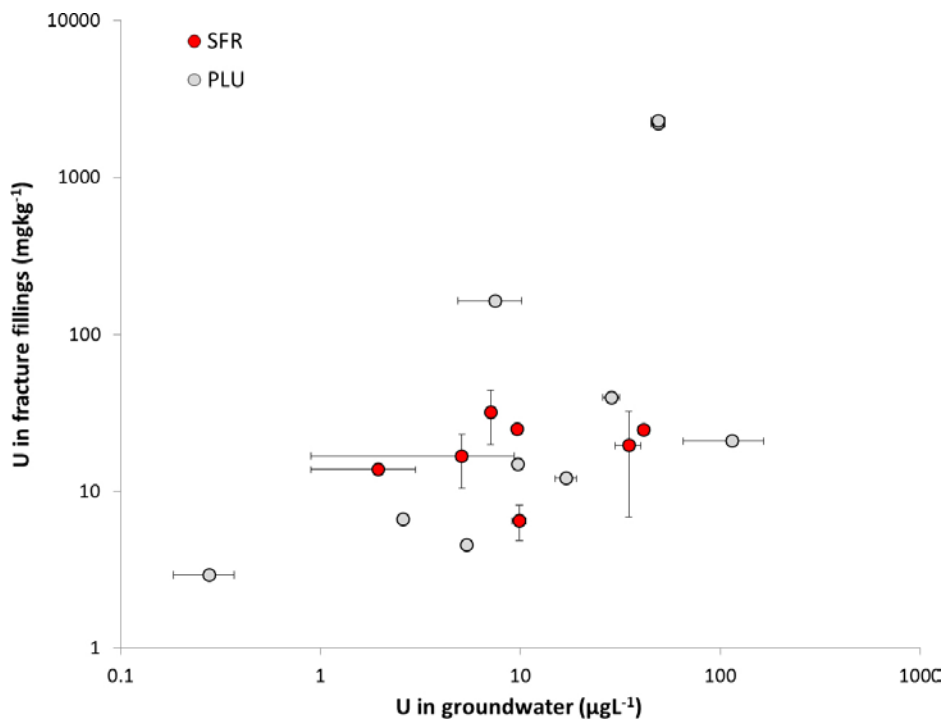
Figure 5-48. *Uranium in groundwater samples plotted versus uranium in fracture filling material from the corresponding borehole sections.*

In two different borehole sections sampled for groundwater from the existing SFR facility, $^{234}U/^{238}U$ activity ratios have been measured at several occasions (cf. Table 5-13). In borehole section KFR7A: –134.43 m.a.s.l. data are available from 1987, 2000 and 2006 showing some variations in uranium content (equivalent to 89.2–121.0 mBq/L ^{238}U) with relatively stable activity ratios at 4.2 to 4.4. The groundwater has remained Littorina-glacial in type but the chloride contents have decreased with time (5,000 to 4,000 mg/L) as also the magnesium values (250 to 174 mg/L); the bicarbonate content has remained stable at 110–115 mg/L. For borehole section KFR01: –94.23 m.a.s.l., data are available from two sampling occasions (1987 and 2006) with the uranium content significantly higher in 2006 (22 and 107 mBq/L ^{238}U respectively). The groundwater in this section has changed from a Littorina-glacial mixture to a Mixed transition type groundwater composition where input of present Baltic Sea is indicated by a slight increase in bicarbonate from 83 to 107 mg/L. It is also possible that the intrusion of the Baltic Seawater has increased the uranium content, but it is interesting to note that the activity ratio remains relatively similar (4.9 ad 4.3). The conclusion from both these sections is that the activity ratios reflect interaction with the uranium phases in the fracture systems and are not restricted to the different groundwater types, once again underlining that differences in uranium contents in the groundwaters reflect the irregular distribution of easily dissolvable uranium phases along the different fracture systems, whereas the amount of actually mobilised uranium is related to the groundwater chemistry together with the availability of dissolvable phases.

Table 5-13. ^{238}U and ^{234}U in mBq/L values measured in boreholes KFR7A and KFR01 at different occasions.

| Borehole section	Sampled year 1987		Sampled year 2000		Sampled year 2006	
	^{238}U mBq/L	^{234}U mBq/L	^{238}U mBq/L	^{234}U mBq/L	^{238}U mBq/L	^{234}U mBq/L
KFR01: –94.23 m.a.s.l.	22.0	108.1	–	–	107.0	462.0
KFR7A: –134.43 m.a.s.l.	104.4	433.2	89.2	395.0	121.0	504.0

Despite the lack of data in some important areas (e.g. uranium isotope data on fracture fillings), the studies can be summarised as follows. The most probable explanation to the elevated dissolved uranium contents from the site investigation at Forsmark was the presence of a dissolvable uranium phase heterogeneously distributed in the fracture system. When coming in contact with groundwaters characterised by an Eh higher than –200 mV and bicarbonate concentrations > 30mg/L, this uranium phase may become mobile. Solubility calculations showed that a stable U(VI)-carbonate complex is probably responsible for the higher uranium concentrations observed in these groundwaters (Gimeno et al. 2008). There are strong indications that most groundwaters at the SFR site, irrespective of groundwater type, have Eh values in the relevant range to support the above explanation. Furthermore, from Figure 5-46 c it is obvious that most samples show bicarbonate concentrations well above 50 mg/L. The study of fracture filling material from some of the sampled sections at the SFR made it possible to identify uranium phases from some of the water conducting fractures and whole bulk chemistry of the filling material supports a remobilisation of U (Th/U > 2) at some time in the past. The measured uranium contents in bulk fracture fillings are, however, not very high (< 45 µg/kg). Ongoing work, which includes fracture mineral sampling together with associated groundwater sampling in the SFR extension borehole KFR106, is focussed on the uranium issue with special emphasis to further locate and describe the solid uranium phases.

5.8.2 Radium and radon

Radium-226 and radon-222 are part of the uranium-238 decay series, radium being the daughter isotope to thorium-230. Radium and radon have been measured in about 20 groundwater samples from the SFR and Figure 5-49 a–d shows ^{226}Ra plotted versus ^{222}Rn, ^{238}U, Cl and SO_4; the plots also include values from the Forsmark site investigations. It can be concluded that with the exception of two (very low) radon values the radium and radon activities at SFR are within the same range as the Forsmark samples (cf. Smellie et al. 2008). Although no clear correlation between radium and radon activity can be seen, the activity of radon exceeds that of radium with at least two orders of magnitude in most of the samples, which corresponds to the Forsmark dataset.
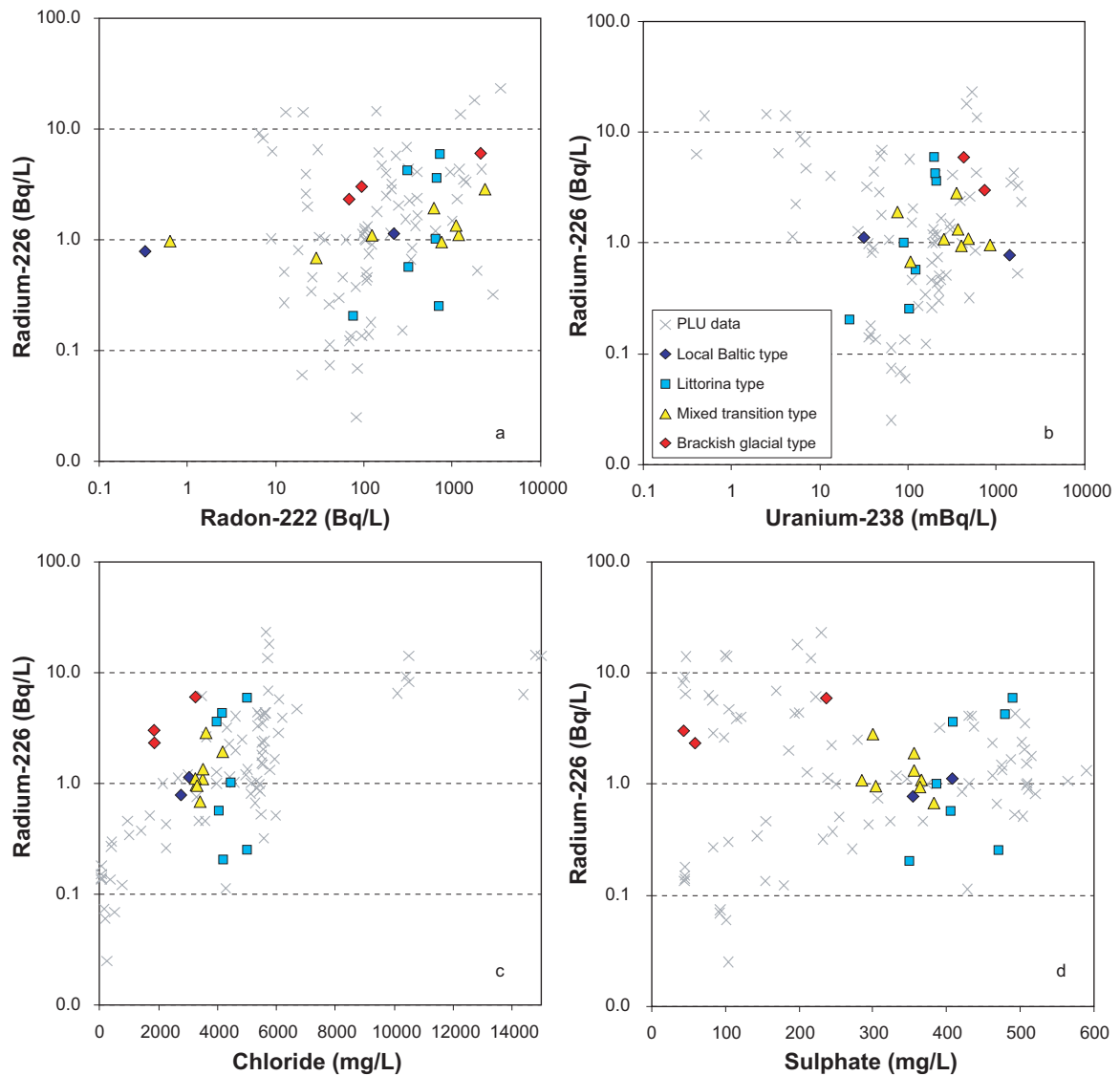
Figure 5-49. *Radium (Bq/L) in groundwater samples from the SFR plotted versus; a) radon-222 (Bq/L), b) uranium-238(mBq/L), c) chloride (mg/L), and d) sulphate (mg/L).*

In most samples only one pair of analyses have been carried out and it is therefore not possible to judge the quality of the measurements. Radon contents in groundwater sampled with the gas lift technique may be too low due to loss of gas during the sampling (e.g. KFR101). The two samples available from borehole section KFR101: –240.25 m.a.s.l. show very similar radium values of 2.3 and 3.0 Bq/L with radon measurements at 95.5 and 69 Bq/L. Compared with data from other borehole sections radon is low in these samples in relation to the measured radium activity.

In summary, measured radium and radon activities are within the interval measured at Forsmark, and there is no obvious correlation between radium, radon and other parameters. On the other hand, the measurements are limited and may only serve to indicate that extreme values are not present.

5.9 Microorganisms and gases

Microorganisms influence the groundwater chemistry in several ways. Microbial diversity and activity were found to be substantial in shallow groundwaters sampled from overburden materials and from shallow rock fractures in Olkiluoto, Finland, typically down to about 20 m (Pedersen et al. 2008). The microbial degradation of organic material from surface vegetation and the oxidation

of methane from deeper groundwater consume oxygen and result in the change of infiltrating groundwater from aerobic to anaerobic. The degradation of organic material continues to greater depth but since the oxygen from the atmosphere is continuously consumed, the microbial processes in groundwater progressively become anaerobic which means that chemical species other than oxygen act as electron acceptors in metabolic processes. Due to the varying energetic output from degradation with different electron acceptors, the processes proceed in a defined order, starting with nitrate, an oxidised nitrogen compound, followed by oxidised species of manganese, iron, sulphur and carbon (cf. Table 5-14). The continuous input of organic material from the surface vegetation keeps the subsurface anaerobic and reduced by means of microbial respiration metabolisms. The resulting products from microbial degradation of organic material and methane depend on the type of electron acceptor elements that are available. If the rock and groundwater is rich in iron oxide containing minerals, the electron acceptor is likely to be ferric iron and the output from the metabolic process will be ferrous iron and a contribution to the amount of dissolved ferrous iron. In another geological setting, the rock may be depleted in iron and manganese but dissolved sulphate may be available in the groundwater, and the resulting metabolic process will then be sulphate reduction to hydrogen sulphide.

What different metabolic processes that will dominate depend also on other factors. The microorganisms in groundwater can be variably sensitive to the flow velocity, salinity or temperature (Hallbeck and Pedersen 2008a, b, c). Deep groundwater has a lower amount of organic material than shallow groundwater, and microorganisms at depth will be more dependent on energy and carbon sources available from depth, such as hydrogen and methane. Results from the microbial analyses during the site investigations in Forsmark and Laxemar showed that the number and activity of microorganisms varied significantly between different borehole sections and depths, but there was no obvious relation with depth (Hallbeck and Pedersen 2008b, c). A similar situation has been recorded in Olkiluoto, Finland (Pedersen 2008, Pedersen et al. 2010).

Table 5-14. Chemical speciation by microorganisms. Microbially mediated chemical speciation reactions possible in groundwater are listed. Potential risks for a repository are indicated.

Element	Reduction	Electron and energy source	Product	Potential risk
Oxygen	$O_2 + 4H^+ + 4e^- \rightarrow 2H_2O$	Org-C	H_2O	None
Nitrogen	$2NO_3^- + 12H^+ + 10e^- \rightarrow N_2 + 6H_2O$ (other recations also occur)	Org-C, H_2	N_2, N_2O, NO, NO_2^-	Gas development
Iron	$Fe(III) + e^- \rightarrow Fe^{2+}$	Org-C; H_2	Fe^{2+}	None
Manganese	$Mn(IV) + 2e^- \rightarrow Mn^{2+}$	Org-C, H_2	Mn^{2+}	None
Sulphur	$SO_4^{2-} + 8e^- + 10H^+ \rightarrow HS^- + H^+ + 4H_2O$	Org-C, H_2	HS^-	Corrosive
Carbon	$CO_2 + 4e^- \; 4H^+ \rightarrow CH_4 + 2H_2O$ $2CO_2 + 4e^- \; 4H^+ \rightarrow CH_3COOH$ $CH_3COOH \rightarrow CH_4 + CO_2$	H_2	CH_4 acetate	Gas development

5.9.1 Microbial investigations in SFR

Due to the few available microbe data, previous (year 2000) and recent (borehole KFR105) microbial investigations in the SFR boreholes are presented together with data from the site investigations in Forsmark (Hallbeck and Pedersen 2008c). The TNC (Total Number of Cells) data from two borehole sections in borehole KFR105 are plotted with early SFR data and all other available TNC data from the site investigation in Forsmark in Figure 5-50. The TNC values from the two depths in KFR105 were 4.8×10^3 and 7.8×10^2 cells mL^{-1}, respectively.

Data from the MPN determinations in KFR105 are shown in Table 5-15. The obtained data were among the smallest numbers found, mostly below detection, when compared with data from the site investigation in Forsmark. This is illustrated by showing the lowest and highest MPN value for each of the physiological groups of microorganisms found during the site investigation in Forsmark. Note that these data come from several different boreholes and sections.

Figure 5-50. *Total number of cells (TNC) per mL of groundwater against depth. The data from sampling in SFR have been labelled with borehole name and depth and colour coded according to the groundwater type definition in Section 3.3. The other data (×) are from the site investigation in Forsmark (Hallbeck and Pedersen 2008c).*

Table 5-15. MPN values from samples from KFR105 and from the site investigation in Forsmark (Hallbeck and Pedersen 2008c).

Borehole section	NRB	IRB	MRB	SRB	AA	HA	AM	HM
KFR105: −128 m	3.30	< 0.20	< 0.20	< 0.20	< 0.20	< 0.20	< 0.20	< 0.20
KFR105: −154 m	70.00	0.20	< 0.20	< 0.20	0.70	0.40	< 0.20	< 0.20
Forsmark								
Highest	46,300	4,000	3,000	13,000	160,000	160,000	1.7	17
Lowest	280	< 0.20	< 0.20	< 0.20	< 0.02	< 0.20	< 0.20	< 0.20

In Figure 5-51, TNC is plotted against corresponding ATP values and the correlation is significant at $p = 0.0003$ for the data. The TNC and ATP data from the two sections in KFR105 are the smallest numbers and concentrations, respectively, in the data set but they still follow the correlation line.
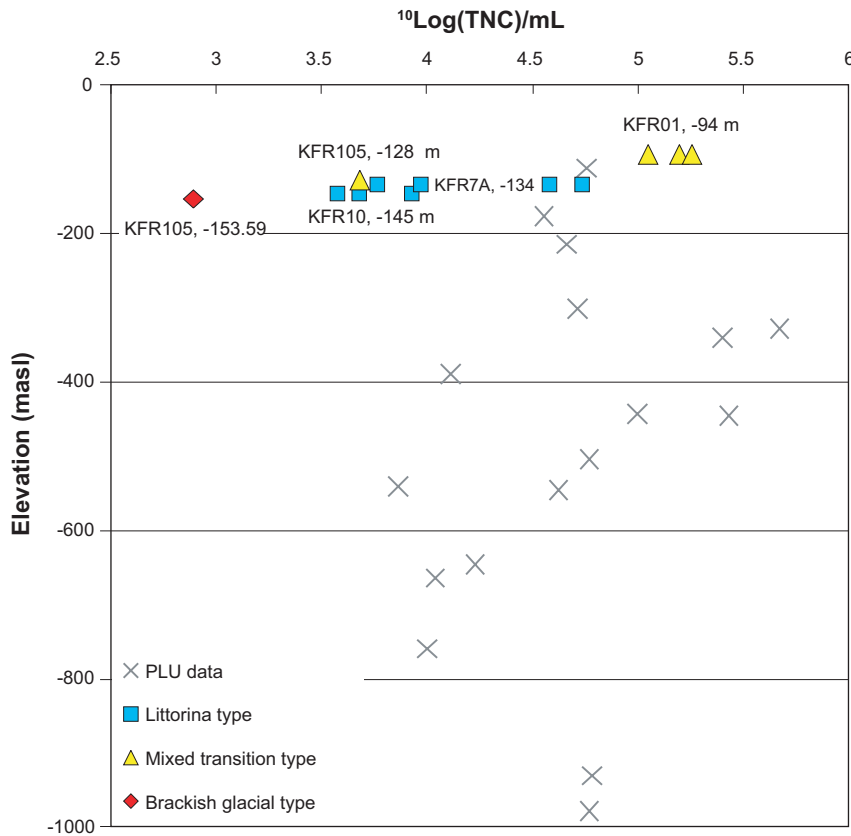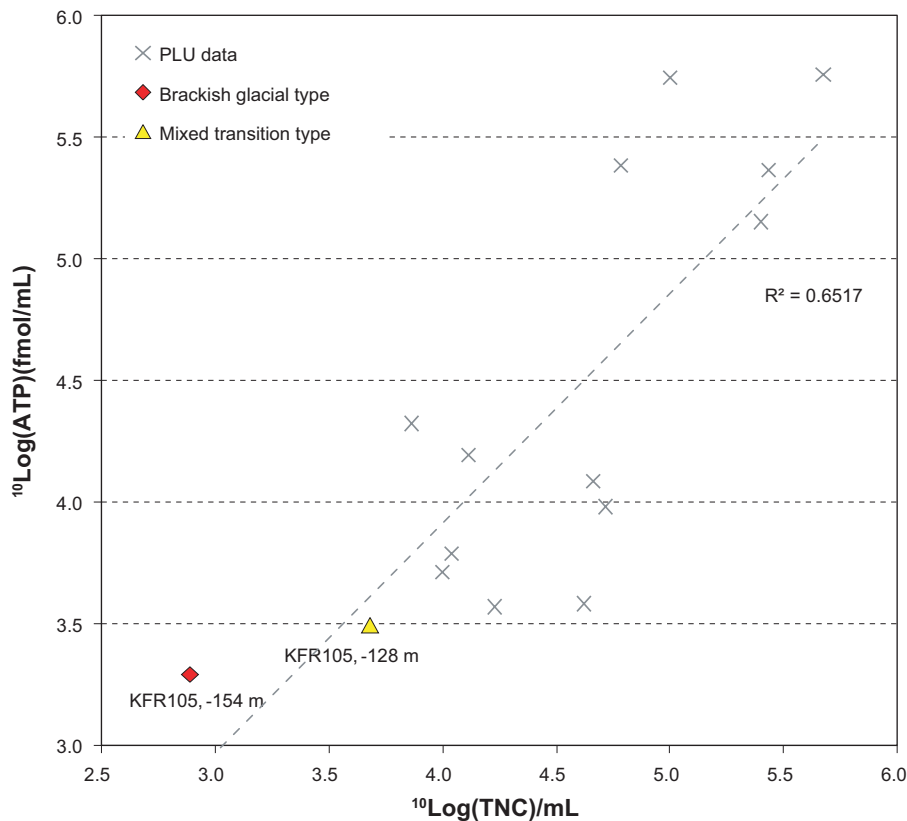
Figure 5-51. *Total number of cells (TNC) per mL of groundwater against ATP. The data from sampling in SFR have been labelled with borehole name and depth and colour coded according to the groundwater type definition in Section 3.3. The other data (×) are from the site investigation in Forsmark (Hallbeck and Pedersen 2008c).*

5.9.2 Discussion

The total number of cells (TNC), the ATP values, as well as the values for cultivable physiological groups (MPN), are all low (in some cases very low) in the groundwater samples from KFR105: –128 m.a.s.l. and KFR105 –154 m.a.s.l. When the chemistry data from these groundwater samples (KFR105: –128 m.a.s.l., being of Mixed transition type, and KFR105: –154 m.a.s.l., of Brackish-glacial type) were compared with samples from other boreholes and borehole sections in the SFR and Forsmark areas, nothing unusual was found. There was, in other words, no obvious explanation for these low numbers in the chemistry and gas data. However, investigations of microorganisms from the Fennoscandian Shield during the last 25 years have shown that the diversity and numbers vary significantly between boreholes and borehole sections, even if they are very close to each other. This was demonstrated by data collected during the site investigation in Forsmark (Hallbeck and Pedersen 2008c), Laxemar (Hallbeck and Pedersen 2008b) and Olkliluoto, Finland (Pedersen et al. 2008). The reasons for this heterogeneity can probably be explained by a combination of different factors such as; a) the presence and activity of phages, b) the availability to electron donors and acceptors for the microorganisms, c) the filtering effects on planktonic microorganisms from gouge and clay materials in the aquifers being pumped or drained, and d) the time and rate of pumping or draining and flowing of groundwater during sampling.

5.9.3 Gases

The gas contents and compositions (total gas volume, carbon dioxide, helium, methane and hydro-gen gas) in groundwater samples collected in the SFR are presented in Figure 5-52 a–f. The gas data are compared to corresponding values for the groundwater samples collected in the Forsmark site investigation. Despite the somewhat higher concentrations of carbon dioxide, the concentrations agree with the general trends found in the Forsmark samples (cf. Section 5.5.1) concerning the carbonate system and pH. The redox context of the gas concentrations are further discussed in Gimeno et al. (2011) and in Section 5.6.
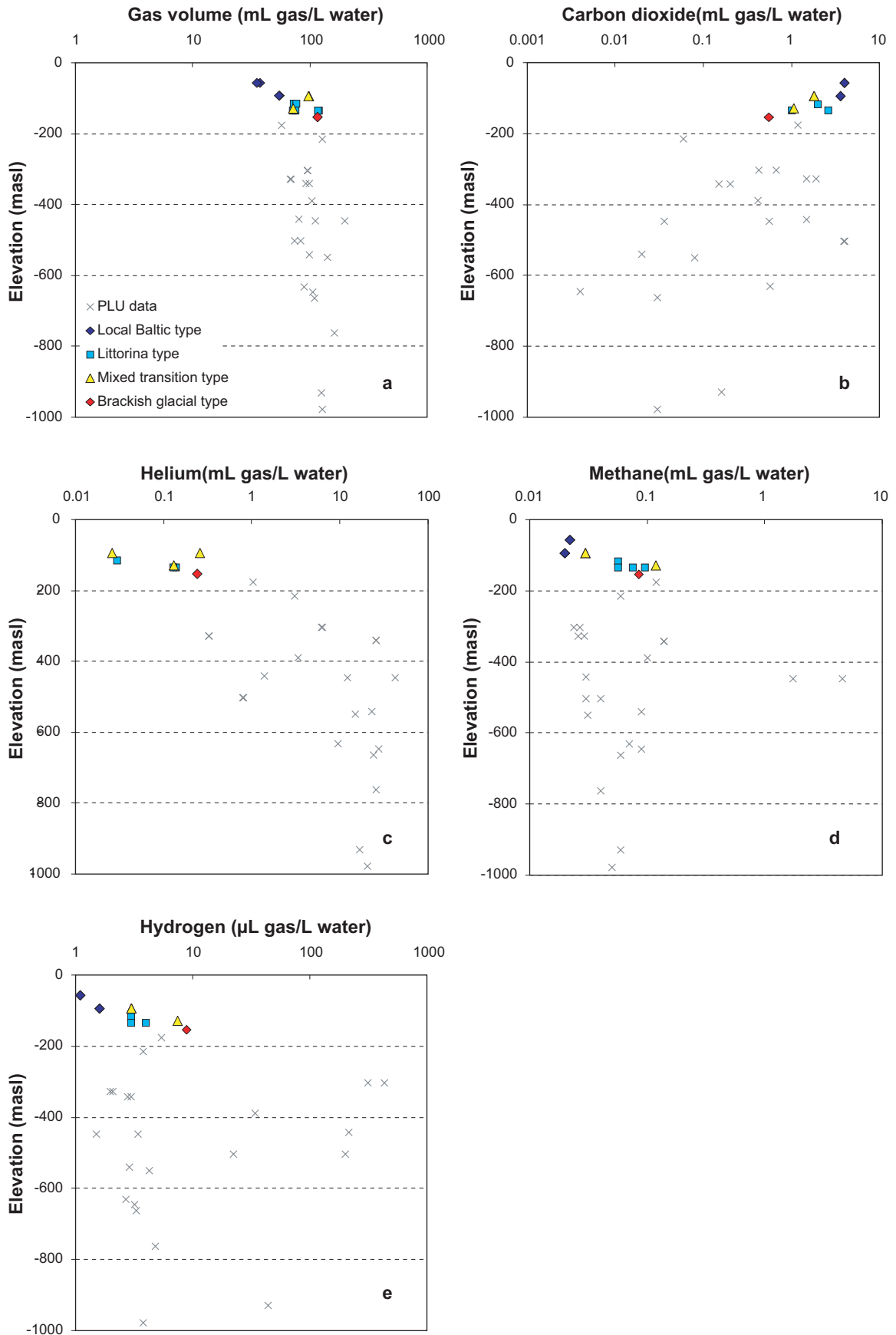
Figure 5-52. *Gas contents in groundwater against depth and related to the different groundwater types defined for the SFR Site in Section 3.3. PLU data includes Forsmark only; a) Total gas volume, b) Carbon dioxide, c) Helium, d) Methane, and e) Hydrogen.*

5.10 Residence times

A key factor in validating the suggested past and present groundwater evolution in the SFR model volume is to constrain the average residence time for each of the defined groundwater types. This can, at least theoretically, be approached qualitatively in terms of groundwater composition, i.e. based on aspects of water/rock reaction kinetics, or on a more quantitative level by using radioactive isotopes (Smellie et al. 2008). In the present investigation the data are restricted to:

A. Tritium (^{3}H) and carbon-14 (as percentage modern carbon, pmC), which can only suggest different periods of isolation from the atmosphere in time scales of decades (tritium) or postglacial time (carbon-14).

B. ^{36}Cl data from a small number of strategic samples covering a time span of several hundreds of thousands of years.

However, in defining the different groundwater types the ratio of the stable oxygen isotopes (expressed as δ^{18}O) has been used also to distinguish groundwaters with cold climate components (glacial meltwater), which in turn provide relative information on residence time.

It is important to keep in mind that the groundwater samples are usually influenced by mixing, and this is especially true for the SFR samples as the present SFR tunnels have changed the hydrogeological conditions resulting in an increased drawdown of young Baltic Seawater along some fracture zones and in others resulting in the mixing of residing groundwater types of different age and origin.

5.10.1 Tritium and radiocarbon

Recharge of meteoric water in Forsmark or, in the case of the SFR site present Baltic Seawater, can be traced by the variation of tritium over the last 50 years since the largest peak of atmospheric thermonuclear tritium dating from the early 1960s. It is still present in the recharging precipitation and in the infiltrating seawater and shallow groundwaters to the bedrock, but probably now also includes a smaller component of tritium related to the Forsmark nuclear power plant and possibly also the SFR storage facility.

Figure 5-53 shows tritium variation in groundwater samples from SFR versus date of sampling. The measurements carried out before year 2000 are relatively few but nevertheless show a larger variation than those later sampled. The present Baltic type waters show generally the highest values
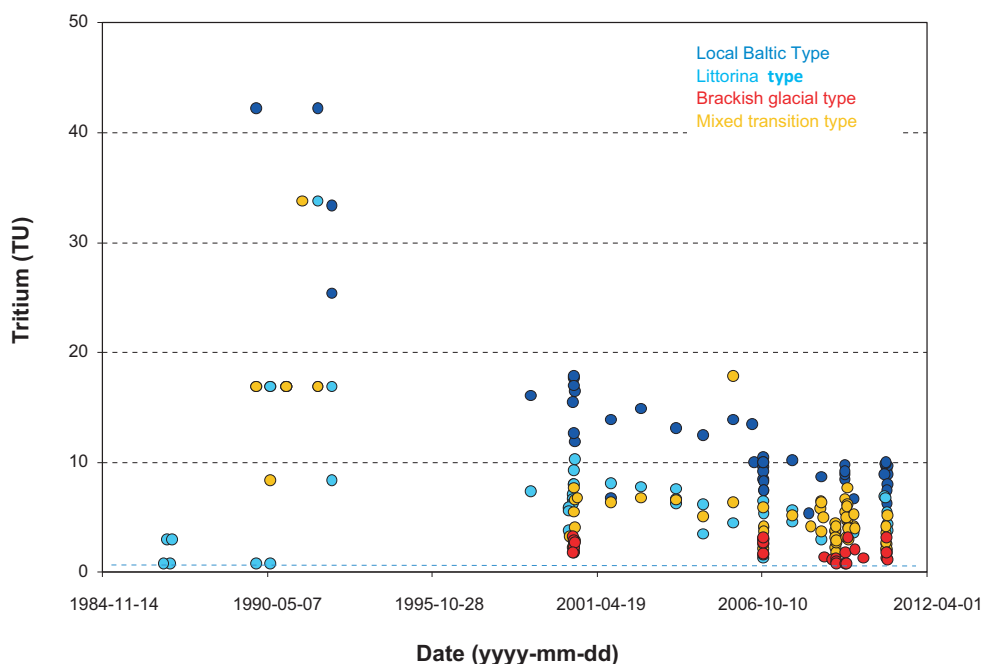
Figure 5-53. Distribution of tritium (TU) with time in the different groundwater types defined for the SFR Site in Section 3.3. All available tritium data during the time period are included. The detection limit at 0.8 TU is given as a blue broken line.

and display also a significant decrease with time largely compatible with the half-life of tritium (about 12 y). This supports that the major source of tritium in the Baltic Seawater is residual tritium from the bomb testing during the early 1960's and that any additional tritium from the power plant is subordinate.

In order to obtain a more compatible dataset only the samples sampled from year 2000 and onwards are used in the plots in Figure 5-54. The plot shows a characteristic decrease in tritium to a depth of around 150–200 m which represents the limit of recharge water of a young age (< 50 years) (Figure 5-54 a). However, measurable tritium content still persists within the entire depth interval which may be due to various sources of contamination (Smellie et al. 2008). In the SFR case, the samples were collected in the vicinity of the repository and also the nuclear power facility which suggest obvious sources for contamination. The few samples with tritium below detection limit (< 0.8 TU) are waters of Brackish-glacial type from sections KFR101:240 m and KFR105:154 m, but the entire group of brackish-glacial waters show tritium values < 3TU, which is lower than the Mixed transition type (1-7 TU) and Littorina type waters (1-10 TU).

The Baltic Seawater close to the SFR shows tritium values in the range of 10 to19 TU. The Baltic type groundwaters show somewhat lower values (5-18 TU) with samples higher than 15 TU all sampled in 2000. The general decrease of TU during the last decade is evident also from Figure 5-54 d showing the decrease in TU for the Baltic type groundwater sampled in KFR08: –93 m.
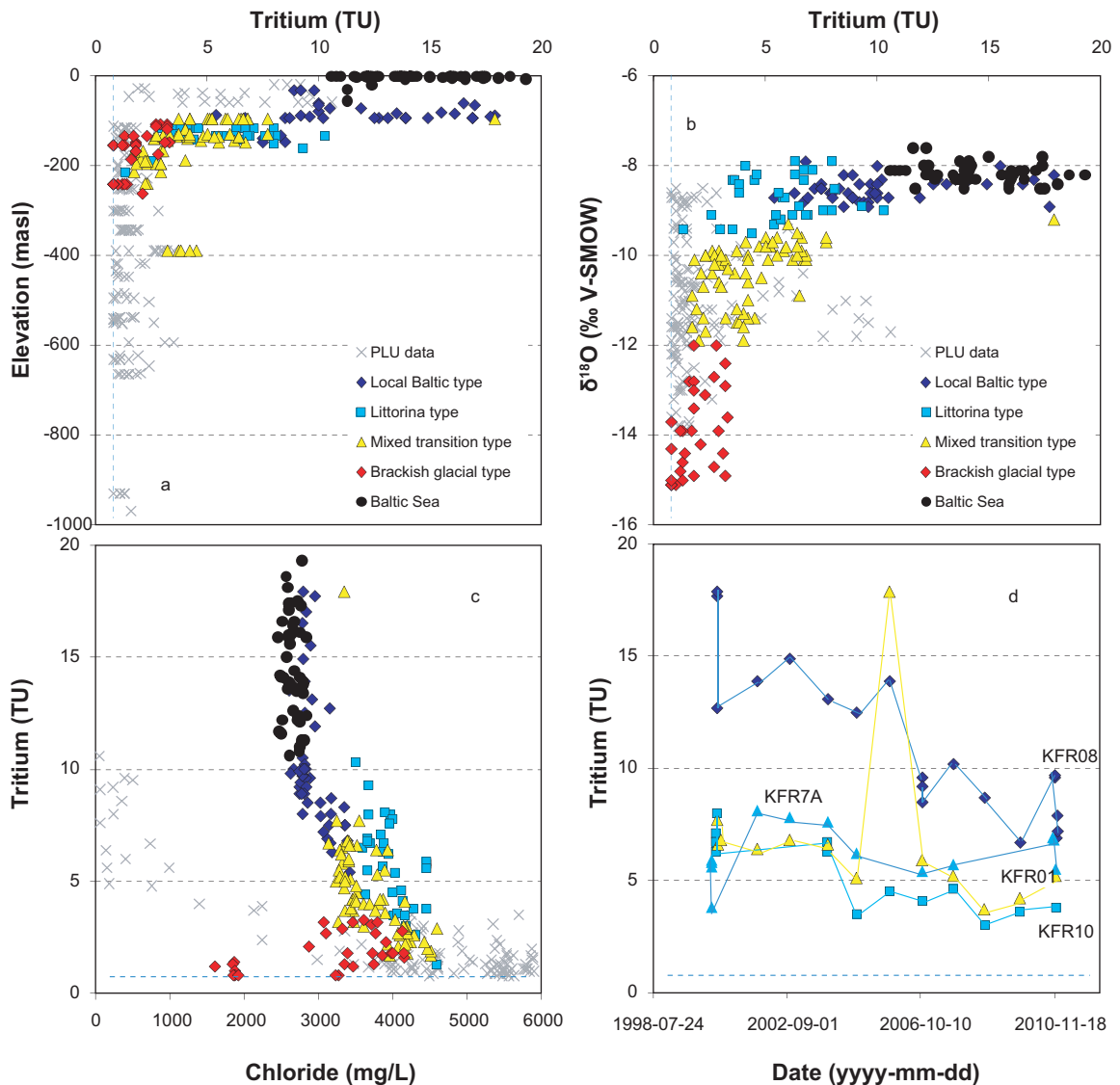
Figure 5-54. Tritium (TU) in the SFR samples plotted together with data from the site investigation at Forsmark. Data are plotted versus elevation (a), δ¹⁸O (b), chloride (c), and for four different sections versus date of sampling (d). The broken blue line refers to the detection limit (0.8 TU).

Generally, the trend of tritium in the different groundwater types corresponds to the conceptual understanding of the groundwater system at SFR (cf. Figure 5-54 a–e). The Baltic type groundwater shows the highest values followed by (and some overlapping with) the Littorina type groundwater. The Brackish-glacial type groundwater shows the lowest values, all below 3.2 TU, and it is only in this group that samples with tritium below detection limit (0.8 TU) are found. As already mentioned, most of the groundwater samples from the SFR show evidence of mixing and this is supported by the presence of tritium in nearly all samples. However, tritium values are a little too high (although still in most cases below 7 TU) for all groundwaters except for the Local Baltic type. This indicates a small contamination in many of the samples and it is presently not understood whether this takes place in the bedrock itself and/or during sampling. There are indications that there can be some contamination (e.g. tritium) during the operational phase of the present SFR, and some also in the water from the upper basin which contains drainage waters from the SFR tunnels which may contain, or have contained, elevated titrium.

Radiocarbon (^{14}C), with a half-life of 5,730 years, extends the range of detection up to 30,000 years for groundwater residence time. Theoretically, this range should cover comfortably the period since the last deglaciation, in particular confirmation of the Littorina Sea transgression; however, this is more complicated in practice. The analyses of carbon isotopes from the SFR site are relatively few and have been mainly carried out during the last 10 years. All carbon analyses are on inorganic carbon (TIC) and Figure 5-55 shows ^{14}C$_{TIC}$ (pmC) versus elevation (a), bicarbonate content (b), δ^{18}O (c), δ^{13}C (d) and tritium (e). It is obvious that the lowest ^{14}C contents are found in groundwaters below –100 m.a.s.l. where bicarbonate contents are less than 110 mg/L. These groundwaters also have the most depleted δ^{18}O, i.e. a large component of glacial water and correspondingly the lowest tritium content (cf. Figure 5-55 a–e). Generally, low ^{14}C corresponds to low δ^{13}C which is contrary to the Forsmark site where the highest ^{14}C corresponds to low δ^{13}C. This underlines the present marine (SFR) versus terrestrial (Forsmark) character of the young groundwaters of the areas.

The general understanding of the relative residence times of the different groundwater types is supported by the four samples representing present Baltic type groundwaters which show the highest ^{14}C contents (45 to 65 pmC) and high tritium values, thus indicating a modern origin (< 50 years old). However, the ^{14}C contents are still lower than expected at 45–65 pmC which supports the influence of reactions that have contributed "dead" carbon to the inorganic system in the groundwaters, either through calcite dissolution or breakdown of old organic material. The contribution from reactions is also supported by the increased bicarbonate values; Baltic Seawaters usually have values around 70–90 mg/L.

The five Littorina type groundwaters show ^{14}C contents between 22 to 42 pmC in agreement with the Forsmark data on Brackish marine type groundwaters. The Brackish-glacial type groundwaters, in contrast, generally show expected low values of 5 to 20 pmC. The Mixed transition type waters show as anticipated a broader range of ^{14}C (5 to 44 pmC) in line with their mixed origins (of which the lowest values correspond to samples from KFR02 and may be influenced by grouting diluting the ^{14}C signal). For the entire data set, higher tritium values, as expected, correspond to higher ^{14}C (cf. Figure 5-55 e). During the site investigations in Forsmark attempts to correct the ^{14}C contents for reactions, mainly based on δ^{13}C, was not judged as successful (Smellie et al. 2008), and therefore has not been applied here.

5.10.2 Helium-4

Helium-4 atoms are continuously produced in rocks by neutralisation of α-particles emitted during the decay of the naturally occurring radioactive elements uranium and thorium (e.g. Andrews et al. 1989a, b). Similar to chloride, helium is chemically inert; unlike chloride, however, its solubility in the atmosphere is very low and the amount of helium recharged via precipitation is insignificant compared to the *in situ* produced helium (^{4}He). Generally, radiogenic helium produced in various uranium- and thorium-bearing minerals in the bedrock is readily released to the associated porewater. Once this happens, the helium atoms are transported either by diffusion or advection into the groundwater of neighbouring fractures and eventually released to the atmosphere at the groundwater discharge. Therefore, increased helium reflects increased residence time. In Figure 5-52 c the He-concentrations measured in the SFR samples (only six samples) are plotted versus elevation together with data from Forsmark. As can be seen, the He concentrations in the SFR samples are generally lower or almost equal to the lowest helium values measured in the Forsmark samples, and these in turn represent the Brackish marine groundwater type (Littorina-glacial groundwater) from Forsmark. The helium data from the SFR data are very few and show no separation between the different groundwater types (in contrast to the tritium and ^{14}C values).
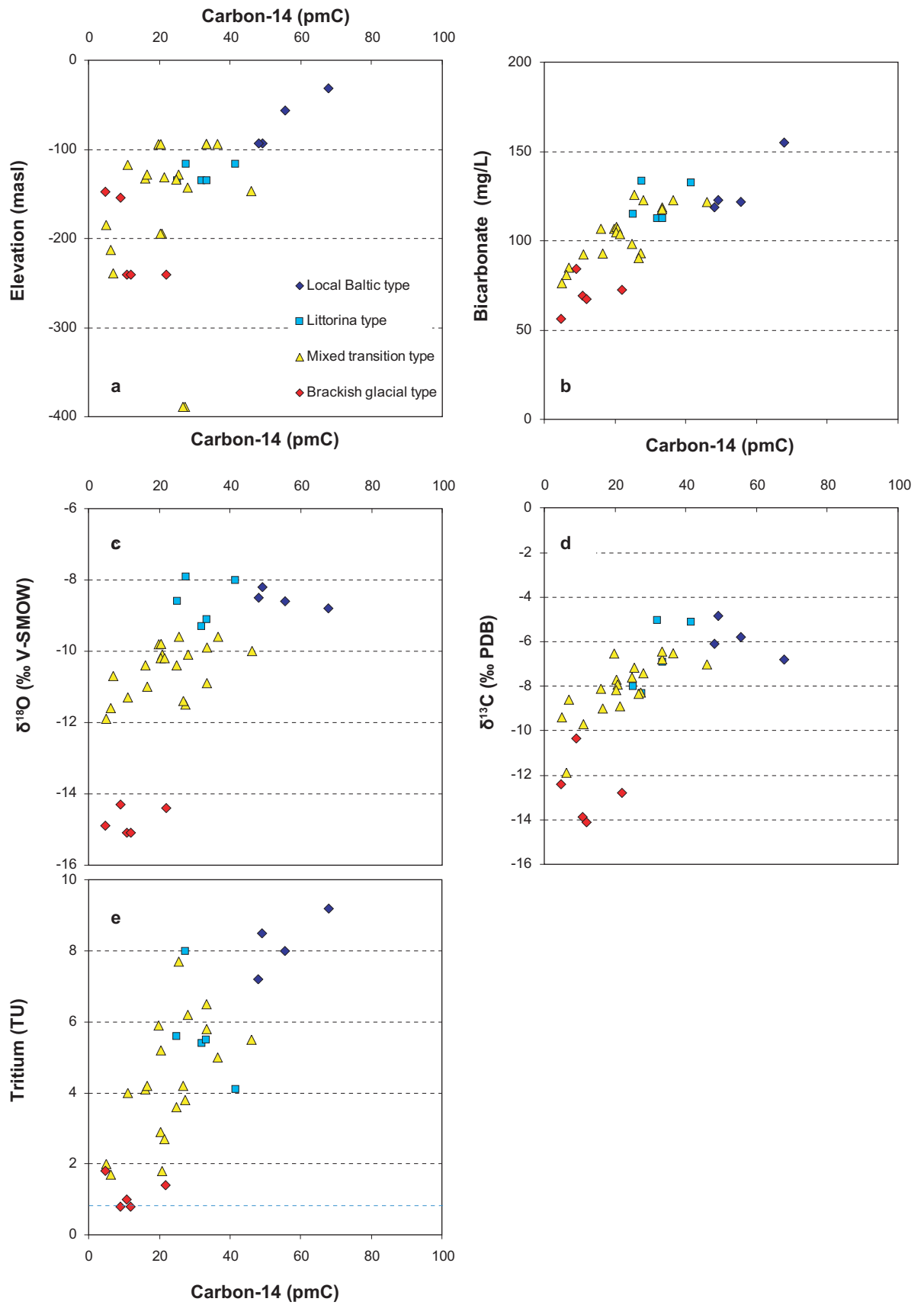
Figure 5-55. *Carbon-14 (TIC) in samples from SFR versus elevation (a), bicarbonate (b), δ¹⁸O (c) δ¹³C (d), and tritium (e). The broken blue line refers to the detection limit (0.8 TU).*

5.10.3 Chlorine-36

Chlorine-36, with a half-life of 301,000 years and generally conservative behaviour in a crystalline bedrock aquifer, is considered very useful for identifying saline waters of different origin and residence times extending as far as back to early Quaternary and late Tertiary times (Andrews et al. 1989a b, Bentley et al. 1986, Andrews and Fontes 1992, Clark and Fritz 1997). Chlorine-36 is therefore a useful compliment to tritium and ^{14}C and by covering ages far beyond the detection limits for these two nuclides.

Radiogenic [36]Cl in groundwaters has three sources; a) cosmogenic [36]Cl produced in the atmosphere and transported to the hydrosphere via precipitation, and b) epigenetic through activation of Cl, K and Ca on the land surface by solar radiation, or c) *in situ* production caused by the neutron flux produced by the decay of naturally occurring radioelements (i.e. U, Th and K) at greater depth in the bedrock. With time [36]Cl in the bedrock aquifer will accumulate and decay until the rate of production equals the rate of decay (i.e. secular equilibrium will have been achieved) after a period of 1.5 million years. Groundwaters showing [36]Cl at secular equilibrium with the *in situ* [36]Cl production of a specific rock will therefore have been shielded from the atmosphere and resided in this rock for at least 1.5 million years.

Table 5-16. [36]Cl analyses of selected SFR groundwater types.

Sample	Depth (m)	Sec. Mid. Elev. (m)	Chloride (mg/L)	at. ^{36}Cl/at. Cl ratio (10^{-15})	Origin
KFR7A	48.0–74.7	−134.43	3,674	$11.83 \cdot 10^{-15} \pm 1.96 \cdot 10^{-15}$	Littorina-glacial
KFR08	63.0–104.0	−93.3	3,126	$13.95 \cdot 10^{-15} \pm 2.44 \cdot 10^{-15}$	Baltic type
KFR101	279.5–341.8	−240.15	1,926	$27.19 \cdot 10^{-15} \pm 3.71 \cdot 10^{-15}$	Brackish-glacial
KFR105	265.0–306.81	−153.59	3,476	$24.86 \cdot 10^{-15} \pm 3.51 \cdot 10^{-15}$	Brackish-glacial

Units measured = Atoms of Cl-36 per total Cl extracted from groundwater; expressed as: atomic ^{36}Cl/atomic Cl = ^{36}Cl/(^{35}Cl+^{37}Cl).

From the SFR boreholes, four different groundwaters were selected for [36]Cl analyses representing; Baltic type groundwater, Littorina type groundwater and two samples of Brackish-glacial type groundwaters of which one shows a relatively low Cl content (1,926 mg/L) and the other a higher value (3,476 mg/L). In Figure 5-56 [36]Cl data from all sites in Sweden and Finland which have undergone hydrogeochemical investigations and where [36]Cl has been analysed, are plotted. Although not exactly the same groundwater type subdivisions have been used for the respective published data, an attempt has been made here to colour code the data according to their origin using eight different groundwater types (cf. Figure 5-56). The shaded fields represent calculated equilibria with the host rock at Äspö-Laxemar (Louvat et al. 1999), Olkiluoto (Gascoyne 2001) and Forsmark (Smellie et al. 2008).

The surface waters show as expected the highest [36]Cl/Cl ratios although the values vary considerably. In contrast, the present Baltic Seawaters and the Brackish marine waters of Littorina type from the different sites show the lowest [36]Cl/Cl ratios. This is in agreement with the earlier stated contribution of Cl from sources shielded from the atmosphere for a long period of time and low [36]Cl/Cl ratios measured in oceanic water (0.24 x10^{-15} ^{36}Cl/Cl) (Mahara et al. 2008). The Littorina type sample from the SFR records the lowest salinity and the highest [36]Cl/Cl ratios of the Littorina type samples analysed from the different sites. One possible explanation is that the Littorina sample is partly diluted with present Baltic Sea which has entered the fracture system as a result of the existing SFR tunnels.

The brackish to saline non-marine waters from all the different sites show significant [36]Cl contents approaching secular equilibria with the host rock, indicating very long residence times, i.e. in the order of at least 1.5 Ma which could indicate Early Quaternary and possibly even Tertiary (cf. Smellie et al. 2008).

Three samples with a significant glacial component have been analysed; two from the SFR and one from Laxemar (KLX04). The extent of the glacial component and the absence of time series sampling in this latter sample is somewhat suspect due to the intersection of a major deformation zone at 873–973 m and should be treated therefore with some caution. However, regardless of this issue, the Cl content in these samples varies from 1,926 to 7,880 mg/L and the interpretation (based on
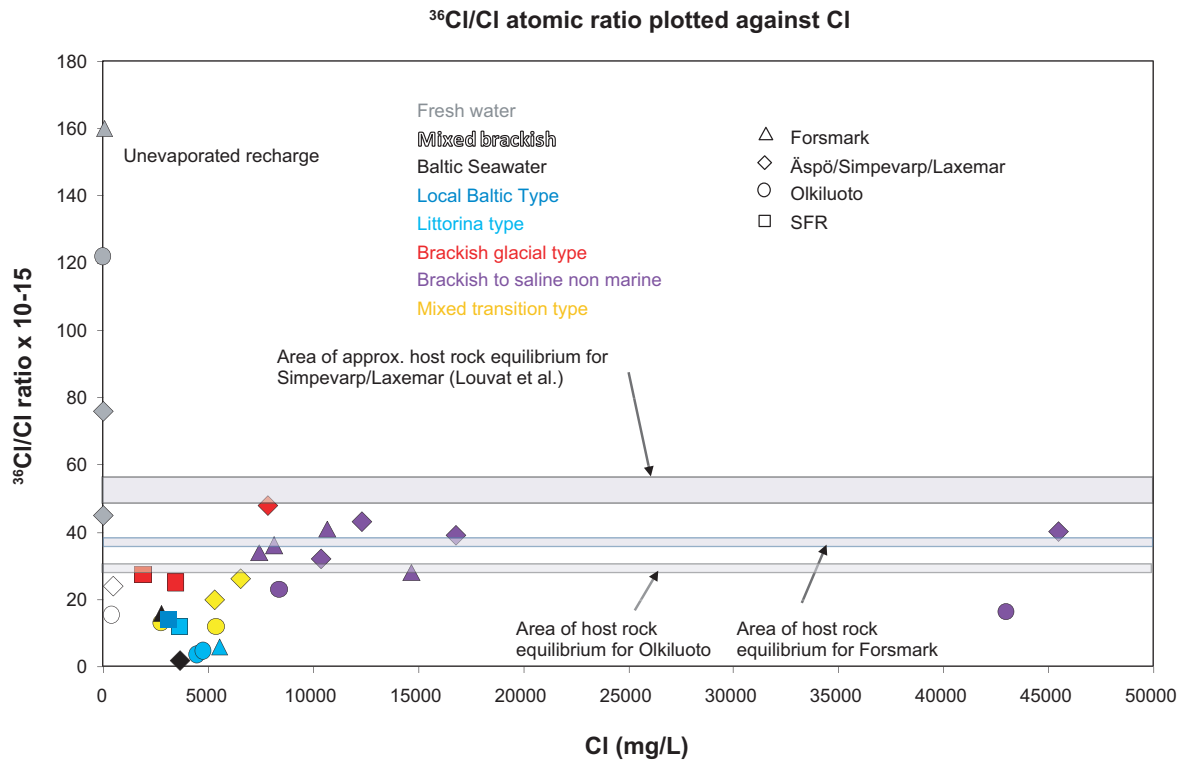
Figure 5-56. *Chloride-36 data from groundwaters at the SFR (this study), Forsmark (Smellie et al. 2008), Laxemar (Laaksoharju et al. 2009), Äspö/Laxemar/Simpevarp (Louvat et al. 1999) and Olkiluoto (Gascoyne 2001) compared to secular equilibrium $^{36}Cl/Cl$ ratios of in situ production in the host rocks (shaded broad horizontal lines).*

geochemical signatures) is that the major saline component in all three groundwaters is non-marine which is in line with the long residence times and equilibira values recorded for all the brackish non-marine to saline groundwater samples (cf. Figure 5-56). For the SFR samples the picture is less clear, but integrating the available information from the other isotopic systems studied, the indication is that these waters are approaching equilibria with the host rock rather than showing an input of young water components (e.g. these Brackish-glacial type groundwaters are very low in ^{14}C and have tritium contents below detection limit).

5.10.4 Conclusions on residence times

Based on the available information from radiometric isotope analyses (tritium, ^{14}C and ^{36}Cl), more quantitative information from $\delta^{18}O$, and the general understanding of the site, the following conclusions can be drawn:

- The oldest groundwater in the SFR area contains significant portions of glacial meltwater identified by depleted $\delta^{18}O$. A possible scenario is that glacial meltwater (most probably from the last deglaciation) has been injected into the fracture zones and further into smaller fractures by large hydraulic heads during the melting of the continental ice sheet. This dilute glacial meltwater subsequently mixed with existing Brackish non-marine type groundwater probably of very old age (i.e. approaching ^{36}Cl equilibria with the host rock) already present in the fracture system.

- In the larger fracture zones, and especially at shallow depth, the groundwater was probably very dilute following deglaciation and during the following period of fresh water accumulation on the sediment/bedrock surface (the Ancylus Lake, cf. Figure 3-1). When the Littorina Sea transgressed (starting some 9,500 years ago with a salinity maximum occurring between 4,500 to 3,000 BC) it intruded into the bedrock driven by density differences mixed with the dilute water depleted in $\delta^{18}O$ present in the fractures after the deglaciation. It is clear that the Littorina water has not penetrated the less transmissive fractured bedrock between the more highly transmissive fracture zones to the same extent as the glacial meltwater.

- The last water type to intrude is the present Baltic Sea. Based on its tritium content, which is similar in many of the SFR sampling sections, this intrusion is relatively late and has been accelerated by the drawdown caused by the SFR facility (cf. Section 6.2).

- The fact that all samples from the SFR model volume contain groundwaters with bicarbonate contents higher than 30 mg/L, and that all carbon isotope analyses show the presence of radio-carbon (5 to 65 pmC), indicate that the major input to the carbon system has occurred after the last deglaciation.

5.11 Late hydrochemical data from borehole KFR104

During the investigation stage, no hydrogeochemical investigations were planned or conducted in borehole KFR104. However, the borehole is located in the Central Block (cf. Figure 1-3) and the modelling and interpretation work revealed modelling difficulties due to shortage of data from this actual target area for the extension of the SFR. Therefore, a sample series of three groundwater samples were collected in section 333.0–454.6 m borehole length (–306.5 m elevation) in June 2011 just before completion of the review version of this report. A separate discussion about these very late data is therefore presented here. The sampled section is very long which may possibly influence the chemistry of the sample. Figures 5-1 (EC) and 5-12 (groundwater types) in 3D include also borehole KFR104. Quality assessment and discussions concerning sampling conditions in this borehole section are presented in Appendix 1, and the sampling details and data are documented in Appendix 2.

KFR104 data are compared to the rest of the SFR dataset in Figures 5-57 a–d and 5-58 a–d where Cl, Mg, HCO_3 and $\delta^{18}O$ are plotted against elevation and Mg, HCO_3 SO_4 and $\delta^{18}O$ are plotted against chloride, respectively. Figure 5-12 presents the water type distribution in 3D and includes also this borehole. From the low magnesium and $\delta^{18}O$ values, it is obvious that this groundwater belongs to the Brackish-glacial groundwater type.

The sampled borehole section is located in a depth range with few other data, 5-57 a–d. However, the groundwater composition shows a close resemblance to that of the previously sampled borehole KFR101 at –240 m elevation, cf. 5-58 a–d. This indicates that the very dilute groundwater of the Brackish-glacial type may be more common than previously expected.

The groundwater of KFR104 at –306.5 m elevation has a somewhat higher chloride and sulphate concentration than borehole KFR101 but the magnesium and bicarbonate concentrations are the lowest in the SFR dataset. Furthermore, the sampled borehole section in KFR104 is twice as long (122 m) as the one in KFR101 and contains three flow anomalies at some distance from each other and these may yield waters of somewhat different compositions, cf. Appendix 1. In contrast, the dominating flow anomalies in borehole KFR101 are concentrated in a very narrow depth range. The drilling water contents in the KFR104 case (recording 0.4%, 4% and 4% respectively) with the Baltic Seawater as drilling water source, cannot explain the small differences in composition during the time series. Instead variable contributions from the three different flow anomalies in the long borehole section may be a more probable explaination, for example, to account for the differences in chloride and sulphate. A comparison of the groundwater composition in the bottom section of KFR104 (Figure 5-58) with other groundwater data from the Central Block (Figure 5-19) shows that the indicator parameters in the KFR104 case plot quite far from the other Central Block data. Furthermore, there is no obvious resemblance with the data from the bottom section of borehole KFR105 which also intersects deformation zone ZFMWNW3267, although this occurs about 150 m above the bottom section of KFR104. Furthermore, similar groundwater from the bottom of KFR101 intersecting the Northern boundary belt diverges even more from the other Northern boundary belt groundwaters (the second deepest is KFR7A some 100 m higher up).

The few investigated borehole sections at depths below –230 m elevation are listed in Table 5-17 and two out of five borehole sections show the dilute Brackish-glacial groundwater type. It is possible that the water composition observed in KFR101 and KFR104 is common at this depth range in fractures lacking contact with the upper part of the bedrock.
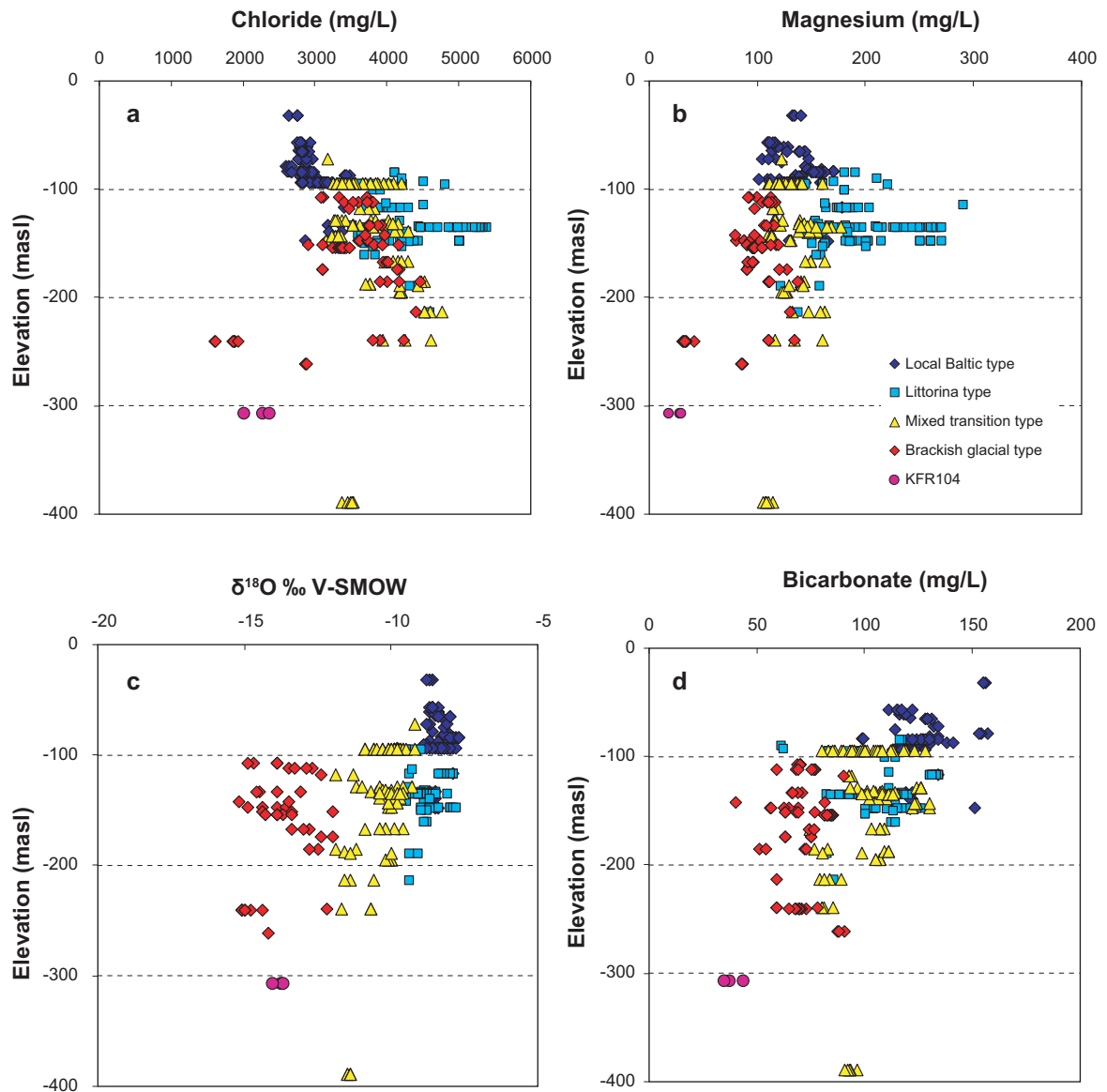
Figure 5-57 a–d. *Groundwater data from borehole KFR104 (cerise) compared to other groundwater data from the SFR site (1986–2010). The plots show the distribution of chloride, magnesium, $\delta^{18}O$ and bicarbonate with depth related to the different groundwater types defined for the SFR Site in Section 3-3.*

In conclusion, the most recent sample from KFR 104 underlines the presence of a non-marine Brackish-glacial groundwater type at intermediate depth in the area of focus for the SFR extension. The most likely explanation for the existence of groundwater with a salinity significantly lower, not only that of the Littorina Seawater but also the present Baltic Seawater, is that this water intruded the bedrock (most probably during the last glaciation/deglaciation) during increased hydraulic head pressure conditions quite different from those prevailing today.

Table 5-17. Sampled borehole sections below –230 m elevation and observed groundwater type.

| Borehole section	Elevation (m)	Water type	Comment
KFR02, 137.0–170 m	–239.08	G → T	Close to SFR, below zone ZFM871
KFR101, 279.5–341.8 m	–240.15	G dilute	Zone 0805A
KFR106, 260.0–300.0 m	–261.03	G	ZFMNNW1034
KFR104, 333–454.6 m	–306.5	G dilute	One of three flow anomalies is located in ZFMWNW3267
KFR102A, 423.0–443.0 m	–388.97	T	Close to SFR, Zone ZFMENE3115
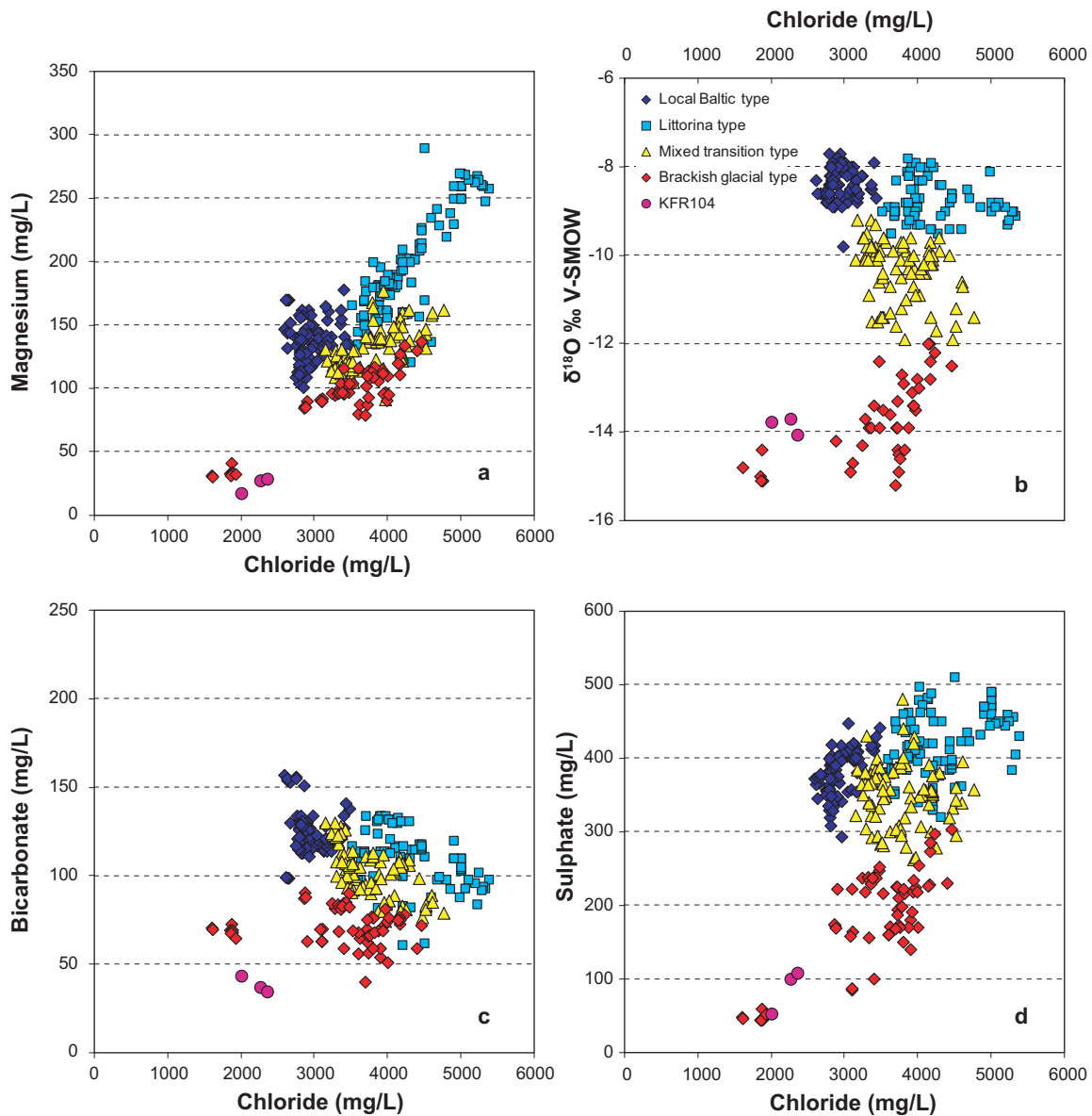
Figure 5-58 a–d. *Groundwater data from borehole KFR104 (cerise) compared to other groundwater data from the SFR site (1986–2010). Plots of magnesium, $\delta^{18}O$, bicarbonate and sulphate versus chloride concentration. The groundwater samples are colour coded according to the different groundwater types defined for the SFR Site in Section 3.3.*

6 Hydrogeochemical site description

6.1 Introduction

The main aim of the hydrogeochemical site descriptive model is to present an understanding of the site based on the measurements, interpretations and model contributions described in the previous chapters. The main objective is to describe the chemistry and distribution of the groundwater, the hydrogeochemical processes involved in its origin and evolution, and to incorporate the use of available geological and hydrogeological site descriptive models. This chapter outlines the visualisation of the SFR hydrogeochemical site descriptive model according to present understanding. The SFR site/target volume with the major deformation zones, the location of the SFR extension boreholes and cross sections A and B relating to the 2D and 3D visualisations, are shown in Figure 6-1.

Visualisation of the SFR major deformation zones, the position of the sampled boreholes and a graphic representation of the major hydrogeological structures, sampling locations and their chemistry, is presented in both 3D and 2D in Figures 6-2 to 6-5.

6.2 Hydrogeochemical visualisation

As described in Chapter 2 (cf. Figures 2-5 to 2-8 and 2-9), Section 5.2 and in other parts of the report, the SFR site/target area is delimited by the Northern and Southern boundary belts, i.e. two major vertical to steeply dipping deformation zones, ZFMWNW0001 (Singö) to the southwest and ZFMNW0805A and B (formerly Zone 8a and b) to the northwest, respectively. Together with the other steeply dipping zones, i.e. ZFMNE0870A and B (formerly Zone 9a and b), ZFMNNW1209 (formerly Zone 6) and ZFMNNE0869 (formerly Zone 3) inside the target area (i.e. the Central Block), they have served as important groundwater flow pathways over long periods of geological time.
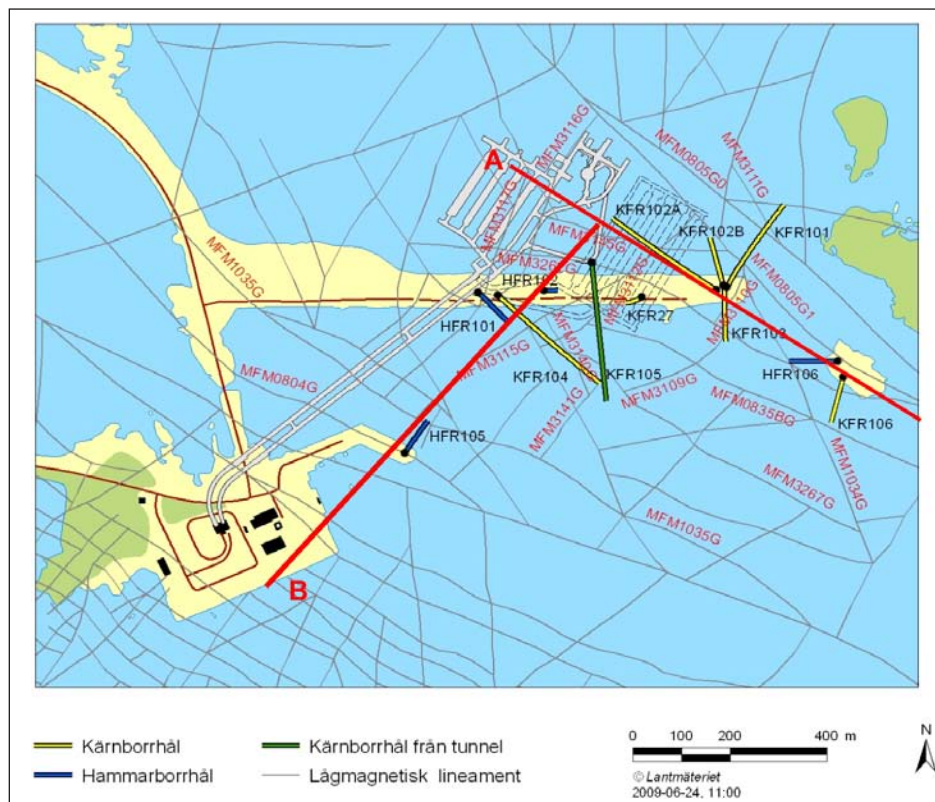
Figure 6-1. The SFR site/target area showing cross sections A and B in relation to the SFR waste storage facility and the series of drilled boreholes representing the SFR extension project. The 3D section chosen is approximately parallel to section A viewed to the northwest.

Some of these vertical zones (e.g. ZFMNNE0869, ZFMNW0805A,B and ZFMNE0870), may have hydraulic contact with the gently dipping deformation zone ZFM871 (formerly Zone H2) which is located just beneath the silo at the SFR and covers most of the local model area.

Prior to the last deglaciation, the groundwaters at the SFR are considered to have comprised non-marine types changing from brackish to saline with increasing depth; mixed in components of an old meteoric water (and maybe also old glacial meltwaters) are also thought to have been present at shallow and intermediate depths. During the last deglaciation (cf. Section 3.2.3), dilute glacial meltwaters under high hydraulic gradients penetrated to maximum depths investigated at the SFR (~ –400 m.a.s.l.) and probably to still greater depths in common with observations at Forsmark (Laaksoharju et al. 2008). These waters mixed with the resident non-marine brackish to saline and old meteoric groundwaters resulting in a range of brackish-glacial mixtures. Subsequently during the Holocene, the Littorina Sea transgression resulted in the density driven infiltration of saline waters into the bedrock along many of the same transmissive flow paths that earlier channelled the glacial meltwaters. This produced varying degrees of mixing, whilst sometimes in less hydraulic conductive fractures or less transmissive rock mass areas between the more major deformation zones, the glacial meltwater appear to have been preserved. This is indicated sometimes by the occurrence of brackish-glacial groundwaters resident at higher levels in the bedrock than the later Littorina type groundwaters.

Prior to the construction of the SFR waste storage facility, the groundwater flow was considered regional, slow moving and discharging upwards along the important flow pathways. With the commencement of the SFR excavation and construction phases, these pathways have facilitated the dynamic drawdown of near surface waters (e.g. Baltic Sea) (cf. Section 2.3) and possibly of mixtures of Littorina and young meteoric water types. The influence of groundwater sampling and/or hydraulic testing in boreholes on groundwater mixing may have some local effects, but these can be considered unimportant compared to the large volumes of drawdown groundwaters which are circulating in the major hydraulically connected fracture systems.
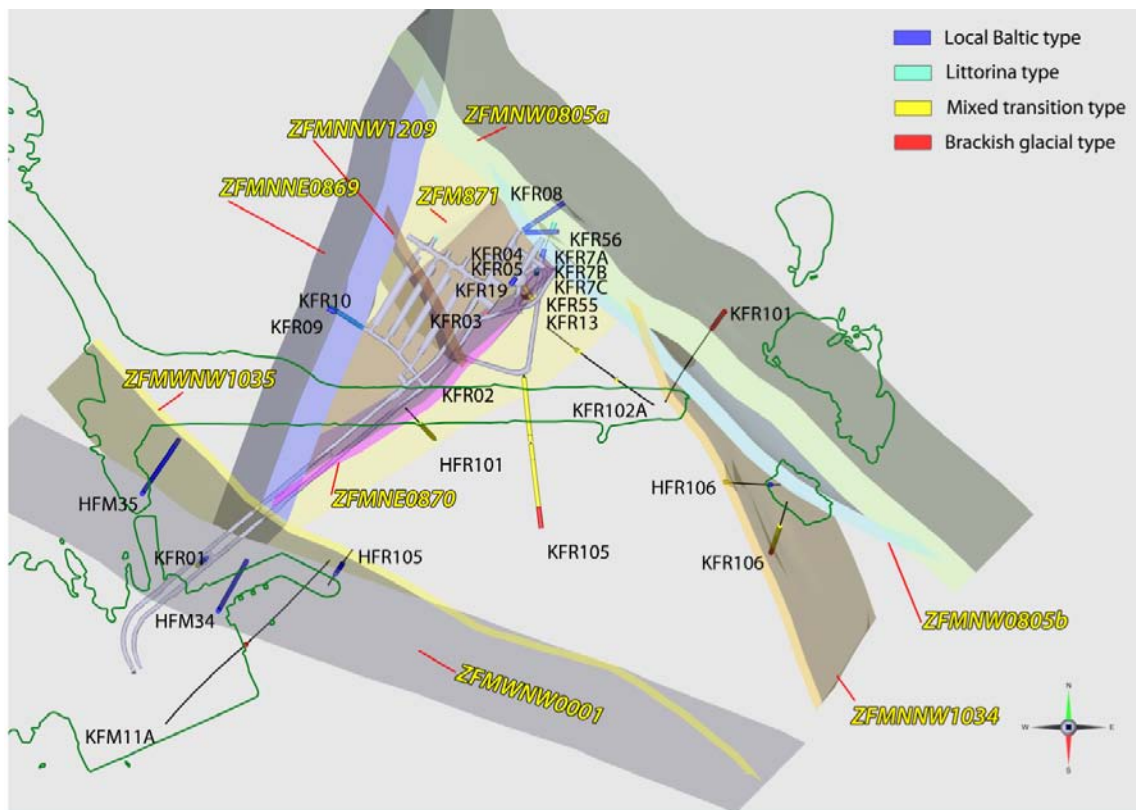
Figure 6-2. *3D presentation viewed from the top of the groundwater type distribution in relation to major zones in the regional model volume. The green outline at the surface demarcates the coastline with the pier and small islets.*
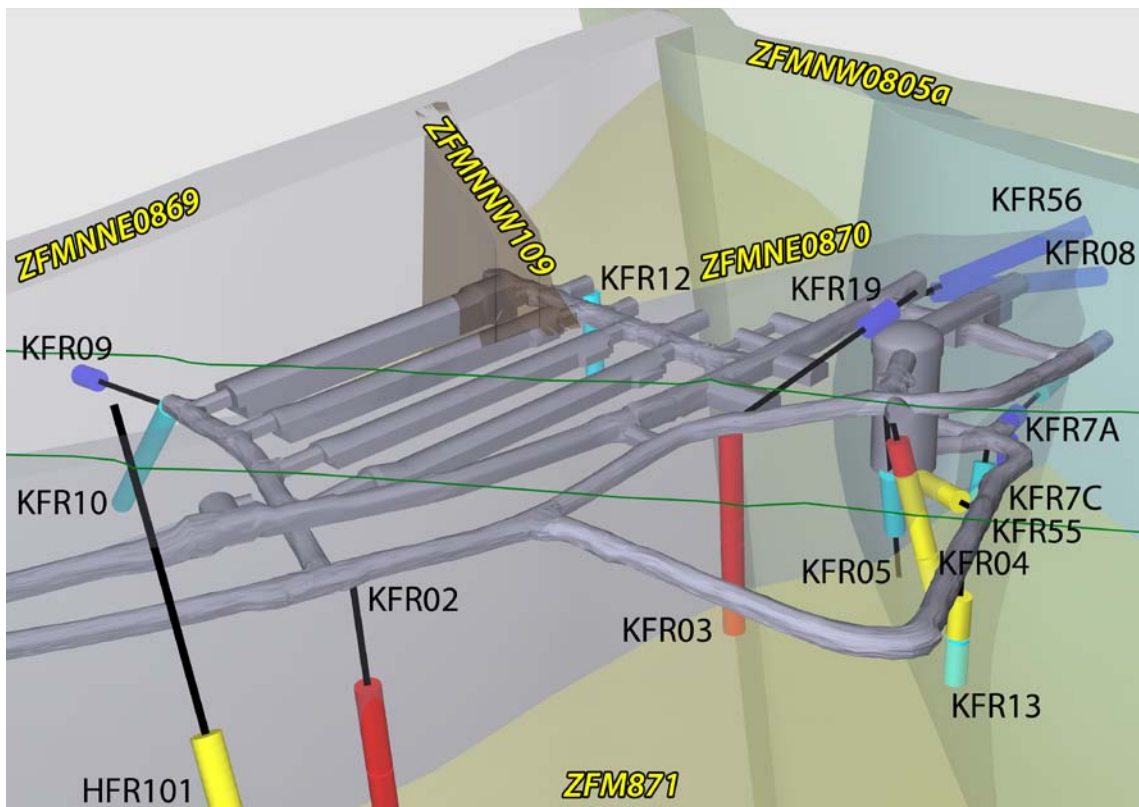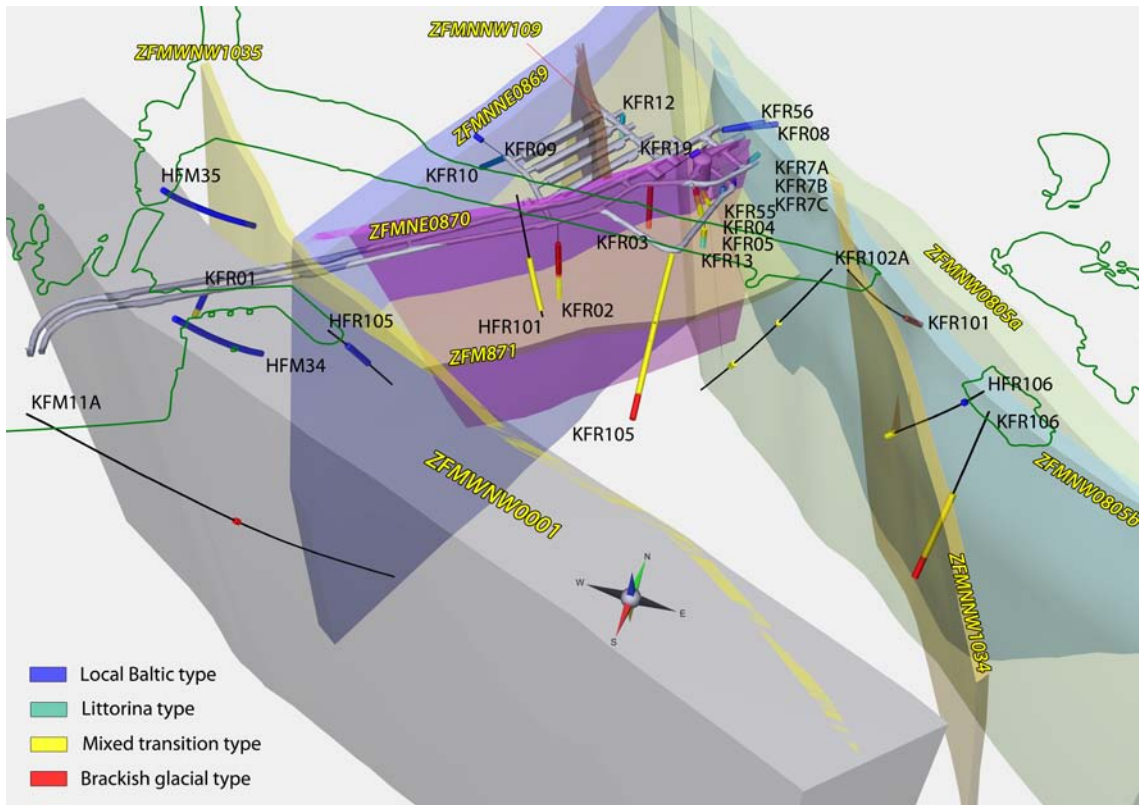
Figure 6-3. *3D presentation, viewed from southeast, of the groundwater type distribution in relation to major zones in the regional model volume. The boreholes drilled from the SFR facility are enlarged in the view at the bottom of the page. The green outline at the surface demarcates the coastline with the pier and small islets. Note the decrease in colour intensity along the boreholes when viewed through a penetrated rock/ deformation zone volume.*

The hydrogeochemical site understanding is based mainly on the exploratory analysis part of the programme outlined in Chapter 5, interfaced with relevant input data from the geological and hydro-geological site descriptive models version 1.0 (Curtis et al. 2011, Öhman et al. 2011). To visualise the groundwater chemistry, two 3D models and two 2D cross sections were selected (Figures 6-2 to 6-5) that best illustrate the SFR site/target volume (regional and local model volume) based on geology and hydrogeology. The two 2D cross sections refer to 'A' and 'B' in Figure 6-1; one 3D visualisation is viewed towards the northeast (i.e. from the southwest) approximately centred along cross section 'B' and the other gives a view from above of the same location (Figure 6-1).

The 3D section was chosen to visualise the distribution of the different groundwaters types and their relation to the important transmissive deformation zones which characterise the SFR site. Attention has been given to the distribution of the different groundwater types along each borehole which has been discussed in Section 5.3. Figures 6-2 and 6-3 therefore provide the general setting to the SFR site showing the dominance of the vertical and highly transmissive deformation zones ZFMNNE0869 (formerly Zone 3), ZFMNNW1209 (Zone 6) and ZFMW0805A, B (formerly Zone 8a and b) and their important hydraulic intersections with the subhorizontal zone ZFM871 (formerly Zone H2); zone ZFMNE0870A, B (formerly Zone 9a and b) may also play a hydraulic role but this is not clear. There is some hydrochemical evidence that zone ZFM871 might extend further towards the southwest, possibly reflecting some discontinuous structures present which may represent irregu-lar flow paths not picked up in the geological and hydrogeological models because of heterogeneity and/or an overall lack of data. Alternatively, it may form part of the Shallow Bedrock Aquifer (SBA) which is discussed in Section 2.2.3.

The two vertical 2D sections (A and B in Figures 6-4 and 6-5) provide simplified visualisa-tions of the SFR volume area where the actual intersections of the structural zones are indicated and the boreholes when not aligned along the section are extrapolated onto the same 2D plane.

Figure 6-4. *Vertical cross section A (cf. Figure 6-1) showing a simplified visualisation of the SFR volume area viewed to the northwest. Groundwater types are colour coded and the upper bedrock division (light beige colour) represents bedrock characterised by a high frequency of interconnected highly water conduct-ing fractures (Shallow Bedrock Aquifer) suggesting near to steady state and transient conditions between the rock matrix pore water and the fracture groundwaters. The bedrock at intermediate depths (dark beige colour) is characterised by a much lower fracture frequency of water conducting fractures suggesting transient conditions between the rock matrix pore water and the fracture groundwaters, i.e. generally greater distances to the nearest water conducting fractures and also a reduction in transmissivity along these fractures. For key to groundwater colour coding see Figure 6-3.*
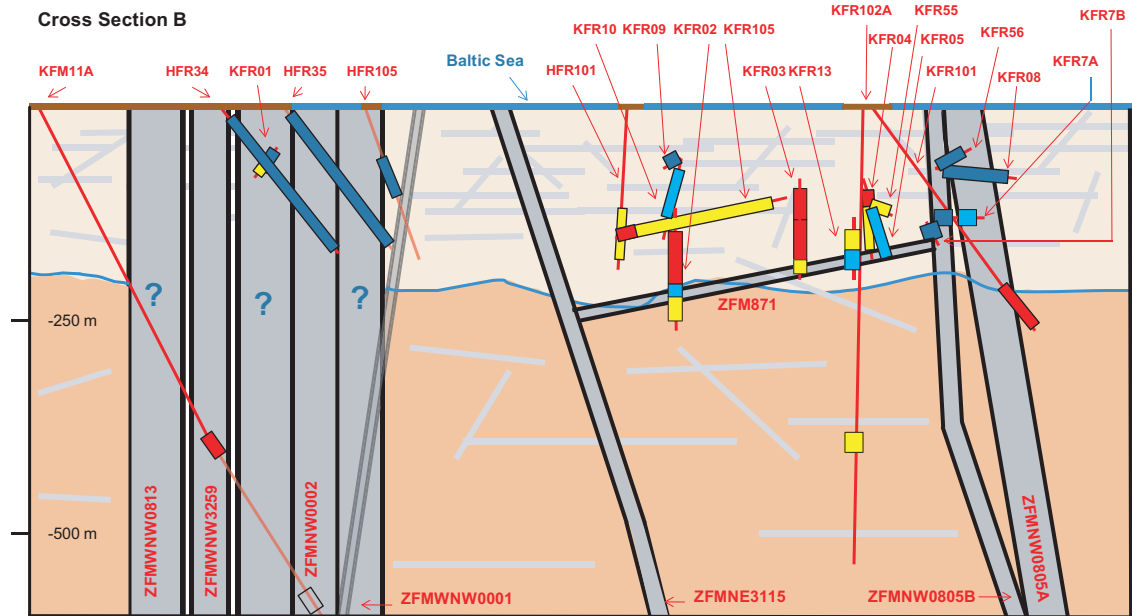
Figure 6-5. Vertical cross section B (cf. Figure 6-1) showing a simplified visualisation of the SFR volume area viewed to the northeast. Groundwater types are colour coded and the upper bedrock division (light beige colour) represents bedrock characterised by a high frequency of interconnected highly water conducting fractures (Shallow Bedrock Aquifer) suggesting near to steady state and transient conditions between the rock matrix pore water and the 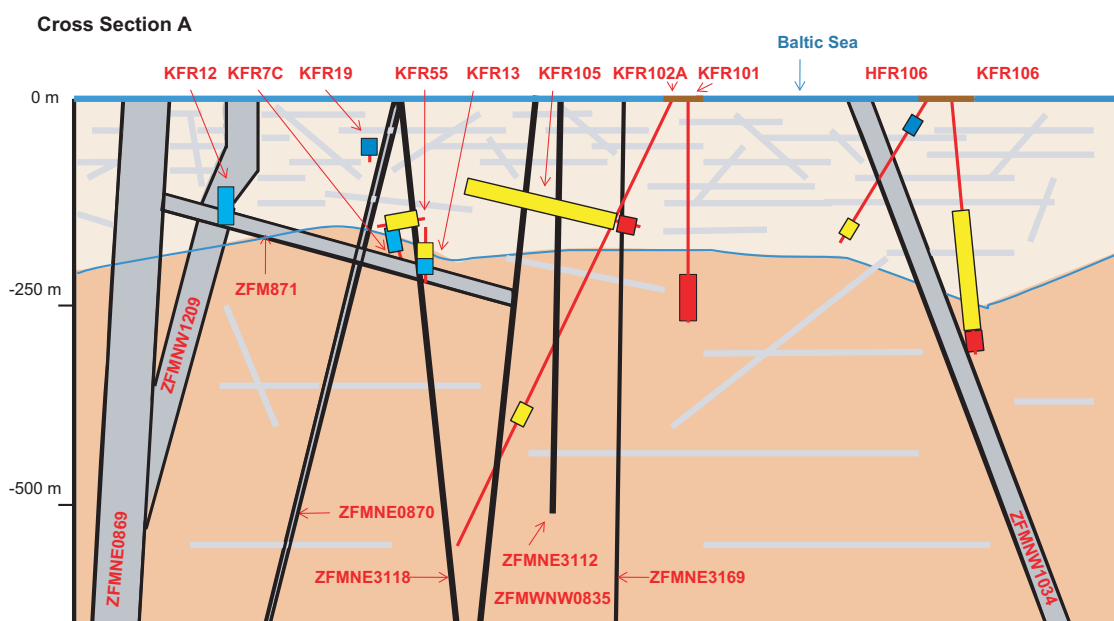fracture groundwaters. The bedrock at intermediate depths (dark beige colour) is characterised by a much lower fracture frequency of water conducting fractures suggesting transient conditions between the rock matrix pore water and the fracture groundwaters, i.e. generally greater distances to the nearest water conducting fractures and also a reduction in transmissivity along these fractures. The question marks indicate the uncertainty as to how these major deformation zones comprising the Southern boundary belt will influence the relationship between the fracture groundwater and the pore waters. Note: Samples from KFR02 taken in 2006 show a Littorina composition within Zone ZFM871; this subsequently changed to a Transition type groundwater similar to that shown below Zone ZFM871. For key to groundwater colour coding see Figure 6-3.

Schematically shown is the division at about –200 m.a.s.l. between the shallow bedrock aquifer (light beige colour) with a high frequency of interconnected transmissive fractures, and the underlying bedrock (darker beige colour) characterised by a decrease of interconnected fracture frequency with depth and therefore of lower transmissivity. As commented on above, the hydrostructural properties of the SFR site have determined the distribution and degree of mixing of the different groundwater types, most of which have been introduced since the last deglaciation. These groundwaters (Local Baltic Sea, Littorina type with a glacial component, Brackish-glacial type, Mixed brackish water (transition type)) residing at shallow to intermediate depths (maximum elevation depth studied about –400 m.a.s.l.) are indicated in Figures 6-2 to 6-5.

As addressed briefly in Section 3.2, when the most recent continental ice melted and retreated (i.e. deglaciation stage approximately 18,000 BC to 8000 BC), glacial meltwater was hydraulically injected under considerable head pressure into the bedrock close to the ice margin. The exact penetration depth is still unknown, but will depend on the hydraulic properties of the bedrock. Because of the shallow depth of the investigated SFR site, penetration of glacial meltwater has been widespread, certainly down to zone ZFM871 (formerly Zone H2) facilitated by the intersecting vertical to steeply dipping transmissive deformation zones described above. These glacial meltwaters underwent mixing with the older, preexisting groundwaters comprising old meteoric waters and deeper non-marine brackish to saline types (depending on depth) to form a range of brackish-glacial groundwater types (Figures 6-2 to 6-5; boreholes KFM11A, KFR03, KFR04 KFR101, KFR105 and KFR106). During the subsequent Littorina Sea transgression, density driven marine waters preferentially followed the same major transmissive pathways to zone ZFM871 and potentially beyond, and permeated the earlier resident old

meteoric and non-marine brackish-glacial groundwaters. This led to the Littorina Seawater under-going degrees of dilution and also forming a range of mixed groundwater types with the Brackish-glacial types (e.g. 'Littorina type water with a glacial component', cf. Section 3.3.1). The strongest Littorina signatures seem to have been preserved in the steeply dipping zones of ZFMNNE0869 (for-merly Zone 3) and ZFMW0805A, B (formerly Zone 8a and b), and within or close to zone ZFM871 (formerly Zone H2). The importance of this hydraulic connection with subhorizontal zone ZFM871 can be seen in all three visualisations, namely, where the main concentration of the Littorina type groundwaters with a variable glacial component are present (Figures 6-2 to 6-5; boreholes KFR05, KFR7A, KFR7C, KFR09, KFR10, KFR12, KFR13).

From the Littorina Sea transgression to present Baltic Sea conditions the SFR area has been continuously submerged and the groundwater flow has been considered regional, slow moving with discharge upwards along the important flow pathways (cf. Section 2.3.3). If anything, this may tend to create a weak upconing of deeper non-marine brackish to saline groundwater, which might have contributed to some further mixing at intermediate depths, In general, however, little change has probably occurred until the investigation, excavation and construction phases of the SFR facility commenced in 1985. Since then, Baltic Seawaters have been infiltrating the SFR site area into the bedrock and mixing with near surface Littorina type groundwaters, and possibly also brackish-glacial type groundwaters, along the more hydraulically conducting pathways (cf. Section 5.2). This is clearly seen in Figure 6-5 where recent 'Local Baltic Sea' (cf. Section 3.3.1) infiltration is associated with the large scale transmissive deformation zones ZFMWNNW0001 (Singö zone) and ZFMNW0805A and B (formerly Zone 8). The total distribution of these Baltic type groundwaters are indicated in Figures 6-2 to 6-5 (boreholes HFR34, HFR35, HFR105, HFR106, KFR01, KFR7A, KFR07B, KFR08, KFR09, KFR19 and KFR56). Of these boreholes, KFR09 and KFR7B have initially been Littorina in type and subsequently changed to Baltic type since investigations have commenced; borehole KFR07A records both types and probably represents a transient stage from Littorina to Baltic types.

Variable mixing of these three major groundwater types under both natural and anthropogenic conditions corresponds to the 'Mixed brackish water (transition type)' (cf. Section 3.3.1). These groundwater types are often located where there is a more dynamic groundwater circulation conducive to mixing processes. It has also been suggested that input of Littorina-young meteoric mixtures may have been introduced from inland sources to the southwest (Forsmark) via the interconnected shallow bedrock aquifer (SBA) structures (cf. Section 5.3). That some of the mixing processes can be linked also to other activities such as hydraulic testing and groundwater sampling campaigns cannot be excluded, but these are considered to be relatively minor compared to the large scale drawdown effects. Nevertheless, combined, the extent of this mixing is difficult to quantify and has involved a major effort in the present SFR study (cf. Sections 3.3 and 4.3). Boreholes associated with mixed brackish transition type groundwaters are HFR101, KFR01, KFR02, KFR04, KFR7A, KFR7C, KFR10, KFR13, KFR55, KFR102A, KFR105, KFR106 (Figures 6-2 to 6-5). Of these, KFR01 shows a change from Baltic to transition, KFR04 a change from glacial to transition, and KFR13 records both Littorina and transition type groundwaters and probably represents a transient stage from Littorina to a transition type.

6.3   Possible pore water trends at the SFR

Pore water studies have been carried out at Forsmark during the site characterisation programme and are documented in (Laaksoharju et al. 2008, Waber et al. 2009); no pore water data exist for the SFR site, and none is planned. The relative homogeneity of the geology and hydrogeology at Forsmark has enabled a degree of extrapolation of the pore water chemistry across the Forsmark site. This generally shows close to steady state conditions in the upper approximately 150 m where there is an increased frequency of interconnected water conducting fractures and a dynamic groundwater circulation dominated by fresh meteoric groundwater (i.e. the shallow bedrock aquifer). At this depth, the density of the fracture network coupled to an active groundwater circulation has enabled the fracture water to achieve rapid near to steady state conditions between the pore water and the fracture groundwaters, i.e. within the last approximately 2,000 years since the Forsmark site emerged from the sea accompanied by the establishment of hydraulic gradients. Steady state or close to steady

state conditions are also indicated from depths greater than approximately 700 m depth where; a) there are much fewer water conducting fractures, b) the groundwater circulation is low to almost stagnant, c) the groundwaters show a transition from 'Brackish Marine' (~8,000 mg/L Cl) to 'Saline' (10,000–20,000 mg/L Cl) in composition, and d) the groundwater ages are extremely old (at least hundreds of thousands of years).

In contrast, from about 200–700 m depth transient conditions dominate, reflecting changes in groundwater compositions related to recent climatic events especially the last deglaciation and subsequent Holocene period, but also some predating events of unknown age. During this interval there has been inadequate time for fracture groundwaters and pore waters to achieve steady state conditions. This reflects a lower frequency of interconnected water conducting fracture networks and therefore a less dynamic groundwater circulation compared to the upper approximately 150 m. In addition, the relatively short time intervals between recent climatic changes resulting in periodic penetration of water types of different composition, have also been an important factor in preventing large scale near steady state conditions being established.

It is possible that these general trends at Forsmark can be further extrapolated to apply to the SFR site although there are geological and hydraulic differences, not least being separated by the major regional Singö deformation zone. The location of the SFR site to the northeast of the northwestern part of the Forsmark candidate area shows a change in geology from a largely medium-grained granite/granodiorite sequence within the Forsmark candidate site, to a granite-metamorphic-aplite and finally a felsic to intermediate volcanic rock metamorphic sequence which hosts the large, regional Singö deformation zone. Further to the northeast of the Singö zone, this last named rock type continues to the SFR site which itself is comprised mainly of pegmatite/pegmatitic granite. Along this sequence, pore water data are only available from the northeast orientated borehole KFM08C which terminates close to the edge of the demarcated Forsmark candidate site

Despite the difference in geology, the upper approximately 200 m at the SFR show similar hydrostructural properties to that at Forsmark, i.e. the shallow bedrock aquifer. The bedrock at the SFR has been divided therefore at about –200 m.a.s.l. into the shallow bedrock aquifer (light beige colour) with a high frequency of interconnected water conducting fractures, and the underlying bedrock (darker beige colour) characterised by a decrease in the frequency of interconnected water conducting fractures with depth and therefore characterised by an overall lower transmissivity (Figures 6-4 and 6-5). This subdivision can be used to speculate on the nature of the rock matrix pore water distribution based on the data from the Forsmark investigations discussed above.

The shallow bedrock (i.e. the shallow bedrock aquifer) probably indicates both near to steady state conditions and also transient conditions established between the rock matrix pore waters and the fracture palaeowaters groundwaters depending on the distances to the nearest water conducting fractures and the fracture transmissivity which is high. Short diffusion distances will achieve steady state more rapidly compared to greater distances, and the heterogeneity of the fractured upper bedrock will result in a range of distances and therefore a variation of steady state and transient conditions. At intermediate depths, i.e. including the deeper –200 to –400 m.a.s.l. part of the SFR target area, transient conditions are expected to dominate because of the generally greater distances to the nearest water conducting fractures and also the reduction in transmissivity along these fractures. At still greater depths (400–700 m) it is expected that near to steady state conditions will gradually dominate with increasing depth, similar to that described for the Forsmark site.

7 Evaluation of uncertainties

7.1 Measured and modelled uncertainties in field data and interpretation methods

7.1.1 Sources of uncertainties

Each phase of the hydrogeochemical investigation programme performed within the SFR extension project introduces uncertainties that have to be accounted for and fully addressed and documented in order to provide confidence in the site descriptive model and subsequent repository safety analyses.

The case with an existing repository in operation within/close to the investigated site introduces conditions not previously encountered in SKB site investigations, for example, significant changes in groundwater flow and associated mixing of different groundwater types. Nevertheless, these conditions also provide some advantages, for example, the possibility to follow groundwater development during the last twenty years and actually know to what extent there have been changes in groundwater composition during that time period. This can be of importance for future predictions of open and more dynamic hydraulic conditions associated with repository construction for the disposal of low and intermediate level radioactive waste. However, to describe such a dynamic groundwater system also implies an additional degree of difficulty and uncertainty to the interpretation work.

Data uncertainty

The fact that undisturbed groundwater samples from boreholes do not exist is even more relevant in the SFR case where most of the studied groundwaters originate from the upper approximately 250 m of bedrock. Several different conditions therefore can impact directly on the integrity of the sampled groundwaters, the most important of which result from drawdown effects and altered flow pathways in the vicinity of the tunnel system; these latter factors comprise part of the model to be developed. Furthermore, data uncertainties have increased with time due to the use of data collected over the last twenty years. These have been archived using different methods and levels of documentation and most probably reflect different quality standards of sampling performance and analyses.

Analytical uncertainties are addressed in Nilsson A-C (2009) and Nilsson et al. (2010a) where uncertainties as reported for the different methods and components are given. The different possible impacts on sampling and sampling conditions are identified and discussed in Section 1.5.2. Appendix 1 includes quality assessment of the samples in the SFR dataset for model version 1.0. The approach is similar to the one used in the Forsmark site investigation and accounts for impacts from sampling conditions as well as from analytical performance; however, at the SFR it had to be adapted to a 25 year long sample time series with all the associated uncertainties outlined above. Generally, rather few of the samples can be considered of the utmost/highest quality but nevertheless most of the data were judged to be of acceptable quality for interpretation purposes. Some of the samples that did not achieve the previously accepted standards used in the Forsmark site investigation were assigned as "good enough" in order to make it possible to cover the major chemical trends during the period 1986 to 2010. Samples with questionable analytical confidence for some single components are evident from some of the plots in, for example, Figures 5-2 to 5-7 where they occur as outliers. Such samples are easily recognisable and can be discarded if required, although they are too few in number to mask the general chemical trends.

- None of the samples collected from the recent boreholes showed drilling water contents exceeding 7% and generally they were around 2–3%. Other impacts from drilling are described in Section 1.5.2.

- The effects from drilling activities on groundwater samples from the early boreholes are likely to be insignificant since the boreholes were drilled more than twenty years ago and have been naturally flushed out.

- The redox effect from the drilling water (recent boreholes) on the groundwater composition is relatively small, due to the large buffer capacity of the rock.

- The errors in the potentiometrically measured Eh is estimated to $\pm$ 50 mV. However, the risk of measuring too high Eh values is large. For example, several positive Eh values measured in the SFR boreholes can be attributed to artefacts related to contamination problems during the Eh measurements (especially in the old measurement campaigns) or to failures in the sealing capacity of the old equipment in the proximity of oxic environments (i.e. the tunnels). Figure 7-1 presents an example of the long stabilisation periods towards reducing conditions that probably reflect the gradual removal of groundwater affected by the oxic environment in the tunnels.

- Most of the available pH data were measured in the laboratory which may represent a serious uncertainty in redox pair modelling and speciation-solubility calculations. Generally, the field pH measurements show higher values than the laboratory measurements and the differences can be within –0.1 to + 0.3 pH units with an average of +0.11 pH units as estimated from more recent samples where both laboratory and field measurements are available. A check of the effects of pH on interpretation and modelling were performed using the calculated pH values obtained by assuming calcite saturation, (cf. Section 5.5).

- The groundwater composition of the time series (short time period) from the different borehole sections is most often quite stable. The relative standard deviation of, for example, the measured chloride concentrations in each series of groundwater samples, generally is well within 5%.

- Individual analytical uncertainties for each chemical and isotopic constituent and their concentration values are reported by the different analytical laboratories, but are not included in the Sicada database as further interpretative use of these uncertainty values are difficult to handle due to the large volumes of analytical data involved. Uncertainties as reported for the different methods, components and concentration ranges are presented for old as well as recent analyses in Nilsson et al. (2010). Analytical errors associated with laboratory measurements are generally in the order of $\pm$ 5 to15% for major ions as exemplified in Figures 7-2 a and b showing $\delta^{18}O$ ($\pm$ 0.2‰ V-SMOW absolute value) versus chloride ($\pm$ 5%) and total sulphur ($\pm$ 12%) by ICP AES versus sulphate ($\pm$ 12%) by ion chromatography, respectively. The general measurement uncertainties for chloride, magnesium and $\delta^{18}O$ are included as error bars in the trend plots presented in Appendix 1 for the time period 1986 to 2010.

- A systematic discrepancy was observed between sulphur analysed by ICP AES and sulphate determinations by ion chromatography, cf. Figure 7-2 b. The deviation is generally within 15% and may be due to other sulphur containing species (sulphide, tiosulphates etc) being present in the groundwater and contributing to the total sulphur concentration by ICP AES.

- The M3 model uncertainty is $\pm$ 10% (in the calculated mixing proportions) within the 90% confidence interval; the model uncertainties are discussed in Gimeno et al. (2011).

- Uncertainties in geochemical models based on the PHREEQC code depend on which code version is being used. The analytical uncertainties and the uncertainties concerning the thermodynamic data bases are of importance in speciation-solubility calculations and care is required also in order to select realistic mineral phases. The uncertainty ranges associated with different saturation index calculations can be seen from the plots in Sections 5.4 and 5.5 and are discussed in detail in Gimeno et al. (2011).

7.1.2 Temporal and spatial variability

Temporal hydrogeochemical variability is largely dependent of the hydraulic conditions in the vicinity of the SFR repository as well as on the hydraulic properties of the boreholes. The variability of different components in the 20 years scale illustrates minor changes in, for example, chloride, bicarbonate, pH and tritium, respectively. This variability appears as more or less stable trends with a certain degree of predictability. Occasional local variations in the groundwater composition may appear due to heavy pumping or discharge of large volumes of groundwater from the sampled borehole or boreholes in its vicinity, as well as due to other temporary conditions that affect the groundwater mixing patterns or flow pathways. Repeated regular sampling from each sampling location may verify and assure hydrogeochemical stability or regular trends. However, all the recent SFR boreholes, except borehole KFR101, have been sampled (collection of a time series of three to four samples) at one occasion only and some uncertainty regarding their stability is justifiable.
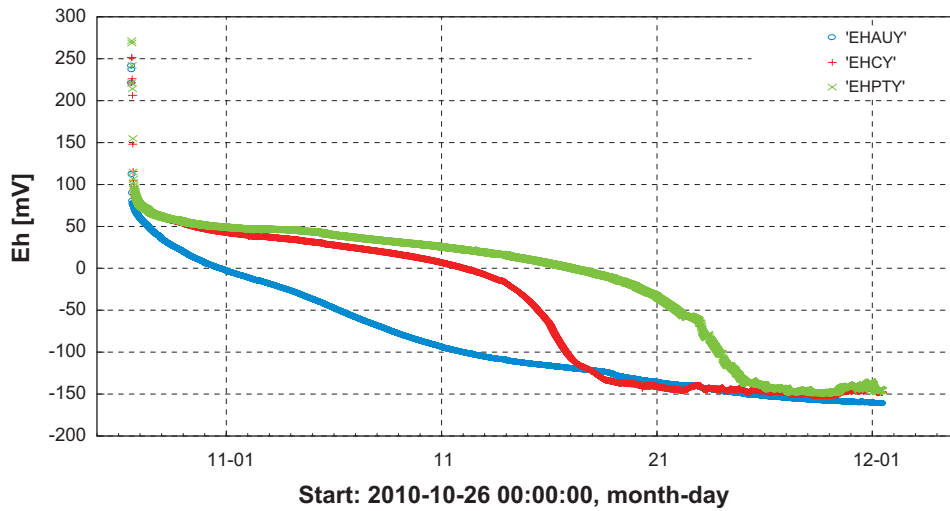
Figure 7-1. *Online redox measurement sequence from borehole KFR7A with three different redox electrodes (gold, glassy carbon and platinum). Methodology issues and problems associated with the potentiometric measurements are thoroughly described in Auqué et al. (2008).*
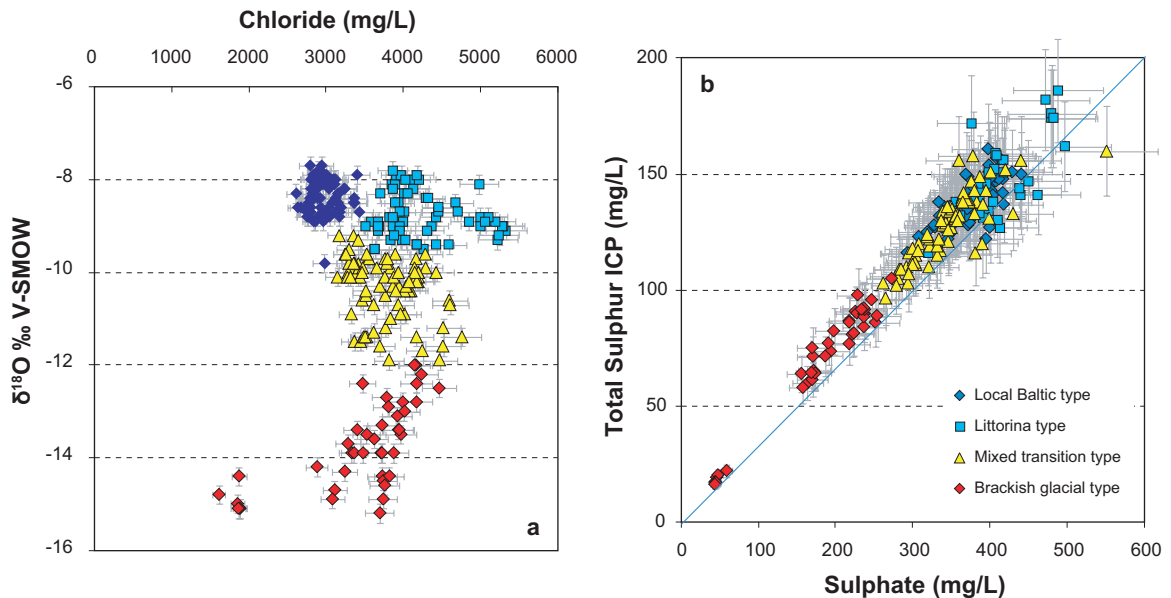
Figure 7-2 a, b. $\delta^{18}O$ *versus chloride with an analytical uncertainty of ± 0.2‰ absolute value and ± 5%, respectively (a), and total sulphur (SO₄-S) versus sulphate by ion chromatography, both having an analytical uncertainty of 12% (b). The broken line represents* $3 \times SO_4\text{-}S = SO_4$ *(mg/L).*

The most obvious cause of uncertainties in spatial variability is low and/or irregular data coverage. The SFR dataset is undoubtedly dominated by samples from closely located early boreholes in the present SFR facility while the borehole data in the area of interest for the repository extension are few. Moreover, most of the data are associated to deformation zones at or close to both the Northern and Southern boundary belts, whereupon the Central Block is less well covered. The spatial variability of the groundwater types reflects the hydrogeology of the shallow bedrock which is considered to be anisotropic with limited contact to the overlying Baltic Sea. The hydraulic conducting fracture system is dominated by subhorizontal fractures where steep deformation zones are expected to play an essential role in any vertical hydraulic connection to the sea. The zones are judged to be heterogeneous, discontinuous in character, and there is abundant evidence of isolated, compartmentalised rock volumes. The spatial variability of the groundwater types therefore would be expected to be

high and this is generally the case, and more so when the impact of the SFR construction is considered. However, the major flow pathways are fairly well established and described hydrogeologically and hydrogeochemically and therefore the uncertainties are low. In contrast, the discrete fractures characterising the lower transmissive bedrock between the major deformation zones are less well known and likewise the spatial variability of groundwater types associated with them.

7.1.3 Other model uncertainties

Other uncertainties can include conceptual uncertainties, degree of confidence in the selected model, and bias in predictions etc.

The mixing calculations (M3 computer software) have proved to be especially complicated at the SFR due to the limited chloride concentration range, the presence of two marine end members (Baltic and Littorina Seawater), and one or more non marine, dilute end member (s) of unknown/ uncertain composition. The extensive testing of end members to be included in the M3 calculation as well as their compositions (based on the Monte Carlo method (Gimeno et al. 2008)), and the specific problems encountered in the SFR extension case, as well as general modelling uncertainties, are described in detail in Gimeno et al. (2011).

The hydrogeochemical site visualisation (cf. Chapter 6) is based on a systematic, step-wise approach to determine depth trends and hydrochemical groupings of the groundwaters as detailed throughout Chapter 3. Understanding of the system therefore reflects the interpretation of hydrochemical data which has undergone a rigorous quality check and categorisation; in other words a good degree of confidence. Coupled with the results of quality assured hydrogeological measurements and modelling, which in turn is based on geological models of high standard, the input properties to the hydrogeochemical visualisation should represent the best quality available at this moment of time. Uncertainties undoubtedly still remain, perhaps stemming from inadequacies (i.e. insufficient data in places) in the geological model which may impact on the hydrogeological interpretation and possibly therefore on the integrity of the hydrogeochemical model and visualisation.

7.2 General confidence level

The following aspects of the hydrogeochemical model are associated with the highest confidence:

- The major outlines regarding development and flow pathways of the defined groundwater types before and after the construction of the SFR repository.

- The origin of the most recent end members (Baltic and Littorina Seawater, glacial meltwater) and the major processes (qualitative control concerning Eh and pH buffer capacity and major reactions) affecting the present groundwater composition at the sampled locations.

- Predictability concerning expected groundwater composition in the sense that no extreme groundwater compositions, other than those already encountered, are likely to occur at the depth ranges considered. However, to predict the groundwater type in different sections of a new borehole in the area may prove difficult due to the experienced heterogeneity. For example, the very dilute brackish-glacial groundwater encountered at the bottom of borehole KFR101 in zone ZFMNNW0805A could not have been predicted beforehand.

- The conceptual models are based on close integration between all three disciplines (geology, hydrogeology and hydrogeochemistry).

The following aspects of the hydrogeochemical model are associated with the lowest confidence:

- The natural hydrogeochemical conditions prior to the construction of the SFR facility are not known since there are no groundwater chemistry data from the first drilling stage prior to the commencement of the excavation phase. For example, it is uncertain if the introduction of the Baltic type groundwater into the bedrock is altogether a consequence of the drawdown around the SFR or if this groundwater type could have been already naturally present at some shallow locations. Furthermore, the occurrence of the mixed transition type groundwater seems to have increased due to the SFR but to what extent is unknown.

- Certain groundwater aspects (pore water, microbes, gas) are treated briefly due to lack of data or very few data from the actual SFR site. The descriptions in these cases are very much based on data and experience from the Forsmark site investigations which lower the confidence.

- The groundwater type distribution in the southwestern part of the Central Block and also outside the deformation zones in the target area is largely unknown due to the locations of the boreholes. Most boreholes in this area are associated with the zones in the Northern and Southern boundary belts. For this reason, groundwater sampling in borehole KFR104, which has not been investigated previously, was performed late in the reporting stage.

- In common with the hydrogeological model, uncertainties exist at the detailed level regarding flowpaths at connections between major vertical zones ZFMNW0805A,B and ZFMNNE0869 and the gently dipping zone ZFM871 (formerly Zone H2). For example, the presence of Littorina type groundwater at these junctions and its absence in the new boreholes in the target area is not fully understood. Moreover, whether mixtures of Littorina and recent meteoric waters from inland contribute to the groundwater within as well as to the east of the Southern boundary belt, is not yet clear from a hydrogeological viewpoint, and in addition it has not been possible to verify from the groundwater chemistry of samples collected in the relevant boreholes.

- Most hydrogeochemical data originate from the well defined major deformation zones compared to the more discrete fractures located between these zones which potentially contain components of much older groundwaters and/or better preserved deglaciation and Holocene waters.

8   Summary and conclusions

8.1   Hydrogeological and palaeohydrogeological implications

The SFR site/target area, occupying the area northwest of Forsmark, is delimited by the vertical to subvertical deformation zones comprising the Northern and Southern boundary belts (cf. Figure 2-5). Together with the other steeply dipping zones within and north of the target area (i.e. the Central Block), they have served as important groundwater flow pathways over long periods of geological time. Some of these steeply dipping zones intersect the gently dipping deformation zone ZFM871 (formerly Zone H2) which is located just beneath the silo at the SFR.

In common with other SKB studied sites and especially that at Forsmark, the palaeohydro-chemistry at the SFR shows the introduction and mixing of different water types of varying salinity mainly dating back to last deglaciation and Holocene times. Prior to the last deglaciation, the groundwaters at the SFR are considered to have comprised non-marine types changing from brackish to saline with increasing depth; mixed in components of an old meteoric water (and maybe also old glacial meltwaters) are also thought to have been present at shallow and intermediate depths. During the last deglaciation (about 13,000 to 8,800 BC) dilute glacial meltwaters under high hydraulic gradients penetrated to maximum depths investigated at the SFR (~ –400 m.a.s.l.) and probably to still greater depths in common with observations at Forsmark. These waters mixed with the resident non-marine brackish to saline and old meteoric groundwaters resulting in a range of brackish-glacial mixtures. Subsequently during the Holocene, dilute meltwaters formed the Ancylus Lake (8,800–7,500 BC) and this was followed by the Littorina Sea transgression (about 7,500 BC to the present) resulting in the density driven infiltration of saline waters into the bedrock along many of the same transmissive flow paths that earlier channelled the glacial meltwaters. This produced varying degrees of mixing, whilst sometimes in less hydraulic conductive fractures or less transmissive rock mass areas between the more major deformation zones, the glacial meltwaters appear to have been preserved. This is indicated sometimes by the occurrence of brackish-glacial groundwaters resident at higher levels in the bedrock than the later Littorina type groundwaters.

Following the Littorina stage (and the subsequent transition to Baltic Sea conditions), the SFR area continued to be submerged, and slow moving, deep regional discharge flow paths within the highly transmissive deformation zones once again became established. This was the likely hydrogeological situation prior to commencement of the SFR investigation phase in 1985.

In contrast to other SKB site investigations (Forsmark and Laxemar), the SFR is unique in that studies are restricted to the upper approximately 400 metres of bedrock, and that the present day hydrochemistry is influenced by anthropogenic mixing of existing palaeo-groundwater types due to hydraulic drawdown (and some upconing) effects resulting from the excavation, construction and finally the operational phases of the SFR. In addition, drawdown has introduced younger local Baltic type waters which, based on their tritium contents, are relatively late reflecting the drawdown. This water type can show similarities in salinity and isotopic characteristics to diluted versions of the older Littorina Sea type groundwaters, and on occasions to differentiate the two sources may be difficult.

Different sediment thicknesses on the seabed have also played a role in the presence of local Baltic type groundwaters. For example, time series hydrochemical data indicate that whilst the Northern boundary belt (i.e. thin sedimentary cover and rapid intrusion of local Baltic type water) strictly follows a mixing line between Littorina and local Baltic type groundwaters, the Southern boundary belt (i.e. thick sedimentary cover which impedes rapid intrusion of local Baltic type water) shows a less marine signature. These differences in composition have been observed in groundwater samples also from the gently dipping heterogeneous zone ZFM871 where closeness to the Northern boundary belt implies more of a marine signature compared to boreholes at some distance from the Northern boundary belt.

An additional water source may include the discharge of shallow inland groundwater from Forsmark via the upper conductive shallow bedrock aquifer (SBA). Potentially, this may supply a groundwater mixture of young meteoric and Littorina origin to this depth interval within the Southern boundary belt. However, it is not clear at the moment whether this mixture could progress further to the northeast beyond the Southern boundary belt to the SFR site.

In general, the greatest groundwater mixing effects have occurred soon after construction of the SFR in 1985 with changes in groundwater pressure and inflow to boreholes and the tunnel system. Since then, conditions have slowly stabilised to reach close to equilibrium about the year 2000. The extent of the changes appear to be restricted to the vicinity of the SFR; new data from the Central Block and the area southeast of zones ZFMENE0870 and ZFM871 which demarcate the recently investigated SFR extension project area, suggest that away from the SFR facility and its immediate surroundings the overall hydrochemistry may not have undergone major changes.

The most important conclusions are:

- The major role that large scale hydraulically active deformation zones have and are playing in influencing the hydrochemistry of the SFR site and its immediate surroundings, both prior to and subsequent to the excavation, construction and operational phases. This is evident from the distribution of defined groundwater types, i.e. younger groundwaters with a marine signature (Baltic type at shallow depth down to –100 m.a.s.l. and Littorina type further down) present in transmissive deformation zones, while older Brackish-glacial type groundwaters are most often present in the less transmissive bedrock between major zones in single discrete fractures.

- Since the year 2000 anthropogenic mixing effects have slowly stabilised to reach close to equilibrium conditions. Stabilised hydrochemistry has been observed since the year 2000 from the annual sampling at four different sampling locations, all of them representing different major vertical zones.

- The extent of the anthropogenic changes appears to be restricted to the vicinity of the SFR; the overall hydrochemistry in the immediate surroundings may not have undergone any major changes since recent Baltic type groundwater is less abundant in the recently investigated target area south of the SFR repository. However, possibly increased mixing (e.g. resulting in transition type samples) cannot yet be distinguished and excluded.

8.2   General hydrochemistry and hydrochemical evolution

The hydrochemical input used in the investigations included; a) all those available data before the operational phase of the SFR (1984 to 1988), b) data from the routine SFR groundwater control or monitoring programme that has been ongoing since 1989, and c) the most recent data (2008–2010) from the SFR extension project. To ensure selection of the most representative groundwater data whilst hydraulic conditions have been changing during the SFR excavation and construction phases, and presently during the operational phase, careful consideration was given to the variation of sampling quality during these long periods of time. This included addressing the impact of different activities on sampling and sampling conditions and techniques, for example, sampling of borehole sections/entire boreholes, air lift pumping consequences, insufficient removal of contaminated water from borehole sections prior to sampling and, importantly, changes in hydrogeological conditions. The most recent SFR extension investigations also included the impact of drilling and drilling water on sample quality.

Based on the complex groundwater mixing processes, coupled to the need to separate groundwaters of different origins and residence times in the bedrock, a modified subdivision of the groundwaters from that applied during the Forsmark Site investigation was necessary. The shallow SFR samples (to about –400 m.a.s.l.) are characterised by a small range in Cl concentration (1,500 to 5,500 mg/L Cl) compared with the Forsmark site (50–16,000 mg/L Cl), but the $\delta^{18}O$ values showed a similar variation (–15.5 to –7.5‰ V-SMOW) to Forsmark. Fresh meteoric water components of present precipitation type are considered to be minor. Magnesium was regarded as a useful indicator of marine water and all the groundwater samples were colour coded accordingly based on their Cl/Mg ratio. This approach was quite successful in not only separating the different groundwater groups, but in some cases also showing the evolutionary mixing trends between groups (cf. Figure 3-4). The hydrochemical variables Cl, Mg and $\delta^{18}O$ indicate a large variation linked to the origin and residence time of the groundwaters despite the relatively small variation in salinity. Based on the variation of these hydrochemical variables, together with the palaeoclimatic considerations, a subdivision of the groundwaters into three major groups (origins) was made:

1) **Local Baltic type** groundwater with a Cl content of 2,500 to 3,500 mg/L, $\delta^{18}O$ at –9 to –7.5‰ V-SMOW and with strong marine signatures based on the Cl/Mg weight ratio and SO_4, K and the Br/Cl ratio. Tritium is also high with contents similar or slightly lower than the present Baltic Sea at the surface. This water is most common down to –100 m.a.s.l. but is found also in a few sections at about –150 m.a.s.l. The inflow of Baltic Seawater is a result of drawdown caused by the SFR facility.

2) **Littorina type** groundwater with a component of glacial water; Cl content is between 3,500 to 6,000 mg/L and $\delta^{18}O$ at –9.5 to –7.5‰ V-SMOW. The salinity is greater than the present Baltic Sea and chemical indicators such as Mg, SO_4 and Br/Cl ratio support a marine origin for the saline component. The slightly depleted $\delta^{18}O$ compared with the original Littorina Sea ($\delta^{18}O$ around –4.5 V-SMOW) indicates a significant component of glacial water probably from the last deglaciation. The Littorina type waters are commonly found at depths between –80 to –200 m.a.s.l. according to the present data set. In the nearby Forsmark area, however, Littorina-glacial waters are found down to 500–600 m depth.

3) **Brackish-glacial type** groundwaters with a Cl content of 1,500 to 5,000 mg/L and $\delta^{18}O$ < –12.0‰ V-SMOW. The marine signature is generally weak and the Br/Cl ratio deviates from that of marine waters. The brackish-glacial waters (at depths > –100 msl) are the oldest present at the SFR and the amounts of post-glacial components are small.

A large number of samples cannot be defined by any of the three groups above because of varying degrees of mixing and therefore a forth group called **Mixed transition type** water is used. Its presence at depths from about 60 to 400 m is indicated from groundwater monitoring over the last two decades showing it becoming more frequent. This is probably a result of the changing hydrogeological conditions in the SFR area influenced by drawdown inflow to the tunnels.

Principal Component Analysis (PCA) and M3 mixing calculations has helped to support the discrimination of groundwater groups described above based on expert judgement, and to obtain an idea of the mixing proportions of the different end-member waters that have contributed to the chemical composition of the SFR groundwaters.

The sequence of events and the possible mixing of different waters are summarised in Table 8-1.

Table 8-1. Origin of groundwaters and sequence of events influencing their chemistry at SFR.

Origin of groundwater	Approximate residence time	Depth	Type of structures	Comment
Present Baltic Sea	Modern water from the last 50 years based on tritium.	Down to 100 m depth.	Steeply dipping fracture zones with surface contact.	It is unclear if Baltic Seawater was present in the fracture zones before construction of the SFR tunnels.
Littorina Sea water	The Littorina maximum took place 4500 to 3000 BC.	80 to 220 m depth.	Most common in the larger fracture zones, especially the vertical zones ZFMNE0870A and B and ZFMNNE0869 (Zones 8 and 3) at the connection with the subhorizontal zone ZFM871 (Zone H2).	The Littorina Seawater is mixed with preexisting glacial meltwaters in the fracture zones, becoming more dilute (lower Cl) and with a significantly more depleted $\delta^{18}O$.
Glacial meltwater	This water is most probably from the last deglaciation which occurred at Forsmark ca 11,000 years ago.	The waters with the most depleted $\delta^{18}O$ values (indicative of glacial meltwater) are found at depths between 100 to 250 m.	Usually confined to single discrete fractures in the less transmissive parts of the bedrock.	The glacial meltwater has mixed with the preexisting brackish non-marine water producing some of the lowest Cl contents (1,600 mg/L Cl in KFR101: –240 m.a.s.l.).
Non-marine brackish water	Older than last deglaciation (> 15,000 a)	This water is only found as relatively small portions mixed with the glacial meltwater and partly also with the brackish marine water of Littorina type.	Usually confined to the less transmissive parts of the bedrock.	The origin of the brackish non-marine water is unclear, but includes probably components of old meteoric water and may also contain older glacial water, together with non-marine water of unknown age.

Differences compared with the hydrochemistry at Forsmark:

- Importantly, because the SFR is situated beneath the Baltic Sea, any input of modern meteoric water is judged to be minor and must result from laterally transported inland waters. The magnesium contents in the sampled waters (30–300 mg/L) are all above the limit used within the Forsmark investigations (< 25 mg/L) to differentiate non-marine brackish to saline waters. In fact, all of the SFR samples except for two sections, KFR101: –240 m.a.s.l. and KFR104: –306 m.a.s.l., are within the range of 70–300 mg/L Mg, which indicates that a marine input can be distinguished in most of the samples, but to variable degrees.

- The bicarbonate contents (40 to 160 mg/L) are relatively high compared with the non-marine brackish waters at Forsmark, which are mostly below 25 mg/L. This probably reflects variable mixing with infiltrated marine waters.

- The most depleted $\delta^{18}O$ values (indicative of portions of glacial meltwater) are found in less saline waters (< 4,000 mg/L Cl) in less transmissive fractures which differs from the Forsmark site where depleted values are found in more saline waters and at greater depths (cf. Figures 6-1 e and 6-5 e) due to a larger portion of glacial meltwater. Most of the brackish non-marine groundwaters at Forsmark have probably been isolated for a longer time than is the case at the SFR.

8.3 Groundwater-mineral systems

The major groundwater/mineral systems have been described which provide fundamental input to understanding the hydrochemistry of the SFR site and therefore of importance to safety analysis considerations. The main conclusions are:

- **Carbonate system and pH:** Most of the geochemical character and trends observed in the SFR groundwaters are similar to those observed at Forsmark, especially if only groundwaters with a marine component are compared. In summary; a) there is no clear pH trend with depth which may reflect the lateral heterogeneity of the groundwater system, b) high and variable HCO_3^- values are found in groundwaters with a marine (both Littorina and present Baltic) signature, as a result of biological activity during infiltration of marine waters through seabed sediments, c) in general, most of the SFR groundwaters seem to be in equilibrium or slightly oversaturated with respect to calcite, and d) fracture calcite is very common but shows no significant variations with depth and thus no obvious clues of calcite dissolution can be deduced from the present data.

- **Sulphate system:** Similar trends to Forsmark showing that; a) the Littorina and Baltic Seas are the main sources of sulphur, b) isotopic data ($\delta^{34}S$) indicate that sulphate reducing microbial activity seems to have played a minor role on the control of dissolved sulphate concentrations, and c) groundwaters are undersaturated with respect to gypsum and celestite and close to equilibrium with respect to barite; however, none of these minerals appear to have appreciably affected the dissolved sulphate contents derived from mixing processes.

- **Silica and fluoride systems:** Dissolved silica and fluoride concentrations are not correlated to chloride contents, indicating mineral solubility control. In the former, incongruent dissolution of feldspars with formation of secondary clays, clay mineral transformations and silica adsorption-desorption reactions in clays, participate. For fluoride, most groundwaters are in equilibrium, and those that are undersaturated correspond mostly to shallow groundwaters affected by the dilution effect associated with the intrusion of present Baltic Seawaters with very low fluoride contents.

- **Measured Eh data and redox pair modelling:** The potentiometric Eh measurements in the SFR groundwaters provide oxidising and reducing values. Reducing values (from −140 to −190 mV) are in line with those measured in the Forsmark groundwaters and are apparently controlled by the occurrence of an iron phase with an intermediate crystallinity and/or by ferrous clay minerals, both of which have been identified. Oxidising values in groundwaters (from +30 to +110 mV) appear to be controlled by amorphous Fe(III) oxyhydroxides and should represent the existence of present or recent oxic environments (artifacts), since these phases quickly recrystallise (e.g. months) to less soluble and more stable phases under reducing conditions. However, the local infiltration of oxidising Baltic type groundwaters can not be totally discarded and this aspect merits further study.

- **Redox sensitive elements:** Few data are available; however some understanding of their importance can be speculated upon.

As for Forsmark, iron and sulphur represent two very important redox systems for the understanding of the redox processes in the SFR groundwaters. The evolution and behaviour of these elements are frequently linked to bacterial activity (iron reducing bacteria –IRB, and sulphate reducing bacteria –SRB). Moreover, dissolved Fe(II) and S(-II) contents in some of the SFR groundwaters seem to be also controlled by inorganic processes, such as equilibrium situations with respect to Fe(II)-monosulphides and to siderite, and reductive dissolution of ferric oxyhydroxides by hydrogen sulphide.

Manganese and nitrogen systems can be used to trace old and present marine mixing events and different inorganic reactions and microbial processes could participate in the control of dissolved manganese in the groundwaters.

For the nitrogen system, the overall main characteristics would support the existence of anoxic-reducing conditions in the groundwaters from the SFR. The higher concentrations of nitrate detected in some groundwaters may be related to anthropogenic disturbances associated with the SFR facility.

8.4   Hydrogeochemical site description

A visualisation integrating the major hydrogeological and hydrogeochemical features of the investigated SFR rock volume (Figure 8-1) is presented based on the hydrogeological 0–1,000 m depth conceptual model after Öhman et al. (2011). Modifications to this model to satisfy hydrochemical considerations include colour coding of the main groundwater types in the three major flow path structures and in less transmissive discrete fractures which characterise the general SFR rock volume between these structures.
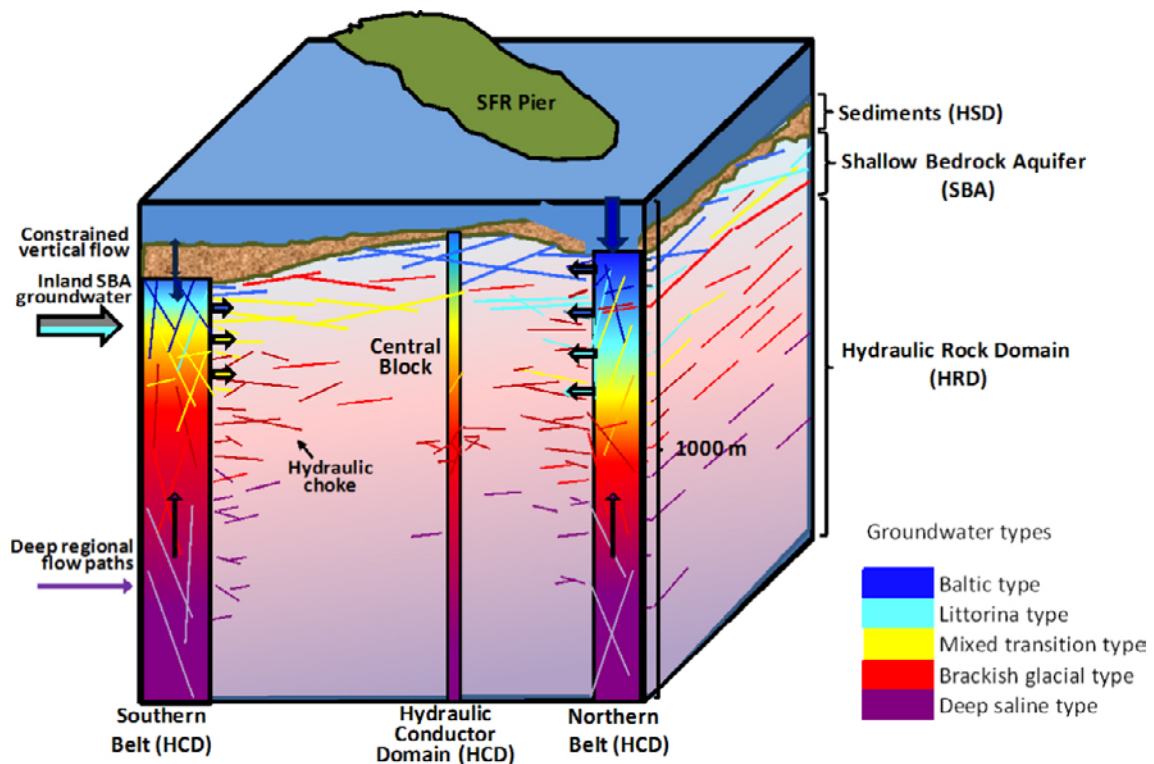
Figure 8-1. Conceptual block model (0–1,000 m depth) integrating the major hydrogeological and hydro-geochemical features of the investigated SFR rock volume. The different groundwater types are indicated by the same colour scheme used in Figures 6-2 to 6-4 with the exception of the deeper saline groundwater which is indicated by lilac and is not present as a dominant groundwater type in the SFR rock volume. See text for explanation to the different arrow types (modified after Öhman et al. 2011).

Based on Forsmark data (because no data below 400 m.a.s.l. are available from SFR), the deepest part of the bedrock is ascribed a saline non-marine groundwater type (deep lilac colour) and is associated with the two highly transmissive deformation areas (i.e. the Southern and Northern boundary belts) and the central Hydraulic Conductor; a weak regional flow direction upwards is indicated by the upward pointing black arrows. A more subdued lilac colour increasing in intensity with depth represents the less transmissive rock volume between these structures characterised by discrete fracture zones of low conductivity. These discrete fractures (and possibly also the rock matrix pore waters) probably represent similar salinities to the deepest groundwaters in the major conducting structures (i.e. deeper than about 700 m based on the Forsmark investigations). Furthermore, preserved components of old meteoric groundwater may be present at intermediate depths, and more so within the lower transmissive rock mass than the highly transmissive fracture zones.

The last deglaciation phase is represented by the introduction of glacial meltwaters particularly along the highly transmissive deformation zones, but also into smaller, less conductive fractures or dead-end fractures (i.e. 'pockets') heterogeneously distributed within the rock mass. Mixing with the older non-marine saline to brackish groundwaters (and components of old meteoric water) has given rise to the brackish-glacial groundwater types (bright red colour). This is followed subsequently by the infiltration of the Littorina Seawaters (turquoise colour), preferentially along the more highly conducting fracture zones but also along some less conducting fracture zones. Mixing of these Littorina type waters has occurred to different degrees with the earlier brackish-glacial groundwaters producing the mixed brackish water (transition) type groundwaters (yellow colour). There are occasions where mixing has not occurred and where the brackish-glacial groundwaters have remained at shallower levels in the bedrock ('pockets') shielded from the passage of the later Littorina type groundwaters; this is schematically indicated as red infilled fractures at higher levels than the maximum depths achieved by the Littorina type groundwaters. Littorina type groundwaters may also have been preserved under special conditions and this is also indicated by the turquoise colour of some of the near surface discrete fractures.

Following the Littorina stage (and the subsequent uninterrupted transition to Baltic Sea conditions) the area continued to be submerged, and slow moving, deep regional discharge flow paths within the highly transmissive deformation zones were once again established (upward pointing black arrows). This was the likely hydrogeological situation prior to commencement of the SFR investigation phase in 1985.

The SFR activities have resulted in the inflow of external waters into the SFR rock volume during the excavation/construction phases, namely modern Baltic Seawaters (dark blue colour) via the highly transmissive deformation zones comprising the Northern and Southern boundary belts as well as zone ZFMNNE0869 (Zone 3). However, sea bottom sedimentation has been much more developed (i.e. thicker) above the Southern boundary belt compared to the Northern one (Figure 6-5; cf. Section 2.2.1), allowing a greater volume of Baltic Sea type water to preferentially infiltrate to the latter (indicated by the larger and thicker downward pointing blue arrow). As indicated by the concentration of short thick horizontal arrows from the upper approximately 400 m parts of the Northern and Southern boundary belts, the SFR drawdown has gradually pulled in groundwaters along conducting fracture zones into the Central Block area and towards the SFR site. These groundwaters, already the product of natural mixing processes affecting Brackish-glacial and Littorina type waters, therefore have undergone additional anthropogenic mixing involving a Baltic Sea input and this has been compounded by the increased flow system resulting from the drawdown effects. Other anthropogenic activities, such as drilling, hydraulic testing and groundwater sampling, are considered of minor importance.

The input flow sources to the Central Block area of mixed groundwaters with components of Brackish-glacial, Littorina and Baltic type waters is visualised to show close to the surface in the Northern boundary belt the dark blue of the Baltic Sea and lower down a dominant Littorina component; in the latter case a component of brackish-glacial water is assumed to be present also. In contrast, the Southern boundary belt is considered to be less transmissive because of the thick sediment cover which has limited initially the amount of Littorina Sea and later the Baltic Sea waters infiltrating into the deformation zones to mix with the resident Brackish-glacial groundwaters. This explains the restricted vertical extent of the Mixed transient groundwater types; compare the depth extent of the yellow colouring between the two belts and note the less dominant Littorina and Baltic components in the Southern boundary belt. The conceptual model also shows a lateral flow direction to the Southern boundary belt from the near surface Shallow Bedrock Aquifer (SBA) which may have transported mixtures of modern meteoric water with some residual Littorina type water from inland, i.e. from the northeastern part of the Forsmark area. However, this is based on too few data and may simply reflect the hydrogeological and hydrogeochemical heterogeneity of the bedrock system.

References

SKB's (Svensk Kärnbränslehantering AB) publications can be found at www.skb.se/publications.

Alexeev S V, Alexeeva L P, 2003. Hydrogeochemistry of the permafrost zone in the central part of the Yakutian diamond-bearing province, Russia. Hydrogeology Journal 11, 574–581.

Anderson C R, Pedersen K, 2003. *In situ* growth of *Gallionella* biofilms and partitioning of lanthanides and actinides between biological material and ferric oxyhydroxides. Geobiology 1, 169–178.

Andersson P S, Wasserburg G J, Chen J H, Papanastassiou D A, Ingri J, 1995. ^{238}U-^{234}U and ^{232}Th-^{230}Th in the Baltic Sea and in river water. Earth and Planetary Science Letters 130, 217–234.

Andrews J N, Fontes J-C, 1992. Importance of the in situ production of ^{36}Cl, ^{36}Ar and ^{14}C in hydrology and hydrogeochemistry. In Proceedings of Symposium on Isotope Techniques in Water Resources Development, Vienna, March 1991, 245–269.

Andrews J N, Davis S N, Fabryka-Martin J, Fontes J-C, Lehmann B E, Loosli H H, Michelot J-L, Moser H, Smith B, Wolf M, 1989a. The *in situ* production of radioisotopes in rock matrices with particular reference to the Stripa granite. Geochimica et Cosmochimica Acta 53, 1803–1815.

Andrews J N, Hussain N, Youngman M J, 1989b. Atmospheric and radiogenic gases in groundwaters from the Stripa granite. Geochimica et Cosmochimica Acta 53, 1831–1841.

Auqué L, Gimeno M J, Gómez J, Nilsson A-C, 2008. Potentiometrically measured Eh in groundwaters from the Scandinavian Shield. Applied Geochemistry 23, 1820–1833.

Ball J W, Nordstrom D K, 2001. User's manual for WATEQ4F, with revised thermodynamic data base and test cases for calculating speciation of major, trace, and redox elements in natural waters. Open File Report 91-183, U.S. Geological Survey, Denver, Colorado.

Banwart S A, 1999. Reduction of iron(III) minerals by natural organic matter in groundwater. Geochimica et Cosmochimica Acta 63, 2919–2928.

Bentley H W, Phillips F M, Davis S N, 1986. Chlorine-36 in the terrestrial environment. In Fritz P, Fontes J-C (eds). Handbook of environmental isotope geochemistry. Vol 2. The terrestrial environment. Amsterdam: Elsevier, 427–480.

Björck S, 1995. A review of the history of the Baltic Sea 13–8 ka. Quarternary International 27, 19–40.

Bosson E, Gustafsson, L-G, Sassner M, 2008. Numerical modelling of surface hydrology and near-surface hydrogeology at Forsmark. Site descriptive modelling, SDM-Site Forsmark. SKB R-08-09, Svensk Kärnbränslehantering AB.

Carlsson A, Christiansson R, 2007. Construction experiences from underground works at Forsmark. Compilation report. SKB R-07-10, Svensk Kärnbränslehantering AB.

Claesson Liljedahl L, Munier R, Sandström B, Drake H, Tullborg E-L, 2011. Assessment of fractures classified as non-mineralised in the Sicada database. SKB R-11-02, Svensk Kärnbränslehantering AB.

Clark I D, Fritz P, 1997. Environmental isotopes in hydrogeology. Boca Raton, FL: Lewis.

Curtis P, Markström I, Petersson J, Triumf C-A, Isaksson H, Mattson H, 2011. Site investigation SFR. Bedrock geology. SKB R-10-49, Svensk Kärnbränslehantering AB.

Deutsch W J, 1997. Groundwater geochemistry: fundamentals and applications to contamination. Boca Raton, FL: Lewis.

Drake H, Tullborg E-L, 2009. Fracture mineralogy Laxemar. Site descriptive modelling, SDM-Site Laxemar. SKB R-08-99, Svensk Kärnbränslehantering AB.

Drake H, Tullborg E-L, MacKenzie A B, 2009. Detecting the near-surface redox front in crystalline bedrock using fracture mineral distribution, geochemistry and U-series disequilibrium. Applied Geochemistry 24, 1023–1039.

Drever J I, 1997. The geochemistry of natural waters: surface and groundwater environments. 3rd ed. Upper Saddle River, NJ: Prentice Hall.

Drew M C, 1983. Plant injury and adaptation to oxygen deficiency in the root environment: a review. Plant and Soil 75, 179–199.

Döse C, Stråhle A, Mattsson K-J, Carlsten S, 2009a. Site investigation SFR. Boremap mapping of core drilled borehole KFR101. SKB P-09-36, Svensk Kärnbränslehantering AB.

Döse C, Winell S, Stråhle A, Carlsten C, 2009b. Site investigation SFR. Boremap mapping of core drilled boreholes KFR102B and KFR103. SKB P-09-38, Svensk Kärnbränslehantering AB.

Eklund S, Mattson K-J, 2009. Forsmark site investigation. Quantitative mapping of fracture minerals in Forsmark. SKB P-08-47, Svensk Kärnbränslehantering AB.

Ferris F G, Konhauser K O, Lyvén B, Pedersen K, 1999. Accumulation of metals by bacteriogenic iron oxides in a subterranean environment. Geomicrobioloy Journal 16,181–192.

Follin S, 2008. Bedrock hydrogeology Forsmark. Site descriptive modelling, SDM-Site Forsmark. SKB R-08-95, Svensk Kärnbränslehantering AB.

Follin S, Johansson P-O, Levén J, Hartley L, Holton D, McCarthy R, Roberts D, 2007a. Updated strategy and test of new concepts for groundwater flow modelling in Forsmark in preparation of site descriptive modelling stage 2.2. SKB R-07-20, Svensk Kärnbränslehantering AB.

Follin S, Levén J, Hartley L, Jackson P, Joyce S, Roberts D, Swift B, 2007b. Hydrogeological characterisation and modelling of deformation zones and fracture domains, Forsmark modelling stage 2.2. SKB R-07-48, Svensk Kärnbränslehantering AB.

Follin S, Stephens M B, Laaksoharju M, Nilsson A-C, Smellie J A T, Tullborg E-L, 2008a. Modelling the evolution of hydrochemical conditions in the Fennoscandian Shield during Holocene time using multidisciplinary information. Applied Geochemistry 23, 2004–2020.

Follin S, Hartley L, Jackson P, Roberts D, Marsic N, 2008b. Hydrogeological conceptual model development and numerical modelling using CONNECTFLOW, Forsmark modelling stage 2.3. SKB R-08-23, Svensk Kärnbränslehantering AB.

Gascoyne M, 2001. ^{36}Cl in Olkiluoto groundwaters: Evidence for intrusion of Littorina seawater. Posiva Working Report 2001-20, Posiva Oy, Finland.

Gershenfeld N A, 1999. The nature of mathematical modeling. Cambridge: Cambridge University Press.

Gimeno M J, Auqué L F, Gómez J, 2006. Mass balance modelling. In SKB. Hydrogeochemical evaluation. Preliminary site description. Laxemar subarea –version 2.1. SKB R-06-70, Svensk Kärnbränslehantering AB, 175–210.

Gimeno M J, Auqué L F, Gómez J B, Acero P, 2008. Water-rock interaction modelling and uncertainties of mixing modelling. SDM-Site Forsmark. SKB R-08-86, Svensk Kärnbränslehantering AB.

Gimeno M J, Auqué L F, Gómez J B, Acero P, 2009. Water-rock interaction modelling and uncertainties of mixing modelling. Site descriptive modelling, SDM-Site Laxemar. SKB R-08-110, Svensk Kärnbränslehantering AB.

Gimeno M J, Auqué L F, Gómez J B, Acero P, 2011. Site investigation SFR. Water-rock interaction and mixing modelling in the SFR. SKB P-11-25, Svensk Kärnbränslehantering AB.

Glamheden R, Maersk Hansen L, Fredriksson A, Bergkvist L, Markström I, Elfström M, 2007. Mechanical modelling of the Singö deformation zone. Site descriptive modelling Forsmark stage 2.1. SKB R-07-06, Svensk Kärnbränslehantering AB.

Gómez J B, Laaksoharju M, Skårman E, Gurban I, 2006. M3 version 3.0: Concepts, methods and mathematical formulation. SKB TR-06-27, Svensk Kärnbränslehantering AB.

Gómez J B, Laaksoharju M, Skårman E, Gurban I, 2009. M3 version 3.0: Verification and Validation. SKB TR-09-05, Svensk Kärnbränslehantering AB.

Grenthe I, Stumm W, Laaksoharju M, Nilsson A-C, Wikberg P, 1992. Redox potentials and redox reactions in deep groundwater systems. Chemical Geology 98, 131–150.

Gustavsson E, Jönsson S, Ludvigson J-E, 2006. Forsmark site investigation. Pumping tests and flow logging. Boreholes HFM33, HFM34 and HFM35. SKB P-06-193, Svensk Kärnbränslehantering AB.

Hallbeck L, Pedersen K, 2008a. Characterization of microbial processes in deep aquifers of the Fennoscandian Shield. Applied Geochemistry 23, 1796–1819.

Hallbeck L, Pedersen K, 2008b. Explorative analysis of microbes, colloids and gases together with microbial modelling. Site description model, SDM-Site Laxemar. SKB R-08-109, Svensk Kärnbränslehantering AB.

Hallbeck L, Pedersen K, 2008c. Explorative analysis of microbes, colloids and gases. SDM-Site Forsmark. SKB R-08-85, Svensk Kärnbränslehantering AB.

Hedenström A, Sohlenius G, 2008. Description of the regolith at Forsmark. Site descriptive modelling, SDM-Site Forsmark. SKB R-08-04, Svensk Kärnbränslehantering AB.

Hedenström A, Sohlenius G, Strömgren M, Brydsten L, Nyman H, 2008. Depth and stratigraphy of regolith at Forsmark. Site desprictive modelling, SDM-Site Forsmark. SKB R-08-07, Svensk Kärnbränslehantering AB.

Heginbottom J A, Dubreuil M A, Harker P A, 1995. Canada – Permafrost. In: The national atlas of Canada. 5th ed. National Atlas Information Service, Natural Resources Canada, MCR 4177.

Holden B, Stotler R L, Frape S K, Ruskeeniemi T, Talikka M, Freifeld B M, 2009. High Lake permafrost comparison site: Permafrost phase IV. NWMO TR-2009-11, Nuclear Waste Management Organization, Canada.

Holmén J G, 2005. SFR-1. Inverse modelling of inflow to tunnels and propagation of estimated uncertainties to predictive stages. SKB R-05-74, Svensk Kärnbränslehantering AB.

Holmén J G, Stigsson M, 2001a. Modelling of future hydrogeological conditions at SFR. SKB R-01-02, Svensk Kärnbränslehantering AB.

Holmén J G, Stigsson M, 2001b. Details of predicted flow in deposition tunnels at SFR, Forsmark. SKB R-01-21, Svensk Kärnbränslehantering AB.

Ivanovich M I, Harmon R S, 1992. Uranium-series disequilibrium: applications to earth, marine and environmental sciences. 2nd ed. Oxford: Clarendon Press.

Jönsson S, Harrström J, Ludvigson J-E, Nilsson A-C, 2008. Site investigation SFR. Hydraulic tests, flow logging and hydrochemical sampling. Boreholes HFR101, HFR102 and HFR105. SKB P-08-87, Svensk Kärnbränslehantering AB.

Kukkonen I T, Šafanda J, 2001. Numerical modelling of permafrost in bedrock in northern Fennoscandia during the Holocene. Global and Planetary Change 29, 259–273.

Kulik D A, Kersten M, Heiser U, Neumann T, 2000. Application of Gibbs energy minimization to model early-diagenetic solid-solution aqueous-solution equilibria involving authigenic rhodochrosites in anoxic Baltic Sea sediments. Aquatic Geochemistry 6, 147–199.

Kölling M, 2000. Comparison of different methods for redox potential determination in natural waters. In Schüring L, Schulz H D, Fischer W R, Böttcher J, Duijnisveld W H M (eds). Redox: fundamentals, processes and applications. Berlin: Springer, 42–54.

Laaksoharju M, Gurban I, 2003. Groundwater chemical changes at SFR in Forsmark. SKB R-03-03, Svensk Kärnbränslehantering AB.

Laaksoharju M, Wallin B (eds), 1997. Evolution of the groundwater chemistry at the Äspö Hard Rock Laboratory. Proceedings of the second Äspö International Geochemistry Workshop, June 6–7, 1995. SKB ICR 97-04, Svensk Kärnbränslehantering AB.

Laaksoharju M, Skårman C, Skårman E, 1999. Multivariate Mixing and Mass-balance (M3) calculations, a new tool for decoding hydrogeochemical information. Applied Geochemistry 14, 861–871.

Laaksoharju M, Smellie J, Tullborg E-L, Gimeno M, Hallbek L, Molinero J, Waber N, 2008. Bedrock hydrogeochemistry Forsmark. Site descriptive modeling SDM-Site Forsmark. SKB R-08-47, Svensk Kärnbränslehantering AB.

Laaksoharju M, Gimeno M, Auqué L F, Gómez, J B, Acero P, Pedersen K, 2009. Hydrogeochemical and microbiological effects on fractures in the Excavation Damaged Zone (EDZ). SKB R-09-05, Svensk Kärnbränslehantering AB.

Langmuir D, 1997. Aqueous environmental geochemistry. Upper Sadle River, NJ: Prentice Hall.

Langmuir D, Melchior D, 1985. The geochemistry of Ca, Sr, Ba and Ra sulfates in some deep brines from the Palo Duro Basin, Texas. Geochimica et Cosmochimica Acta 49, 2423–2432.

Lindquist A, Nilsson K, 2010. Site investigation SFR. Hydrochemical characterisation of groundwater in borehole KFR105. Results from five investigated borehole sections. SKB P-10-02, Svensk Kärnbränslehantering AB.

Louvat D, Michelot J L, Aranyossy J F, 1999. Origin and residence time of salinity in the Äspö groundwater system. Applied Geochemistry 14, 917–925.

Lundin L, Lode E, Stendahl J, Melkerud P-A, Björkvald L, Thorstensson A, 2004. Soils and site types in the Forsmark area. SKB R-04-08, Svensk Kärnbränslehantering AB.

Löfgren M, Sidborn M, 2010. Statistical analysis of results from the quantitative mapping of fracture minerals in Laxemar. Site descriptive modelling – complementary studies. SKB R-09-31, Svensk Kärnbränslehantering AB.

Mahara Y, Hasegawa T, Miyakawa K, Ohta T, 2008. Correlation between dissolved ^{4}He concentration and ^{36}Cl in groundwater at Äspö, Sweden. Applied Geochemistry 23, 3305–3320.

Molinero-Huguet J, Samper-Calvete J, Zhang G, Yang C, 2004. Biogeochemical reactive transport model of the Redox Zone experiment of the Äspö Hard Rock Laboratory in Sweden. Nuclear Technology 148, 151–165.

Neumann T, Heiser U, Leosson M A, Kersten M, 2002. Early diagenetic processes during Mn-carbonate formation: evidence from the isotopic composition of authigenic Ca-rhodochrosites of the Baltic Sea. Geochimica et Cosmochimica Acta 66, 867–879.

Nilsson A-C, 2009. Site investigation SFR. Presentation and evaluation of hydrogeochemical data from SFR-boreholes, 1984–2007. SKB P-09-45, Svensk Kärnbränslehantering AB.

Nilsson A-C, Tullborg E-L, Smellie J, 2010a. Preliminary hydrogeochemical site description SFR (version 0.2). SKB R-10-38, Svensk Kärnbränslehantering AB.

Nilsson A-C (ed), Berg C, Harrström J, Jönsson S, Thur P, Borgiel M, Qvarfordt S, 2010b. Forsmark site investigation. Hydrochemical monitoring of groundwaters and surface waters. Results from water sampling in the Forsmark area, January –December 2009. SKB P-10-40, Svensk Kärnbränslehantering AB.

Nilsson G, 2009. Site investigation SFR. Drilling of the cored borehole KFR105. SKB P-09-41, Svensk Kärnbränslehantering AB.

Nilsson K, 2011. Site investigation SFR. Hydrochemical characterisation of groundwater in the SFR repository. Sampling and analysis during 2010. Extended investigations in KFR7A: 48.0 to 74.7 m, KFR08: 63.0 to 104.0 m and KFR19: 95.0 to 110.0 m. SKB P-11-14, Svensk Kärnbränslehantering AB.

Nordstrom D K, 2005. Modeling low-temperature geochemical processes. In Drever J I (ed). Treatise on Geochemistry. Vol 5. Surface and ground water, weathering, and soils. Amsterdam: Elsevier, 37–72.

Nordstrom D K, Ball J W, Donahoe R J, Whittemore D, 1989. Groundwater chemistry and water–rock interactions at Stripa. Geochimica et Cosmochimica Acta 53, 1727–1740.

Noseck U, Tullborg E-L, Suksi J, Laaksoharju M, Havlová V, Denecke M A, Buckau G, 2012. Real system analyses/natural analogues. Applied Geochemistry 27, 490–500.

Odén M, 2009. Site investigation SFR. Hydrogeological modelling at SFR using DarcyTools. Site description SFR version 0.0. SKB P-08-94, Svensk Kärnbränslehantering AB.

Olofsson I, Simeonov A, Stephens M, Follin S, Nilsson A-C, Röshoff K, Lindberg U, Lanaro F, Fredriksson A, Persson L, 2007. Site descriptive modeling Forsmark, stage 2.2. A fracture domain concept as a basis for the statistical modeling of fractures and minor deformation zones, and inter-disciplinary coordination. SKB R-07-15, Svensk Kärnbränslehantering AB.

Parkhurst D L, Appelo C A J, 1999. User's guide to PHREEQC (version 2): a computer program for speciation, batch-reaction, one-dimensional transport, and inverse geochemical calculations. Water-Resources Investigations Report 99-4259, U.S. Geological Survey, Denver, Colorado.

Pedersen K, 2006. Microbiology of transitional groundwater of the porous overburden and underlying fractured bedrock aquifers in Olkiluoto 2004, Finland. Posiva Working Report 2006-09, Posiva Oy, Finland.

Pedersen K, 2008. Microbiology of Olkiluoto groundwater 2004–2006. Posiva 2008-02, Posiva Oy, Finland.

Pedersen K, Arlinger J, Eriksson S, Hallbeck A, Hallbeck L, Johansson J, 2008. Numbers, biomass and cultivable diversity of microbial populations relate to depth and borehole-specific conditions in groundwater from depths of 4–450 m in Olkiluoto, Finland. The ISME Journal 2, 760–775.

Pedersen K, Arlinger J, Edlund J, Eriksson L, Lydmark S, Johansson J, Jägevall S, Rabe L, 2010. Microbiology of Olkiluoto and ONKALO groundwater. Results and interpretations, 2008–2009, Posiva Working Report 2010-60, Posiva Oy, Finland.

Pitkänen P, Luukkonen A, Ruotsalainen P, Leino-Forsman H, Vuorinen U, 1999. Geochemical modelling of groundwater evolution and residence time at the Olkiluoto site. Posiva 98-10, Posiva Oy, Finland.

Pitkänen P, Partamies S, Luukkonen A, 2004. Hydrogeochemical interpretation of baseline groundwater conditions at the Olkiluoto site. Posiva 2003-07, Posiva Oy, Finland.

Påsse T, 1997. A mathematical model of past, present and future shore level displacement in Fennoscandia. SKB TR 97-28, Svensk Kärnbränslehantering AB.

Ruskeeniemi T, Paananen M, Ahonen L, Kaija J, Kuivamäki A, Frape S, Moren L, Degnan P, 2002. Permafrost at Lupin: report of Phase I. Report YST-112, Geological Survey of Finland, Nuclear Waste Disposal Research.

Ruskeeniemi T, Ahonen L, Paananen M, Frape S, Stotler R, Hobbs M, Kaija J, Degnan P, Blomqvist R, Jensen M, Lehto K, Moren L, Puigdomenech I, Snellman M, 2004. Permafrost at Lupin: report of Phase II. Report YST-119, Geological Survey of Finland, Nuclear Waste Disposal Research.

Sandström B, Stephens M B, 2009. Mineralogy, geochemistry, porosity and redox properties of rocks from Forsmark.Compilation of data from the regional model volume for SR-Site. SKB R-09-51, Svensk Kärnbränslehantering AB.

Sandström B, Tullborg E-L, 2009. Episodic fluid migration in the Fennoscandian Shield recorded by stable isotopes, rare earth elements and fluid inclusions in fracture minerals at Forsmark, Sweden. Chemical Geology 266, 135–151.

Sandström B, Tullborg E-L, 2011. Site investigation SFR. Fracture mineralogy and geochemistry of borehole sections sampled for groundwater chemistry and Eh. Results from boreholes KFR01, KFR08, KFR10, KFR19, KFR7A and KFR105. SKB P-11-01, Svensk Kärnbränslehantering AB.

Sandström B, Tullborg E-L, de Torres T, Ortiz J E, 2006. The occurrence and potential origin of asphaltite in bedrock fractures, Forsmark, central Sweden. GFF 128, 233–242.

Sandström B, Tullborg E-L, Smellie J, MacKenzie AB, Suksi J, 2008. Fracture mineralogy of the Forsmark site. SDM-Site Forsmark. SKB R-08-102, Svensk Kärnbränslehantering AB.

Sandström B, Tullborg E-L, Larson S Å, Page L, 2009. Brittle tectonothermal evolution in the Forsmark area, central Fennoscandian Shield, recorded by paragenesis, orientation and ^{40}Ar/^{39}Ar geochronology of fracture minerals. Tectonophysics 478, 158–174.

Sandström B, Annersten H, Tullborg E-L, 2010. Fracture-related hydrothermal alteration of metagranitic rock and associated changes in mineralogy, geochemistry and degree of oxidation: a case study at Forsmark, central Sweden. International Journal of Earth Sciences 99, 1–25.

Sandström B, Nilsson K, Tullborg E-L, 2011. Site investigation SFR. Fracture mineralogy including identification of uranium phases and hydrochemical characterisation of groundwater in borehole KFR106. SKB P-11-41, Svensk Kärnbränslehantering AB.

Sidborn M, Sandström B, Tullborg E-L, Salas J, Flávia M, Delos A, Molinero J, Hallbeck L, Pedersen K, 2010. SR-Site: Oxygen ingress in the rock at Forsmark during a glacial cycle. SKB TR-10-57, Svensk Kärnbränslehantering AB.

Silver W L, Lugo A E, Keller M, 1999. Soil oxygen availability and biogeochemistry along rainfall and topographic gradients in upland wet tropical forest soils. Biogeochemistry 44, 301–328.

SKB, 2001. Site investigations. Investigation methods and general execution programme. SKB TR-01-29, Svensk Kärnbränslehantering AB.

SKB, 2008. Geovetenskapligt undersökningsprogram för utbyggnad av SFR. SKB R-08-67, Svensk Kärnbränslehantering AB. (In Swedish.)

Smellie J, Tullborg E-L, Nilsson A-C, Sandström B, Waber N, Gimeno M, Gascoyne M, 2008. Explorative analysis of major components and isotopes. SDM-Site Forsmark. SKB R-08-84, Svensk Kärnbränslehantering AB.

Stephens M B, Fox A, La Pointe P, Simeonov A, Isaksson H, Hermansson J, Öhman J, 2007. Geology Forsmark. Site descriptive modelling Forsmark stage 2.2. SKB R-07-45, Svensk Kärnbränslehantering AB.

Svensson U, 1996. SKB Palaeohydrogeological programme. Regional groundwater flow due to advancing and retreating glacier – scoping calculations. SKB Utveckling Progress Report U-96-35, Svensk Kärnbränslehantering AB.

Svensson U, Follin S, 2010. Groundwater flow modelling of the excavation and operation phases – Forsmark. SKB R-09-19, Svensk Kärnbränslehantering AB.

Söderbäck B (ed), 2008. Geological evolution, palaeoclimate and historical development of the Forsmark and Laxemar-Simpevarp areas. Site descriptive modeling, SDM-Site. SKB R-08-19, Svensk Kärnbränslehantering AB.

Tarasov L, Peltier W R, 2007. Coevolution of continental ice cover and permafrost extent over the last glacial-interglacial cycle in North America. Journal of Geophysical Research 112, F02S08. doi:10.1029/2006JF000661

Thorstenson D C, 1984. The concept of electron activity and its relation to redox potentials in aqueous geochemical systems. Open File Report 84-072, U.S. Geological Survey, Denver, Colorado.

Thur P, Nilsson K, 2009a. Site investigation SFR. Hydrogeochemical characterisation of groundwater in borehole KFR101 and results from water sampling and analyses in boreholes KFR02, KFR7A, KFR08 and KFR56. Sampling during winter 2008–2009. SKB P-09-53, Svensk Kärnbränslehantering AB.

Thur P, Nilsson K, 2009b. Site investigation SFR. Hydrogeochemical characterisation of groundwater in borehole KFR102A. Results from water sampling and analyses during March 2009. SKB P-09-50, Svensk Kärnbränslehantering AB.

Thur P, Jönsson S, Harrström J, Ludvigson J-E, 2009. Site investigation SFR. Hydraulic tests, flow logging and chemical sampling. Borehole HFR106. SKB P-09-54, Svensk Kärnbränslehantering AB.

Trotignon L, Michaud V, Lartigue J-E, Ambrosi J-P, Eisenlohr L, Griffault L, de Combarieu M, Daumas S, 2002. Laboratory simulation of an oxidizing perturbation in a deep granite environment. Geochimica et Cosmochimica Acta 66, 2583–2601.

Tröjbom M, Söderbäck B, Johansson P-O, 2007. Hydrochemistry in surface water and shallow groundwater. Site descriptive modelling, SDM-Site Forsmark. SKB R-07-55, Svensk Kärnbränslehantering AB.

Tullborg E-L, Drake H, Sandström B, 2008. Palaeohydrogeology: a methodology based on fracture mineral studies. Applied Geochemistry 23, 1881–1897.

Tullborg E-L, Smellie J, Nilsson A-C, Gimeno M J, Auqué LF, Bruchert V, Molinero J, 2010. SR-Site – sulphide content in the groundwater at Forsmark. SKB TR-10-39, Svensk Kärnbränslehantering AB.

Waber H N, Gimmi T, deHaller A, Smellie J A T, 2009. Porewater in the rock matrix. Site descriptive modelling, SDM-Site Laxemar. SKB R-08-112, Svensk Kärnbränslehantering AB.

Welin E, 1964. Uranium dissemination and vein fillings in iron ores of norhern Uppland, central Sweden. Geologiska Föreningens i Stockholm Förhandlingar 86, 51–82.

Westman P, Wastegård S, Schoning K, Gustafsson B, Omstedt A, 1999. Salinity change in the Baltic Sea during the last 8,500 years: evidence, causes and models. SKB TR-99-38, Svensk Kärnbränslehantering AB.

Winell S, 2009. Site investigation SFR. Boremap mapping of core drilled borehole KFR105. SKB P-09-59, Svensk Kärnbränslehantering AB.

Winell S, Döse C, Stråhle A, Carlsten S, Selnert E, 2009a. Site investigation SFR. Boremap mapping of core drilled boreholes KFR104 and KFR27 (from 147.5 m). SKB P-09-39, Svensk Kärnbränslehantering AB.

Winell S, Carlsten S, Stråhle A, 2009b. Site investigation SFR. Boremap mapping of core drilled borehole KFR102A. SKB P-09-52, Svensk Kärnbränslehantering AB.

Öhman J, Follin S, 2010. Site investigation SFR. Hydrogeological modelling of SFR. Data review and parameterisation of model version 0.1. SKB P-09-49, Svensk Kärnbränslehantering AB.

Öhman J, Bockgård N, Follin S, 2011. Site investigation SFR. Hydrogeological modelling of SFR. Data review and parameterisation. SKB R-11-03, Svensk Kärnbränslehantering AB.

Sample quality assessment

A1.1   Background

As described in Section 1.5.2, the quality or representativity of groundwater samples may be influenced by different conditions in the borehole or at the sampling occasion. Furthermore, the quality of the samples in the SFR dataset, in particular, is especially variable and complex to judge since it covers a time period of more than 20 years. During this time both equipment and the methods employed have undergone development in addition to the increase in experience and knowledge concerning groundwater investigations. Despite these modifications, an attempt was made to assess as close as possible the sample quality of the SFR dataset based on experience from the previous Forsmark and Laxemar site investigations (Smellie et al. 2008).

This classification of groundwater samples into five quality categories requires evaluation of hydraulic conditions in the borehole, in the section being sampled, and also in the surrounding bedrock. Furthermore, when assessing the sample quality category for each borehole section several procedures which can influence the groundwater quality have to be considered; a) contamination from drilling (e.g. rock flour and drilling water), b) possible impacts caused by sampling conditions (e.g. which techniques are used; what sampling times should be used), c) analytical performance and integration of data from different sources, and d) is the coverage satisfactory for interpretation purposes?

In reality, the SFR dataset differs from the Forsmark and Laxemar datasets in several aspects. Furthermore, the available hydrogeological information concerning the early SFR boreholes is far less extensive and differs in character from that of the Forsmark and Laxemar boreholes. Therefore, some modifications of the previous approach have been necessary in order to provide a judicious subdivision of the SFR samples into quality categories. The following aspects were taken into consideration;

- Despite the fact that sampling in the early SFR boreholes has been ongoing since 1984, practically the same sampling method has been used for old as well as new boreholes (if the few samples collected during drilling are excluded). As a consequence, sampling method criteria can be disregarded.

- Previously in the Forsmark site investigation, flow logging information was used to evaluate the risk of short circuiting between borehole sections. Although this information is missing from the early SFR boreholes, it has been possible to detect short circuiting between sections from pressure registrations in adjacent borehole sections during sampling. In fact, regular/continuous pressure monitoring is applied to all the sampled borehole sections, both early and recently drilled boreholes. Furthermore, this pressure monitoring helps to explain unstable groundwater compositions in a few cases were pressure gradients exist. The hydraulic effect criterion was therefore changed to "Pressure responses between sections" and the conditions causing unstable groundwater composition can sometimes be identified from this pressure data.

- Sampling has been performed both sporadically and sometimes regularly (annually or every 5th year) and on occasions as a series of samples during a continuous discharge of groundwater (for days or weeks). These different conditions can affect confidence in the data and this led to the term "sample series" being introduced to denote long term monitoring, while "time series" was used for a short term series of sample collection. Adequate time series and/or sample series are considered important quality criteria.

- Finally, while the data quality assessment for the datasets from Forsmark and Laxemar centred on each borehole section, the quality assessment for the SFR dataset had to focus on each sample due to the very heterogeneous dataset for each borehole section and also the varying range of analyses for each sample. Consequently, a table corresponding to Tables A1-1 or A1-2 has been produced for each one of the 360 samples in the SFR dataset. A summary of this extensive documentation is given for each borehole section below in Chapter 3.

A1.2 Categorisation criteria

Table A1-1 and Table A1-2 outline the approach for judging the groundwater quality categories for cored boreholes and percussion drilled boreholes used in Chapter 3. The different criteria are commented on in the text below the two tables.

Drilling water content

A major consideration in evaluating the quality of groundwater samples is the potential impact of flushing or drilling water from core drilling on the chemistry of the collected samples. Historically at SKB, a maximum of 1% drilling water (based on the amount of uranine tracer) has been used to indicate samples of the highest quality. This limit may be relevant for parameters like trace metals, TOC/DOC and ^{14}C (pmC). The choice of the drilling water source is of great importance because the greater the difference in composition the greater the impact of unwanted contamination. Of special importance in the SFR extension project was to avoid any change in the groundwater marine signature that might impact on the evaluation of the groundwater origin. The strategy for selecting drilling water sources for the boreholes drilled in the SFR extension project and the expected impacts on the chemistry is described in Section 1.5 in the main report. The gradual decrease in quality was assessed according to the drilling water content limits $\leq 1\%$, $\leq 5\%$ and $\leq 10\%$.

Table A1-1. Categorisation criteria for core drilled boreholes.

Cored boreholes Aspects/Conditions	1	2	3	4	5	Comment
Drilling water (≤ 1%)	X	X	X	X	X	Valid for all tunnel boreholes, new and old.
Drilling water (≤ 5%)		X	X	X	X	Valid for most of the new surface borehole samples.
Drilling water (≤ 10%)			X	X	X	Valid for the rest of the new surface boreholes. No drilling water content > 6.5%.
Time series* adequate	X	X	X	X	X	All new locations. Only a few locations in early boreholes from 1986–87, 1995, 2000, 2006 and 2010.
Time series absent		X	X	X	X	The remaining other locations.
Sample series** adequate	X	X	X	X	X	Four old sampling locations (annual sampling), KFR101 and inner section of KFR105.
Sample series inadequate		X	X	X	X	Most of the remaining old locations (~each fifth year).
Sample series absent			X	X	X	Most new boreholes; a few early locations sampled once.
Suitable section length	X	X	X	X	X	Generally, section length > 20 m = category 3 and section lengths > 100 m = category 4. The sample quality depends also on the number of flow anomalies in the section, and if the water volume to be exchanged prior to sampling was sufficient. When possible, this volume was estimated using plug flow calculations.
Sampling during drilling				X	X	Few samples; all of them in new boreholes.
Charge balance ≤ ± 5%	X	X	X	X		The first investigation in 1984–86 was discarded together with a few other samples.
Major ions complete	X	X	X	X	X	Absent for many early samples.
Major ions incomplete			X	X	X	
Environmental isotopes complete	X	X	X	X	X	Absent for many early samples.
Environmental isotopes incomplete		X	X	X	X	
Instable composition in time series (generally due to pressure gradients in borehole)					X	
Pressure responses between sections			X	X	X	Category no. depends on size of response.

*Time series = at least three samples collected during continuous pumping or discharge from tunnel borehole (duration of days or weeks). An adequate time series refers to a sufficient number of samples to show that the groundwater composition has achieved stability with time (i.e. hours, days to weeks) following drilling and other borehole activities, prior to and during groundwater sampling.

**Sample series = several separate sampling occasions (annually, each fifth year or weeks to months inbetween the main occasions). An adequate sample series refers to a sufficient number of groundwater samples to be able to trace changes in groundwater composition with time (i.e. months to years), for example, the gradual transient effects of drawdown due to excavation and construction at the SFR. Availability increases the quality but stability or trends do not influence the quality categorisation.

Table A1-2. Categorisation criteria for percussion drilled boreholes.

Percussion boreholes Aspects/Conditions	1	2	3	4	5	Comment
Flow log available	X	X	X	X	X	
Time series* adequate	X	X	X	X	X	
Time series absent		X	X	X	X	
Sample series** adequate	X	X	X	X	X	
Sample series inadequate		X	X	X	X	
Sample series absent			X	X	X	
Suitable section length	X	X	X	X	X	Section length > 20 m = category 3. Section lengths > 100 m = category 4. The sample quality depends also on number of flow anomalies in the section and if the necessary water volume to be exchanged prior to sampling is calculated using plug flow calculations.
Charge balance ≤ ± 5%	X	X	X	X		
Major ions complete	X	X	X	X	X	
Major ions incomplete			X	X	X	
Environmental isotopes complete	X	X	X	X	X	
Environmental isotopes incomplete		X	X	X	X	
Instable composition in time series (generally due to pressure gradients in borehole)					X	
Pressure responses between sections			X	X	X	Depends on size of response

*Time series = at least three samples collected during continuous pumping or discharge from tunnel borehole (days or weeks duration). An adequate time series refers to a sufficient number of samples to show that the groundwater composition has achieved stability with time (i.e. hours, days to weeks) following drilling and other borehole activities prior to and during groundwater sampling.

**Sample series = several separate sampling occasions (annually, each fifth year or weeks to months inbetween the main occasions). An adequate sample series refers to a sufficient number of groundwater samples to be able to trace changes in groundwater composition with time (i.e. months to years), for example, the gradual transient effects of draw-down due to excavation and construction at the SFR. Availability increases the quality but stability or trends do not influence the quality categorisation.

Time series and sample series data

The possible impacts on analytical quality and sample representativity from different causes may to some extent be excluded or verified by other samples from the same borehole section. Available time series data, i.e. several samples collected during continuous discharge from the borehole section (during days/weeks), is desired in order to prove the stability/representativity of the water composition or to discover trends during sampling that reveal sampling and representativity problems and may be an effect of, for example, introduction of shallower water due to pressure gradients. Time series groundwater samples were collected routinely within the SFR extension project, but from the early stages of the SFR repository only a few time series from a few borehole sections and sampling occasions are available. The time series are either adequate (minimum three samples) or absent which effects the quality assessment. Furthermore, stability improves and trends decrease the sample quality.

On the other hand, the long sample series of single samples collected regularly between 1986 and 2010 are also useful for the quality evaluation of data. Plots of chloride, magnesium and $\delta^{18}O$ trends with time are presented below for each borehole section if enough data are available. A stable water composition or a clear trend in the data strengthens the reliability but an unstable or irregular composition during the time period in question may be quite representative and does not necessarily reflect poor sampling quality. The sample series are either adequate, inadequate or absent which effects the quality assessment. Stability improves, but instability does not necessarily lower the quality.

Section lengths

The length of the borehole section being sampled, in combination with the number and position of the flow anomalies present in the section, impact on the sample quality in two aspects. First, it affects the possibilities to resolve the differences in groundwater composition along the borehole.

Secondly, the risk that the sample contains a significant contribution of unrepresentative or contaminated water that has remained in the borehole section for some time increases with increasing section length. Since flow logging data are not available from the early boreholes, no plug flow calculations could be performed in order to estimate the discharge volume needed in order to obtain samples with an insignificant contribution from water remaining in the borehole section. The section length limits > 20 m and > 100 m lowered the quality to categories 3 and 4, respectively.

Charge balance

Historically at SKB, a maximum charge imbalance of ± 5% (valid for all groundwaters in the salinity range encountered at SFR) has been considered acceptable. With greater imbalance, the samples are excluded for modelling purposes (category 5).

Complete sets of analyses

The major ions should be complete, i.e. it should be possible to calculate a relevant charge balance, and otherwise the sample is assessed as a category 4. If only minor, but important ions such as Fe or Mn are missing, the sample is assessed as a category 3.

Pressure responses between sections

All sampling, including the time period 1986 to 2010 as well as from all boreholes, early SFR repository boreholes as well as recent SFR extension project boreholes, have been conducted in borehole sections equipped with fixed packer equipment and pressure sensors for pressure measurements. Therefore, pressure responses may be revealed in adjacent borehole sections during sampling and these may be due to connection via the fracture system in the bedrock (indicated by delayed response) or leakage over the packers (immediate response). The implication for the sample quality is obviously that groundwater representing different borehole sections and flow anomalies are mixed.

Factors not considered

Other factors that may affect the sample quality but have been disregarded as quality criteria are:

1. Gas lift pumping could lower the quality; this is commented on in Section 1.5.2.

2. Calculated volume of water to be exchanged before sampling (Plug flow calculation) could increase/verify the quality, especially in cases with long section lengths.

3. The inclusion of old analyses, prior to the use of ICP AES as a routine procedure (i.e. before 1990), may lower the analytical quality.

A1.3   Results

The results of the sample quality assessment performed for the samples representing the SFR extension boreholes (time period 2007 to 2010) and the SFR repository boreholes (time period 1986/87 to 2010) are presented in this chapter. For the repository boreholes and for borehole KFR101, the borehole specific presentation includes also time series plots of chloride, magnesium and $\delta^{18}O$ for the time periods 1986/87 to 2010 and November 2008 to December 2010, respectively. These constituents/variables are plotted since they represent the basis for the groundwater type classification and their stability/instability has therefore some implications. A summary presenting the number of samples belonging to each quality category (the rejected samples, i.e. category 5, are not included) each year is given in Figure 3-1. It should be remembered that even though to assess the sample quality is not a straightforward procedure, it is still believed that this categorisation as presented in Figure 3-1 provides a good general idea of the quality of the dataset used in the SFR modelling.

It may be commented on that the large number of category 4 samples in 1995 was due mainly to incomplete analyses and that the single category 1 sample in the spring of 2000 represented only borehole KFR01. The three category 1 samples in 2010 all represented the extended SFR investigation in borehole KFR19.
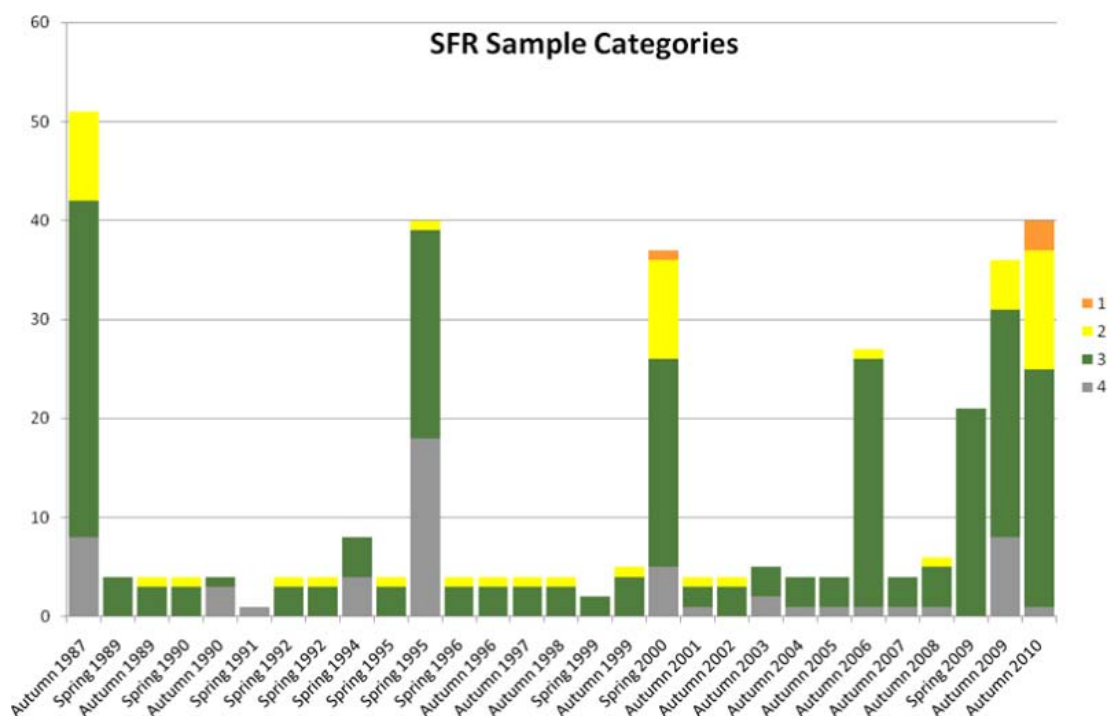
Figure A1-1. *Relation of sample numbers assessed to each of the four chosen quality categories represent-ing each year and season during the time period 1986/87 to 2010.*

A1.3.1 SFR extension boreholes

The SFR extension boreholes have PFL-f data (i.e. water yielding fractures identified by Posiva flow log) and therefore the number and position of the flow anomalies that exceed the detection limit (generally 1E–9 m^2s^{-1}) is known. This information along the boreholes and the sampled sections are provided for each borehole to give a general idea of the borehole characteristics and the sampling conditions. For example, the section lengths and the number of the flow anomalies contained in the borehole section and their transmissivities determine the possibility to obtain representative enough samples. Flow anomaly information is necessary in order to estimate roughly the volumes that have to be exchanged in order to obtain suitable formation groundwater samples from fractures in the bedrock, i.e. avoiding volumes of stagnant, possibly contaminated water that has been for some time in the borehole. Furthermore, sample time series (days to weeks) have been collected from all the sampled SFR extension boreholes to verify stable water composition during pumping or discharge of water by overpressure (tunnel borehole KFR105).

Borehole KFR101

Borehole KFR101 was completed in July 2008 and packer equipment was installed in September 2008. Initially, this borehole was not planned for hydrogeochemical sampling, however, due to the observed very low EC (600 mS/m) measured at the bottom of the borehole during PFL logging, groundwater sampling turned out to be essential for site understanding.

Drilling water: Tap water (sampled and analysed) was used as the drilling water source and found to decrease from 3.4% in the first sample to 1.2% in the last sample.

Hydraulic/hydrogeological information: Transmissivity values from the PFL-f logging plotted along the borehole are given in Figure A1-2. The largest transmissivities are found in deformation zone ZFMNW0805A (the sampled section) and B, and at the intersection with zone DZ3. This latter zone is subhorizontal and is included in the deterministic subhorizontal 'Shallow Bedrock Aquifer' feature SBA6 (see Section 2.2.3 and Öhman et al. (2011)).

Groundwater sampling: Groundwater samples from the bottom section in KFR101 at 279.5 to 341.8 m were collected at three different occasions; the first in November 2008 and then in February 2009 (3 samples), in March 2009 (4 samples) and the last sample in December 2010 (Thur and Nilsson 2009a). This final sample was also selected for [36]Cl isotope determinations. The chloride, magnesium and $\delta^{18}O$ trends are displayed in Figure A1-3 a–c. Since the sampled section is of the simple type for pressure measurements and not a circulation section, air lift pumping with nitrogen gas was used to pump the groundwater to the ground surface during sampling. The possible impacts are treated in Section 1.5.2 in the main report. Plug flow calculations were conducted in order to interpret the volume to be removed from the relatively long borehole section prior to sampling.

Sample quality assessment for borehole KFR101.

Borehole section and vertical elevation	Number of samples in Dataset I	Sample quality categories and number of samples in each category.					Comments
		1	2	3	4	5	Category 1 is of the highest, and category 5 is of the lowest, quality.
KFR101:1 279.5–341.8 m **Mid. vertical elevation –240.2 m**	9			8		1	Due to the long section, eight samples are assigned to a category 3. Otherwise five of the samples would have been category 2 (sample series are inadequate but time series are adequate). Fe and Mn are missing for two samples. One sample is of category 5 due to charge imbalance and therefore transferred to Dataset II.
Adequate time series		**Time period**					**Comments**
Time series, 3 samples		February 2009					Stable composition. Some major concentrations are lower than in samples collected before and after this occasion.
Time series, 4 samples		**March 2009**					**Stable composition.**
Two single samples		November 2008 December 2010					Composition similar to sample series collected in March 2009. [36]Cl isotope determinations carried out in December 2010

Borehole section information: The section transects the deformation zone ZFMNW0805a (formerly Zone 8a) at 242.0 to 341.76 m, Figure A1-2.

Pressure responses: No clear responses in the other borehole sections were observed during pumping and sampling, and their absence indicates that no short-circuiting has affected the samples.

Available/missing data: Complete analyses including isotopes and trace metals. In addition, this borehole section has been analysed for [36]Cl, i.e. KFR101:1, KFR105:1, KFR08:1 and KFR7A:1.

Questionable data: None.

Groundwater composition: The available time series samples (short term) and the repeated sampling in 2008, 2009 and 2010 (sample series), verifies that the dilute water composition is quite stable. From EC logging it is concluded that the salinity in the shallower parts of the borehole is higher than in the sampled bottom section. The water samples from the bottom section are less saline than the Baltic Sea water and the [18]O values show a clear glacial meltwater signature. Furthermore, the carbon-14 and the [36]Cl values support long residence times. All samples have been classified as belonging to the Brackish-glacial groundwater type. Very late samples (June 2011) from the bottom section of borehole KFR104 show similar groundwater compositions which indicate that very dilute groundwaters may be more common than earlier believed.

KFR101 (50.7º/ 33.5º), Length = 341.76 m
PFL-logged (13.72-330.76 m)
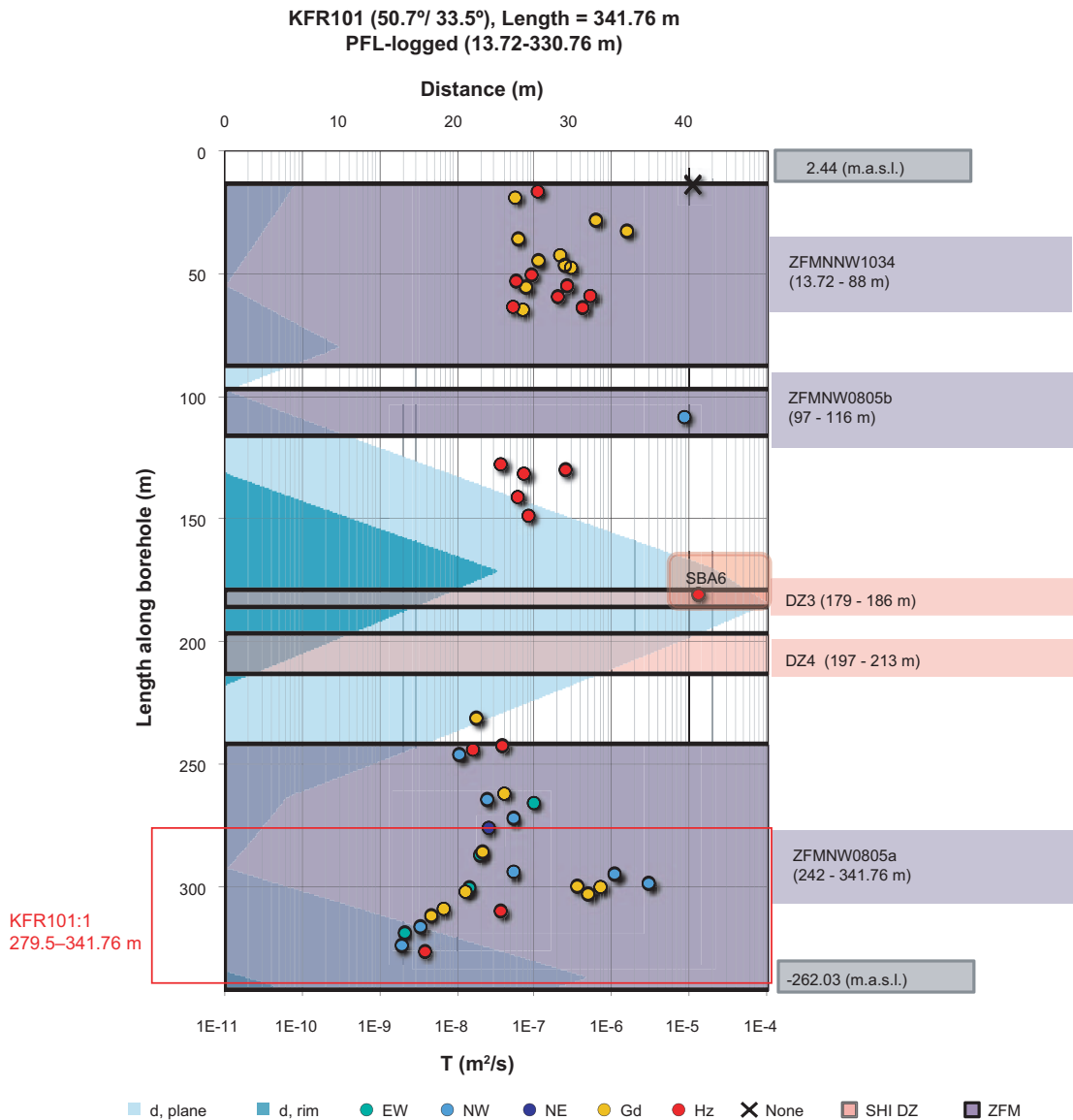
Figure A1-2. *Hydraulic data for KFR101 with the sampled borehole section at the bottom of the borehole framed in red. Groundwater from high transmissive NW-striking steep PFL-f structures at 300 m dominates in the flow from the borehole section. Blue shadings show distance to the central plane and the rim of nearest deformation zone, respectively. The PFL-f structure at 13.7 m borehole length is assumed to reflect a leaking casing. High transmissive NW-striking steep PFL-f structures occur within WNW0805A and B. The PFL-f data outside major zones are few and indicate low transmissivity (modified after Öhman et al. 2011).*
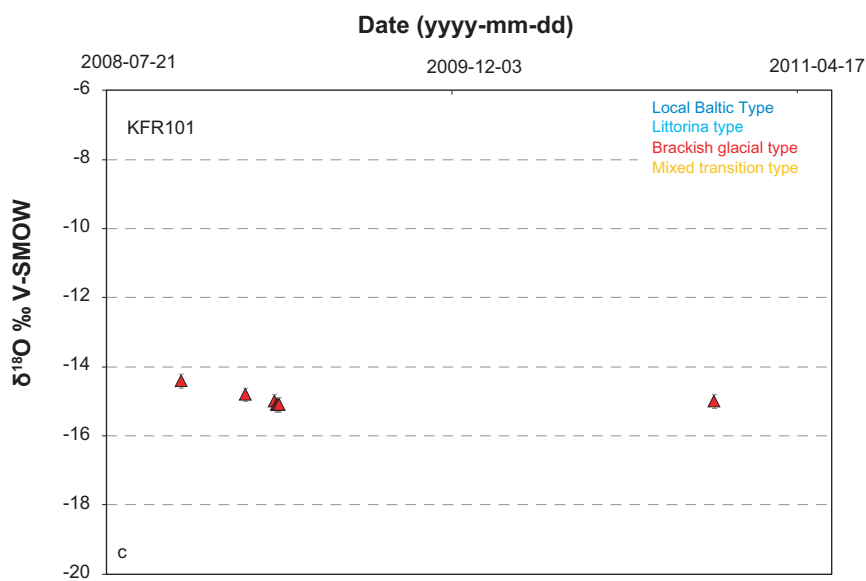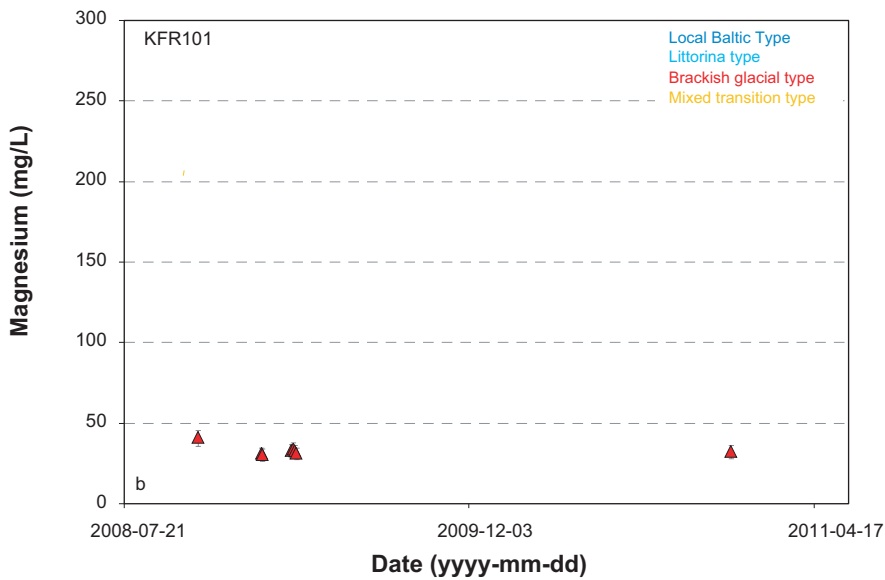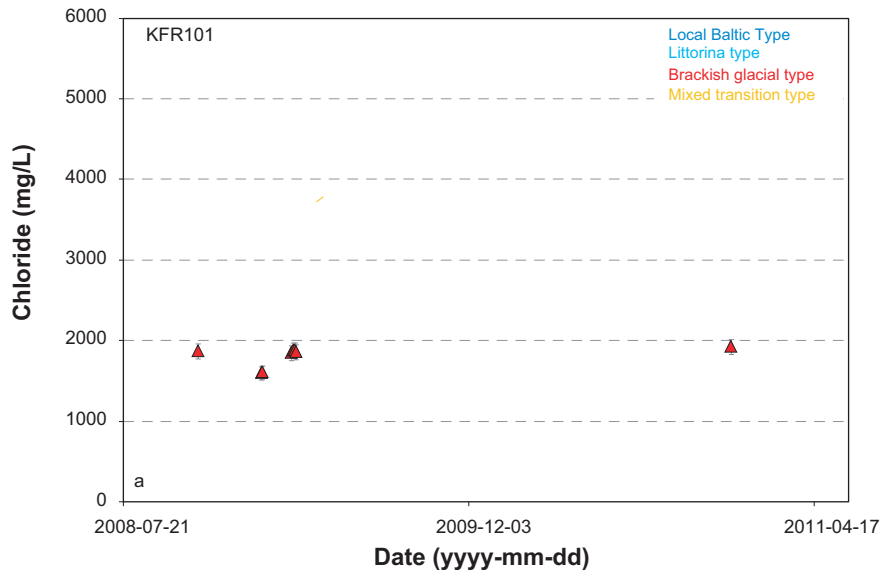
Figure A1-3 a–c. *Borehole KFR101; chloride, magnesium and δ¹⁸O trends from 2008 to 2010. The error bars represent 5%, 12% and 0.2 (‰ V-SMOW), respectively.*

Borehole KFR102A

Borehole KFR102A is the deepest borehole drilled during the SFR extension project and it was completed in December 2008 with packer equipment installed in March 2009. This is the only borehole of the telescopic type, otherwise used as a standard during the previous Forsmark site investigations. Two of the installed borehole sections, one at intermediate depth and one at the bottom, are circulation sections and intended for groundwater sampling.

Hydraulic/hydrogeological information: Transmissivity values from PFL logging are plotted along the borehole in Figure A1-4. The shallowest PFL-f structure, located at 72 m borehole length, is assumed to reflect an inflow at the interval 70.4 to 72 m borehole length that is hidden behind the steel pipe. These upper PFL-f structures are possibly related to the horizontal structure SBA2. Highly transmissive flow anomalies are detected at approximately 190–205 m borehole length and have been alternatively modelled as a shallow hydrogeological structure SBA6. The sampled section at around 215 m borehole length, just below the very transmissive flow anomalies, was selected for groundwater sampling to lower the risk of excessive drilling water contamination. There is also a horizontal radar reflector just below this interval (71°/12°) at 215 m borehole length. The bedrock between ZFMNE3112 and ZFMENE3115 is remarkable in that there is an absence of detected PFL-f inflows. A gently dipping PFL-f structure with high transmissivity is found in porous granite inside the intercept of ZFMENE3115 which is the steeply dipping deformation zone that terminates ZFM871 to the southeast. The deepest part of KFR102A, below its intersection of ZFMENE3115, is located underneath ZFM871 (Zone H2) (Öhman et al. 2011).

Drilling water: Tap water (sampled and analysed) was used as the drilling water source and found to vary between 2 and 3% in both borehole sections with no decreasing trend observed.

Groundwater sampling: The samples (two time series of five groundwater samples each) from the two borehole sections were all collected in March 2009 (Thur and Nilsson, 2009b). Plug flow calculations were conducted in order to interpret the volume to be removed from both borehole sections prior to sampling and the subsequent time series were collected during ten days of pumping. Pumping was performed in a stand pipe connected to the installed circulation section.

Sample quality assessment for borehole KFR102.

Borehole section and vertical elevation	Total number of samples in Dataset I	Sample quality categories and number of samples in each category					Comments
		1	2	3	4	5	Category 1 is of the highest, and category 5 is of the lowest, quality.
KFR102A:4 214.0–219.0 m Mid. vertical elevation −194.6 m	5		5				The drilling water content ≤ 5% and the absence of sample series classify the samples as category 2.
KFR102A:2 423.0–443.0 m Mid. vertical elevation −388.97 m	5		5				The drilling water content ≤ 5% and the absence of sample series classify the samples as category 2.

Section information: The upper section represents flow anomalies just below a water bearing structure (SBA6) (see Section 2.2.3) and is not defined as a deformation zone. The lower section intersects deformation zone ZFMENE3115 at 422 to 503 m (see Figure A1-4).

Pressure responses: No clear responses in the other borehole sections were observed during pumping and sampling in either borehole section; this indicates no short circuiting between the sections that could have affected the samples.

Available/missing data: Complete analyses including isotopes and trace elements.

Questionable data: None.

Groundwater composition: The groundwater samples from the intermediate section are more saline than the bottom section; all samples have been classified as mixed Transition groundwater type.
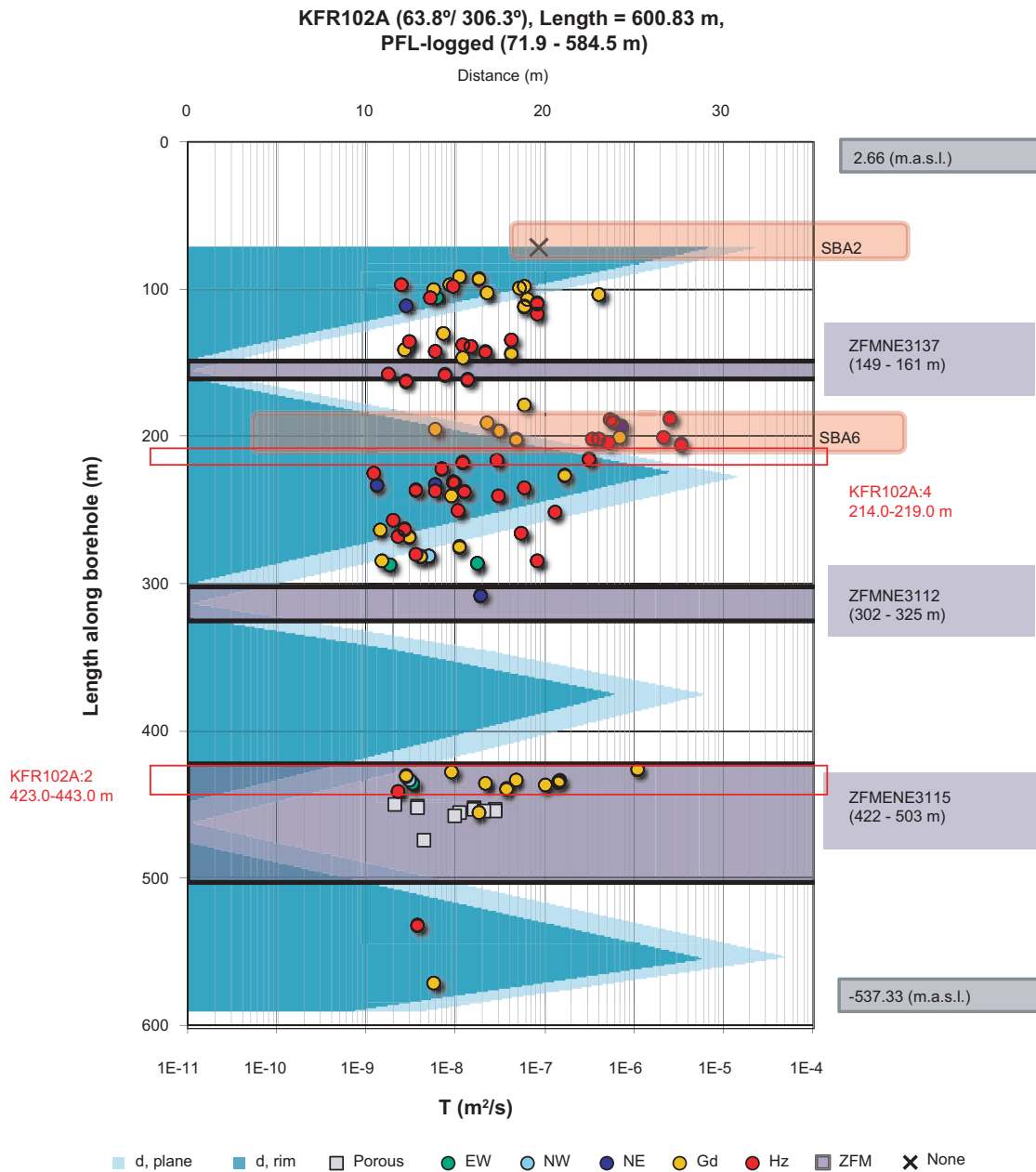
Figure A1-4. *Hydraulic data for KFR102A with the sampled borehole sections below 200 m and 400 m framed in red. Blue shadings show distance to the central plane and the rim of the nearest deformation zone, respectively. The sampled sections represent two parts of the borehole with high transmissive horizontal PFL-f structures at about 200 m and gently dipping PFL-f structures at about 415 m, respectively, whilst the part between ENE3112 and ENE3115 has a remarkable lack of PFL-f inflow (modified after Öhman et al. 2011).*

Borehole KFR104

Borehole KFR104 is located inside the Central Block and was completed in September 2008. It is of the conventional type whichprevents the installation of circulation sections for groundwater sampling. Initially no sampling was planned but in the late modelling stage it became apparent that the lack of data in the Central Block was a serious shortcoming which had to be rectified.

Hydraulic/hydrogeological information: Transmissivity values from PFL logging are plotted along the borehole in Figure A1-5 showing that the frequency and transmissivity of the flow anomalies decreases notably with depth. An exceptionally large *in situ* drawdown was estimated from the PFL-f data in the interval 145 to 320 m borehole length which reflects an indirect hydraulic connection to SFR or ZFM871 (Zone H2). However, the groundwater in the sampled section represents three isolated PFL-f structures, two in bedrock between zones and one within deformation zone ZFMWNW3267 (Öhman et al. 2011).

Drilling water: Borehole HFR101 was used as the drilling water source which increased from insignificant to about 4% in the samples during pumping. This may explain the somewhat increasing salinity in the three samples with time since the drilling water was of the Baltic groundwater type, i.e. more saline than the groundwater in the sampled borehole section.

Groundwater sampling: Three groundwater samples from the bottom section at 333.0 to 454.6 m were collected in June and July 2011. Since the sampled section is of the simple type for pressure monitoring and not a circulation section, air lift pumping with nitrogen gas was used to transport the groundwater to the ground surface during sampling; possible impacts are treated in Section 1.5.2 in the main report. Plug flow calculations were conducted in order to interpret the volumes (0.7, 1.5 and 2.5 m^3) to be discharged from this long borehole section prior to collection of the three samples.

Sample quality assessment for borehole KFR104.

Borehole section and vertical elevation	Total number of samples in Dataset I	Sample quality categories and number of samples in each category					Comments
		1	2	3	4	5	Category 1 is of the highest, and category 5 is of the lowest, quality.
KFR104:1 333.0–454.57 m mid. vertical elevation –306.2 m					3		Due to the long borehole section the three samples are assigned to a category 4

Section information: The sampled section is located within deformation zone ZFMWNW3267 and in the Central Block.

Pressure responses: No clear pressure responses in the other near-vicinity borehole sections were observed during pumping and sampling.

Available/missing data: Reduced analytical programme included basic water analyses and tritium, deuterium and δ^{18}O (SKB class 3). No other isotope determinations or trace metal analyses were performed.

Questionable data: None.

Groundwater composition: An extreme water composition with very low salinity was encountered in the bottom section of KFR104; this was less saline than the Baltic Sea water and the ^{18}O values show a clear glacial meltwater signature. The three time series samples (short term) indicate a somewhat increasing salinity trend that cannot be entirely explained by increasing drilling water content. A more probable explanation is different contributions from the three flow anomalies in the borehole section with varying groundwater composition. From EC logging it is concluded that the salinity in the shallower parts of the borehole is higher than in the sampled bottom section. All samples have been classified as belonging to the brackish-glacial groundwater type. The previous samples from the bottom section of borehole KFR101 showed similar groundwater compositions, which suggest that very dilute groundwaters may be present at more locations than earlier believed.

KFR104 (51.3º/ 132.2º), Length = 454.57 m
PFL-logged (8.7 -240 m), coarsely (240 - 438.2 m)
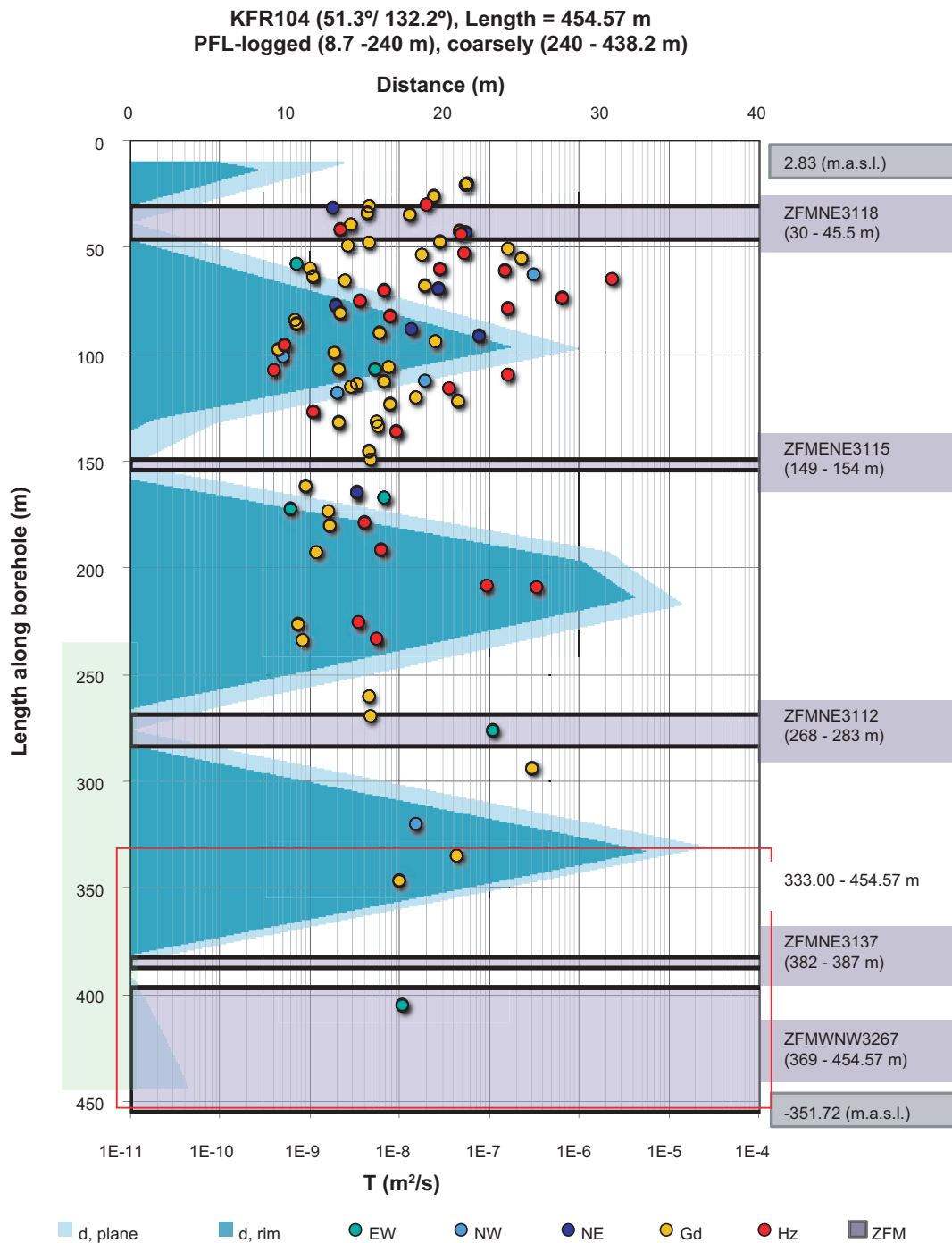
Figure A1-5. _Hydraulic data for KFR104 with the sampled borehole section at the bottom of the borehole framed in red. Blue shadings show distance to the central plane and the rim of nearest deformation zone, respectively. Steep EW-striking PFL-f structures are found in ENE3112 and in WNW3267. The horizontal high transmissive PFL-f structure at about 210 m borehole length has the lowest fresh water head (–15.9 m), suggesting hydraulic connection to the SFR (modified from Öhman et al. 2011)._

Borehole KFR105

Borehole KFR105 was completed in October 2008 and packer equipment to delimit five borehole sections was then installed. This borehole is located inside the Central Block and is a borehole drilled subhorizontally underground south from the lower construction tunnel of the SFR. The depth difference along the borehole from top to bottom is about 40 m and the borehole location is given in Figure 1-3 in the main report.

Hydraulic/hydrogeological information: Transmissivity values from the PFL-f logging are plotted along the borehole in Figure A1-6. KFR105 intersects three NE- to ENE-striking deformation structures, ZFMENE3115, ZFMNE3112, and ZFMNE3137, as well as the two WNW-striking zones ZFMWNW8042 and ZFMWNW3267. With the exception of ZFMWNW8042, there are no general signs of increased transmissivity within the deformation zone intercepts.

Drilling water: The lower drainage basin provided the drilling water (sampled and analysed); for location of the basin, see Figure 2-17 in the main report. As expected, no drilling water content was measured (0%) in any of the collected samples since the water flow is directed towards the tunnel and the risk of contamination from drilling, drilling water or other activities is small.

Groundwater sampling: Samples (time series of 4 to 10 groundwater samples) were collected by opening valves (the flow is obtained due to pressure gradients) from the five borehole sections between July 2009 and December 2010 (Lindquist and Nilsson 2010). Redox measurements and exdended sampling/analyses were conducted from sections KFR105:1 and KFR105:4. Plug flow calculations were performed in order to interpret the volume to be removed from the borehole sections prior to sampling.

Sample quality assessment for borehole KFR102.

Borehole section and vertical elevation	Total number of samples in Dataset I	Sample quality categories and number of samples in each category					Comments
		1	2	3	4	5	Category 1 is of the highest, and category 5 is of the lowest, quality.
KFR105:5 4.0–119.0 m Mid. vertical elevation –117.4 m	4				4		The long borehole section implies category 4. Otherwise the quality corresponds to category 2.
KFR105:4 120.0–134.0 m Mid. vertical elevation –128.4 m	5		5				Extended investigations and analyses were judged to assign a category 2. Gas and microbe data are available. Responses were observed between the three intermediate borehole sections in this borehole. Due to the subhorizontal direction of the borehole and the small difference in depth between the three sections, the samples were not assigned a category 4.
KFR105:3 138.0–169.0 m Mid. vertical elevation –132.7 m	4			4			The long borehole section implies category 3. Responses were observed between the three intermediate borehole sections in this borehole. Due to the subhorizontal direction of the borehole and the small difference in depth between the three sections, the samples were not assigned a category 4.
KFR105:2 170.0– 264.0 m Mid. vertical elevation –142.9 m	4			4			The long borehole section implies a category 3. Responses were observed between the three intermediate borehole sections in this borehole. Due to the subhorizontal direction of the borehole and small difference in depth between the three sections, the samples were not assigned a category 4.
KFR105:1 265.0–306.8 m Mid. vertical elevation –153.6 m	10			10			Extended investigations and analyses; Eh, gas and microbe data are available. Four sampling occasions; time series of 5 samples from 2009-07-14 to 2009-07-27. Time series of 3 samples from 2010-01-18 to 2010-02-15. Two single samples from 2009-08-11 and 2010-12-03. The long borehole section implies category 3.

Section information: Section 4.0–119.0 m includes the deformation zones ZFMENE3115 and ZFMNE3112; sections 120.0–134.0 m and 138.0–169.0 m are completely within the bedrock between the deformation zones. Section 170.0–264.0 m intersects the three deformation zones ZFMWNW8042, ZFMWNW3267 and ZFMNE3137. Finally, section 265.0–306.8 m intersects deformation zone ZFMWNW3267.

Pressure responses: Pressure responses were observed between the three intermediate borehole sections; the similar water composition indicates that these sections are short circuited.

Available/missing data: Complete analyses including isotopes and trace metals. The bottom borehole section has also Eh measurements and ^{36}Cl isotope determinations are available for KFR101:1, KFR105:1, KFR08:1 and KFR7A:1.

Questionable data: None.

Groundwater composition: Generally, the samples from the first to fourth sections provide groundwater of the mixed Transition type while the groundwater samples from the bottom section are all clearly Brackish-glacial type. The three intermediate sections have very similar groundwater compositions, clearly on the mixed Transition type side, and the groundwater from the first section is close to the borderline between Brackish-glacial and mixed Transition type.
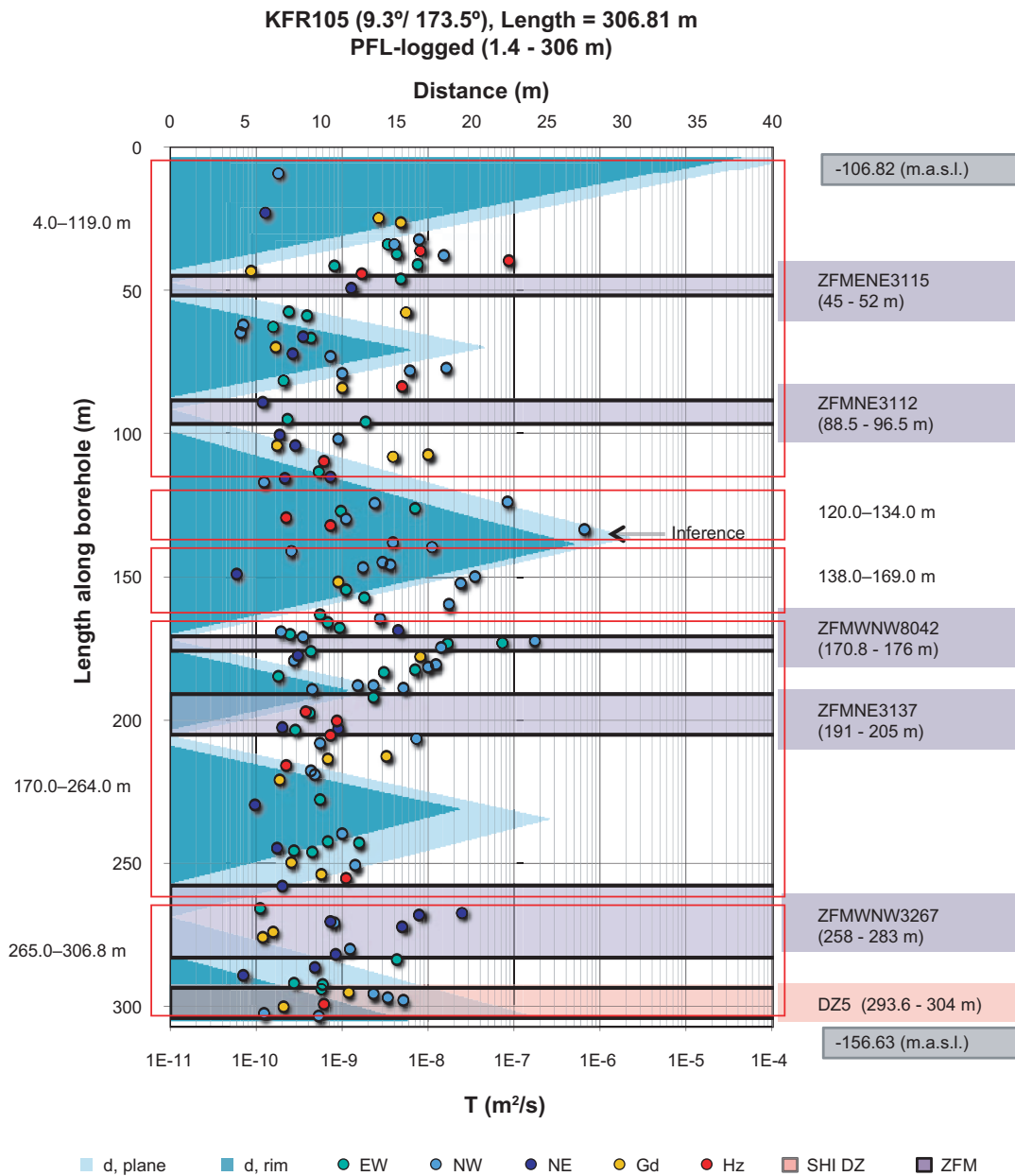

Figure A1-6. Hydraulic data for KFR105 with the sampled borehole sections along the borehole framed in red.Blue shadings show distance to the central plane and the rim of nearest deformation zone, respectively. Inferences were registered in surrounding boreholes when the drilling of KFR105 reached 133 m length (arrow) (modified from Öhman et al. 2011).

Borehole KFR106

Borehole KFR106 was completed in September 2009 and packer equipment to delimit three borehole sections was installed. It was drilled from a small island outside the SFR harbour; the location is given in Figure 1-3 in the main report. Although the borehole was not originally intended for hydrogeochemical sampling, it was decided following the recorded possible presence of solid phase uranium (Sandström et al. 2011) to characterise the groundwater chemistry as a complement to the mineralogy.

Hydraulic/hydrogeological information: Transmissivity values from the PFL logging are plotted along the borehole in Figure A1-7 showing that KFR106 reflects a strong hydraulic character typical of the Northern boundary belt. The borehole is dominated by horizontal, high-transmissive PFL-f structures, not only within the deformation zone intercepts, but also in the less fractured rock in between (Öhman et al. 2011).

Drilling water: Seawater (sampled and analysed) provided the drilling water which decreased in content in the upper borehole section from 5.5 to 4.8% in the final sample, and in the lower borehole section from 6.4 to 6%.

Groundwater sampling: Samples (time series of 3 groundwater samples) were collected by air lift pumping using nitrogen gas in November 2009 (Sandström et al. 2011). Plug flow calculations were performed for the long borehole sections in order to check the possibility of suitable representative samples and to interpret the volume to be removed prior to sampling. The two lower of the three sealed borehole sections were judged suitable for sampling.

Sample quality assessment for borehole KFR106.

Borehole section and vertical elevation	Total number of samples in Dataset I	Sample quality categories and number of samples in each category					Comments
		1	2	3	4	5	Category 1 is of the highest, and category 5 is of the lowest, quality.
KFR106:2 143.0–259.0 m Mid. vertical elevation –117.4 m	3				3		The long borehole section implies category 4. Otherwise, the quality corresponds to category 2 and 3 depending on drilling water content.
KFR106:1 260.0–300.0 m Mid. vertical elevation –261.0 m	3			3			Because of the section length and the drilling water content, a category 3 was assigned.

Borehole section information: Both borehole sections intersect deformation zone ZFMNNW1034 at 256 to 266 m.

Pressure responses: Equipment for pressure measurements was not installed during the sampling occasion and possible responses between sections could not be revealed.

Available/missing data: Complete analyses including isotopes and trace metals.

Questionable data: None.

Groundwater composition: The two time series from each borehole section show stable groundwater compositions. The samples from the central borehole section show mixed Transition type groundwater while the bottom section provides groundwater of Brackish-glacial type.

KFR106, PFL-logged (9.1-293.6 m)
69.4º/ 197.6º , Length = 300.13 m
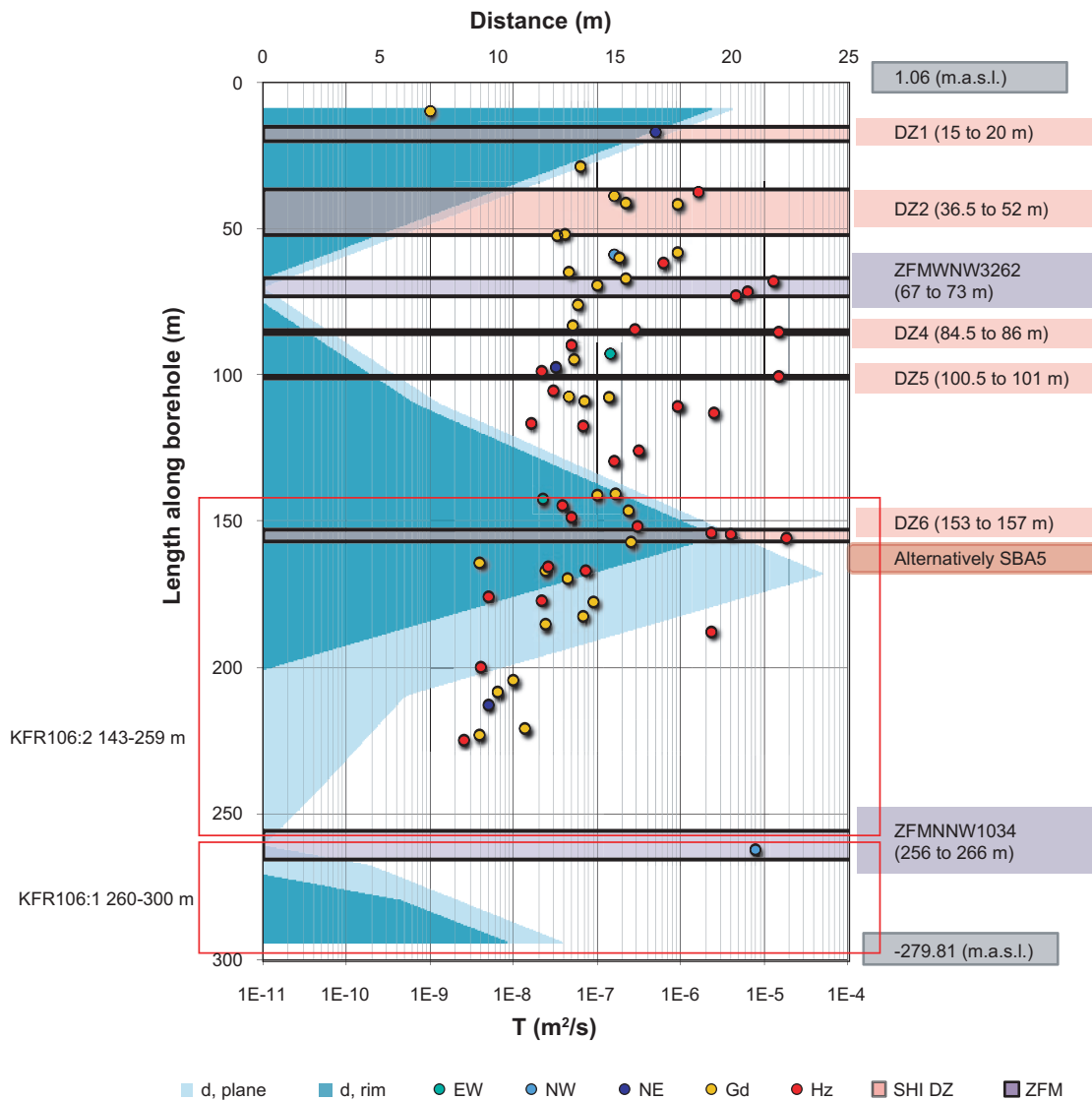
Figure A1-7. Hydraulic data for KFR106 with the two sampled borehole sections framed in red. Blue shadings show distance to the central plane and the rim of the nearest deformation zone, respectively. High transmissive horizontal PFL-f structures are found in zone KFR106_DZ6 and a single high transmissive, steep NW-striking PFL-f structure is found in zone NNW1034. Under undisturbed conditions outward directed flow is only measured in ZFMWNW3262, KFR106_DZ4, KFR106_DZ5 and NNW1034, suggesting distant connections to the SFR (modified after Öhman et al. 2011).

Borehole HFR101

The 209.0 m long percussion borehole HFR101 was completed in May 2008.

Hydraulic/hydrogeological information. Hydraulic tests using the HTHB equipment (Hydro-Testutrustning för HammarBorrhål) located two flow anomalies; a shallow one from 107.3 to 108.0 m borehole length is dominating (T(total) = 2.8E–6 m^{2}S^{-1}, T(anomaly) = 2.6E–6m^{2}s^{-1}), see Figure A1-8.

Groundwater sampling: Samples (time series of 3 groundwater samples) were collected from the entire borehole using the HTHB equipment in May 2008. Three samples were also collected from the drilling water line in September–October 2008 when the borehole was used as a drilling water source.

Sample quality assessment for borehole HFR101.

Borehole section and vertical elevation	Total number of samples in Dataset I	Sample quality categories and number of samples in each category					Comments
		1	2	3	4	5	Category 1 is of the highest, and category 5 is of the lowest, quality.
HFR101 0.0–209.0 m mid. vertical elevation –71.58 m	6				6		The long borehole section implies category 4. The actual sampled section may be considered to be between 107.3 to 108.0 m, since this flow anomaly is clearly dominating.

Borehole information: The borehole intersects deformation zones ZFMNE0870 and ZFMNE3118 at 28 to 41 m, and 190 to 202 m, respectively.

Groundwater composition: Comparison of the two time series from the entire open borehole indicate a minor decrease in salinity and somewhat increasing marine signature (increase in Na and decrease in Ca) with time; however, the difference is not that significant and the $\delta^{18}O$ values all lie between –9.6 and –10.6 (V-SMOW), i.e. the groundwater is classified as being of mixed Transition type.

Borehole HFR105

The 200.5 m long percussion borehole HFR105 was completed in April 2008.

Hydraulic/hydrogeological information: Hydraulic tests were carried out using the HTHB equipment (HydroTestutrustning för HammarBorrhål). The flow log shows that the major input occurs between 55.6 and 120.0 m borehole length, (T(total) = $2.3E–5\ m^2S^{-1}$), see Figure A1-8.

Groundwater sampling: Samples (time series of 3 groundwater samples) were collected in April 2008 from the entire open borehole using the HTHB equipment.

Sample quality assessment for borehole HFR105.

Borehole section and vertical elevation	Total number of samples in Dataset I	Sample quality categories and number of samples in each category					Comments
		1	2	3	4	5	Category 1 is of the highest, and category 5 is of the lowest, quality.
KFR105 0.0–200.5 m Mid. vertical elevation –86.73 m	3				3		The long borehole section implies category 4. The actual sampled section may be considered to be between 55.6 to 120.0 m where the major input occurs.

Borehole information: The borehole intersects deformation zones ZFMWNW0001 (i.e. Singö) and ZFMWNW1035 at 21 to 92 m and 119 to 147 m, respectively.

Groundwater composition: The time series data show stable groundwater composition and the borehole is characterised by groundwaters of Baltic Sea type.

Borehole HFR106

The 209.0 m long percussion borehole HFR106 was completed in July 2008.

Hydraulic/hydrogeological information.: Hydraulic tests were carried out using the HTHB equipment (HydroTestutrustning för HammarBorrhål). Two highly transmissive flow anomalies were observed, the shallow one (38–40 borehole length) with T(anomaly) = $1.2E–5m^2s^{-1}$, and the deeper one (178–180 m borehole length) with T(anomaly) = $1.1E–5m^2s^{-1}$, see Figure A1-8.

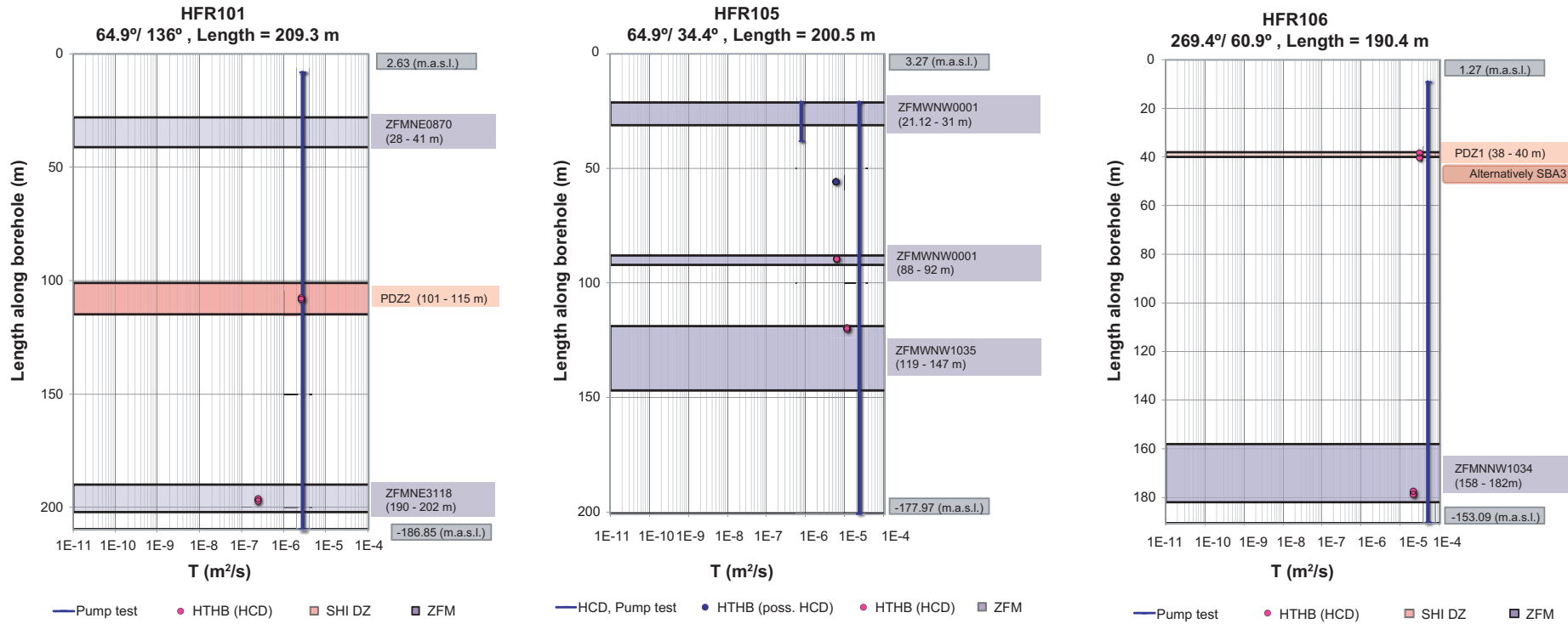**Figure A1-8.** *Hydraulic data of HFR101, HFR105 and HFR106 together with locations of deformation zones as defined by the geology and the possible deformation zones observed from single hole interpretations. The samples from HFR101 and HFR105 represented the entire boreholes. Two delimited sections were sampled in HFR106 at 36.0–41.0 m and 175.0–190.4 m borehole lengths (Öhman et al. 2011).*

Groundwater sampling: Samples (time series of 3 groundwater samples) were collected from two delimited borehole sections at 36.0 to 41.0 m and 175.0 to 195.4 m using the HTHB equipment in July 2009 (Thur et al. 2009).

Sample quality assessment for borehole HFR106.

Borehole section and vertical elevation	Total number of samples in Dataset I	Sample quality categories and number of samples in each category					Comments
		1	2	3	4	5	Category 1 is of the highest, and category 5 is of the lowest, quality.
HFR106 36.0–41.0 m Mid. vertical elevation –31.36 m	3			3			Sample series are absent but time series are adequate and the samples are assigned a category 3.
HFR106 175.0–190.4 m Mid. vertical elevation –146.9 m	3				3		Sample series are absent but time series are adequate. However, the samples show an increasing salinity trend and therefore the samples are assigned a category 4.

Borehole information: The bottom borehole section intersects deformation zone ZFMNNW1034 at 158 to 182 m borehole length.

Groundwater composition: The time series from the two borehole sections show increasing salinity trends. The trend in the upper section is rather insignificant and the groundwater in the three samples is of the Baltic type. The lower section provides water of the Baltic type and of similar composition to the previous section in the first sample, but then the following samples show an increasing salinity which do not stabilise, and the groundwater subsequently changes to the mixed Transition type. This is probably due to a pressure gradient established between the sections that has resulted in the introduction of a more dilute, shallow groundwater to the deeper section following drilling.

A1.3.2 SFR repository boreholes

The SFR repository boreholes have less available and useful transmissivity information, and also flow anomaly data are missing. Hydraulic conductivities as estimated from pressure build-up tests or water injection tests are given in the text; transmissivities may be obtained by multiplying with the borehole section length in metres. Some sample time series (short term in days or weeks) are available from 1986/87, 1995, 2000, 2006 and 2010, however, single samples are more common. Annual sampling has been performed since 1989 in the bottom section of boreholes KFR01, KFR08, KFR10 and KFR7B, and these also have the most extensive analytical protocols. Plots of chloride, magnesium and $\delta^{18}O$ data with time are included in the following borehole presentations if more than three data points are available for one of the sections at different years.

Borehole KFR01

Borehole KFR01 was drilled and packer equipment was installed in November–December 1984. During 2008 this equipment was replaced and the packer position and borehole length were checked and subsequently corrected/adjusted by +0.15 m; the previous positions are given in the table below.

Drilling water: Unknown drilling water source; drilling water content is not relevant more than 20 years after drilling.

Hydraulic/hydrogeological information: The borehole penetrates deformation zone ZFMWNW0001 (formerly the Singö Zone). Of the pressure build-up tests conducted in the borehole, a hydraulic conductivity of 7×10^{-7} m/s was obtained in the crushed core of the zone represented by the inner section (44.5–53.4 m) of the tests carried out. In the more peripheral part of the zone, represented by the outer section, the hydraulic conductivity was estimated to 10^{-9} m/s. Unlike many other borehole sections in the SFR, the pressure variations in KFR01 are not obviously correlated to the Baltic Sealevel fluctuation.
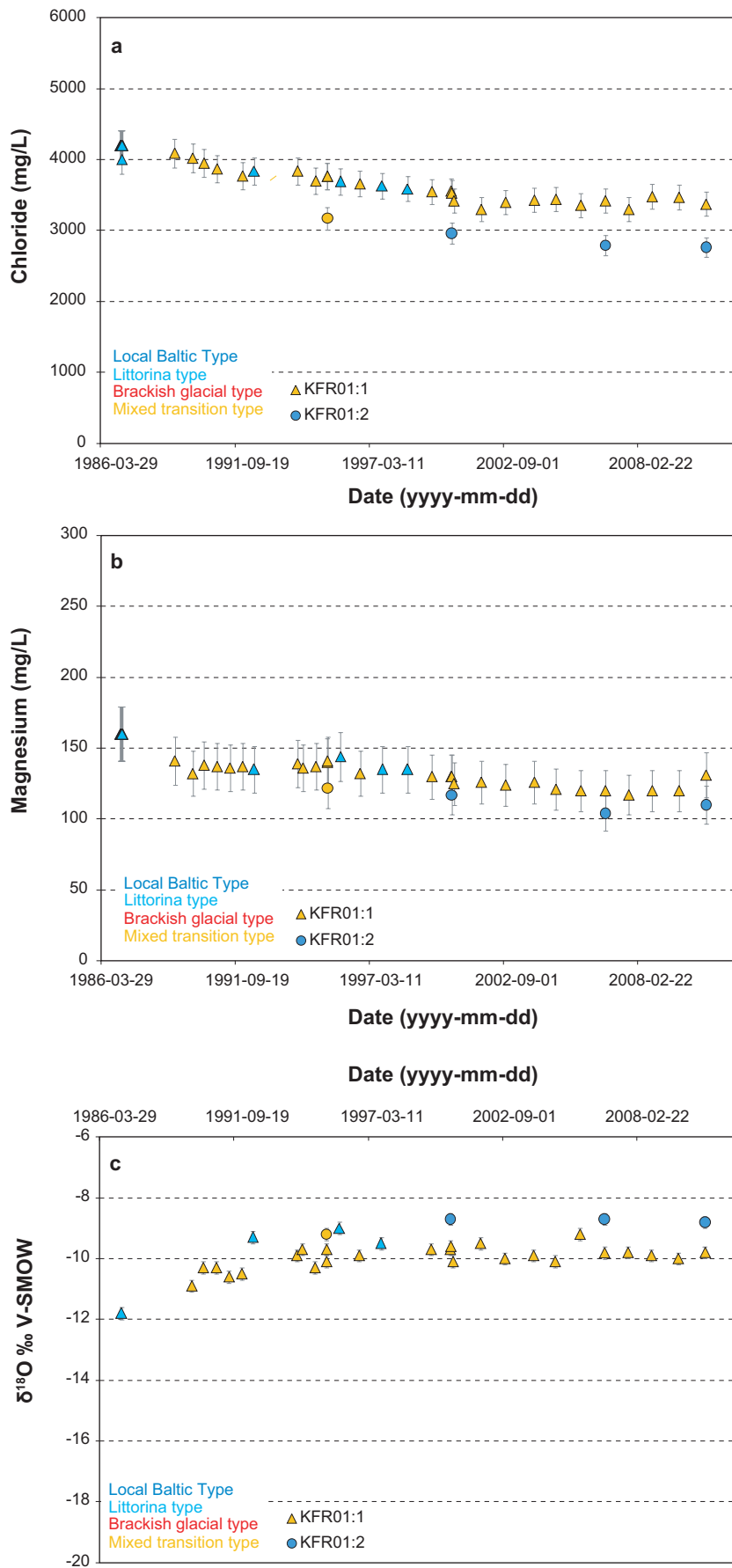
Figure A1-9 a–c. *Borehole KFR01; chloride, magnesium and δ¹⁸O trends from 1987 to 2010. The error bars represent 5%, 12% and 0.2 (‰ V-SMOW), respectively.*

Sampled borehole sections: Two sections (11.0–43.5 m and 44.5–53.4 m) have been sampled for groundwater; the bottom one has been sampled annually while the other less regularly. Data trends (Cl, Mg, δ^{18}O) with time for the two sections are presented in Figure A1-9 a–c.

Sample quality assessment for borehole KFR01.

Borehole section and vertical elevation	Total number of samples in Dataset I	Sample quality categories and number of samples in each category					Comments
		1	2	3	4	5	Category 1 is of the highest, and category 5 is of the lowest, quality.
KFR01:2 **11.0–43.5 m** **Mid. vertical elevation –71.6 m**	4		1	1	2	3	Four samples were collected in 1995, 2000, 2006 and 2010. Sample series are inadequate and time series are absent (which implies category 2). Major ions are incomplete for the category 3 and 4 samples.
KFR01:1 **44.5 62.3 m** **Mid. vertical elevation –94.2 m**	42	1	21	15	5	21	Early sampling in 1987 and annual sampling from 1989 to 2010. Time series from 1987-01-13 to1987-02-16 (12 samples). Time series from 2000-07-11 tp 2000-08-22 (3 samples). Stable major components and redox measurements at both occasions. The later Eh values are questionable

Borehole section information: The entire borehole (both sampled sections) is located in deformation zone ZFMWNW0001 (formerly the Singö Zone).

Available/missing data: The shallow section has tritium, deuterium and δ^{18}O isotope data but lacks trace metal data. The dataset from the deeper section includes additional isotope determinations as well as trace metal analyses from time to time (i.e. about each fifth year).

Questionable data: It is possible that the magnesium values from 1987 (Sample nos. 1298, 1300, 1302, 1305, 1307, 1308, 1312, 1314, 1316, 1318 and 1321) may be systematically somewhat too high. Two anomalously high sulphate-sulphur values (sample nos. 13446 and 13470) were observed also for the deepest section.

Groundwater composition: Section 11.0–43.5 m; the four samples show a somewhat decreasing salinity with time. The first sample from 1995 is classified as mixed Transition type groundwater due to a weakly depleted δ^{18}O (–9.2‰ V-SMOW) while all subsequent samples are of the Baltic groundwater type.

Section 44.5–62.3 m; the samples show a slow decrease in salinity with time. The first samples from 1987 are, although questionable, classified as Littorina type groundwater due to the high chloride and magnesium concentrations, while later samples change to mixed Transition groundwater types. It is, however, equally likely that the first magnesium values are erroneous and more attention should have been paid to the single δ^{18}O value which indicates a mixed Transition type groundwater already from the start.

Borehole KFR02

Borehole KFR02 was drilled in November 1984 (117 m) and extended to 170.3 m in 1986. During 2008 the packer equipment was replaced and the packer positions and borehole lengths were checked.

Drilling water: Unknown drilling water source; drilling water content is not relevant more than 20 years after drilling.

Hydraulic/hydrogeological information: Water injection tests in 10 m sections have been performed in the borehole indicating a slightly higher hydraulic conductivity in the interval 105–125 m. The hydraulic conductivity in the four borehole sections sampled is rather low ranging from $9 \cdot 10^{-10}$–$5 \cdot 10^{-9}$ m/s.

Other information/comments: The pressure level in the different borehole sections has been sensitive to sudden and rather large variations associated with disturbances in the borehole, for example during water sampling, deflation of packers or re-instrumentations. No satisfying explanation to this behaviour has been found so far, but it is suspected to be a "near-borehole" effect (for example in the borehole wall) rather than further out in the surrounding aquifer.

Sampled borehole sections: Four sections have groundwater samples, see below. None of the sections have been sampled annually, but nevertheless sampling is conducted quite frequently (1986, 1995, 2000, 2006 and 2010); see Figure A1-10 a–c for trend plots with time (Cl, Mg and $\delta^{18}O$ data).

Sample quality assessment for borehole KFR02.

Borehole section and vertical elevation	Total number of samples in Dataset I	Sample quality categories and number of samples in each category					Comments
		1	2	3	4	5	Category 1 is of the highest, and category 5 is of the lowest, quality.
KFR02:4 43.0–80.0 m Mid. vertical elevation –146.9 m	5			5		4	Five samples collected in 1986, 1995, 2000, 2006 and 2010. Sample series are inadequate and time series are absent (which implies category 2). However, due to section length > 20 m all samples are defined as category 3. Furthermore, some of the samples lack some major ions (Fe, Mn).
KFR02:3 81.0–118.0 m Mid. vertical elevation –184.9 m	6			6		7	Six samples collected in 1986, 1986, 1995, 2000, 2006 and 2010. Sample series are inadequate and time series are absent (which implies category 2). However, due to section length > 20 m all samples are defined as category 3. Some ions and tritium are missing for some of the samples.
KFR02:2 119.0–136.0 m Mid. vertical elevation –212.9 m	6		3	3		1	Six samples collected in 1986, 1995, 2000, 2006, 2009 and 2010. Sample series are inadequate and time series are absent (which implies category 2). Some ions and tritium are missing for the samples of category 3.
KFR02:1 137.0–170.0 m Mid. vertical elevation –239.1 m	6			6		1	Six samples collected in 1986, 1986, 1995, 2000, 2006 and 2010. Sample series are inadequate and time series are absent (which implies category 2). However, due to the section length > 20 m all samples are defined as category 3. Some ions and tritium are missing for some of the samples.

Section 43.0–80.0 m is located above zone ZFM871 (formerly Zone H2) and within the vertical zone ZFMNE0870 (formerly Zone 9).

Section 81.0–118.0 m is located partly within zone ZFM871 (formerly Zone H2).

Section 119.0–136.0 m is located partly within zone ZFM871 (formerly Zone H2).

Section 137.0–170.0 m is located below zone ZFM871 (formerly Zone H2).

Available/missing data: Rather complete datasets with deuterium, tritium and $\delta^{18}O$ data except for the earliest samples; trace metals were determined for the 2010 samples.

Questionable data: None.

Groundwater composition: Typical for the borehole is a marked change of groundwater composition (more contribution of marine Littorina water) along the borehole at the intersection with zone ZFM871 (formerly Zone H2) at 109.2 to 130.2 m borehole length. As a consequence, the salinity is higher in section 119.0–136.0 m than in the bottom section. Overall, the groundwater composition shows a weak trend towards increased mixing with time in the borehole sections except the upper section. Here, the water composition is quite stable and maintains the Brackish-glacial signature up to the last collected sample in year 2010. However questionable, the sample collected in section 119.0–136.0 m in 2006 was classified as Littorina type solely due to the high $\delta^{18}O$ value.
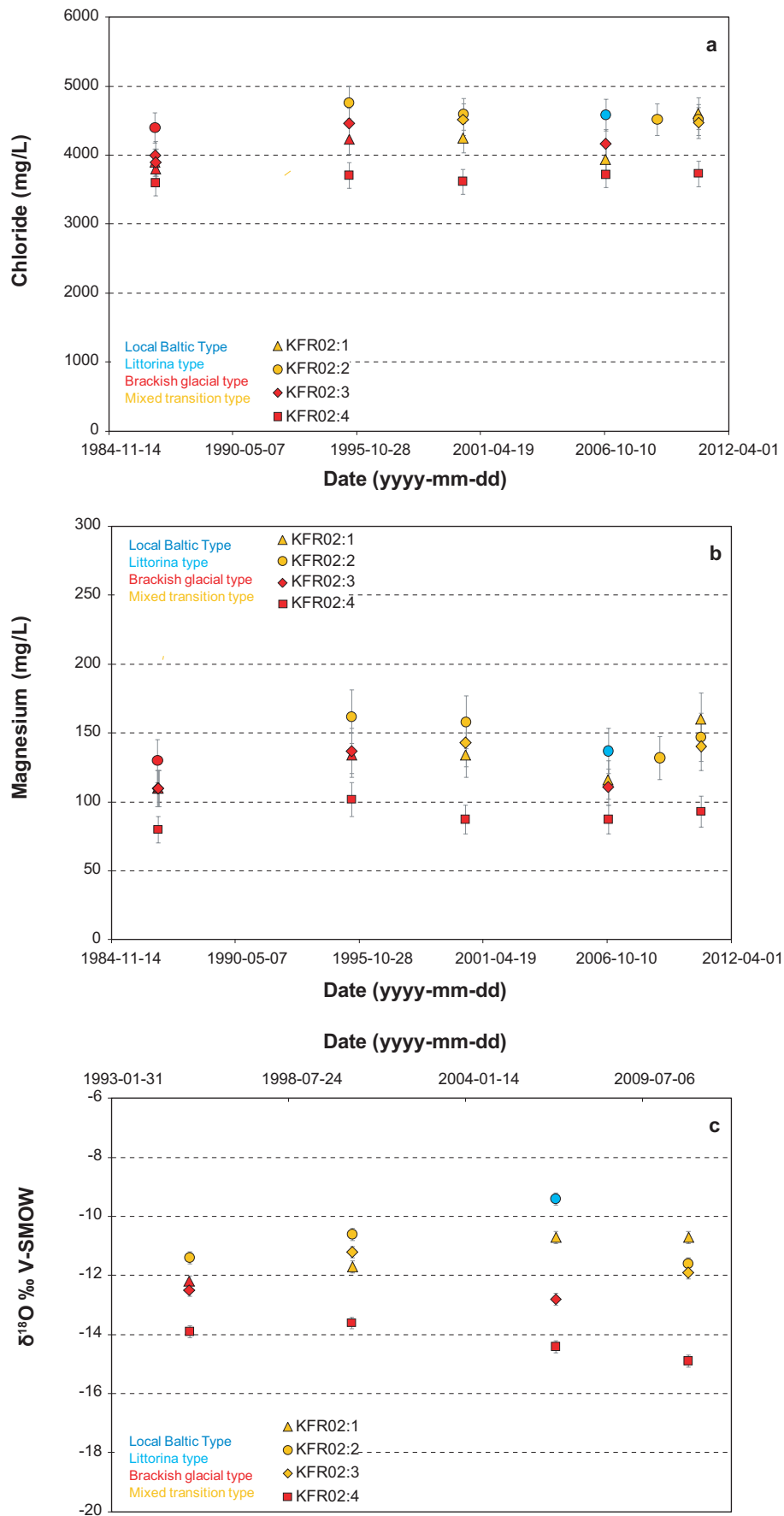
Figure A1-10 a–c. *Borehole KFR02; chloride, magnesium and δ¹⁸O (from 1995) trends from 1986 to 2010. The error bars represent 5%, 12% and 0.2 (‰ V-SMOW), respectively.*

Borehole KFR03

Borehole KFR03 was drilled in 1985 and packer equipment was installed shortly after drilling and subsequently replaced in 2008 when packer positions and borehole length were checked. The packer positions were corrected/adjusted by +0.16 m; the previous positions are given in the table below.

Drilling water: Unknown drilling water source; drilling water content is not relevant more than 20 years after drilling.

Hydraulic/hydrogeological information: Pressure build-up tests were performed in the four sections resulting in a hydraulic conductivity of about $3 \cdot 10^{-8}$ m/s in the two outermost sections and about 10^{-9} m/s in the two inner sections.

Other information/comments: The pressure level in the borehole sections is only a few metres above air pressure causing release of gas in the tubes and a correspondingly low flow, especially from section KFR03:1 but also from KFR03:2 (about 2 and 50 mL/min respectively).

Sampled borehole sections: Four sections have groundwater samples, see below. None of the sections have been sampled annually but sampling has been conducted during 1995, 2000, 2006 and 2010. See Figure A1-11 a–c for sample series plots (Cl, Mg and $\delta^{18}O$ data).

Sample quality assessment for borehole KFR03.

Borehole section and vertical elevtion	Total number of samples in Dataset I	Sample quality categories and number of samples in each category					Comments
		1	2	3	4	5	Category 1 is of the highest, and category 5 is of the lowest, quality.
KFR03:4 5.0–44.0 m **Mid. vertical elevation** –106.9 m	4			4		2	Four samples collected in 1995, 2000, 2006 and 2010. Sample series are inadequate and time series are absent (which implies category 2). However, due to the section length > 20 m all samples are defined as category 3. Fe, Mn and sometimes tritium are missing for some of the samples.
KFR03:3 45.0–56.0 m **Mid. vertical elevation** –132.9 m	4		2	2		2	Four samples collected in 1995, 2000, 2006 and 2010. Sample series are inadequate and time series are absent (which implies category 2). Some ions (Fe, Mn) and sometimes tritium are missing for the samples of category 3.
KFR03:2 57.0–80.0 m **Mid. vertical elevation** –150.9 m	5			5		2	Five samples collected in 1987, 1987, 1995, 2000 and 2010. Sample series are inadequate and time series are absent (which implies category 2). However, due to section length > 20 m all samples are defined as category 3. Some ions (Fe, Mn) and sometimes tritium are missing for some of the samples.
KFR03:1 81.0–101.6 m **Mid. vertical elevation** –173.7 m	4		2	2		2	Four samples collected in 1986, 1987, 1995 and 2000. Sample series are inadequate and time series are absent (which implies category 2). Some ions (Fe, Mn) and tritium are missing for the category 3 sample.

Section 5.0–44.0 m is located within zone ZFMNE0870 (formerly Zone 9) and above zone ZFM871 (formerly Zone H2).

Section 45.0–56.0 m is located within zone ZFMNE0870 (formerly Zone 9) and above zone ZFM871 (formerly Zone H2).

Section 57.0–80.0 m is located within zone ZFMNE0870 (formerly Zone 9) and above zone ZFM871 (formerly Zone H2).

Section 81.0–101.6 m is located within the zones ZFMNE0870 (formerly Zone 9) and ZFM871 (formerly Zone H2).
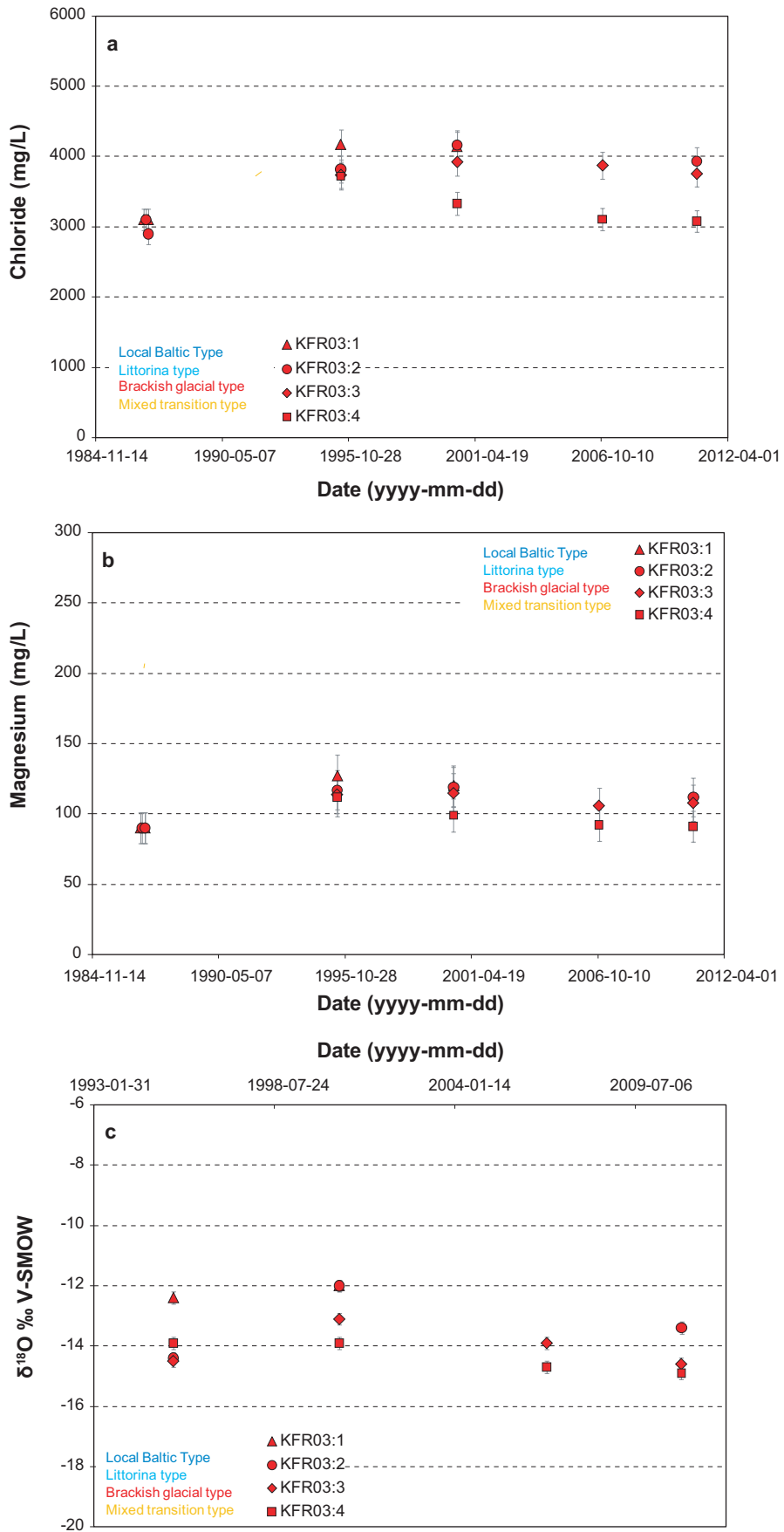
***Figure A1-11 a–c.** Borehole KFR03; chloride, magnesium and δ¹⁸O (starting 1995) trends from 1986 to 2010. The error bars represent 5%, 12% and 0.2 (‰ V-SMOW), respectively.*

Available/missing data: The four borehole sections lack trace metals but have some late $\delta^{18}O$ data (starting in 1995).

Questionable data: None.

Groundwater composition: The groundwater composition is rather similar in the four borehole sections and the Brackish-glacial groundwater type is maintained also in the most recent samples. An almost insignificant elevation in salinity is observed along the borehole at its intersection with zone ZFM871 (formerly Zone H2) at 78.3 to 99.7 m borehole length (i.e. in the bottom section). The groundwater composition in the four sections shows first a somewhat increasing salinity from the first to the second sampling occasions, and then a weakly decreasing trend. However, all samples preserve their Brackish-glacial character and the trend is rather towards a larger contribution of glacial meltwater than towards an increased contribution of marine water.

Borehole KFR04

Borehole KFR04 was drilled in February 1985 and packer equipment was installed in March of the same year and subsequently replaced in 2008 when the packer positions and borehole length were checked. The packer positions were corrected/adjusted by +0.09 m; the old positions are given in the table below.

Drilling water: Unknown drilling water source; drilling water content is not relevant more than 20 years after drilling.

Hydraulic/hydrogeological information: Pressure build-up tests in the four borehole sections show hydraulic conductivity values close to 10^{-8} m/s.

Other information/comments: No water can be extracted from section KFR04:4 where the pressure level is close to air pressure.

Sampled borehole sections: Three sections have groundwater samples, see below. None of the sections have been sampled annually but nevertheless it is conducted quite frequently (1986, 1995, 2000, 2006 and 2010). See Figure A1-12 a–c for sample series plots (Cl, Mg and $\delta^{18}O$ data).

Sample quality assessment for borehole KFR04.

Borehole section and vertical elevation	Total number of samples in Dataset I	Sample quality categories and number of samples in each category					Comments
		1	2	3	4	5	Category 1 is of the highest, and category 5 is of the lowest, quality.
KFR04:3 28.0–43.0 m **Mid. vertical elevation** –111.5 m	6		4	2			Six samples collected in 1987, 1987, 1995, 2000, 2006 and 2010. Sample series are inadequate and time series are absent (which implies category 2). Some ions (Fe, Mn) and sometimes tritium are missing for the samples of category 3.
KFR04:2 44.0–83.0 m **Mid. vertical elevation** –138.5 m	4			4			Four samples collected in 1995, 2000, 2006 and 2010. Sample series are inadequate and time series are absent which implies category 2. However, due to the long section (> 20 m) all samples are classified as category 3.
KFR04:1 84.0–100.5 m **Mid. vertical elevation** –166.3 m	4		2	2			Four samples collected in 1995, 2000, 2006 and 2010. Sample series are inadequate and time series are absent (which implies category 2). Some ions (Fe, Mn) and sometimes tritium are missing for the category 3 samples.

Section 28.0–43.0 m is located within zone ZFMNE0870 (formerly Zone 9) and above zone ZFM871 (formerly Zone H2).

Section 44.0–83.0 m is located within zone ZFMNE0870 (formerly Zone 9) and above zone ZFM871 (formerly Zone H2).

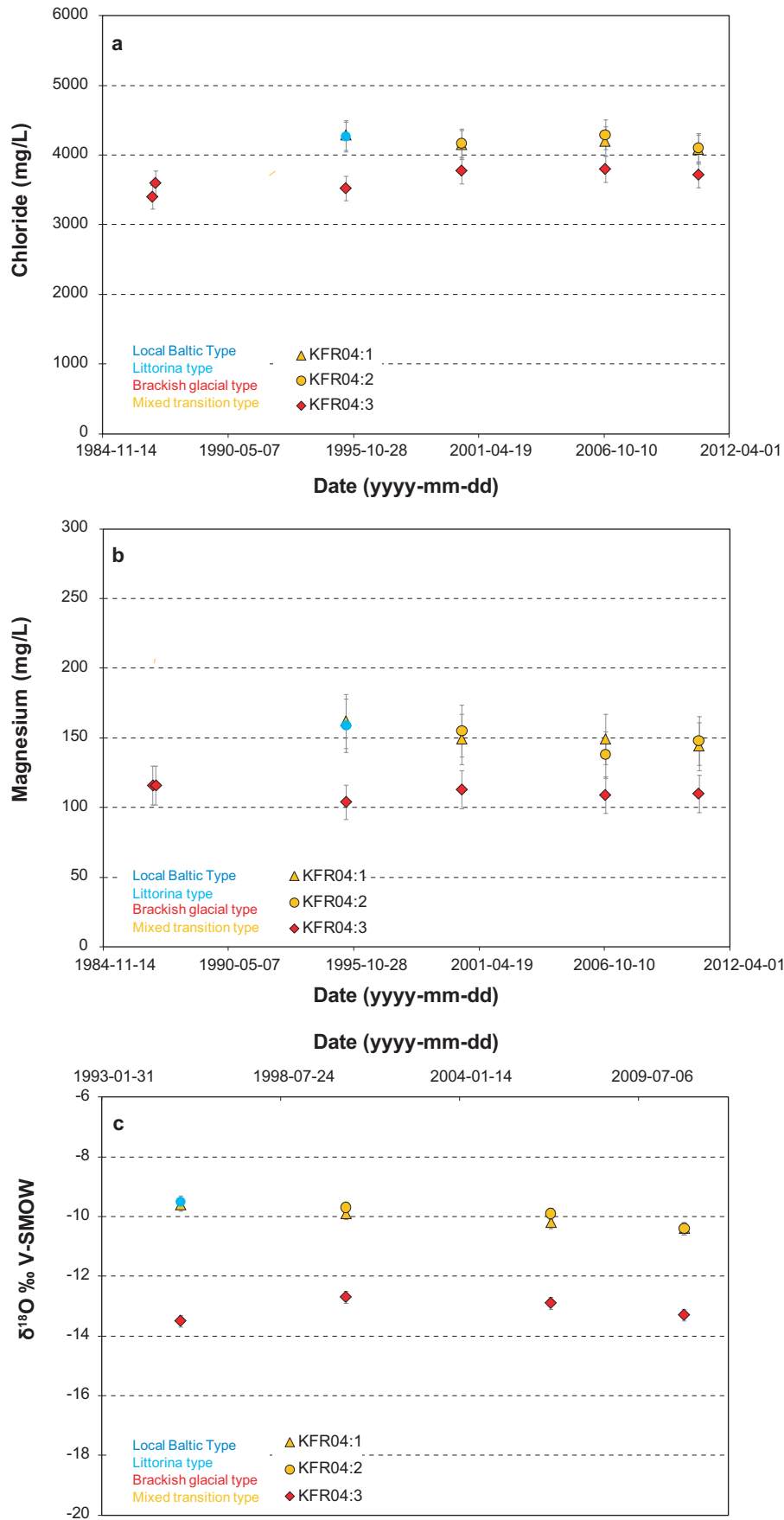**Section 84.0–100.5 m** is located within zone ZFM871 (formerly Zone H2).

Figure A1-12 a–c. Borehole KFR04; chloride, magnesium and δ18O (starting 1995) trends during the time period 1987 to 2010. The error bars represent 5%, 12% and 0.2 (‰ V-SMOW), respectively.

Available/missing data: No trace metal analyses but deuterium and tritium are available from the three sections which started in 1995.

Questionable data: None.

Groundwater composition: In common with borehole KFR02, the groundwater composition diverges along the borehole at and close to the transection of zone ZFM871 (formerly Zone H2). The upper section shows stable water composition with groundwater of Brackish-glacial type while the two lower sections show a slowly decreasing salinity trend and increased mixing.

Borehole KFR05

Borehole KFR05 was drilled in June 1985 and packer equipment was installed shortly after the drilling and subsequently replaced during 2008 when the packer positions and borehole length were checked; the packer positions were corrected/adjusted by +0.15 m.

Drilling water: Unknown drilling water source; drilling water content is not relevant more than 20 years after drilling.

Hydraulic/hydrogeological information: Water injection tests at two metre interval sections have been conducted only along a restricted portion of the borehole, between 40 and 66 m. In this section the highest hydraulic conductivity ($8 \cdot 10^{-8}$ m/s) was recorded in section 58–60 m.

Other information/comments: After the re-instrumentation, in the spring of 2008, the water pressure was insignificant in sections KFR05:1, KFR05:3 and KFR05:4 and therefore no water could be extracted.

Sampled borehole sections: Groundwater sampling has been performed in two different borehole sections at two sampling occasions and each at different times. It may be the case that one of the section registrations are erroneous since the water composition of the two sections is very similar.

Sample quality assessment for borehole KFR05.

Borehole section and vertical elevation	Total number of samples in Dataset I	Sample quality categories and number of samples in each category					Comments
		1	2	3	4	5	Category 1 is of the highest, and category 5 is of the lowest, quality.
KFR05:2 57.0–79.0 m **Mid. vertical elevation** −141.1 m	2			2		1	Two samples collected in 2006 and 2010. Both sample series and time series are absent (which implies category 3). Fe and Mn are missing for one of the samples.
KFR05:1 80.0–96.0 m **Mid. vertical elevation** −159.9 m	2			2		1	Two samples collected in 1995 and 2000. Both sample series and time series are absent (which implies category 3). Fe and Mn are missing for one of the samples.

Section 57.0–79.0 m is located above zone ZFM871 (formerly Zone H2).

Section 80.0–96.0 m is located partly within zone ZFM871 (formerly Zone H2).

Available/missing data: No trace metal analyses but deuterium and tritium are available starting in 1995.

Questionable data: None.

Groundwater composition: The two samples from each section have a similar groundwater composition, i.e. Littorina groundwater type.

Borehole KFR08

Borehole KFR08 was drilled at the end of 1985to the beginning of 1986 and packer equipment to delimit three borehole sections was installed shortly after the drilling and subsequently replaced during 2008 when the packer positions and borehole length were checked. The packer positions were corrected/adjusted by –0.05 m; the previous positions are given in the Table below.

Drilling water: Unknown drilling water source; drilling water content is not relevant more than 20 years after drilling.

Hydraulic/hydrogeological information: The hydraulic conductivity has been evaluated from pressure build-up tests to about $2 \cdot 10^{-7}$ m/s in section KFR08:1, $5 \cdot 10^{-7}$ m/s in section KFR08:2 and $3 \cdot 10^{-8}$ m/s in section KFR08:3. All three sections show pressure variations strongly correlated to the level in the Baltic Sea.

Sampled borehole sections: Groundwater samples have been collected from all the delimited sections of the borehole; see Figure A1-13 a–c for trends with time (Cl, Mg and δ^{18}O). The first groundwater sampling including all the sections was performed in 1995. The bottom section at 63–104.4 m was added to the annual sampling programme to represent the deformation zone ZFMNW0805a (formerly Zone 8a) and data exist since 1989. This bottom section (deepest section) of the borehole was selected for extended investigations, including redox measurements, in 2010, due to its relatively shallow location and the Baltic type groundwater signature (Nilsson K 2011). This choice of borehole was based on the fact that it was considered as one of the most likely boreholes to yield oxic groundwater, if it exists at all in the SFR repository boreholes.

Sample quality assessment for borehole KFR08.

Borehole section and vertical elevation	Total number of samples in Dataset I	Sample quality categories and number of samples in each category					Comments
		1	2	3	4	5	Category 1 is of the highest, and category 5 is of the lowest, quality.
KFR08:3 **6.0–35.0 m** Mid. vertical elevation **–87.8 m**	4			2	2	1	The samples were collected in 1995, 2000, 2006 and 2010. Sample series are inadequate and time series are absent (which implies category 3). Some ions and isotopes are missing for two of the samples (category 4).
KFR08:2 **36.0–62.0 m** Mid. vertical elevation **–90.3 m**	5			4	1	1	The samples were collected in 1995, 2000, 2006, 2009 and 2010. Sample series are inadequate and time series are absent (which implies category 3). Some anions are missing for one of the samples (category 4).
KFR08:1 **63.0–104.4 m** Mid. vertical elevation **–93.3 m**	31			28	3	3	The annual sampling started in 1989. Sample series are adequate and time series were collected in 2010; the section length implies category 3. Time series, 3 samples collected from 2010-12-07 to 2010-12-20. Stable water composition; successful redox measurements.

Borehole section 6.0–35.0 m is located in deformation zone ZFMNW0805b (formerly Zone 8b) (intersection at 3–19 m).

Both sections 36.0–62.0 m and 63.0–104.4 m are located partly in deformation zone ZFMNW0805a (formerly Zone 8a) (intersection at 41–104.4 m).

Available/missing data: The first two sections have sporadic analyses of the isotopes tritium, deuterium and δ^{18}O, but no trace metals. The samples from the bottom section have generally a more complete analyses and, in addition, ^{36}Cl isotope data from 2010 are available for KFR101:1, KFR105:1, KFR08:1 and KFR7A:1.

Questionable values/data: The ^{18}O signature (–9.8‰ V-SMOW) from spring 1996 (Sample no 17000) deviates and is likely to be a misprint or confused samples.

Groundwater composition: The samples show a minor slow decrease in salinity with time. All samples, including the first samples collected in 1989 in section 63.0 to 104.4 m, belong to the Baltic groundwater type.
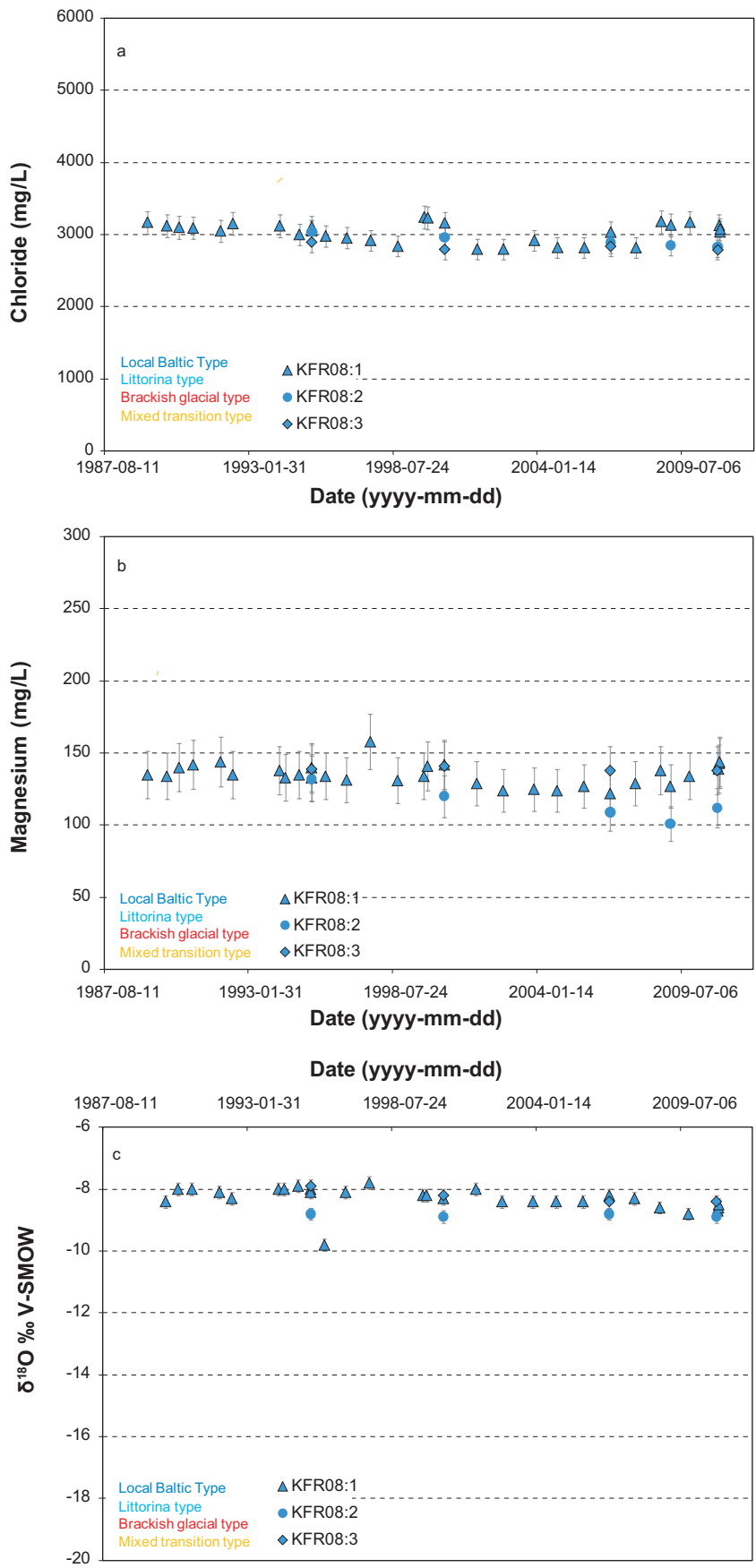
Figure A1-13 a–c. *Borehole KFR08; chloride, magnesium and $\delta^{18}O$ trends from 1989 to 2010. The error bars represent 5%, 12% and 0.2 (‰ V-SMOW), respectively.*

Borehole KFR09

Borehole KFR09 was drilled in 1985 and packer equipment was installed to delimit sections 43.0–62.0 m and 63.0–80.24 m prior to the first sampling occasion in 1986. This packer equipment was replaced by one close to the borehole orifice a short time thereafter, probably around 1987. However, the exact date/year is unknown and samples from the bottom section record an erroneous upper section limit of 63 m in Sicada until 2000. During 2008 new packer equipment was installed.

Drilling water: Unknown drilling water source; drilling water content is not relevant more than 20 years after drilling.

Hydraulic/hydrogeological information: From pressure build-up tests during an earlier instrumentation (probably in the mid-1980s) with four sections in the borehole, the highest hydraulic conductivity, $1.9 \cdot 10^{-6}$ m/s, was measured in section 43–62 m from the tunnel wall. This section is interpreted to penetrate deformation zone ZFMNNE0869 (formerly Zone 3). A relatively high value is also measured in section 24–42 m, about $5 \cdot 10^{-7}$ m/s, while the values are lower in sections 7–23 m (about $6 \cdot 10^{-8}$ m/s) and 63–81 m (about $2 \cdot 10^{-9}$ m/s).

Other information/comments: Today the whole borehole represents one section with a packer installed about 2 m from the tunnel wall. Due to the high hydraulic transmissivity for the whole borehole and a large diameter connection through the packer, high flow and rapid replacement of borehole water before sampling can be obtained when the valve is opened.

Sampled borehole sections: Below it is assumed that the two samples collected in 1986 and 1987 represent the shorter section, while all other samples represent the entire borehole. By mistake this borehole was sampled instead of borehole KFR10 (a borehole which is included in the annual sampling programme) between 1992 and 1998. The trends with time in chloride, magnesium and $\delta^{18}O$ are presented in Figure A1-14 a–c.

Sample quality assessment for borehole KFR09.

Borehole section and vertical elevation	Number of samples in Dataset I	Sample quality categories and number of samples in each category					Comments
		1	2	3	4	5	Category 1 is of highest and category 5 is of the lowest, quality.
KFR09:1 63.0–80.2 m Mid. vertical elevation –83.7 m	2			2		3	The two single samples were collected in 1986 and 1987, respectively. Both samples are of Category 3 due to the lack of sample series and time series.
KFR09:entire 0.00–80.2 m Mid. vertical elevation –80.9 m (section uncertain)	13			11	2		The samples were collected from 1992 to 2000 and in 2010, respectively. All samples are of Category 3 due to the section length and the lack of sample series and time series. Two of the samples lack some major constituents.

Section information: The sampled long section penetrates deformation zone ZFMNNE0869 (formerly Zone 3) at 0–58.7 m borehole length.

Available/missing data: The borehole has sporadic analyses of the isotopes tritium, deuterium and $\delta^{18}O$ but no trace metals.

Questionable values/data: None.

Groundwater composition: Samples collected in 1986 and 1987 show a Littorina type groundwater; subsequent samples collected are less saline and of Baltic type groundwater. This difference may be due to either changes in groundwater composition due to drawdown effects from the SFR repository, or that the Littorina type groundwater dominates in the flow anomalies contained in the short section.

Figure A1-14 a–c. *Borehole KFR09; Chloride, magnesium and δ¹⁸O (starting 1995) trends during the time period 1986 to 2010. The error bars represent 5%, 12% and 0.2 (‰ V-SMOW), respectively. Note that the first two samples were collected from a short section of 63.0–80.2 m length and are classified as Littorina type groundwater.*

Borehole KFR10

Borehole KFR10 was drilled in 1985 and packer equipment was installed to delimit section 87.0–107.28 m prior to the first sampling occasion at the end of 1985. This packer equipment was replaced with one close to the borehole orifice a short time thereafter, probably around 1987. However, the exact date/year is unknown and the samples from the bottom section recorded an erroneous upper section limit of 87 m in the SKB database Sicada until 2000.

Drilling water: Unknown drilling water source; drilling water content is not relevant more than 20 years after drilling.

Hydraulic/hydrogeological information: The borehole partly penetrates zone ZFMNNE0869 (formerly Zone 3); in an earlier instrumentation the borehole was packed off into four sections. Results from pressure build-up tests show high values of hydraulic conductivity at $1.4 \cdot 10^{-6}$ m/s for the innermost section (87–108 m) and about $1.2 \cdot 10^{-6}$ m/s in the nearby section (66–86 m), but low hydraulic conductivity just above 10^{-9} m/s in the two outermost sections (7–50 and 56–65 m).

Other information/comments: Today the borehole is equipped with only one mechanical packer installed about 2 m inside the tunnel wall. Due to the high hydraulic transmissivity for the whole borehole and a large diameter connection through the packer, high flow and rapid replacement of borehole water can be obtained when the valve is opened.

Sampled borehole sections: Below it is assumed that the eleven samples collected in 1986 and 1987 represent the shorter section, while all other samples represent the entire borehole. However, borehole KFR10 is included in the annual sampling programme by mistake and borehole KFR09 was sampled between 1992 and 1998. The trends with time in chloride, magnesium and $\delta^{18}O$ are presented in Figure A1-15 a–c.

Sample quality assessment for borehole KFR10.

Borehole section and vertical elevation	Number of samples in Dataset I	Sample quality categories and number of samples in each category					Comments
		1	2	3	4	5	Category 1 is of the highest, and category 5 is of the lowest, quality.
KFR10:1 87.0–107.28 m	11			6	5	12	The samples were collected in 1986 and 1987. The samples are of category 3 due to section length and category 4 due to incomplete data. Time series data exist from 1986-11-20 to1987-01-07 as well as Eh measurements
KFR10:entire 0.00–107.28 m **Mid. vertical elevation −116.23 m (section uncertain)**					22	1	The samples are of category 4 due to the considerable section length and in some cases incomplete data. Time series data exist from 2000-06-22 to 2000-07-04 and Eh measurements are unreliable.

Section information: The section (irrespectable of length) is located in deformation zone ZFMNNE0869 (formerly Zone 3) and the bottom of the borehole most likely may be connected to zone ZFM871.

Questionable values/data: A single chloride value from 2001 (Sample no 17073) may be somewhat too low since a corresponding change is not shown in any of the other components and the charge imbalance is positive (4%).

Groundwater composition: The samples show a slow decrease in salinity with time until 2000 but maintain the Littorina type groundwater signature; after this date a stabilisation or a weak increase in salinity occurs. The samples collected in 1986/87 are considerably more saline than subsequent samples which may have resulted from either changes in groundwater composition due to drawdown effects from the SFR repository, or that more saline groundwater dominates in the flow anomalies contained in this short section.
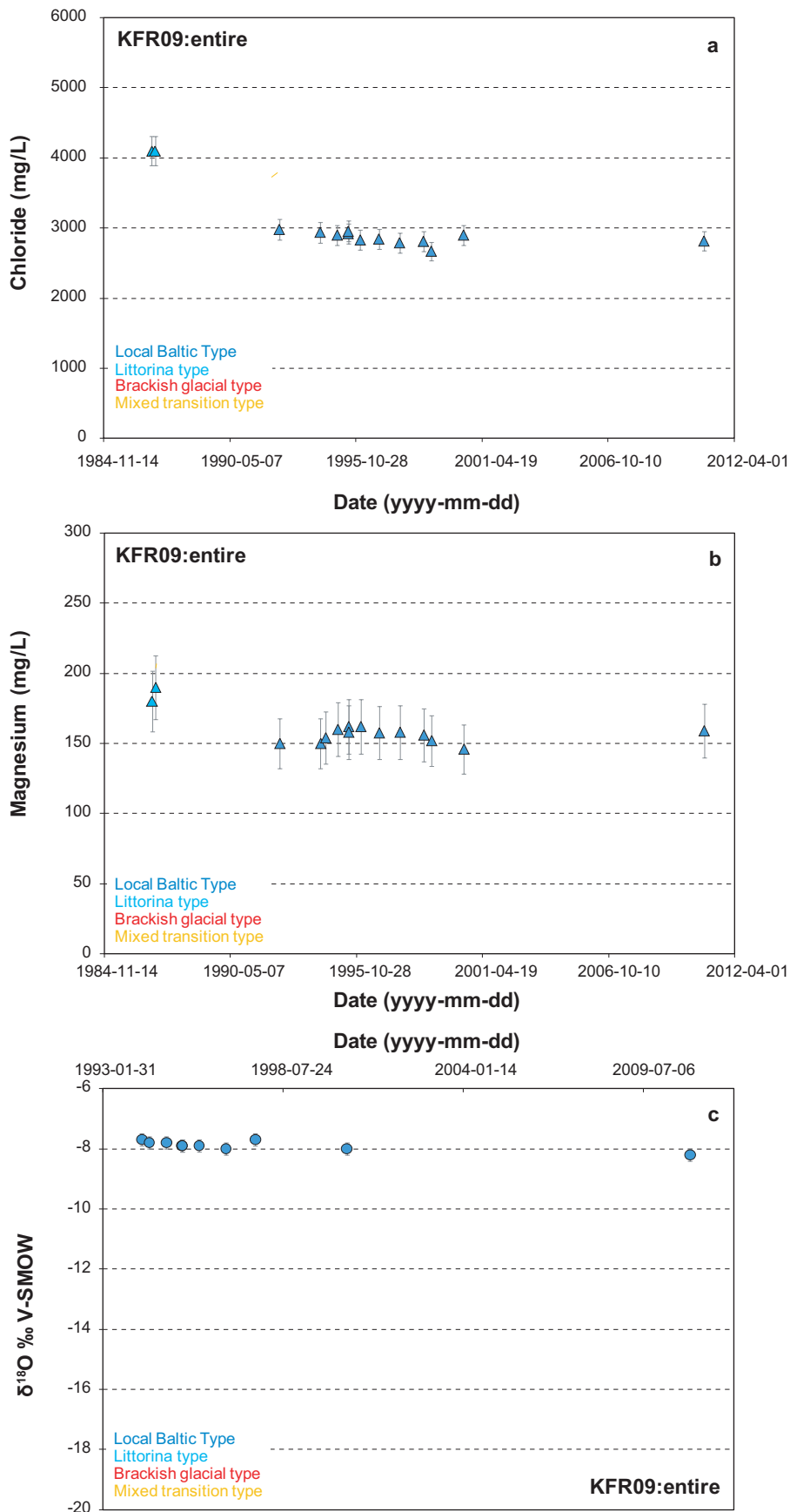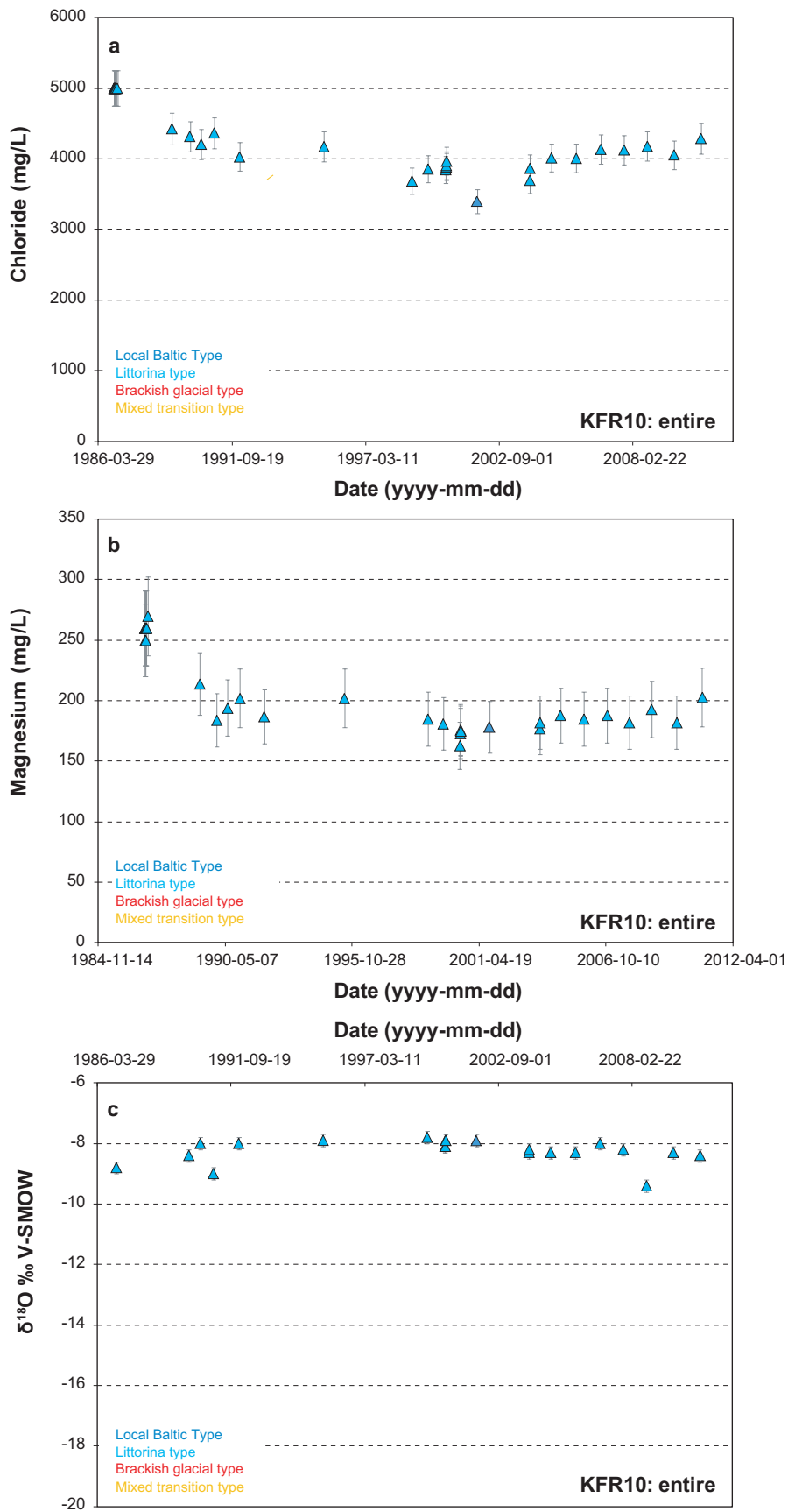
Figure A1-15 a–c. *Borehole KFR10; Chloride, magnesium and δ^{18}O trends during the time period 1986 to 2010. The error bars represent 5%, 12% and 0.2 (‰ V-SMOW), respectively. Note that the first three samples were collected from a short section of 87.0–107.28 m.*

Borehole KFR11

Borehole KFR11 was drilled in December 1985 and packer equipment was installed to delimit four sections prior to the first sampling occasion in 1986. The packer equipment was subsequently dismantled and removed and no more sampling has been conducted after 1987. It is believed that the borehole has been sealed with cement.

Drilling water: Unknown drilling water source; drilling water content is not relevant more than 20 years after drilling.

Hydraulic/hydrogeological information: The estimated hydraulic conductivities derived from pressure build-up tests in the different sections are: KFR11:1 at $-2 \cdot 10^{-6}$ m/s, KFR11:2 at $-5 \cdot 10^{-8}$ m/s, KFR11:3 at $-8 \cdot 10^{-9}$ m/s and KFR11:4 at $-7 \cdot 10^{-7}$ m/s.

Sampled borehole sections: Only a few (one or two in Dataset I) groundwater samples have been collected from each of the four borehole sections representing the entire borehole. Since all samples were taken very early on (1986/87) there exist no sample series or any recorded changes in groundwater composition due to the presence of the repository.

Sample quality assessment for borehole KFR11.

Borehole section and vertical depth	Number of samples in Dataset I	Sample quality categories and number of samples in each category					Comments
		1	2	3	4	5	Category 1 is of the highest, and category 5 is of the lowest, quality.
KFR11:4 7.0–24.0 m Mid. vertical elevation –89.2 m	1			1		1	The samples were collected in 1986 and 1987 and belong to category 3 due to the absence of sample series and time series. 14 very early samples belong to category 5 and Dataset II.
KFR11:3 25.0–39.0 m Mid. vertical elevation –92.1 m	1			1		1	
KFR11:2 40.0–55.0 m Mid. vertical elevation –94.8 m	1			1		1	
KFR11:1 56.0–98.1 m Mid. vertical elevation –99.9 m	2			2		11	

Section information: Section 7.0–24.0 m (almost the entire section) is located in zone ZFM-NW0805b (0–18.77 m); the three other sections transect zone ZFMNW0805a at between 41.45 and 95.65 m (Formerly Zones 8B and 8A).

Available/missing data: Isotope and trace metal data are not available.

Questionable values/data: None.

Groundwater composition: The samples have been classified as belonging to the Littorina type groundwater due to the relatively high magnesium concentrations which seems reasonable also from the position of the borehole. However, there is a clear difference in the concentrations of the major components (especially sulphate) in the bottom section compared to the other sections.

Borehole KFR12

Borehole KFR12 was drilled in 1986 and packer equipment was installed to delimit section 20.0–33.0 m prior to the first sampling occasion at the end of 1985. This packer equipment was dismantled some time after, probably around 1987.

Drilling water: Unknown drilling water source; drilling water content is not relevant more than 20 years after drilling.

Hydraulic/hydrogeological information: The estimated hydraulic conductivities from pressure build-up tests in the two sections are: KFR12:1 at $-1 \cdot 10^{-8}$ m/s and KFR12:2 at $-3 \cdot 10^{-7}$ m/s.

Sampled borehole sections: Only two groundwater samples have been collected from this borehole, with the later sample collected from the entire borehole. There are no sample series to plot and the change in the groundwater composition (dilution) cannot be relied on since it may be due to the fact that different parts of the borehole were sampled at the two sampling occasions.

Sample quality assessment for borehole KFR12.

Borehole section and vertical elevation	Number of samples in Dataset I	Sample quality categories and number of samples in each category					Comments
		1	2	3	4	5	Category 1 is of the highest, and category 5 is of the lowest, quality.
KFR12:2 20.0–33.0 m mid. vertical elevation –113.6 m				1			The sample was collected in 1987 and belongs to category 3 because the sample series and time series are absent and the environmental isotopes are incomplete.
KFR12:entire 0.00–50.25 m mid. vertical elevation –112.25 m					1		The sample was collected in 1995 and belongs to category 4 due to incomplete data. Sample series and time series are absent and the environmental isotopes are incomplete.

Section information: The sections (irrespective of length) are located partly within the gently dipping deformation zone ZFM871 (formerly Zone H2), with the borehole transecting the zone between 21.25–31.50 m borehole length.

Available/missing data: Deuterium and $\delta^{18}O$ values exist for one of the samples; trace metal data are not available.

Questionable values/data: None.

General: In common with KFR11, the information from this borehole is also very limited although a $\delta^{18}O$ value exists for the late sample from 1995. The value confirms the marine origin of the groundwater and, since both samples are quite saline (4,500 mg/L for the delimited section and 3,800 mg/L for the entire borehole), they were classified as belonging to the Littorina type groundwater. The PCA supports this classification and it seems reasonable also from the position of the borehole (i.e. transects zone ZFM871).

Borehole KFR13

Borehole KFR13 was drilled in 1986 and packer equipment was installed to delimit three sections prior to the first sampling occasion at the end of 1985. The packer equipment was subsequently replaced during 2008 and the packer positions and section lengths were checked and then corrected/adjusted by –0.25 m; the previous positions are given in the Table below.

Drilling water: Unknown drilling water source; drilling water content is not relevant more than 20 years after drilling.

Hydraulic/hydrogeological information: The hydraulic conductivity in the three borehole sections is decreasing with increasing distance along the borehole with estimated values from pressure build-up tests showing KFR13:1 at $–9 \cdot 10^{-8}$ m/s, KFR13:2 at $–6 \cdot 10^{-10}$ m/s and KFR13:3 at $–8 \cdot 10^{-11}$ m/s.

Other information/comments: Due to the low hydraulic transmissivity in section 3 (4.0–33.0 m) the flow from the water sampling tube in this section is less than 50 mL/min.

Sampled borehole sections: Since the first sampling in 1995, a few groundwater samples have been collected from each of the three borehole sections covering the entire borehole; the chloride, magnesium and $\delta^{18}O$ trends are presented in Figure A1-16 a–c.

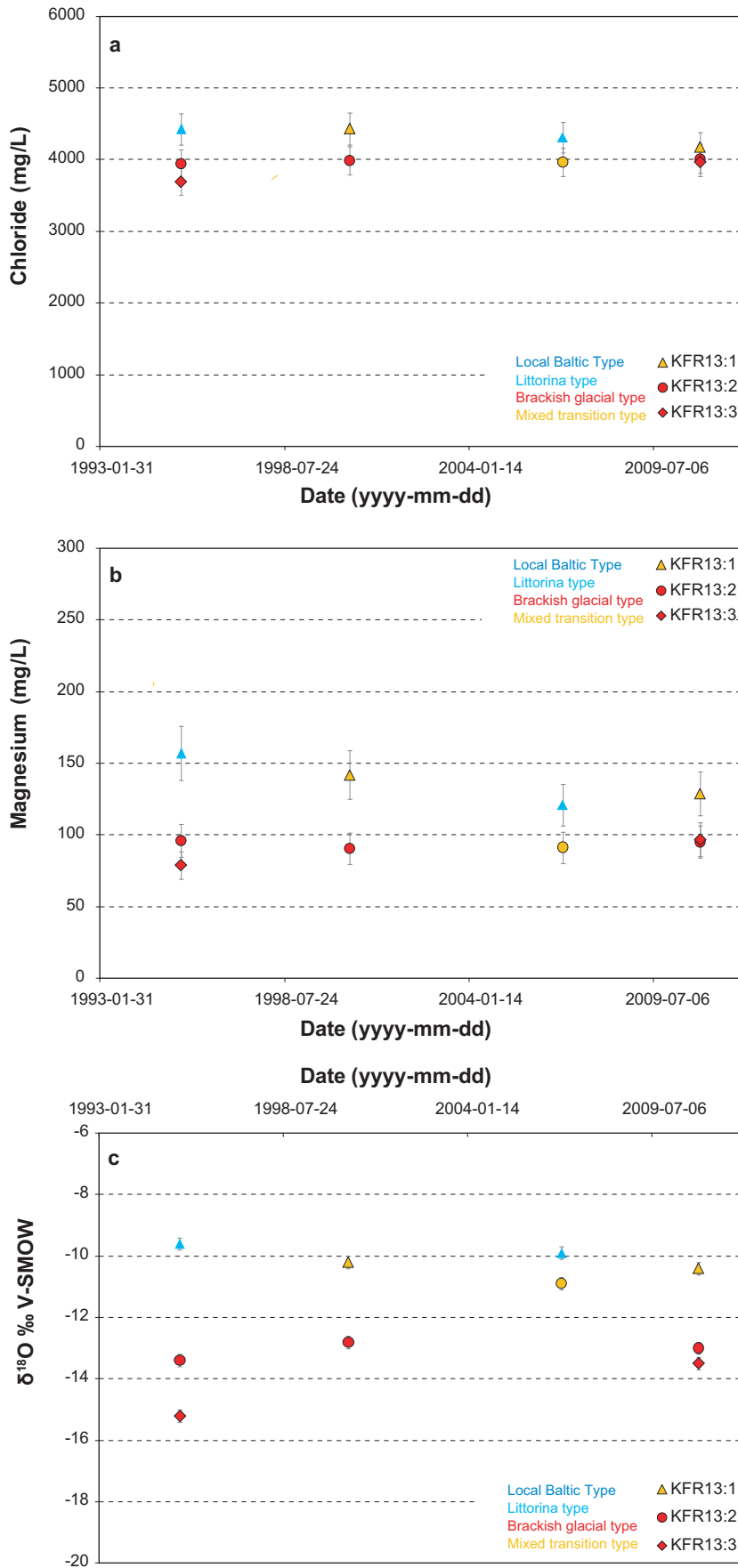***Figure A1-16 a–c.*** *Borehole KFR13; Chloride, magnesium and δ¹⁸O trends from 1995 to 2010. The error bars represent 5%, 12% and 0.2 (‰ V-SMOW), respectively.*

Sample quality assessment for borehole KFR13.

Borehole section and vertical elevation	Number of samples in Dataset I	Sample quality categories and number of samples in each category					Comments
		1	2	3	4	5	Category 1 is of the highest, and category 5 is of the lowest, quality.
KFR13:3 4.0–33.0 m Mid. vertical elevation –141.8 m	2			2		1	The samples were collected in 1995 and 2010. Both samples belong to category 3 due to the fact that the sample series and time series are absent and the environmental isotopes are incomplete. One sample from 1992 has very incomplete analyses and is assigned category 5 (Dataset II)
KFR13:2 34.0–53.0 m Mid. vertical elevation –166.8 m	4		2	1	1	1	The samples were collected in 1995, 2000, 2006 and 2010. Sample series are adequate but time series are absent (category 2). Major ions and environmental isotopes are more or less incomplete (categories 3 and 4) for two of the samples. One sample from 1992 has very incomplete analyses and is assigned category 5 (Dataset II).
KFR13:1 54.0–76.6 m Mid. vertical elevation –188.6 m	4			3	1	1	The samples were collected in 1995, 2000, 2006 and 2010. Sample series are adequate but time series are absent. Major ions and environmental isotopes are more or less incomplete (categories 3 and 4) for two of the samples. One sample from 1992 has very incomplete analyses and is assigned category 5 (Dataset II).

Section information: The bottom section is transecting deformation zone ZFM871 (formerly Zone H2) at 61to 68 m borehole length. Besides ZFM871, the two lower sections are also intersecting zone zfmne3118, while the upper section is located in the bedrock between zones.

Available/missing data: Deuterium and $\delta^{18}O$ values exist for all the samples; trace metal data are not available.

Questionable values/data: None.

Groundwater composition: Typical also for this borehole is the clear change of groundwater composition (i.e. greater contribution of marine Littorina water) in the bottom section at 54.0–76.6 m which corresponds to the intersection with zone ZFM871 (formerly Zone H2) at 53.36 to 74.99 m borehole length. The two upper sections generally maintain a stable composition of a Brackish-glacial groundwater type signature, while the bottom section shows a slow decrease in salinity and alternates between groundwaters of Littorina type and those of mixed Transition type. However questionable, the water type classification changes in 2006 for two of the borehole sections/samples, due solely to increased $\delta^{18}O$ values.

Borehole KFR19

Borehole KFR19, directed upwards from the tunnel, was completed in January 1985 and packer equipment to delimit borehole sections was installed in February 1985; the previous section lengths as given in Sicada are 3–50 m, 66–76 m 77–94 m and 95–110.17 m. However, during 2008 the packer equipment was replaced and packer positions and borehole lengths were checked resulting in somewhat different section lengths. This may be due to faulty information from the early years or small changes in the packer positions. The new lengths are given below except for section 3–50 m which does not have a pressure sensor and has been sampled only once.

Drilling water: Unknown drilling water source; drilling water content is not relevant more than 20 years after drilling.
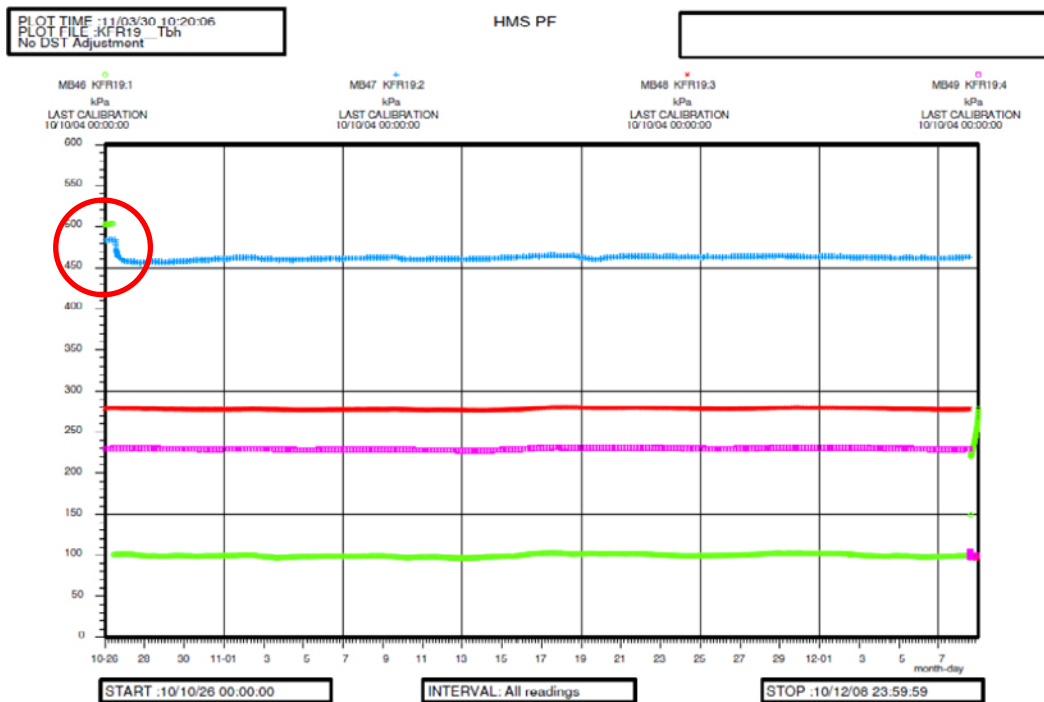
Figure A1-17. *Pressure registration during the hydrochemical investigation in KFR19 (October to December 2010). The figure shows the pressure registration in all four sections in KFR19, where section 1 was cut for the investigation. A pressure response can be noticed in section KFR19:2 (77.6 m to 94.6 m borehole length), see red circle.*

Hydraulic/hydrogeological information: Rather low hydraulic conductivities ranging from $4 \cdot 10^{-11}$ m/s to $-5 \cdot 10^{-10}$ m/s are obtained for all four sections. The pressure level in the innermost two sections is almost the same but more than 200 kPa higher than in the two outermost sections. There is also an ongoing pressure decline in the two innermost sections, not seen in sections KFR19:3 and KFR19:4.

Other information/comments: From the beginning of 2006 and until the re-instrumentation of the borehole in the spring of 2008 there has been a leakage in the tube from section 1, probably somewhere outside section 4. This is most probably due to clogging in the tubes; no water could be obtained from the tubes in sections KFR19:1 and KFR19:4 during a flow test in 1996; after the re-instrumentation in 2008 the flow from all tubes about 300–500 mL/min.

Sampled borehole sections: Since the first sampling in 1995, only a few groundwater samples have been collected from each one of the three borehole sections representing the entire borehole. However, the bottom section (shallowest depth) of the borehole was selected for extended investigations and redox measurements in 2010 due to its shallow location and the Baltic type groundwater signature (Nilsson K 2011). This borehole was considered as one of the most likely to yield oxic groundwater, if it exists at all in the SFR repository boreholes. A pressure response has been observed between sections 1 (95.6–110.2 m) and 2 (77.6–94.6 m), see Figure A1-17 and SKB P-11-14. The chloride, magnesium and $\delta^{18}O$ trends are presented in Figure A1-18 a–c
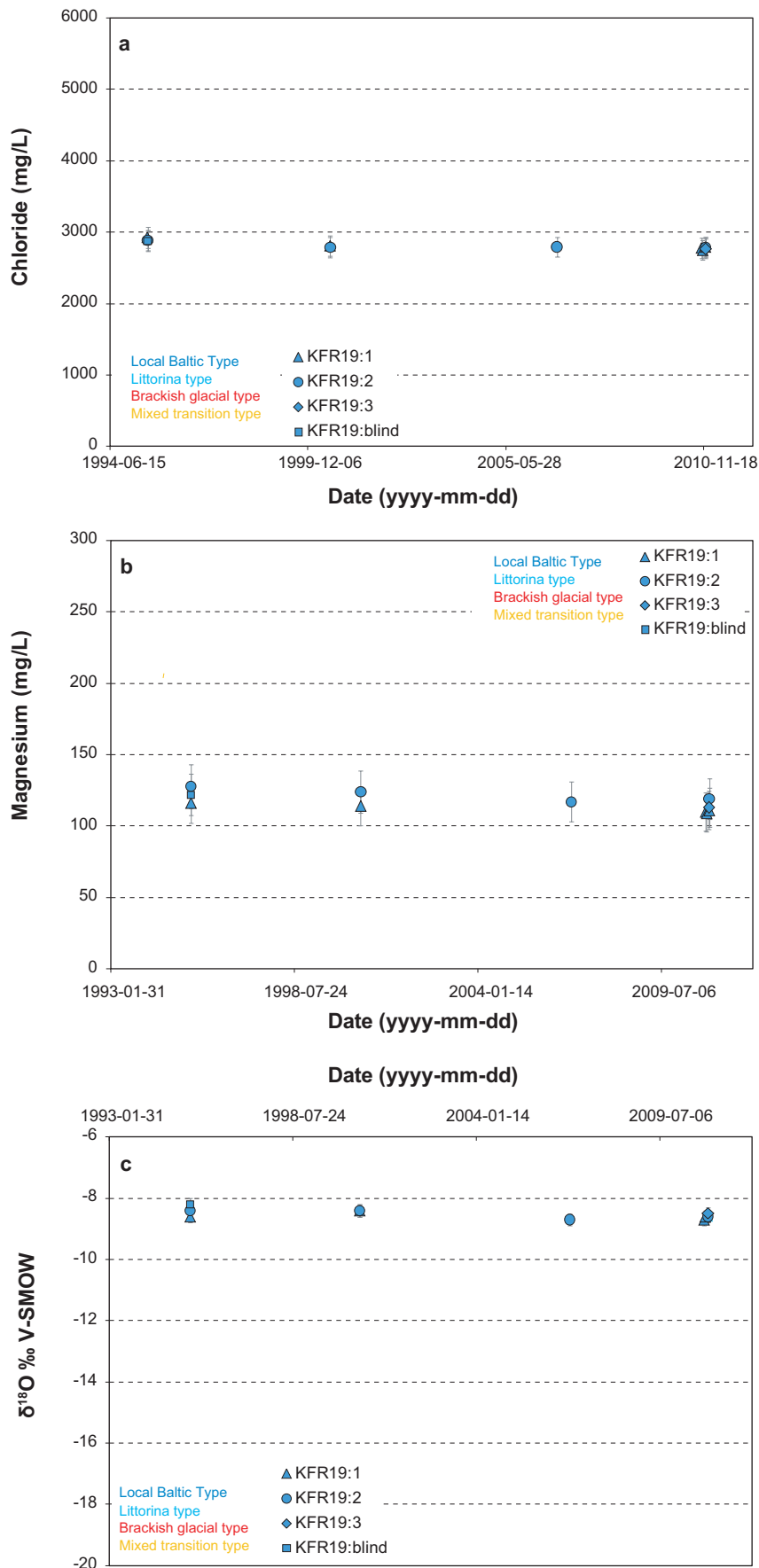
Figure A1-18 a–c. *Borehole KFR19; chloride, magnesium and δ¹⁸O trends during the time period 1995 to 2010. The error bars represent 5%, 12% and 0.2 (‰ V-SMOW), respectively.*

Sample quality assessment for borehole KFR19.

Borehole section and vertical elevation	Number of samples in Dataset I	Sample quality categories and number of samples in each category					Comments
		1	2	3	4	5	Category 1 is of the highest, and category 5 is of the lowest, quality.
KFR19:blind 3.0–50.0 m **Mid. vertical elevation** –74.50 m	1			1			One sample collected in 1995 which belongs to category 3 due to; 1) section length, 2) that sample series and time series are absent, and 3) Fe, Mn and the environmental isotopes are incomplete.
KFR19:3 66.8–76.6 m **Mid. vertical elevation** –63.72 m	1			1			One sample collected in 1995 which belongs to category 3, due to an absence of time series and the environmental isotopes are incomplete.
KFR19:2 77.6–94.6 m **Mid. vertical elevation** –60.29 m	4		2	2		1	The samples are collected in 1995, 2000, 2006 and 2010. Sample series are adequate but time series are absent. Major ions and environmental isotopes are more or less incomplete (category 3) for two of the samples. One sample from 1992 has very incomplete analyses and is assigned to category 5 (Dataset II). A pressure response was observed in section 1 (95.6–110.2 m); see Figure A1-17 and SKB P-11-14
KFR19:1 95.6–110.2 m **Mid. vertical elevation** –56.30 m	5	3	1	1		1	Sample series are adequate (sampling in 1995, 2000 and 2010) and time series were sampled in 2010. Time series: 3 samples from 2010-12-07 to 2010-12-20. Stable water composition and successful redox measurements. A pressure response was observed in section 2 (77.6–94.6 m); see Figure A1-17 and SKB P-11-14. The subhorizontal direction of the borehole and the small difference in vertical depth between the two sections motivate an unchanged quality category.

Section information: This borehole is not interpreted to penetrate any deformation zone; however, it is one of the shallowest boreholes in the SFR and it is directed upwards from the tunnel.

Available/missing data: Deuterium and $\delta^{18}O$ values exist for all samples; trace metal data exist for the last sample from 2010.

Questionable data: None.

Groundwater composition: The groundwater composition is very stable which strengthens its reliability but it is also very similar in all the borehole sections, and all samples therefore have been assigned to a Baltic type groundwater. Despite the young groundwater and the shallow sampling location, the groundwater was still found to be reduced from redox measurements performed in 2010.

Borehole KFR20

Borehole KFR20 was drilled in 1984 and was used until 1996.

Drilling water: Unknown drilling water source;.drilling water content is not relevant more than 20 years after drilling.

Hydraulic/hydrogeological information: The highest estimated hydraulic conductivities from pressure build-up tests in four sections from an earlier instrumentation are: 91–110 m at $-4 \cdot 10^{-9}$ m/s, 74–90 m at $-2 \cdot 10^{-10}$ m/s, 44–58 m at $-8 \cdot 10^{-8}$ m/s and 91–110 m at $-7 \cdot 10^{-9}$ m/s.

Sampled borehole sections: Only a single groundwater sample was collected from the entire borehole in 1995 and therefore no sample series to plot.

Sample quality assessment for borehole KFR20.

Borehole section and vertical elevation	Number of samples in Dataset I	Sample quality categories and number of samples in each category					Comments
		1	2	3	4	5	Category 1 is of the highest, and category 5 is of lowest, quality.
KFR20:entire 0.0–109.7 m Mid. vertical elevation –71.24 m	1				1		One single sample was collected in 1995. Due to that: 1) Sample series and time series are absent, 2) Bicarbonate, Fe, Mn and tritium are missing, and that 3) the entire borehole of 109.7 m length was sampled, The sample is assigned a category 4.

Borehole section information: The entire borehole is located in bedrock between deformation zones.

Available/missing data: Deuterium and $\delta^{18}O$ values exist for the single sample; trace metal data are not available.

Questionable data: None**.**

Groundwater composition: The single sample was considered as Baltic groundwater type due to low salinity, a high $\delta^{18}O$ value and a shallow borehole location.

Borehole KFR55

Borehole KFR55 was drilled in 1985 and packer equipment to delimit the borehole sections was installed after completion of the drilling; the previous section lengths as given in Sicada are 8–21 m, 22–39 m, 40–48 m and 49–61.89 m. During 2008 the packer equipment was replaced and packer positions and borehole length were checked. However, the new section lengths measured were somewhat different which may be explained by faulty information or small changes in the packer positions. The new lengths are given below even if most of the data originate from the period before 2008.

Sample quality assessment for borehole KFR55.

| Borehole section and vertical elevation	Number of samples in Dataset I	Sample quality categories and number of samples in each category					Comments
		1	2	3	4	5	Category 1 is of the highest, and category 5 is of the lowest, quality.
KFR55:3 7.53–20.53 m Mid. vertical elevation –128.3 m	4		2	1	1	1	Samples were collected in 1995, 2000, 2006 and 2010. Sample series adequate but time series are absent. Bicarbonate, Fe, Mn and the environmental isotopes are incomplete in two samples assigned a category 3 and 4. One sample from 1992 is very incomplete (category 5 transferred to Dataset II).
KFR55:2 21.53–38.53 m Mid. vertical elevation –131.4 m	4		2	1	1	1	Samples collected in 1995, 2000, 2006 and 2010. Sample series adequate but time series are absent. Bicarbonate, Fe, Mn and the environmental isotopes are incomplete in two samples assigned categories 3 and 4. One sample from 1992 is very incomplete (category 5 transferred to Dataset II).
KFR55:1 39.53–47.53 m Mid. vertical elevation –134.0 m	4		2	2		1	Samples collected in 1995, 2000, 2006 and 2010. Sample series adequate but time series are absent. Fe, Mn and the environmental isotopes are incomplete in two samples assigned category 3. One sample from 1992 is very incomplete (category 5 transferred to Dataset II).
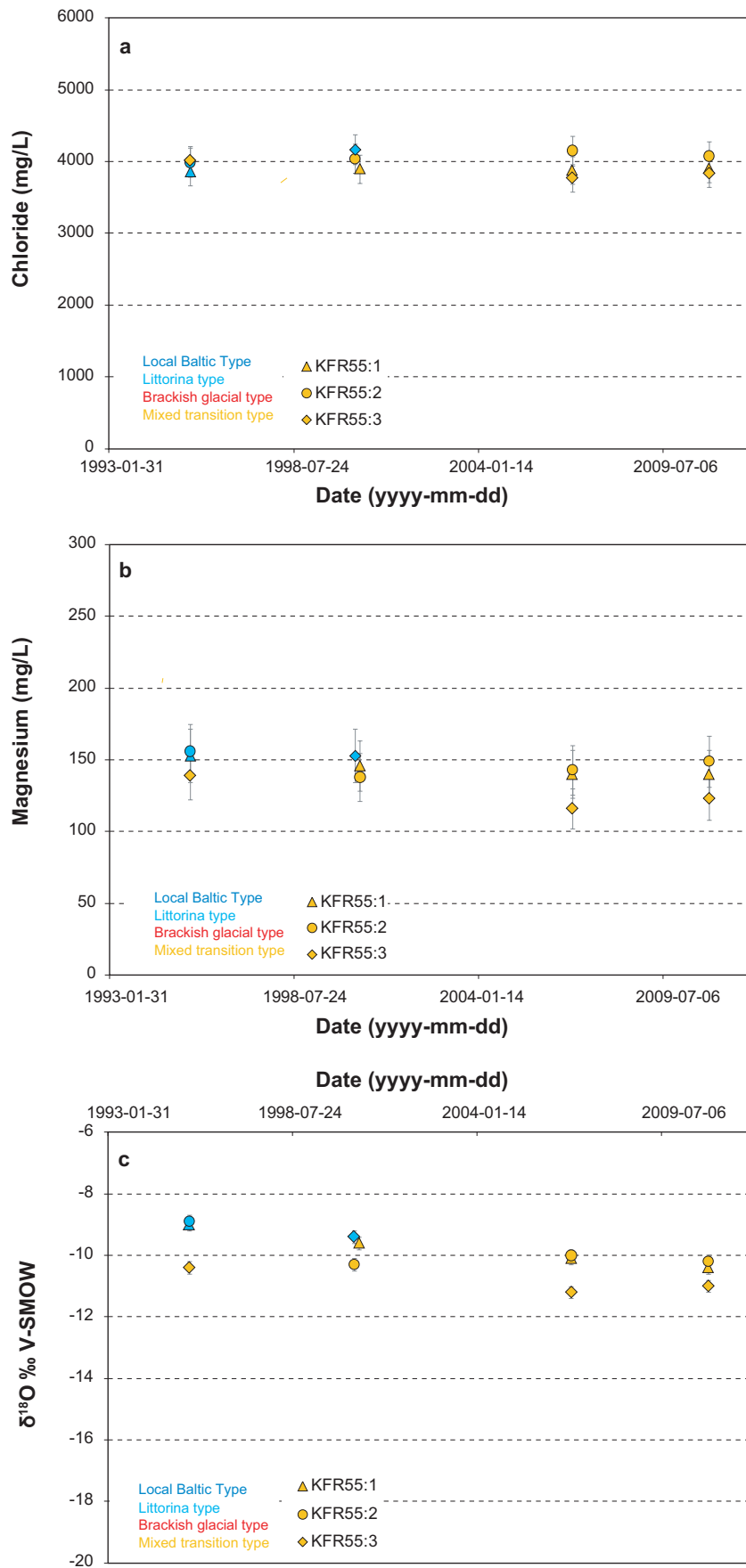
Figure A1-19 a–c. Borehole KFR55; Chloride, magnesium and δ¹⁸O trends from 1995 to 2010. The error bars represent 5%, 12% and 0.2 (‰ V-SMOW), respectively.

Drilling water: Unknown drilling water source; drilling water content is not relevant more than 20 years after drilling.

Hydraulic/hydrogeological information: The hydraulic conductivity in sections 1 and 2 is close to 10^{-8} m/s (no information exists for sections 3 and 4). Following re-instrumentation the pressure in section 1 was close to air pressure and therefore no water was obtained from the section; presently, a slow pressure recovery is ongoing in this section.

Sampled borehole sections: Samples have been collected in the three borehole sections covering the entire borehole since 1995; the chloride, magnesium and δ^{18}O trends are presented in Figure A1-19 a–c.

Borehole section information: The two upper borehole sections are located in deformation zone ZFMNE0870 (formerly Zone 9) between 17 and 38 m borehole length. The first section intersects also zone ZFMNE3118 between 8 and 17 m borehole length.

Available/missing data: Deuterium and δ^{18}O values exist for all samples; trace metal data are not available.

Questionable data: None

Groundwater composition: The groundwater composition in the three borehole sections is rather similar, although a weak decrease in salinity and δ^{18}O trends implies increased mixing.

Borehole KFR56

Borehole KFR56 was drilled in 1985 and includes only one borehole section from a packer located between 8 and 9 m to the bottom of the borehole. New equipment was installed in the borehole during 2008 and packer positions and borehole length were checked.

Drilling water: Unknown drilling water source; drilling water content is not relevant more than 20 years after drilling.

Hydraulic/hydrogeological information: From a pressure build-up test the hydraulic conductivity was estimated to about $4 \cdot 10^{-8}$ m/s.

Other information/comments: The water yield from the borehole is relatively high, about 1,700 mL/min.

Sampled borehole sections: Groundwater samples have been collected quite regularly from a borehole section representing the entire borehole since 1995; the chloride, magnesium and δ^{18}O trends are presented in Figure A1-20 a–c.

Sample quality assessment for borehole KFR56.

| Borehole section and vertical elevation	Number of samples in Dataset I	Sample quality categories and number of samples in each category.					Comments
		1	2	3	4	5	Category 1 is of the highest, and category 5 is of the lowest, quality.
KFR56:1 **9.0–81.7 m** **Mid. vertical elevation** **–64.7 m**	5			4	1	1	Samples were collected in 1995, 2000, 2006, 2009 and 2010. Sample series adequate but time series are absent. The section length of more than 20 m assignes a category 3. Bicarbonate, Fe, Mn and the environmental isotopes are incomplete in one sample of category 4. One sample from 1992 is very incomplete (category 5 transferred to Dataset II)
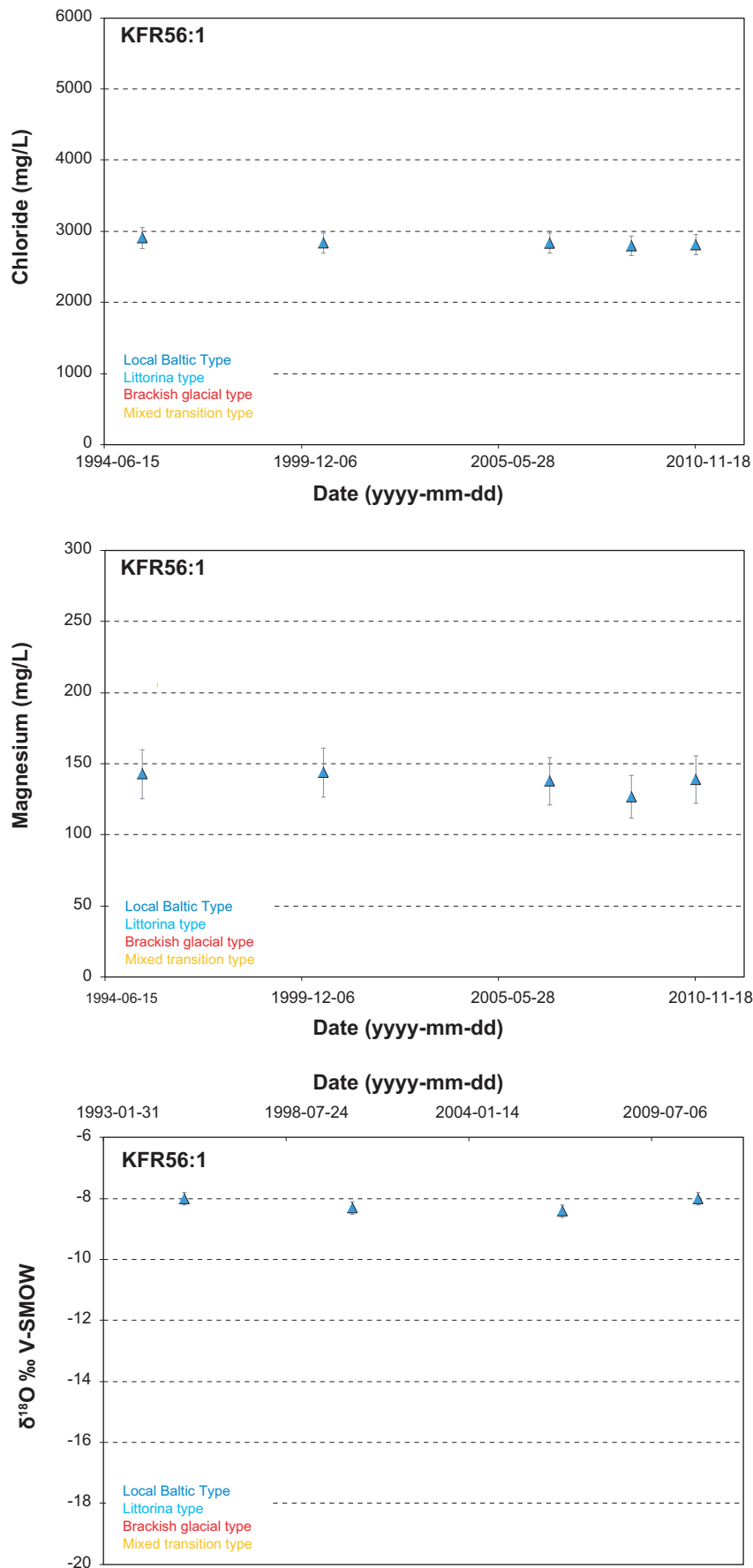
Figure A1-20 a–c. *Borehole KFR56; chloride, magnesium and δ¹⁸O trends during the time period 1995 to 2010. The error bars represent 5%, 12% and 0.2 (‰ V-SMOW), respectively.*

Borehole section information: The borehole section is transecting two deformation zones: ZFM-NW0805b and ZFMNW0805a (formerly Zones 8a and 8b).

Available/missing data: Deuterium and $\delta^{18}O$ values exist for most of the samples; trace metal data are not available.

Questionable data: None.

Groundwater composition: The groundwater composition in the borehole is stable within the measurement uncertainties and all groundwater samples show a Baltic type signature typical for shallow sampling locations.

Borehole KFR7A

Borehole KFR7A was drilled in 1984 followed by the installation of packer equipment to delimit three borehole sections. During 2008 this equipment was replaced and packer positions and borehole length were checked; the first groundwater sampling was performed in 1987.

Drilling water: Unknown drilling water source; drilling water content is not relevant more than 20 years after drilling.

Hydraulic/hydrogeological information: The estimated hydraulic conductivities from pressure build-up tests in the three sections are: KFR7A:1 at $-4 \cdot 10^{-6}$ m/s, KFR7A:2 at $-7 \cdot 10^{-7}$ m/s and KFR7A:3 at $-8 \cdot 10^{-9}$ m/s.

Other information/comments: There has been a leakage in the instrumentation installed between sections 1 and 2, probably already from 2000 until re-instrumentation in 2008. The effect of the leakage could be seen as a pressure influence between the two sections, and most likely is responsible for the brake in trend plots (clearest in the chloride trend plot) in Figure A1-21 a–c below. Following re-instrumentation the pressure in section 2 was still similar to section 3 when the leakage was occurring; the flow rate from section 2 is very low, about.10 ml/min.

Sampled borehole sections: In the bottom section, extensive investigations including collection of time series samples and redox measurements were conducted already in 1987 and repeated in 2000 and 2010. The borehole section, sampled annually since 1989, was selected for extended investigations and further redox measurements in 2010 in order to trace possible changes in redox conditions (Nilsson K 2011). The two upper sections have not been subjected to the same thorough studies and only a few relatively late samples exist. Trend plots of chloride, magnesium and $\delta^{18}O$ with time are presented in Figure A1-22 a–c.

Sample quality assessment for borehole KFR7A.

| Borehole section and vertical elevation	Number of samples in Dataset I	Sample quality categories and number of samples in each category.					Comments
		1	2	3	4	5	Category 1 is of the highest, and category 5 is of the lowest, quality.
2.0–19.0 m **Mid. vertical elevation –132.6 m**	4		2	1	1	1	The samples were collected in 1995, 2000, 2006 and 2010. Sample series are inadequate and time series are absent (which implies category 2). Some ions and isotopes are missing for the two samples assigned categories 3 and 4.
20.0–47.0 m **Mid. vertical elevation –133.5 m**	1				1	2	The sample was collected in 1995. Sample series and time series are absent (which implies category 3). Some anions, Fe, Mn and tritium, are missing for the sample (category 4).
48.0–74.7 m **Mid. vertical elevation –134.4 m**	35			32	3	18	The annual sampling started in 1989. Sample series are adequate and time series were collected in 1987 (5 samples) 2000 (4 samples) and 2010 (3 samples). The section length implies category 3. Successful redox measurements were performed in 1987 and 2010 and more questionable measurements were conducted in 2000.
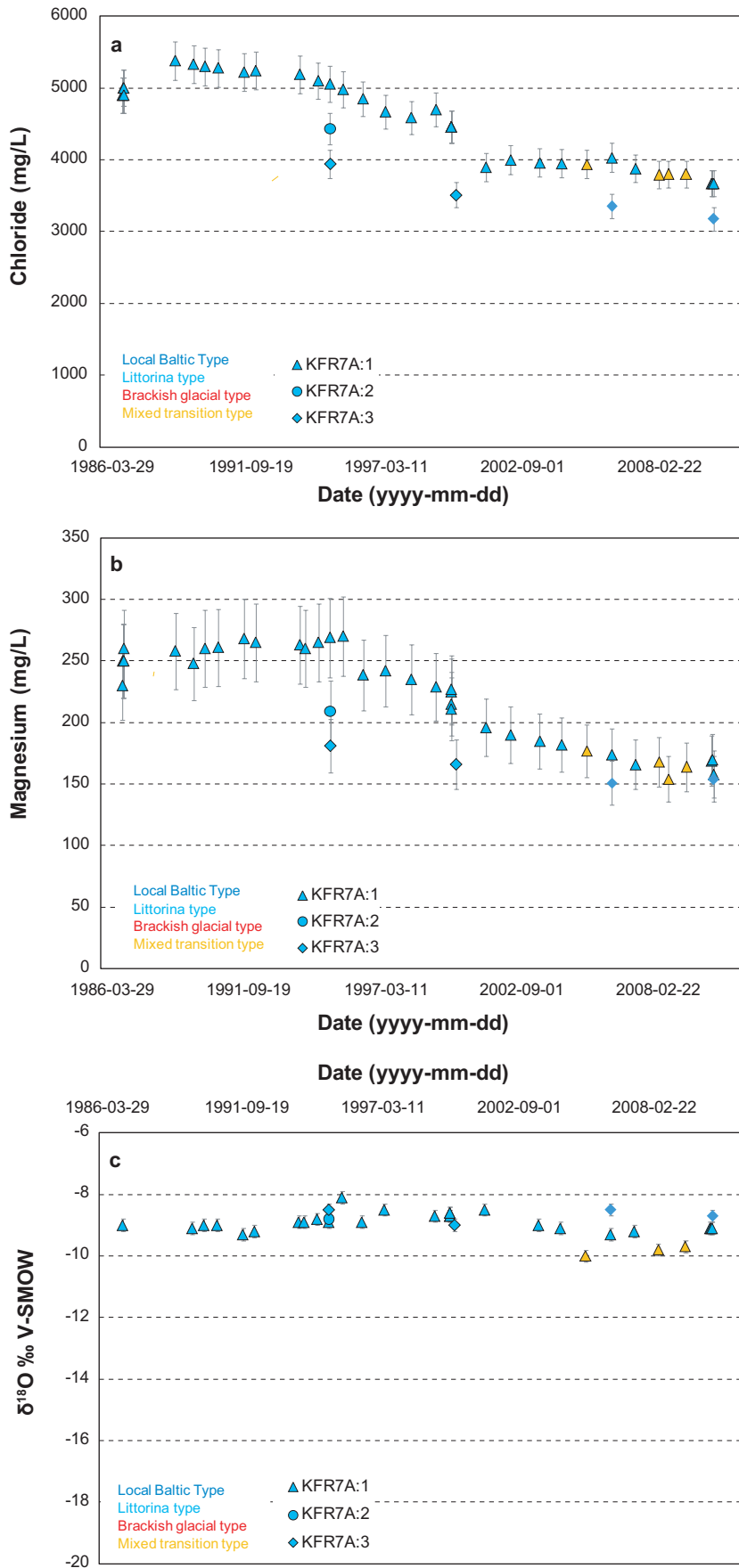
Figure A1-21 a–c. *Borehole KFR7A; chloride, magnesium and $\delta^{18}O$ trends duri ng the time period 1986 to 2010. The error bars represent 5%, 12% and 0.2 (‰ V-SMOW), respectively.*

Borehole section information: The borehole length from 43.6 m to 74.45 m is within deformation zone ZFMNW0805a (formerly Zone 8A) and within deformation zone ZFMNW0805b (formerly Zone 8B) from 3.5 to 43 m. The borehole may also have contact with the gently dipping deformation zone ZFM871 (formerly Zone H2).

Available/missing data: The first two sections have sporadic analyses of the isotopes tritium, deuterium and $\delta^{18}O$ but no trace metals. The samples from the bottom section have generally more complete analyses including Eh measurements and ^{36}Cl isotope data from 2010 (available for KFR101:1, KFR105:1, KFR08:1 and KFR7A:1).

Questionable data: A deviating and too high sulphate value was obtained for sample no. 16094 and the sodium concentration was faulty for sample no 16206.

Groundwater composition: The upper and lower sections both show decreasing chloride and magnesium trends and there is only one sample with intermediate concentrations representing the middle section. Most of the groundwater samples are of the Littorina type, however, despite that the $\delta^{18}O$ signatures are quite similar; the trends reveal a change to Baltic type water in the final samples from the upper section and a change towards mixed Transition type groundwaters in the deep section.

Borehole KFR7B

Borehole KFR7B was drilled in 1985 and packer equipment was installed prior to the first sampling occasion at the end of 1985. New equipment was installed in the borehole during 2008 and packer positions and borehole length were checked.

Drilling water: Unknown drilling water source; drilling water content is not relevant more than 20 years after drilling.

Hydraulic/hydrogeological information: The estimated hydraulic conductivities from pressure build-up tests in the two sections are: KFR7B:1 at $-3\cdot10^{-5}$ m/s and KFR7B:2 at $-2\cdot10^{-8}$ m/s.

Other information/comments: A leakage between the two sections that may have existed since late in 1990 was repaired in May 2001.

Sampled borehole sections: Groundwater samples have been collected from two borehole sections 4–7.6 m and 8.6–21.1 m since 1995 and 1986, respectively; the chloride, magnesium and $\delta^{18}O$ trends are presented in Figure A1-22 a–c.

Sample quality assessment for borehole KFR7B.

| Borehole section and vertical elevation	Number of samples in Dataset I	Sample quality categories and number of samples in each category.					Comments
		1	2	3	4	5	Category 1 is of the highest, and category 5 is of the lowest, quality.
KFR7B:2 4.0– 7.6 m **Mid. vertical elevation** −138.9 m	3		1	1	1	2	Samples were collected in 1995, 2006 and 2010. Sample series adequate but time series are absent (Category 2). Fe and Mn missing (Category 3). Bicarbonate, Fe, Mn and the environmental isotopes are incomplete in samples of category 4. Two samples from 1992 and 2000 are very incomplete (category 5 transferred to Dataset II)
KFR7B:1 8.6–21.1 m **Mid. vertical elevation** −147.6 m	5		2	2	1	2	Samples collected in 1986, 1987, 1995, 2006 and 2010. Sample series adequate but time series are absent (Category 2). Fe and Mn missing (Category 3). Bicarbonate, Fe, Mn and the environmental isotopes are incomplete in samples of category 4. Two samples from 1992 and 2000 are very incomplete (category 5 transferred to Dataset II)
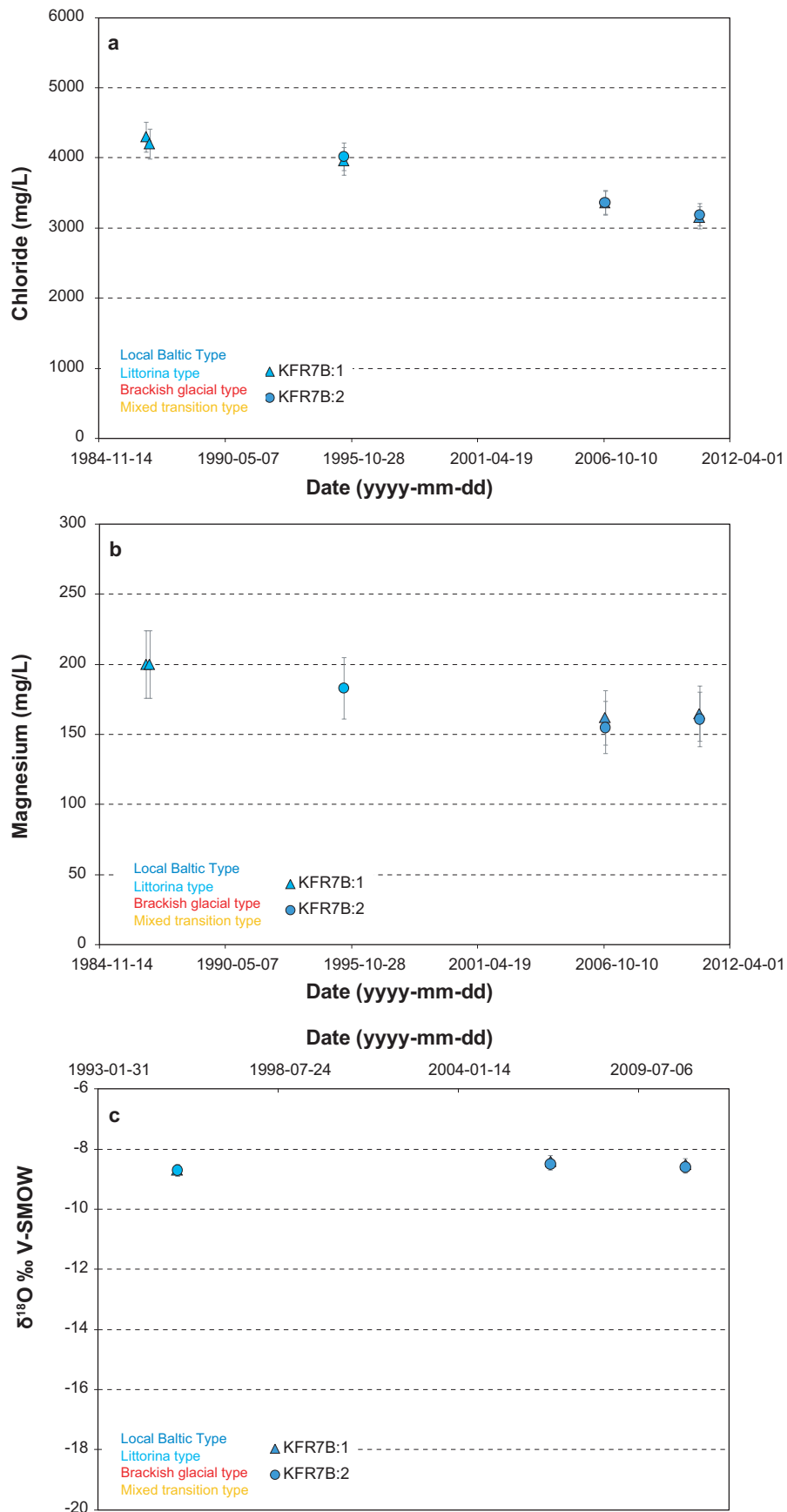
Figure A1-22 a–c. *Borehole KFR7B; chloride, magnesium and δ¹⁸O (starting 1995) trends during the time period 1986 to 2010. The error bars represent 5%, 12% and 0.2 (‰ V-SMOW), respectively.*

Borehole section information: Both sections are located within the gently dipping deformation zone ZFM871 (formerly Zone H2) between 0 to 17 m borehole length, and the bottom section also transects deformation zone ZFMNE0870 (formerly Zone 9) at 20.27 to 21.1 m borehole length.

Questionable data: None.

Groundwater composition: Both borehole sections show very similar groundwater compositions with decreasing salinity trends and a gradual change from Littorina type to Baltic type groundwater. The prevailing marine signature is indicated from the relatively constant and high δ^{18}O value.

Borehole KFR7C

Borehole KFR7C was drilled in 1986 and one single packer was installed close to the borehole orifice prior to the first sampling occasion in 1986. No new equipment was installed in this borehole during 2008 since it was not included in the hydrogeological control programme (pressure monitoring).

Drilling water: Unknown drilling water source; drilling water content is not relevant more than 20 years after drilling.

Hydraulic/hydrogeological information: A pressure build-up test for section 6–34 m recorded a hydraulic conductivity about $2 \cdot 10^{-8}$ m/s.

Sampled borehole sections: Four groundwater samples have been collected from a section representing the entire borehole, or most of the borehole, depending on the existence or not of a packer at the orifice. The chloride, magnesium and δ^{18}O trends are presented in Figure A1-23 a–c.

Sample quality assessment for borehole KFR7C.

Borehole section and vertical elevation	Number of samples in Dataset I	Sample quality categories and number of samples in each category.					Comments
		1	2	3	4	5	Category 1 is of the highest and category 5 is of the lowest, quality.
KFR7C:1 0.0–34.0 m or 6.0–34.0 m Mid. vertical elevation −149.4 m or −152.2 m	4			3	1		Samples were collected in 1986, 1987, 1995 and 2000. Sample series are inadequate and time series are absent (Category 3). The section length results in Category 3. Bicarbonate, Fe, Mn and the environmental isotopes are incomplete in one sample of category 4.

Borehole section information: The borehole section represents the entire borehole, the most of which is within deformation zones ZFMNE0870 (formerly Zone 9 intersecting at 6.23–7.15 m borehole length) and ZFM871 (formerly Zone H2 intersecting at 6–32 m borehole length).

Questionable data: None.

General: The few samples show a somewhat decreasing salinity with time but the Littorina type groundwater signature is maintained also in the last sample from 2000.
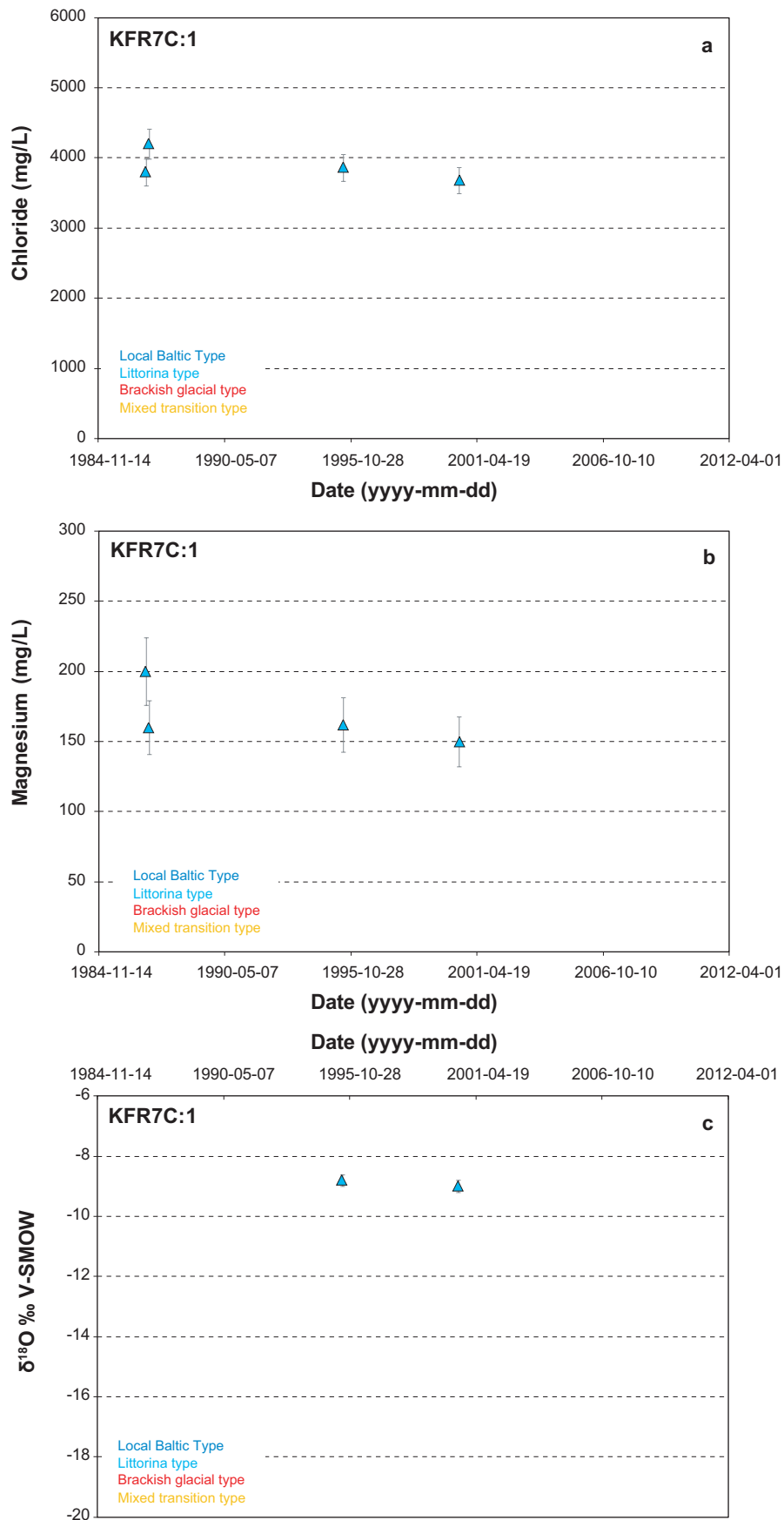
Figure A1-23 a–c. Borehole KFR7C; chloride, magnesium and δ18O (starting 1995) trends from 1986 to 2010. The error bars represent 5%, 12% and 0.2 (‰ V-SMOW), respectively.

Late groundwater sampling in borehole KFR104.

A time series of three groundwater samples were collected in borehole KFR104, section 333.0–454.6 m borehole length (–306.5 m elevation) in June/July 2011 due to shortage of data from the Central Block. The obtained hydrochemical data are not reported in any P-report, therefore a short summary of the performance and a presentation of the data are given in this Appendix.

The controlling documents for performing the sampling activity are given in Table A2-1. Information on sampling conditions is presented in Table A2-2 and the analytical data including basic water analyses (Na, K, Ca, Mg, SO$_4$, SO$_4$-S, HCO$_3$, Cl, Br, F, Si, Fe, Mn, Li, laboratory measurements of pH and electrical conductivity) as well as the isotopes δ^2H and δ^{18}O are displayed in Table A2-3. The sampled section is very long which probably influences the chemistry of the sample. Quality assessment and discussions about sampling conditions in this borehole section are presented in Appendix 1.

Table A2-1. Controlling documents for performance of the activity.

Activity plan	Number	Version
Provtagning och analys i KFR106	AP SFR-10-029	2.0
Method descriptions		
Metodbeskrivning för provtagning och analys i instrumenterade borrhål	SKB MD 425.001	1.0
Mätsystembeskrivning – Handhavandedel; System för hydrologisk och meterologisk datainsamling. Vattenprovtagning och utspädningsmätning i instrumenterade borrhål	SKB MD 368.010	1.0
Provtagning och analys – kemilaboratorium	SKB MD 452.001 to 019	–

Table A2-2. Sampling information.

Idcode	Sample no.	Secup	Seclow	Elevation (m)	Sampling date (yyyy-mm-dd)	Flow rate (L/min)	Minimum discharge volume (m^3) prior to each sampe (1.5, 3 and 5 plug flow volumes*)	Actual pumped volume (m^3) prior to sampling
KFR104	21095	333.0	454.6	–306.5	2011-06-23	0.06	0.735	0.867
KFR104	21096	333.0	454.6	–306.5	2011-07-01	0.06	1.47	2.08
KFR104	21097	333.0	454.6	–306.5	2011-07-13	0.06	2.45	2.59

* Nilsson et al. 2010b

Table A2-3. Hydrochemical data compilation from borehole KFR104, section 333.0–454.6 m borehole length.

Idcode	Secup (m)	Secup (m)	Elevation (m)	Sample no.	Na (mg/L)	K (mg/L)	Ca (mg/L)	Mg (mg/L)	HCO$_3$ (mg/L)	
KFR104	333.0	454.6	–306.5	21095	742	5.44	401	17.3	43.4	
KFR104	333.0	454.6	–306.5	21096	836	5.56	485	27.4	37.0	
KFR104	333.0	454.6	–306.5	21097	859	5.17	531	28.7	34.5	
Idcode	Secup (m)	Secup (m)	Elevation (m)	Sample no.	Cl (mg/L)	SO$_4$ (mg/L)	SO$_4$.S (mg/L)	Br (mg/L)	F (mg/L)	
KFR104	333.0	454.6	–306.5	21095	2,004	52.6	19.5	10.7	1.47	
KFR104	333.0	454.6	–306.5	21096	2,264	99.8	36.8	11.9	1.29	
KFR104	333.0	454.6	–306.5	21097	2,357	108.0	41.1	14.7	1.29	

Idcode	Secup (m)	Secup (m)	Elevation (m)	Sample no.	Si (mg/L)	Fe (mg/L)	Mn (mg/L)	Li (mg/L)	Sr (mg/L)	
KFR104	333.0	454.6	–306.5	21095	5.73	0.0246	0.135	0.0213	6.29	
KFR104	333.0	454.6	–306.5	21096	5.74	0.120	0.170	0.0294	7.63	
KFR104	333.0	454.6	–306.5	21097	5.80	0.167	0.181	0.0314	8.37	
Idcode	**Secup (m)**	**Secup (m)**	**Elevation (m)**	**Sample no.**	**pH-L (pH-unit)**	**EC-L (mS/m)**	**I (mg/L)**	**δD (‰ SMOW)**	**δ^{18}O (‰ SMOW)**	**Drill_w (%)**
KFR104	333.0	454.6	–306.5	21095	7.85	605.5	0.152	–99.5	–13.8	0.4
KFR104	333.0	454.6	–306.5	21096	7.88	682.5	0.106	–99.7	–13.7	4.0
KFR104	333.0	454.6	–306.5	21097	7.89	723.5	0.104	–99.6	–14.1	4.0

Idcode   borehole name.

Secup   upper section limit (m borehole length).

Seclow   lower section limit (m borehole length).

pH-L   pH measured in the laboratory at 25°C.

EC-L   Electrical Conductivity measured in the laboratory. Value corrected to 25°C.

Drill_w   Percentage drilling water contamination in the sample.